THE ADDITION OF HALOMETHYL RADICALS TO FLUOROETHYLENES

John Purdie Sloan

A Thesis Submitted for the Degree of PhD
at the
University of St Andrews

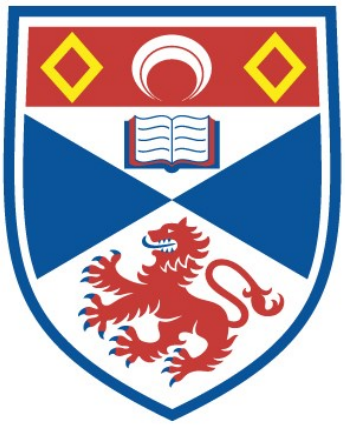

1974

THE ADDITION OF HALOMETHYL RADICALS TO FLUOROETHYLENES

being a Thesis

presented by

JOHN PURDIE SLOAN, B.Sc.

to the

UNIVERSITY OF ST. ANDREWS

in application for

THE DEGREE OF DOCTOR OF PHILOSOPHY

1974

Th 8353

SUMMARY

The thesis records the competitive addition reactions of $CFBr_2\cdot$, $CF_2I\cdot$, $CHF_2\cdot$ and $CH_2F\cdot$ radicals to each of vinyl fluoride, 1,1-difluoroethylene, trifluoroethylene and tetrafluoroethylene in the presence of ethylene, and a few additional reactions in the absence of ethylene. The results are discussed in conjunction with the corresponding results for addition of $C_3F_7\cdot$, $(CF_3)_2CF\cdot$, $C_2F_5\cdot$, $CF_3\cdot$, $CF_2Br\cdot$, $CCl_3\cdot$ and $CH_3\cdot$ radicals.

Part 1 records the photolytic reactions of $CFBr_3$. At short wavelengths both $CFBr_2\cdot$ and :CFBr are formed but the contribution to product formation from the carbene was insignificant in the kinetic series conducted at 366 nm. Competitive addition of $CFBr_2\cdot$ gave, from the Arrhenius plots, the A-factor and activation energy differences and the relative rates of the addition steps. The activation energy differences showed a good correlation with atom localisation energies for $C_3F_7\cdot$, $CF_3\cdot$, $CF_2Br\cdot$, $CCl_3\cdot$ and $CFBr_2\cdot$ radicals.

The photolytic reactions of CHF_2I and CH_2FI with the fluoroethylenes are recorded in parts 2 and 3 respectively. The primary photolysis step with CHF_2I gives difluoromethyl radicals and excited iodine atoms. The excited $I^*(^3P_{\frac{1}{2}})$ atoms abstract hydrogen from CHF_2I giving a system containing both $CHF_2\cdot$ and $CF_2I\cdot$ radicals. The Arrhenius plots for addition of $CF_2I\cdot$ radicals follow the same pattern as for $CFBr_2\cdot$ with much reduced selectivity. Addition of difluoromethyl and fluoromethyl radicals, apart from the normal Arrhenius behaviour observed for competitive addition between ethylene and tetrafluoroethylene, show anomalous Arrhenius behaviour with negative slopes corresponding to diverging adduct ratios with increasing temperatures, and A-factors varying by up to three orders of magnitude. Several potential factors causing the anomalies are considered and excluded: dimerisation and cross combination of radical species; telomerisation of and hydrogen abstraction by the adduct radicals; elimination of HI

from the adducts; and reversibility of the addition steps. The evidence favours joint participation of ground state ($CHF_2^{\cdot}$, $CH_2F^{\cdot}$) and vibrationally excited (CHF_2^{*}, CH_2F^{*}) radicals in non reversible addition reactions, ground state radicals predominating at high temperature and excited state at low temperature. Analysis of the complete set of results indicates that, for fully halogenated alkyl radicals, orientation of addition to unsymmetrical fluoroethylenes is a function of steric factors: the logarithms of orientation ratios at 150°C give a linear correlation with radical radii. With partially halogenated alkyl radicals the strong polar differences between hydrogen and halogen atoms requires the introduction of a polar term, which, combined with radical radii, gives a linear correlation including both partially and fully halogenated alkyl radicals with logarithms of the orientation ratios.

to the memory of my mother

ELSPETH PURDIE

1913-1968

DECLARATION

I declare that this thesis is based on the results of experiments carried out by me, that it is my own composition, and has not been submitted previously in application for a higher degree.

CERTIFICATE

I hereby certify that John Purdie Sloan, B.Sc. has spent eleven terms at research work under my supervision, has fulfilled the conditions of the Resolution of the University Court, 1967 No. 1, and is qualified to submit the accompanying thesis in application for the degree of Doctor of Philosophy.

PROFESSOR LORD TEDDER

UNIVERSITY CAREER

I entered the University of St. Andrews in October 1967, and subsequently graduated B.Sc. with Second Class Honours (Division I) in Chemistry in June 1971.

In October 1971, I was awarded a Science Research Council Studentship, and, from then until July 1974, I carried out work which is embodied in this thesis in the Department of Chemistry, University of St. Andrews under the supervision of Professor Lord Tedder.

ACKNOWLEDGEMENTS

I express my gratitude to Professor Lord Tedder and Dr. John Walton for their advice and guidance, and for continued interest in this work.

Thanks are also due to the technical staff of the Department of Chemistry for their valuable assistance, to Pat, Sharon and Wilma for preparing the typescript and to Tom McQueen for printing the manuscript.

Finally, I thank the Science Research Council for the award of a Research Studentship which enabled me to carry out this research.

CONTENTS

SUMMARY

The thesis records the competitive addition reactions of $CFBr_2\cdot$, $CF_2I\cdot$, $CHF_2\cdot$ and $CH_2F\cdot$ radicals to each of vinyl fluoride, 1,1-difluoroethylene, trifluoroethylene and tetrafluoroethylene in the presence of ethylene, and a few additional reactions in the absence of ethylene. The results are discussed in conjunction with the corresponding results for addition of $C_3F_7\cdot$, $(CF_3)_2CF\cdot$, $C_2F_5\cdot$, $CF_3\cdot$, $CF_2Br\cdot$, $CCl_3\cdot$ and $CH_3\cdot$ radicals.

Part 1 records the photolytic reactions of $CFBr_3$. At short wavelengths both $CFBr_2\cdot$ and :CFBr are formed but the contribution to product formation from the carbene was insignificant in the kinetic series conducted at 366 nm. Competitive addition of $CFBr_2\cdot$ gave, from the Arrhenius plots, the A-factor and activation energy differences and the relative rates of the addition steps. The activation energy differences showed a good correlation with atom localisation energies for $C_3F_7\cdot$, $CF_3\cdot$, $CF_2Br\cdot$, $CCl_3\cdot$ and $CFBr_2\cdot$ radicals.

The photolytic reactions of CHF_2I and CH_2FI with the fluoroethylenes are recorded in parts 2 and 3 respectively. The primary photolysis step with CHF_2I gives difluoromethyl radicals and excited iodine atoms. The excited I^* ($^3P_{\frac{1}{2}}$) atoms abstract hydrogen from CHF_2I giving a system containing both $CHF_2\cdot$ and $CF_2I\cdot$ radicals. The Arrhenius plots for addition of $CF_2I\cdot$ radicals follow the same pattern as for $CFBr_2\cdot$ with much reduced selectivity. Addition of difluoromethyl and fluoromethyl radicals, apart from the normal Arrhenius behaviour observed for competitive addition between ethylene and tetrafluoroethylene, show anomalous Arrhenius behaviour with negative slopes corresponding to diverging adduct ratios with increasing temperatures, and A-factors varying by up to three orders of magnitude. Several potential factors causing the anomalies are considered and excluded: dimerisation and cross combination of radical species; telomerisation of and hydrogen abstraction by the adduct radicals; elimination of HI

from the adducts; and reversibility of the addition steps. The evidence favours joint participation of ground state ($CHF_2^{\cdot}$, $CH_2F^{\cdot}$) and vibrationally excited (CHF_2^{*}, CH_2F^{*}) radicals in non reversible addition reactions, ground state radicals predominating at high temperature and excited state at low temperature. Analysis of the complete set of results indicates that, for fully halogenated alkyl radicals, orientation of addition to unsymmetrical fluoroethylenes is a function of steric factors: the logarithms of orientation ratios at 150°C give a linear correlation with radical radii. With partially halogenated alkyl radicals the strong polar differences between hydrogen and halogen atoms requires the introduction of a polar term, which, combined with radical radii, gives a linear correlation including both partially and fully halogenated alkyl radicals with logarithms of the orientation ratios.

General Introduction

Chemical reactions proceed by either concerted mechanisms or by heterolytic or homolytic fission of chemical bonds. During the nineteenth century no substantiated homolytic fission reactions were reported in the literature and all reactions were explained in terms of heterolytic bond fission yielding oppositely charged entities.

$$A\text{-}B \longrightarrow A^{+} + B^{-}$$

The goal of observing homolytic bond fission, which eluded numerous investigators for half a century, was achieved by M. Gomberg[1] in 1900 while attempting the preparation of hexaphenylethane. The solution reacted instantly with oxygen and iodine and could only be explained on the basis of dissociation of hexaphenylethane into triphenylmethyl radicals.

$$Ph_3C\text{-}CPh_3 \rightleftharpoons 2PH_3C^{\cdot}$$

Homolysis of a chemical bond gives two electrically neutral free radical or atomic species, each with one unpaired electron. In 1925 Taylor[2] proposed a chain mechanism incorporating free radical intermediates in the mercury photosensitised hydrogenation of ethylene.

$$H_2 + Hg(6\ ^3P_1) \longrightarrow 2H^{\cdot} + Hg(6\ ^1S_0)$$

$$H^{\cdot} + C_2H_4 \longrightarrow C_2H_5^{\cdot}$$

$$C_2H_5^{\cdot} + H_2 \longrightarrow C_2H_6 + H^{\cdot}$$

Conclusive evidence for the existence of methyl radicals was obtained in 1929 by Paneth and Hofeditz[3]. They pyrolised tetramethyl lead in a tube flushed with hydrogen and the resulting methyl radicals removed a lead mirror further downstream. Methyl radical lifetimes of approximately 10^{-3} S were calculated. The acceptance of free radical mechanisms enabled Hey and Waters[4] to explain among other reactions the anti-Markovnikov addition of hydrogen bromide to olefins.

The sequence of radical chain reactions is; initiation, in which

radicals are formed; propagation, in which new radical sites are formed while the total number of radical sites remain constant; and termination, in which radicals are destroyed.

Three of the main methods of initiation are:

i) the thermal decomposition of azo compounds producing two radical species for each molecule of nitrogen formed,

$$CH_3\text{-}N{=}N\text{-}CH_3 \xrightarrow{\text{heat}} 2CH_3\cdot + N_2$$

ii) the cleavage of a two electron bond producing a pair of radical sites as in the dissociation of a peroxide,

$$(CH_3)_3C\text{-}OO\text{-}C(CH_3)_3 \longrightarrow 2(CH_3)_3CO\cdot$$

iii) the photolysis of a compound producing two radical sites from cleavage of the weakest bond.

$$CF_3I \xrightarrow{h\nu} CF_3\cdot + I\cdot$$

Propagation reactions fall broadly into four main types:

i) the atom transfer reaction involving mainly hydrogen or halogen abstraction,

$$R\cdot + R'H \longrightarrow RH + R'\cdot$$

$$R\cdot + R'Br \longrightarrow RBr + R'\cdot$$

ii) the addition reaction in which a radical adds to an unsaturated centre,

$$R\cdot + R'CH{=}CH_2 \longrightarrow R'\dot{C}HCH_2R$$

iii) the fragmentation reaction in which a pair of electrons, β to the odd electron, split up to give a radical fragment and an unsaturated molecule: this is the reverse of the addition reaction,

$$R'\dot{C}CH_2R \longrightarrow R\cdot + R'CH{=}CH_2$$

iv) the rearrangement reaction in which a more stable radical is formed.

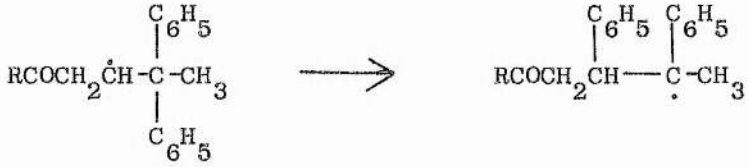

Termination reactions proceed by either combination, in which two radical species combine, or disproportionation in which an atom from one radical is transferred to another radical giving two molecular

products, one with a saturated and the other with an unsaturated terminal group.

$$R\cdot + R'\cdot \xrightarrow{\text{combination}} RR'$$

$$2(CH_3)_2\dot{C}H \xrightarrow{\text{combination}} (CH_3)_2CHCH(CH_3)_2$$

$$2(CH_3)_2\dot{C}H \xrightarrow{\text{disproportionation}} CH_3CH_2CH_3 + CH_3CH{=}CH_2$$

Although the free radical reactions of carbon have received most attention by research workers, the other elements of group IV and the elements of groups V and VI undergo many reactions by free radical mechanisms. Radical reactions of group II are limited[64]: there is some evidence available for the existence of the monohydride and monohalide radicals, and additionally there is kinetic evidence for the formation of the monoalkyl radicals of group IIb elements (Zn, Cd, Hg). Group III elements display a greater variety of free radical reactions mainly due to the stepwise decomposition of the trihydrides and trialkyls. With the lower members of the group (B, Al) there is a tendency for the trialkyl compounds to form π-bonded groups; the higher members (Ga, In, Tl) show a tendency to polymerise.

$$MR_3 \longrightarrow R_2M{=}CHR'$$

$$nMCH_3: \longrightarrow (MCH_3)_n$$

The diversity of free radical reactions exhibited by carbon is not repeated by other members of group IV. Nevertheless the trialkyl hydrides do add to olefinic and acetylenic multiple bonds, and the silanes and germanes readily polymerise. By way of contrast with carbon, silicon preferentially abstracts halogen rather than hydrogen due to the greater strength of the silicon-halogen bonds. Disproportionations are unfavourable as carbon is the only element in the group which readily forms double bonds. Although carbon radicals have a strong affinity for iodine atoms and exhibit no tendency to abstract alkyl groups in transfer reactions, trialkyl tin has been observed to abstract a trifluoromethyl group in preference to an iodine atom in trifluoroiodomethane[65]. This reaction is referred

to as bimolecular homolytic substitution.

In group V the most reactive radicals are those derived from phosphorus. The relatively low reactivity of nitrogen radicals is to some extent due to the high stability of N_2. Very few addition reactions of amino radicals to olefinic double bonds have been reported[66]; the radicals readily dimerise, disproportionate, decompose and abstract hydrogen. The main addition reactions involving an unpaired electron centred on nitrogen are those of the nitro radical ($\cdot NO_2$) and amino radicals ($R_2N\cdot$) which add readily to polyhaloethylenes, terminal and internal olefins, cyclic olefins and conjugated dienes[67]. On the other hand, phosphine, dichlorophosphine and dialkylphosphine readily add to internal and cyclic olefins. In the addition of phosphine to terminal olefins all of the P-H bonds can participate giving mono, di and tri substituted phosphines. Transfer of a hydrogen atom from phosphine occurs readily and this facilitates the formation of one to one adducts. Alkyl and aryl dihalophosphines readily copolymerise with olefins and dienes. The free radicals from the higher members of group V (As, Sb, Bi) have not been observed to participate in addition reactions, but they show a tendency to decompose to the elements.

The free radical reactions of the first two members of group VI (O, S) are profuse. The diversity of the alkoxyl radical encompasses:[68]

i) association with other radicals;

$$RO\cdot + R'\cdot \longrightarrow ROR'$$

ii) addition to unsaturated centres;

$$RO\cdot + \diagdown\!\!\!\!C{=}C\!\!\!\!\diagup \longrightarrow RO\overset{|}{C}\text{-}\overset{|}{C}\cdot$$

iii) abstraction of hydrogen;

$$RO\cdot + R'H \longrightarrow ROH + R'\cdot$$

iv) disproportionation;

$$2RR'CHO\cdot \longrightarrow RR'CHOH + RR'CO$$

v) rearrangement;

$$RR'R''CO\cdot \longrightarrow RR'\dot{C}OR''$$

vi) decomposition by hydrogen atom elimination;

$$RCH_2O\cdot \longrightarrow RCHO + H\cdot$$

vii) decomposition by carbon radical elimination;

$$RCH_2O\cdot \longrightarrow R\cdot + CH_2O$$

$$RR'CHO\cdot \longrightarrow R\cdot + R'CHO$$

Sulphur analogues contain the relatively weak S-H bond, whose fission produces the analogues of alkoxy radicals which undergo similar reactions. The main difference is the high stability of the S-S link which readily facilitates dimerisation. Most types of thiol compounds readily enter into addition reactions with olefins and acetylenes. Sulphur chloride pentafluoride also adds across unsaturated centres. There is evidence for the formation of mono alkyl radicals of selenium and tellurium[69] but the objectionable properties of the alkyl selenides and tellurenides have been responsible for the small amount of work which has been done.

The utility of free radical addition reactions[9] in organic chemistry is apparent from the extensive range of synthetic routes.

Radical addition to alkynes give vinyl radicals.

$$R\cdot + CH\equiv CR' \longrightarrow RHC=\dot{C}R'$$

Further addition of the vinyl radicals gives conjugated dienes.

$$RHC=\dot{C}R' + CH\equiv CR' \longrightarrow RHC=CR'CH=\dot{C}R'$$

Radical addition to benzene gives a stabilised radical intermediate with the unpaired electron delocalised around the six membered ring; further reaction leads to aromatic substitution products[72].

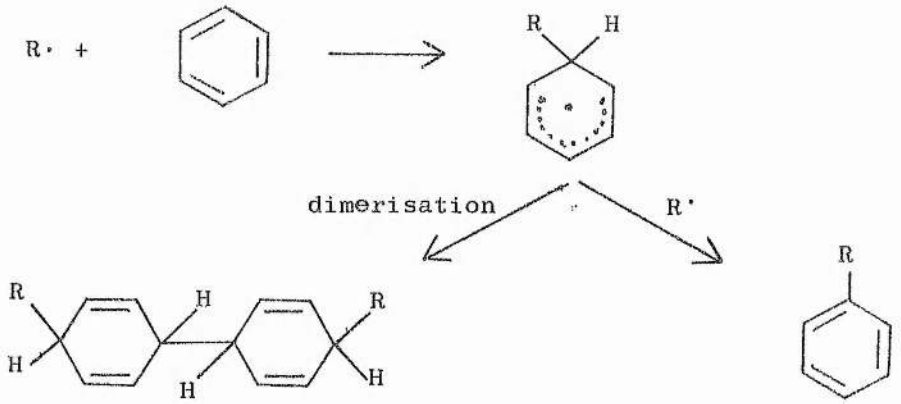

Radical addition to a cyano group gives an intermediate hetero-atom radical with the lone electron sited at a nitrogen atom.

$$R\cdot + R'\text{-}C\equiv N \longrightarrow RR'C=N\cdot$$

Radical addition to a mono olefin followed by a transfer reaction leads to saturation of the olefinic double bond.

$$R\cdot + >C=C< \longrightarrow R\overset{|}{C}\text{-}\overset{|}{\dot{C}}\text{-} \xrightarrow{R'X} R\overset{|}{C}\text{-}\overset{|}{C}X + R'\cdot$$

The fate of the intermediate radical in addition reactions is sensitive to experimental conditions and the nature of available substrates: abstraction of a hydrogen or halogen atom gives the one to one adduct; further addition to another unsaturated molecule followed by abstraction gives the two to one telomer; a large number of addition steps prior to abstraction gives a polymer. Formation of one to one adducts is facilitated by relatively low concentrations of unsaturated substrate and a high transfer coefficient. The transfer coefficient is the ratio of the rate of abstraction to the rate of addition. These free radical addition reactions allow the conversion of; polyhalomethanes to halogenated hydrocarbons; aldehydes to ketones; primary alcohols to secondary alcohols; secondary alcohols to tertiary alcohols; and the alkylation of esters, ethers and amines on the carbon atom α to the functional group.

In the present study the main reaction of interest is the addition reaction of halomethyl radicals to the fluoroethylenes with the aim of elucidating the factors influencing the nature of the addition process. Initially the observations of Mayo and Walling[10] that orientation of addition resulted in the more stable intermediate radical was sufficient to explain the observed products, but recent observations by Tedder and Walton[11] highlight the oversimplicity of this explanation, and they suggest that emphasis should be focussed on the strength of the bond formed. No adequate theory for explaining the directive effects of free radical addition to olefins exists. Evans and Polanyi[12] gave an illustration of activation energies of reaction by constructing two intersecting potential

energy surfaces, one for the bond assignment of the initial state and the other for that of the final state. In 1946 Waters[13] suggested that free halogen atoms are electrophilic in character, and thus attack the point of highest electron density. In 1948 Evans[14] et al. concluded that the most important factor in determining the activation energies is the heat of reactions, and that variation of the heat of reactions can be expressed in terms of the resonance energies of the reacting radicals and olefins. Furthermore, they stressed the repulsion between the reacting centres influenced by the charge distribution on these centres, and the steric effect of substituent groups. In 1953 Haszeldine[15], on the Walling approach, postulated that radical stability decreases as the number of hydrogen atoms, attached directly to the carbon atom carrying the lone electron, is increased.

With the advent of vapour phase chromatography, coupled glc mass spectroscopy and nuclear magnetic resonance, complex product mixtures from the gas phase reactions of radicals with olefins can be satisfactorily analysed qualitatively and quantitatively. Such reactions in the gas phase minimise polar and solvent effects that may be present in liquid phase reactions[73]. The first kinetic data for addition of a free radical to both ends of unsymmetrical olefins was obtained by Walton who studied the addition of trichloromethyl radicals to the fluoroethylenes[16] and fluoropropenes[17]. The results disprove the existing theory, at least for radical addition to fluoroolefins. Walton found reasonable correlation between experimental activation energies and the atom localisation energies. Stefani[19] et al. discusses the distinction between a π- and a σ-transition state in the activated complex and conclude that the correlation of activation energies for the products will be with atom localisation energies and with the strengths of the newly formed bonds.

Development of a theory to elucidate the factors influencing the

orientation of free radical addition to unsymmetrical olefins may involve steric and polar considerations. Part 1 of this thesis reports on the addition of dibromofluoromethyl radicals to the fluoroethylenes, which in conjunction with the results on the addition of trifluoromethyl[20], n-heptafluoropropyl[21], bromodifluoromethyl[22] and trichloromethyl[23] radicals to the same olefins gives a series where steric influences may be examined.

Part 2 reports the addition of difluoromethyl and difluoroiodomethyl radicals to the series of fluoroethylenes: the radicals were generated during the photolysis of difluoroiodomethane.

Part 3 reports the addition of fluoromethyl radicals to the fluoroethylenes. In the trifluoromethyl, difluoromethyl, fluoromethyl and methyl radical series, steric factors are similar, but polar factors change enabling discussion and prediction on polar effects.

PART 1

The Addition of Dibromofluoromethyl Radicals to Fluoroethylenes

INTRODUCTION

Many physical properties of tribromofluoromethane are documented in the chemical literature. Wouters and Hemptinne[24] calculated the interatomic distances. The infrared, raman, nuclear quadrupole resonance and ^{19}F nuclear magnetic resonance spectra have been recorded. Pisanskii and Tsyashchenko[25] recorded the infrared absorption spectrum of $CFBr_3$. Meister[26] et al. systematically studied raman displacements, quantitative depolarisation factors and infrared absorption frequencies of the halotribromomethanes, assigned the raman and infrared bands and calculated force constants. Stepanov[27] calculated the theoretical vibrational frequencies for tribromofluoromethane and other halomethanes. Delwaulle and Francois[28] also measured the raman spectrum bands of $CFBr_3$ and calculated the depolarisation factors and intensities. Biryukov[29] et al. observed the nuclear quadrupole resonance (NQR) spectrum and observed a linear correlation between the mean frequency of the ^{79}Br and ^{81}Br NQR and the Taft inductive constants (σ^*) for the substituents of the halomethanes; σ^* values for thirteen radicals were determined. Filipovich and Tiers[30] measured the ^{19}F nmr spectrum of $CFBr_3$ and other halomethanes over a range of concentration, and extrapolated their results to infinite dilution relative to the solvent and internal reference which was trichlorofluoromethane (CCl_3F). Venkateswarlu[31] et al. have tabulated the force constant data for various stereoisomers of halomethanes and halomethyl radicals and discussed the methods of central force field, orbital valence force field, Urey-Bradley force field and the Wilson F-G matrix. Bernstein[32] has used an interaction scheme to correlate properties of halomethanes such as heats of formation, diamagnetic susceptibility, molar refraction and volume, heat capacity, zero point energy, entropy and free energy. Miller and Smyth[33] have recorded the microwave absorption spectra of halomethanes in the liquid phase

and have tabulated many physical constants such as induced electronic and atomic polarisations, dipole moments, molar refraction and volume, boiling points, viscosity and critical wavelengths: the molecular shapes and rotational degrees of freedom in the solid state[34] have also been recorded. Gelles and Pitzer[35] have tabulated the thermodynamic functions (Cp, $H^{o}-H^{o}_{o}$, $-(F^{o}-H^{o}_{o})/T$ and S^{o}) of thirtynine halomethanes between 100 and 1500°K. Maslov and Maslov[36] have calculated, in the gas phase at 25°C, the heats of formation of many halomethanes including tribromofluoromethane (44 kcal mol^{-1}) and also of vinyl fluoride (28 kcal mol^{-1}), 1,1-difluoroethylene (69 kcal mol^{-1}) and trifluoroethylene (110.4 kcal mol^{-1}).

Very few reactions of tribromofluoromethane are documented in the literature. Hellman[37] et al, pyrolised tribromofluoromethane and obtained hexafluorobenzene as the main product. Edgell and Parts[38] reduced tribromofluoromethane with lithium aluminium hydride and obtained methane and fluoromethane. Simons and Yarwood[63] observed CF as a transient intermediate in the flash photolysis of tribromofluoromethane.

The first kinetic study of radical addition to a series of unsymmetrical olefins in the gas phase yielding products from the addition to both ends of the double bond were conducted by Walton[39] who studied the addition of trichloromethyl radicals to the fluoroethylenes and fluoropropenes. Since then the competitive addition of several free radicals to ethylene and the fluoroethylenes have been studied by Tedder and coworkers. Walton[22] has studied the addition of bromodifluoromethyl, Winton[21] the addition of n-heptafluoropropyl and Greig[20] the addition of trifluoromethyl radicals to the fluoroethylenes in competition with addition to ethylene. Sidebottom[40] studied the addition of the strongly electrophilic pentafluorosulphur radical to the fluoroethylenes but failed to gain quantitative results for addition to the most substituted ends of the olefins owing to the radicals overwhelming preference for

addition to the least substituted ends. Ashton[41] et al. have determined the orientation ratios for addition of $CF_3\cdot$, $C_2F_5\cdot$, $n\text{-}C_3F_7\cdot$, $n\text{-}C_4F_9\cdot$, $n\text{-}C_7F_{15}\cdot$, $n\text{-}C_8F_{17}\cdot$ and $(CF_3)_2CF\cdot$ radicals to vinylfluoride, 1,1-difluoroethylene and trifluoroethylene in the gas phase at 150°C.

Some haloalkyl addition reactions conducted in the liquid phase have been reported. The majority of these are qualitative rather than quantitative in nature. Haszeldine[15] has extensively studied the addition of trifluoroiodomethane to olefins. Coscia[70] measured the normal to reverse adduct ratio for the addition of bromodifluoromethyl radicals to trifluoroethylene, and Dougherty[71] measured the corresponding ratio for the addition of trifluoromethyl radicals to vinyl fluoride.

The competitive addition of dibromofluoromethyl radicals is now recorded and the results are discussed in relation to the accumulated data on free radical addition to ethylenes and the fluoroethylenes.

Fig. 1.1 Diagram of Experimental Apparatus

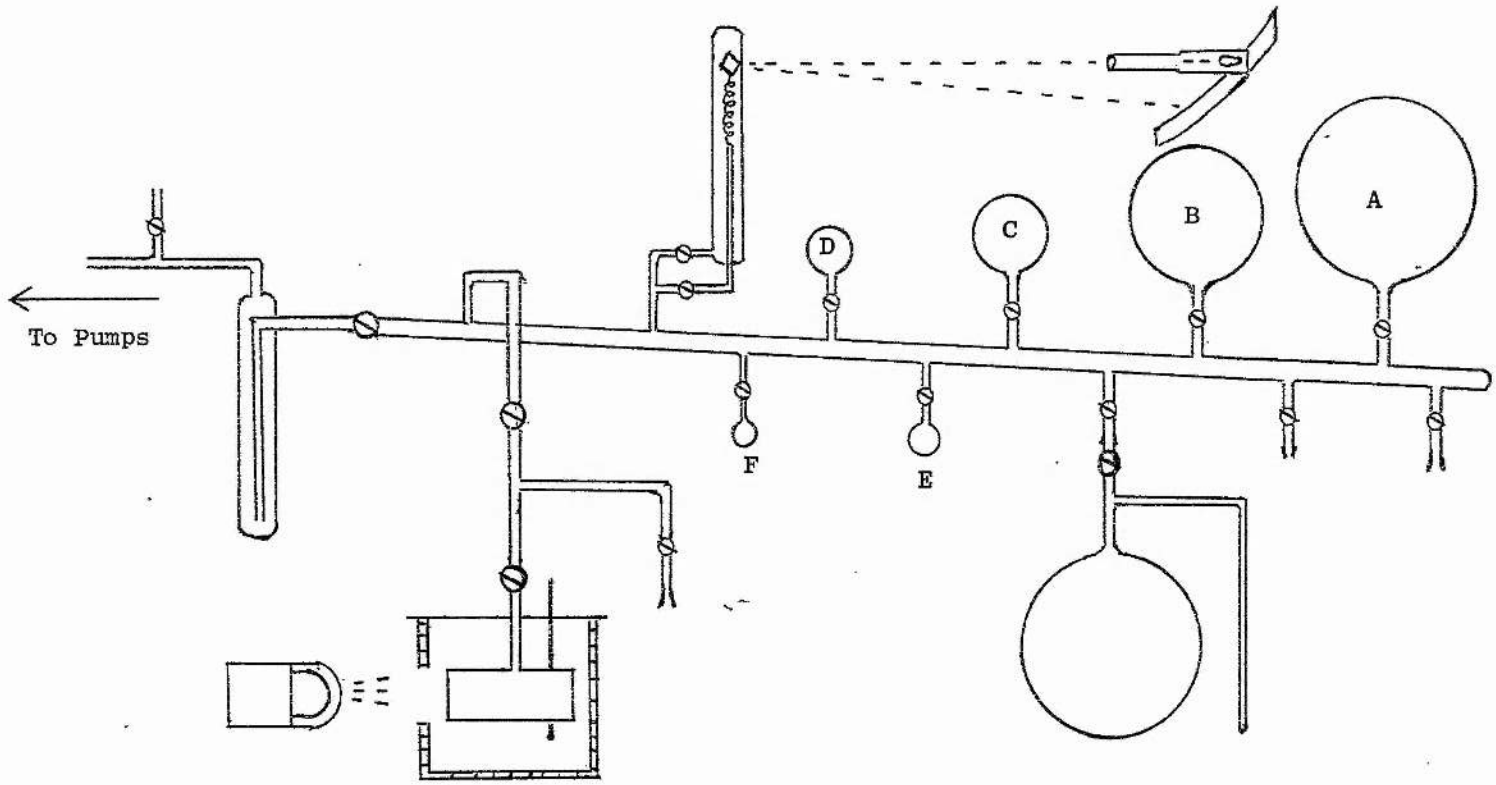

EXPERIMENTAL

REACTANTS

(1) Tribromofluoromethane was prepared by J.C. Walton and D.S. Ashton using a modified Swartz synthesis[42]. A dry mixture of carbon tetrabromide and antimony trifluoride containing a trace of bromine gave a small yield of tribromofluoromethane upon heating to 130°C. The product, upon formation, was distilled directly into a receiver flask. Final purification was achieved by preparative glc which gave material of at least 99.5% purity. The only detectable impurity was dibromodifluoromethane.

(2) The fluoroethylenes were obtained commercially and purified by trap to trap distillation.

(3) The dibromides CH_2BrCH_2Br, $CHFBrCH_2Br$, CF_2BrCH_2Br, $CHFBrCF_2Br$ and CF_2BrCF_2Br were prepared by direct interaction of bromine (20 torr in 2 l) with the appropriate olefin (22 torr in 2 l) in the gas phase in the presence of daylight. They were used for identification purposes only.

APPARATUS

The apparatus consisted of a conventional Pyrex glass vacuum line (fig. 1-1) having five storage bulbs A, B, C, D and E of capacity 2,270 ml, 1,130 ml, 317 ml, 122 ml and 70 ml respectively. The vacuum was maintained by a silicone oil diffusion pump backed by a "Speedivac" rotary oil pump. Reactant pressures were measured using a glass spiral gauge incorporating a "Scalamp" optical system, with one cm deflection equivalent to 4.46 torr. The reaction vessel and side arm were fitted with greaseless taps: all of the other taps were of ground glass and lubricated with Apiezon "N" grease. A vacuum of 10^{-3} to 10^{-5} torr was considered adequate and checked by an "Edwards H.F. coil". The reactor was a cylindrical Quartz glass vessel of 140 ml capacity, and was connected to the

vacuum line by a short (11 cm) medium bore tube to minimise reaction occurring outside the main reaction vessel.

The furnace consisted of an insulated aluminium cylinder with an asbestos lid, electrically heated hot plate base, a circular opening of 2" diameter to permit illumination and an adjustable shutter. The temperature, measured with a mercury in glass thermometer, was uniform throughout the furnace and could be maintained to $\pm 2^{\circ}C$ using a 0-250 volt "variac" transformer. The light source for a particular series of reactions was either a "Hanovia" UVS 220 medium pressure mercury arc or a "Hanovia" UVS 500 medium pressure mercury arc. Unfiltered light was used in the preparative and exploratory experiments, but a Barr and Stroud interference filter of band width 10 nm centred on 366 nm was used in the kinetic experiments. Other Barr and Stroud interference filters having transmission bands centred at 254, 265, 313 and 420 nm were used in the experiments with light of different wavelengths.

Experimental Procedure

Tribromofluoromethane (bp $106^{\circ}C$) was stored in a small tube attached to the main line and surrounded by liquid nitrogen. Ethylene and the fluoroethylenes were stored in two litre glass storage bulbs each fitted with a glass side arm to enable freezing by surrounding with liquid nitrogen, and measurement of requisite pressures on the vacuum line. Each compound was individually "degassed" by allowing the frozen compound to warm up to room temperature and expand into the vacuum line. It was then refrozen and the main manifold was opened to the pumps. This procedure was repeated several times for each compound.

The required quantity of tribromofluoromethane was measured by allowing the frozen "degassed" tribromofluoromethane to expand into the evacuated line and bulb C. When the required pressure was obtained the bulb was isolated and the tribromofluoromethane remaining in the line was distilled into the storage tube by cooling

in liquid nitrogen. Similarly the fluoroethylene was measured into bulb D and the ethylene into bulb E. The reaction vessel and vacuum line were then thoroughly evacuated. The reactants were then transferred to the reaction vessel by surrounding the evacuated reaction vessel with liquid nitrogen and opening the bulb taps. Twenty minutes were allowed for the reactants to distil into the reaction vessel. The pre-heated furnace was then raised around the reaction vessel and the temperature allowed to stabilise. After striking the mercury arc lamp it was allowed to reach its normal working range before removing the shutter to commence the photolysis reaction. At the end of the reaction the product mixture was distilled into a small tube attached to the main line.

Analysis

A Griffin and George D6 gas chromatograph was used for all quantitative analytical work. The instrument employs a Martin and James gas density balance for which the relationship $q = KAM/(M-m)$ holds for all compounds (q = weight of compound with molecular weight M, A = peak area on chromatogram, K = constant and m = molecular weight of carrier gas which was nitrogen). The concentration of each compound is given by $q/M = KA/(M-m)$ and thus from the identified peaks of a chromatogram, relative concentrations are readily obtained. A stainless steel column measuring 6' x 3/16" and packed with 20% silicone oil on 60/100 mesh Embacel was used. The column temperature was maintained at approximately 105^{o}C with the exception of the trifluoroethylene reaction products for which approximately 65^{o}C was used to improve the separation of the two adducts. The nitrogen carrier gas flow rate was maintained at 75 ml min^{-1}. The chart speed was set at 48" hr^{-1}. Injections onto the column were made using a 4 µl stainless steel capillary needle. Single injections per chromatogram were used except for analysis of the vinylidene

fluoride products for which double injections were used to improve peak height. The chromatogram peak areas were measured using a Du Pont 310 Curve Resolver.

Identification of Products

Reaction products were identified by coupled gas chromatography-mass spectroscopy. For each olefin a preparative run was carried out in which unfiltered light was used, and the reaction was allowed to proceed until most of the reactants were consumed. A sample (4 μl) of this reaction mixture was injected into a Pye 104 chromatograph fitted with a 6 ft glass spiral column packed with 10% silicone oil on 60-100 mesh Embacel and maintained at a suitable temperature in the range 60-120°C. Helium carrier gas was used at a pressure of 10 lb in^{-2}. A fraction of the eluted material was led, via a single stage Bieman separator, directly into the source of an AEI MS 902 mass spectrometer. A mass spectrum of each component of the mixture was thus obtained upon entering the spectrometer source. Typical mass spectrometer settings were:- magnet range 5; decrease 9; ionisation current 70 ev; acceleration potential 8 Kv; band width 500 cs^{-1}; and chart speed .15 $in.s^{-1}$. The identities of the dibromides were confirmed by comparing the retention times with those of the authentic materials run under exactly the same chromatographic conditions. For each of the olefins, ethylene, trifluoroethylene and vinyl fluoride, a series of preparative runs was carried out, and the accumulated products were then separated by preparative glc using a 10% silicone oil column in a Pye 105 gas chromatograph. The main reaction products yielded sufficient material for ^{1}H and ^{19}F nmr spectra to be recorded. A Varian HA-100 instrument, operating at 100 MHz, was employed for recording the ^{1}H and ^{19}F nmr spectra at room temperature on CCl_4 solutions of the products containing tetramethylsilane and CCl_3F as internal reference standards.

The ultraviolet spectrum[43], the mass spectrum and the ^{19}F nmr spectrum of bromotrifluoromethane were recorded.

Ultraviolet spectra of samples in the gas phase were obtained at various pressures (5, 10 and 22 torr) on Unicam SP800 UV spectrometer using a quartz cell (81.4 ml). The spectra show two peaks at 206 nm and 231 nm. The corresponding molar extinction coefficients are:

$$\varepsilon_{206} = 1330 \text{ lmol}^{-1}\text{cm}^{-1}, \qquad \varepsilon_{231} = 1020 \text{ lmol}^{-1}\text{cm}^{-1}.$$

Mass Spectrum of $CFBr_3$

m/e	Relative Intensity	Assignment
79,81	1,1	Br^+
91,93	1,1	CBr^+
110,112	11,11	$CFBr^+$
158,160,162	.5,1,.5	Br_2^+
170,172,174	1,2,1	CBr_2^+
189,191,193	50,100,50	$CFBr_2^+$
249,251,253,255	.2,.5,.5,.2	CBr_3^+
268,270,272,274	.1,.3,.3,.1	$CFBr_3^+$

The ^{19}F nmr spectrum of $CFBr_3$ contained a singlet placed 7.21 ppm downfield from CCl_3F ($\phi = -7.21$). This is in good agreement with Filopovich and Tiers'[30] value of $\phi = -7.397$.

The impurty in the $CFBr_3$ was identified as CF_2Br_2 by glc-ms.

Mass Spectrum of CF_2Br_2

m/e	Relative Intensity	Assignment
79,81	29,29	Br^+
110,112	26,26	$CFBr^+$
129,131	100,100	CF_2Br^+
189,191,193	6,12,6	$CFBr_2^+$
208,210,212	4,8,4	$CF_2Br_2^+$

A ethylene

Preparative runs were carried out with $CFBr_3$ (2.22×10^{-3} mol l^{-1}) and $CH_2{=}CH_2$ (1.11×10^{-3} mol l^{-1}). Eight product peaks were observed by glc-ms.

Peak A-1

m/e	Relative Intensity	Assignment
79,81	21,21	Br^+
80,82	9,9	HBr^+
91,93	7,7	CBr^+
92,94	3,3	$CHBr^+$
103,105	3,3	C_2Br^+
104,106	7,7	C_2HBr^+
105,107	4,4	$C_2H_2Br^+$
106,108	93,100	$C_2H_3Br^+$
107,109	4,4	$C_2H_4Br^+$

Identified as bromoethylene (CH_2=CHBr)

Peak A-2

29	40	$C_2H_5^+$
79,81	6,6	Br^+
80,82	9,9	HBr^+
93,95	5,5	CH_2Br^+
108,110	100,100	$C_2H_5Br^+$

Identified as ethyl bromide (CH_3CH_2Br) and confirmed by comparison of retention time with pure material.

Peak A-3

57	>100	$C_3H_2F^+$
59	>>100	$C_3H_4F^+$
79,81	25,25	Br^+
80,82	16,16	HBr^+
93,95	15,15	CH_2Br^+
110,112	7,7	$CFBr^+$
111,113	24,24	$CHFBr^+$
137,139	22,22	$C_3H_3FBr^+$
138,140	100,100	$C_3H_4FBr^+$

The empirical formula of this peak is C_3H_4FBr (cf. Peak D-1)

Peak A-4

m/e	Relative Intensity	Assignment
79,81	14,14	Br^+
80,82	9,9	HBr^+
91,93	16,16	CBr^+
103,105	2,2	C_2Br^+
110,112	7,7	$CFBr^+$
122,124	7,7	C_2FBr^+
141,143	44,44	$C_2F_2Br^+$
201,203,205	1,2,1	$C_2FBr_2^+$
220,222,224	50,100,50	$C_2F_2Br_2^+$

Identified as 1,2-dibromo-1,2-difluoroethylene (CFBr=CFBr)

Peak A-5

79,81	37,37	Br^+
80,82	11,11	HBr^+
91,93	28,28	CBr^+
92,94	24,24	$CHBr^+$
110,112	8,8	$CFBr^+$
111,113	>>100,100	$CHFBr^+$
158,160,162	5,10,5	Br_2^+
170,172,174	1.5,3,1.5	CBr_2^+
171,173,175	2.5,5,2.5	$CHBr_2^+$
189,191,193	2,4,2	$CFBr_2^+$
190,192,194	50,100,50	$CHFBr_2^+$

Identified as dibromofluoromethane ($CHFBr_2$) and confirmed by ^1H and ^{19}F spectra. The ^1H nmr spectrum contains a doublet τ 2.37 (J_{HF} = 50.5), and the ^{19}F nmr spectrum also contains a doublet ϕ 48.0. (J values are in Hz; τ and ϕ values are in ppm).

Peak A-6

59	>>100	$C_3H_4F^+$
60	100	$C_3H_5F^+$
117,119	13,13	$C_3H_2Br^+$
119,121	38,38	$C_3H_4Br^+$
120,122	2,2	$C_3H_5Br^+$
123,125	13,13	C_2HFBr^+
124,126	38,38	$C_2H_2FBr^+$
139,141	>>100	$C_3H_5FBr^+$
184,186,188	2,4,2	$C_2H_2Br_2^+$
203,205,207	2,4,2	$C_2H_2FBr_2^+$

Identified as 1,1-dibromo-1-fluoropropane ($CFBr_2CH_2CH_3$). A few additional fragments attributable to peak 7, dibromoethane, were also present owing to the relatively poor resolution of the two peaks.

Peak A-7

m/e	Relative Intensity	Assignment
79,81	59,59	Br^+
80,82	100,100	$HBr^{+\cdot}$
93,95	30,30	CH_2Br^+
107,109	>>100,100	$C_2H_4Br^+$
186,188,190	15,30,15	$C_2H_4Br_2^+$

Identified as 1,2-dibromoethane (CH_2BrCH_2Br) and confirmed by comparison of retention time with authenic material.

Peak A-8

57	16	$C_3H_2F^+$
59	12	$C_3H_4F^+$
79,81	7,7	Br^+
80,82	11,11	HBr^+
93,95	20,20	CH_2Br^+
137,139	38,38	$C_3H_3FBr^+$
138,140	4,4	$C_3H_4FBr^+$
171,173,175	6,12,6	$CHBr_2^+$
189,191,193	3,6,3	$CFBr_2^+$
217,219,221	50,100,50	$C_3H_4FBr_2^+$

The ^1H nmr spectrum contains a complex multiplet τ 6.6 ppm and the ^{19}F spectrum contained a triplet at ϕ 48.0 ppm (J_{FH}=14Hz). Peak identified as the ethylene adduct, 1,1,3-tribromo-1-fluoropropane ($CFBr_2CH_2CH_2Br$).

B vinyl fluoride

A preparative run with $CFBr_3$ (2.22×10^{-3} mol l^{-1}) and CH_2=CHF (1.11×10^{-3} mol l^{-1}) at 200°C gave four products. These were identified by a combination of nmr and glc-ms.

Peak B-1

m/e	Relative Intensity	Assignment
45	58	$C_2H_2F^+$
56	59	C_3HF^+
57	100	$C_3H_2F^+$
79,81	10,10	Br^+
91,93	4,4	CBr^+
105,107	5,5	$C_2H_2Br^+$
124,126	20,20	$C_2H_2FBr^+$

This peak probably has the empirical formula $C_3H_3F_2Br$. Several unsuccessful attempts were made to separate sufficient of the material to run nmr spectra and confirm the structure as the substituted cyclopropane (cf. Peak D-1).

Peak B-2 was identified as $CHFBr_2$ (same as Peak A-5).

Peak B-3

75	12	$C_3HF_2^+$
76	3	$C_3H_2F_2^+$
77	10	$C_3H_3F_2^+$
79,81	10,10	Br^+
80,82	12,12	HBr^+
91,93	2,2	CBr^+
105,107	5,5	$C_2H_2Br^+$
110,112	6,6	$CFBr^+$
111,113	9,9	$CHFBr^+$
124,126	2,2	$C_2H_2FBr^+$
125,127	1,1	$C_2H_3FBr^+$
129,131	6,6	CF_2Br^+
155,157	9,9	$C_3H_2F_2Br^+$
170,172,174	31,62,31	CBr_2^+
189,191,193	6,12,6	$CFBr_2^+$
215,217,219	2,4,2	$C_3H_2FBr_2^+$
234,236,238	50,100,50	$C_3H_2F_2Br_2^+$
235,237,239	2,4,2	$^{13}CC_2H_2F_2Br_2^+$

On the basis of previous work[16,44] it was expected that the normal adduct from addition to the $CH_2^{=}$ end would be eluted first. The significant ions on peak 3 at m/e 111, 113 ($CHFBr^+$), m/e 124, 126 ($C_2H_2FBr^+$) and on peak 4 at m/e 93,95 (CH_2Br^+) and m/e

142,144 ($C_2HF_2Br^+$) facilitate assigning peak 3 to the normal adduct and peak 4 to the reverse adduct. Identified as the normal adduct, 1,1,3-tribromo-1,3-difluoropropane ($CFBr_2CH_2CHFBr$).

Sufficient material from preparative runs was obtained for nmr spectra on peak 3.

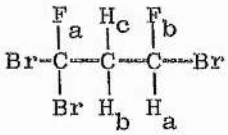

The ^1H spectrum showed a complex multiplet at τ 6.4 (H_b and H_c) and a double double doublet at τ 3.3 (H_a, $J_{H_aF_b}$ = 51, $J_{H_aH_b}$ = 7, $J_{H_aH_c}$ = 3). The ^{19}F spectrum showed two signals, ϕ 135.3 (F_b, 10 lines) and ϕ49.1 (F_a, 7 lines). (J values are in Hz; τ and ϕ values are in ppm).

Peak B-4

m/e	Relative Intensity	Assignment
75	24	$C_3HF_2^+$
77	27	$C_3H_3F_2^+$
79,81	23,23	Br^+
80,82	14,14	HBr^+
91,93	4,4	CBr^+
92,94	3,3	$CHBr^+$
93,95	40,40	CH_2Br^+
105,107	14,14	$C_2H_2Br^+$
110,112	9,9	$CFBr^+$
111,113	40,40	$CHFBr^+$
125,127	9,9	$C_2H_3FBr^+$
129,131	18,18	CF_2Br^+
142,144	10,10	$C_2HF_2Br^+$
155,157	19,19	$C_3H_2F_2Br^+$
170,172,174	1,2,1	CBr_2^+
171,173,175	33,66,33	$CHBr_2^+$
189,191,193	13,26,13	$CFBr_2^+$
235,237,239	50,100,50	$C_3H_3F_2Br_2^+$

Identified as the reverse adduct, 1,1,3-tribromo-1,2-difluoropropane ($CFBr_2CHFCH_2Br$).

C 1,1-difluoroethylene

Two preparative runs, one with $CFBr_3$ (2.00×10^{-3} mol l^{-1}) and $CH_2=CF_2$ (1.50×10^{-3} mol l^{-1}) at 211°C for 1.8 h, and the other with $CFBr_3$ (1.00×10^{-3} mol l^{-1}) and $CH_2=CF_2$ (0.25×10^{-3} mol l^{-1}) at 63°C for 9.8 h gave nine product peaks which were identified by glc-ms.

Peak C-1

m/e	Relative Intensity	Assignment
75	100	$C_3HF_2^+$
95	>>100	$C_3H_2F_3^+$
124,126	62,62	$C_2H_2FBr^+$
173,175	6,6	$C_3HF_3Br^+$
174,176	4,4	$C_3H_2F_3Br^+$

Identified as 1-bromo-1,2,2-trifluorocyclopropane (cf. Peak D-1).

Peak C-2 Identified as 1,2-dibromo-1,2-difluoroethylene (CFBr=CFBr) (same as Peak A-4).

Peak C-3 Identified as $CHFBr_2$ (same as Peak A-5).

Peak C-4

79,81	33,33	Br^+
80,82	19,19	HBr^+
93,95	26,26	CH_2Br^+
104,106	8,8	C_2HBr^+
110,112	6,6	$CFBr^+$
123,125	20,20	C_2HFBr^+
124,126	7,7	$C_2H_2FBr^+$
129,131	59,59	CF_2Br^+
143,145	100,100	$C_2H_2F_2Br^+$
202,204,206	6,12,6	$C_2HFBr_2^+$
222,224,226	.5,1.5	$C_2H_2F_2Br_2^+$

Identified as 1,2-dibromo-1,1-difluoroethane (CH_2BrCF_2Br) and confirmed by comparison of its retention time with authentic material.

Peak C-5

m/e	Relative Intensity	Assignment
79,81	17,17	Br^+
80,82	18,18	HBr^+
129,131	8,8	CF_2Br^+
142,144	36,36	$C_2HF_2Br^+$
171,173,175	8,16,8	$CHBr_2^+$
221,223,225	50,100,50	$C_2HF_2Br_2^+$
300,302,304,306	2,7,7,2	$C_2HF_2Br_3^+$

Identified as 1,1,2-tribromo-2,2-difluoroethane ($CHBr_2CF_2Br$)

Peak C-6

75	10	$C_3HF_2^+$
79,81	5,5	Br^+
80,82	5,5	HBr^+
91,93	1,1	CBr^+
93	2	$C_3F_3^+$
94	3	$C_3HF_3^+$
95	6	$C_3H_2F_3^+$
104,106	1,1	C_2HBr^+
105,107	3,3	$C_2H_2Br^+$
110,112	2,2	$CFBr^+$
124,126	7,7	$C_2H_2FBr^+$
129,131	37,37	CF_2Br^+
173,175	4,4	$C_3HF_3Br^+$
189,191,193	26,52,26	$CFBr_2^+$
253,255,257	50,100,50	$C_3H_2F_3Br_2^+$
332,334,336,338	.1,.3,.3,.1	$C_3H_2F_3Br_3^+$

Identified as the normal adduct, 1,1,3-tribromo-1,3,3-trifluoropropane ($CFBr_2CH_2CF_2Br$)

Peak C-7

75	7	$C_3HF_2^+$
79,81	5,5	Br^+
80,82	5,5	HBr^+
91,93	2,2	CBr^+
93,95	14,14	CH_2Br^+
94	2	$C_3HF_3^+$
105,107	2,2	$C_2H_2Br^+$
110,112	3,3	$CFBr^+$
123,125	3,3	C_2HFBr^+

Peak C-7(cont)

m/e	Relative Intensity	Assignment
124,126	3,3	$C_2H_2FBr^+$
129,131	26,26	CF_2Br^+
142,144	2,2	$C_2HF_2Br^+$
143,145	11,11	$C_2H_2F_2Br^+$
160,162	3,3	$C_2F_3Br^+$
189,191,193	12,24,12	$CFBr_2^+$
233,235,237	2,4,2	$C_3HF_2Br_2^+$
253,255,257	50,100,50	$C_3H_2F_3Br_2^+$
332,334,336,338	.7,2,2,.7	$C_3H_2F_3Br_3^+$

Identified as the reverse adduct, 1,1,3-tribromo-1,2,2-trifluoropropane ($CFBr_2CF_2CH_2Br$). The peak at m/e 129,131 (CF_2Br) is an impurity from the normal adduct.

Peak C-8

62	9	$C_2F_2^+$
79,81	16,16	Br^+
91,93	16,16	CBr^+
103,105	2,2	C_2Br^+
110,112	7,7	$CFBr^+$
122,124	10,10	C_2FBr^+
141,143	29,29	$C_2F_2Br^+$
158,160,162	1,2,1	Br_2^+
170,172,174	3,6,3	CBr_2^+
189,191,193	16,32,16	$CFBr_2^+$
201,203,205	1,2,1	$C_2FBr_2^+$
220,222,224	39,78,39	$C_2F_2Br_2^+$
280,282,284,286	1,3,3,1	$C_2FBr_3^+$
299,301,303,305	33,100,100,33	$C_2F_2Br_3^+$
378,380,382,384,386	2,7,10,7,2	$C_2F_2Br_4^+$

Identified as the dimer, 1,1,2,2-tetrabromo-1,2-difluoroethane ($CFBr_2CFBr_2$). An analytical quantity of the dimer was obtained only in the low temperature run with a four to one excess of $CFBr_3$.

Peak C-9

m/e	Relative Intensity	Assignment
64	40	$C_2H_2F_2^+$
79,81	40,40	Br^+
80,82	96,96	HBr^+
95	49	$C_3H_2F_3^+$
113	77	$C_3HF_4^+$
128	28	$C_4H_4F_4^+$
129,131	85,85	CF_2Br^+
155	15	$C_5F_5^+$
157	9	$C_5H_2F_5^+$
159	6	$C_5H_4F_5^+$
173,175	40,40	$C_3HF_3Br^+$
189,191,193	21,42,21	$CFBr_2^+$
236,238	100,100	$C_5H_2F_5Br^+$
317,319,321	30,60,30	$C_5H_4F_5Br_2^+$

The empirical formula of peak 9 corresponds to the two to one telomer, $C_5H_4F_5Br_3$. The ion at m/e 129,131 identifies the terminal group as $-CF_2Br$. In the first addition step the dibromofluoromethyl radical adds preferentially to the $=CH_2$ end by a factor of approximately thirty to one. Therefore peak nine is probably $CFBr_2CH_2CF_2CH_2CF_2Br$.

D trifluoroethylene

A preparative run with $CFBr_3$ (2.22×10^{-3} mol l^{-1}) and $CHF=CF_2$ (1.11×10^{-3} mol l^{-1}) photolysed for 12 h at 150°C gave a mixture containing seven product peaks. These were identified by glc-ms. The adducts were confirmed by ^1H and ^{19}F nmr spectra.

Peak D-1

75	2	$C_3HF_2^+$
82	6	$C_2HF_3^+$
93	4	$C_2F_3^+$
94	3	$C_3HF_3^+$
113	100	$C_3HF_4^+$
142,144	7,7	$C_2HF_2Br^+$
160,162	.5,.5	$C_2F_3Br^+$
173,175	1,1	$C_3HF_3Br^+$

The empirical formula of C_3HF_4Br fits the substituted propenes (3) and 1-bromo-1,2,2,3-tetrafluorocyclopropane. Formation of these products is feasible by a bromofluoro carbene intermediate pathway; the propenes by insertion into a C-F or C-H bond and the cyclopropane by addition across the double bond. Absence of a strong molecular ion peak detracts from a propene assignment. Additionally, the decomposition ions are in good agreement with the observations of Deen and Roboz[45] that generally the decomposition ions of halocyclopropanes include, $CBrX^+$, $C_2HQ_2X^{+\cdot}$ and $C_3HQ_2X_2^{+\cdot}$ (X = a halogen atom; Q = either a halogen or a hydrogen atom). The evidence from the variation of wavelength experiments showing negligible C_3HF_4Br formation at 420 nm is indicative of product formation by the highly reactive carbene (:CFBr) intermediate. The evidence favours assigning peak D-1 to the cyclopropane. By an analogous deduction the corresponding peaks in the ethylene, vinyl fluoride and 1,1-difluoroethylene preparative runs may justifiably be assigned to the substituted cyclopropanes.

Peak D-2 Identified as $CHFBr_2$ (same as Peak A-5).

Peak D-3

m/e	Relative Intensity	Assignment
82	44	$C_2HF_3^+$
111,113	44,44	$CHFBr^+$
129,131	6,6	CF_2Br^+
142,144	9,9	$C_2HF_2Br^+$
161,163	100,100	$C_2HF_3Br^+$
240,242,244	1.5,3,1.5	$C_2HF_3Br_2^+$

Identified as the dibromide, 1,2-dibromo-1,1,2-trifluoroethane ($CHFBrCF_2Br$), and confirmed by retention time comparison with authentic material, and by ^1H and ^{19}F nmr spectra.

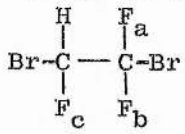

The ^{1}H nmr spectrum showed a double double doublet τ 3.58 (J_{HF_c}=48, J_{HF_a}=9, J_{HF_b}=4). The ^{19}F nmr spectrum showed three double double doublets ϕ 59.3 (F_b, $J_{F_bF_a}$ = 127, $J_{F_bF_c}$ = 23, J_{F_bH} = 4) ϕ 64.0 (F_a, $J_{F_aF_b}$=127, $J_{F_aF_c}$ = 21, J_{F_aH} = 9) ϕ 149.3 (F_c, $J_{F_cF_b}$ = 23, $J_{F_cF_a}$ = 21, J_{F_cH} = 48)
(J values are in Hz; τ and ϕ values are in ppm).

Peak D-4

m/e	Relative Intensity	Assignment
111,113	100,100	$CHFBr^+$
129,131	38,38	CF_2Br^+
173,175	38,38	$C_3HF_3Br^+$
243,245	50,50	$C_4H_2F_6Br^+$

Identified as the two to one telomer, from addition of bromine atoms, $CF_2BrCHFCF_2CHFBr$.

Peak D-5

82	30	$C_2HF_3^+$
113	60	$C_3HF_4^+$
129,131	100,97	CF_2Br^+
142,144	40,40	$C_2HF_2Br^+$
161,163	5,5	$C_2HF_3Br^+$
173,175	13,13	$C_3HF_3Br^+$
189,191,193	43,86,43	$CFBr_2^+$
271,273,275	30,60,30	$C_3HF_4Br_2^+$

Identified as the normal adduct, 1,1,3-tribromo-1,2,3,3-tetrafluoropropane ($CFBr_2CHFCF_2Br$), and confirmed by ^{1}H and ^{19}F nmr spectra.

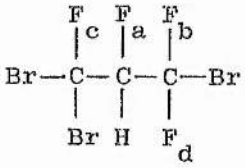

The ^{1}H spectrum showed a symmetrical multiplet at τ 5.0 (J_{HF_a} = 42, J_{HF_b} = 4, J_{HF_a} = 9, J_{HF_d} = 13) and the ^{19}F spectrum showed four symmetrical multiplets at ϕ 171.9 (F_a, $J_{F_aF_c}$ = 30, $J_{F_aF_b}$ = 18, $J_{F_aF_d}$ = 17, J_{F_aH} = 42), ϕ 68.5 (F_c, $J_{F_cF_a}$ = 30, $J_{F_cF_b}$ = 14, $J_{F_cF_d}$ = 13,

J_{F_cH} = 9), ϕ 59.3 (F_d, $J_{F_dF_b}$ = 174, $J_{F_dF_a}$ = 17, $J_{F_cF_d}$ = 13, J_{F_dH} = 13), ϕ 53.4 (F_b, $J_{F_bF_d}$ = 174, $J_{F_bF_a}$ =18, $J_{F_bF_c}$ =14, J_{F_bH} = 4). (J values are in Hz; τ and ϕ values are in ppm).

Peak D-6

m/e	Relative Intensity	Assignment
82	22	$C_2HF_3^+$
111,113	83,83	$CHFBr^+$
113	50	$C_3HF_4^+$
129,131	66,61	CF_2Br^+
142,144	33,33	$C_2HF_2Br^+$
160,162	17,17	$C_2F_3Br^+$
161,163	11,11	$C_2HF_3Br^+$
173,175	11,11	$C_3HF_3Br^+$
189,191,193	50,100,50	$CFBr_2^+$
271,273,275	28,56,28	$C_3HF_4Br_2^+$

Identified as the reverse adduct, 1,1,3-tribromo-1,2,2,3-tetrafluoropropane ($CFBr_2CF_2CHFBr$), and confirmed by ^1H and ^{19}F nmr spectra.

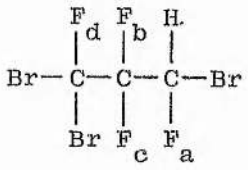

The ^1H spectrum showed a double doublet at τ 3.0 (J_{HF_a} = 48, J_{HF_b} = 17), indicating restricted rotation about the carbon carbon bond at room temperature. The ^{19}F spectrum showed four symmetrical multiplets at ϕ 154.1 (F_a, $J_{F_aF_c}$ = 20, $J_{F_aF_b}$ = 17, $J_{F_aF_d}$ = 20, J_{F_aH} = 48), ϕ 119.9 (F_b, $J_{F_bF_c}$ = 261, $J_{F_bF_a}$ = 17, $J_{F_aF_d}$ = 15, J_{F_bH} = 17), ϕ 104.9 (F_c, $J_{F_cF_b}$ = 261, $J_{F_cF_a}$ = 20, $J_{F_cF_d}$ = 15, J_{F_cH} = 0), ϕ 71.4 (F_d, $J_{F_dF_b}$ = 15, $J_{F_dF_c}$ = 15, $J_{F_dF_a}$ = 20, J_{F_dH} = 0) (J values are in Hz; τ and ϕ values are in ppm).

Peak D-7 Identified as the dimer $CFBr_2CFBr_2$ (see Peak C-8)

E tetrafluoroethylene

Four products were identified from the glc-ms analysis of the preparative run with $CFBr_3$ (1.00×10^{-3} mol l^{-1}) and C_2F_4 (0.17×10^{-3} mol l^{-1}) photolysed for 1 hr at 177°C.

Peak E-1

m/e	Relative Intensity	Assignment
79,81	7,7	Br^+
80,82	8,8	HBr^+
100	40	$C_2F_4^+$
110,112	6,6	$CFBr^+$
129,131	100,100	CF_2Br^+
160,162	17,17	$C_2F_3Br^+$
179,181	>>100,100	$C_2F_4Br^+$
239,241,243	8,15,8	$C_2F_3Br_2^+$
258,260,262	4,8,4	$C_2F_4Br_2^+$

Identified as the dibromide, 1,2-dibromo-1,1,2,2-tetrafluoroethane (CF_2BrCF_2Br), and confirmed by retention time comparison with an authentic sample.

Peak E-2

79,81	16,16	Br^+
80,82	18,18	HBr^+
93	20,20	$C_3F_3^+$
110,112	16,16	$CFBr^+$
112	4	$C_3F_4^+$
122,124	3,3	C_2FBr^+
129,131	>>100,100	CF_2Br^+
141,143	5,5	$C_2F_2Br^+$
153,155	1,1	$C_3F_2Br^+$
160,162	41,41	$C_2F_3Br^+$
170,172,174	2,4,2	CBr_2^+
189,191,193	50,100,50	$CFBr_2^+$
201,203,205	.5,1,.5	$C_2FBr_2^+$
210,212	14,14	$C_3F_5Br^+$
220,222,224	3,6,3	$C_2F_2Br_2^+$
239,241,243	2,4,2	$C_2F_3Br_2^+$
270,272,274	.5,1,.5	$C_3F_4Br_2^+$
289,291,293	>>50,100,50	$C_3F_5Br_2^+$
368,370,372,374	3,10,10,3	$C_3F_5Br_3^+$

Identified as the tetrafluoroethylene adduct, 1,1,3-tribromoperfluoropropane ($CFBr_2CF_2CF_2Br$).

Peak E-3

m/e	Relative Intensity	Assignment
79,81	7,7	Br^+
80,82	11,11	HBr^+
93	12	$C_3F_3^+$
100	18	$C_2F_4^+$
110,112	5,5	$CFBr^+$
112	4	$C_3F_4^+$
119	20	$C_2F_5^+$
129,131	96,100	CF_2Br^+
160,162	14,15	$C_2F_3Br^+$
169	10	$C_3F_7^+$
179,181	80,80	$C_2F_4Br^+$
189,191,193	18,36,18	$CFBr_2^+$
191,193	7,7	$C_3F_4Br^+$
210,212	1,1	$C_3F_5Br^+$
220,222,224	1.5,3,1.5	$C_2F_2Br_2^+$
229,231	8,8	$C_3F_6Br^+$
239,241,243	2,4,2	$C_2F_3Br_2^+$
251,253,255	4,8,4	$C_3F_3Br_2^+$
289,291,293	1.5,3,1.5	$C_3F_5Br_2^+$
301,303,305	4,8,4	$C_4F_5Br_2^+$
389,391,393	18,34,16	$C_5F_9Br_2^+$

Identified as the two to one telomer, 1,1,5-tribromoperfluoropentane ($CFBr_2(CF_2CF_2)_2Br$).

Peak E-4

79,81	18,18	Br^+
80,82	27,27	HBr^+
93	17	$C_3F_3^+$
100	31	$C_2F_4^+$
110,112	7,7	$CFBr^+$
112	6	$C_3F_4^+$
119	58	$C_2F_5^+$
129,131	100,100	CF_2Br^+
131	44	$C_3F_5^+$

Peak E-4(cont)

m/e	Relative Intensity	Assignment
143	4	$C_4F_5^+$
160,162	28,28	$C_2F_3Br^+$
169	23	$C_3F_7^+$
179,181	61,68	$C_2F_4Br^+$
189,191,193	33,66,33	$CFBr_2^+$
191,193	26,26	$C_3F_4Br^+$
219	10	$C_4F_9^+$
229,231	30,32	$C_3F_6Br^+$
239,241,243	3,6,3	$C_2F_3Br_2^+$
241,243	3,3	$C_4F_6Br^+$
251,253,255	3,6,3	$C_3F_3Br_2^+$
279,281	11,11	$C_4F_8Br^+$
289,291,293	2,4,2	$C_3F_5Br_2^+$
291,293	2,2	$C_5F_8Br^+$
301,303,305	2,4,2	$C_4F_5Br_2^+$
329,331	1,1	$C_5F_{10}Br^+$
331	1	$C_7F_{13}^+$
341,343	2,2	$C_6F_{10}Br^+$
351,353,355	1,2,1	$C_5F_7Br_2^+$

Identified as the three to one telomer, 1,1,7-tribromoperfluoroheptane ($CFBr_2(CF_2CF_2)_3Br$).

F tetrafluoroethylene plus ethylene

Two additional product peaks were identified by glc-ms from the photolysis of $CFBr_3$ (1.00×10^{-3} mol l^{-1}), C_2F_4 (0.33×10^{-3} mol l^{-1}) and C_2H_4 (0.17×10^{-3} mol l^{-1}) at 147°C for 1 h.

Peak F-1

77	36	$C_3H_3F_2^+$
79,81	22,22	Br^+
80,82	31,31	HBr^+
91,93	8,8	CBr^+
93,95	11,11	CH_2Br^+
100	12	$C_2F_4^+$

Peak F-1 (cont)

m/e	Relative Intensity	Assignment
107	6	$C_4H_2F_3^+$
108	9	$C_4H_3F_3^+$
109	6	$C_4H_4F_3^+$
110,112	13,13	$CFBr^+$
127	46	$C_4H_3F_4^+$
129,131	100,100	CF_2Br^+
137,139	8,8	$C_3H_3FBr^+$
141,143	3,3	$C_2F_2Br^+$
157,159	10,10	$C_3H_4F_2Br^+$
160,162	22,22	$C_2F_3Br^+$
179,181	2,2	$C_2F_4Br^+$
207,209	47,47	$C_4H_4F_4Br^+$
286,288,290	4,8,4	$C_4H_4F_4Br_2^+$

Identified as the mixed telomer from bromine atom addition, 1,4-dibromo-1,1,2,2-tetrafluorobutane ($CH_2BrCH_2CF_2CF_2Br$).

Peak F-2

77	100	$C_3H_3F_2^+$
79,81	10,10	Br^+
80,82	21,21	HBr^+
107,109	9,9	$C_2H_4Br^+$
111,113	9,9	$CHFBr^+$
115	26	$C_3H_3F_4^+$
129,131	12,12	CF_2Br^+
137,139	4,4	$C_3H_3FBr^+$
155,157	6,6	$C_3H_2F_2Br^+$
160,162	13,13	$C_2F_3Br^+$
173,175	5,5	$C_3HF_3Br^+$
189,191,193	15,30,15	$CFBr_2^+$
217,219	6,6	$C_5H_2F_4Br^+$
237,239	42,42	$C_5H_3F_5Br^+$
294,296,298	5,10,5	$C_5F_4Br_2^+$
313,315,317	38,76,38	$C_5F_5Br_2^+$
396,398,400,402	2,7,7,2	$C_5H_4F_5Br_3^+$

Identified as the mixed telomer, 1,1,5-tribromo-1,2,2,3,3-pentafluoropentane ($CFBr_2CF_2CF_2CH_2CH_2Br$).

Competitive experiments with tetrafluoroethylene and ethylene, using similar conditions to the other olefins, gave as main products the ethylene adduct ($CFBr_2CH_2CH_2Br$) and the cross telomer ($CFBr_2CF_2CF_2CH_2CH_2Br$) with only traces of the tetrafluoroethylene adduct.

Relative Chromatographic Retention Times

OPERATING CONDITIONS: COLUMN 6' x 3/16" stainless steel packed with 20% Silicone Oil on 60-100 mesh embacel

OVEN TEMP. 78-111°C, but mainly 111°C

CARRIER GAS Nitrogen-flow rate 75 ml min^{-1}

The retention times (R_t') relative to the retention time for $CFBr_3$ (2.1 minutes) are quoted.

CYCLOPROPANES	R_t'
C_3HF_4Br	0.26
$C_3H_2F_3Br$	0.27
$C_3H_3F_2Br$	0.27
C_3H_4FBr	0.34

DIBROMIDES	R_t'
CF_2BrCF_2Br	0.22
$CHFBrCF_2Br$	0.49
CH_2BrCF_2Br	0.62
CH_2BrCH_2Br	1.22

OLEFINS	R_t'
$CH_2{=}CHBr$	0.19
$CFBr{=}CFBr$	0.43

MISCELLANEOUS	R_t'
CF_2Br_2 (impurity)	0.23
$CHFBr_2$	0.46
$CHBr_2CF_2Br$	1.94

ADDUCTS	R_t'
$CFBr_2CF_2CF_2Br$	1.69
$CFBr_2CHFCF_2Br$	2.51
$CFBr_2CF_2CHFBr$	2.94
$CFBr_2CH_2CF_2Br$	2.70
$CFBr_2CF_2CH_2Br$	3.83
$CFBr_2CH_2CHFBr$	3.76
$CFBr_2CHFCH_2Br$	4.69
$CFBr_2CH_2CH_2Br$	4.58

TELOMERS	R_t'
$CF_2BrCHFCF_2CHFBr$	1.20
$CF_2BrCF_2CH_2CH_2Br$	1.70
$CFBr_2(CF_2)_4Br$	3.18
$CFBr_2(CF_2)_6Br$	6.04
$CFBr_2CF_2CF_2CH_2CH_2Br$	9.30

DIMER	R_t'
$CFBr_2CFBr_2$	8.62

PROTON NMR SPECTRA (Internal ref TMS)

COMPOUND	CHEMICAL SHIFT τ (ppm)	REMARKS AND COUPLING CONSTANTS (Hz)
$CHFBr_2$	2.37	doublet $J_{HF} = 50.5$
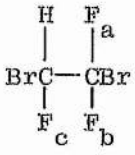	3.58	double double doublet $J_{HF_c} = 48$, $J_{HF_a} = 9$, $J_{HF_b} = 4$
$CFBr_2CH_2CH_2Br$	6.6	complex multiplet $J_{HF} = 14$
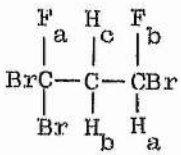	6.4 3.3	(H_b, H_c) complex multiplet (H_a) double double doublet $J_{H_aF_b} = 51$, $J_{H_aH_b} = 7$, $J_{H_aH_c} = 3$
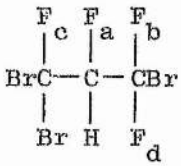	5.0	symmetrical multiplet $J_{HF_a} = 42$, $J_{HF_b} = 4$, $J_{HF_c} = 9$, $J_{HF_d} = 13$
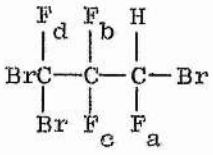	3.0	double doublet $J_{HF_a} = 48$, $J_{HF_b} = 17$

^{19}F NMR SPECTRA (Internal Ref CCl_3F)

COMPOUND	CHEMICAL SHIFT ϕ (ppm)	REMARKS AND COUPLING CONSTANTS (Hz)
$CFBr_3$	-7.21	Singlet
$CHFBr_2$	48.0	doublet $J_{FH} = 50.5$
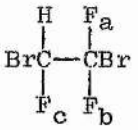	59.3(F_b)	double double doublet $J_{F_bF_a} = 127$, $J_{F_bF_c} = 23$, $J_{F_bH} = 4$
	64.0(F_a)	double double doublet $J_{F_aF_b} = 127$, $J_{F_aF_c} = 21$, $J_{F_aH} = 9$
	149.3(F_c)	double double doublet $J_{F_cF_b} = 23$, $J_{F_cF_a} = 21$, $J_{F_cH} = 48$
$CFBr_2CH_2CH_2Br$	48.0	triplet $J_{HF} = 14$
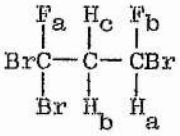	49.1(F_a)	seven lines
	135.3(F_b)	ten lines $J_{F_bH_a} = 51$
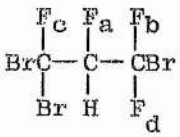	53.4(F_b)	asymmetrical double double double doublet $J_{F_bF_d}$=174, $J_{F_bF_a}$=18, $J_{F_bF_c}$=14, J_{F_bH}=4
	59.3(F_d)	asymmetrical double double triplet $J_{F_dF_b}$=174, $J_{F_dF_a}$=17, $J_{F_dF_c}$=13, J_{F_dH} = 13
	68.5(F_c)	symmetrical multiplet $J_{F_cF_a}$=30, $J_{F_cF_b}$=14, $J_{F_cF_d}$=13, J_{F_cH} = 9
	171.9(F_a)	symmetrical multiplet $J_{F_aF_c}$=30, $J_{F_aF_b}$=18, $J_{F_aF_d}$=17, J_{F_aH} = 42
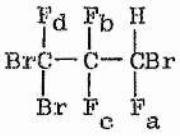	71.4(F_d)	symmetrical double triplet $J_{F_dF_b}$=15, $J_{F_dF_c}$=15, $J_{F_dF_a}$=20, J_{F_dH} = 0
	104.9(F_c)	asymmetrical double double doublet $J_{F_cF_b}$=261, $J_{F_cF_a}$=20, $J_{F_cF_d}$=15, J_{F_cH} = 0
	119.9(F_b)	asymmetrical double double triplet $J_{F_bF_c}$=261, $J_{F_bF_a}$=17, $J_{F_bF_d}$=15, J_{F_bH} = 17
	154.1(F_a)	asymmetrical double double triplet $J_{F_aF_c}$=20, $J_{F_aF_b}$=17, $J_{F_aF_d}$=20, J_{F_aH} = 48

RESULTS

The reactions of tribromofluoromethane with trifluoroethylene

1) Variation of Wavelength

The preparative runs for glc-ms analysis were conducted using unfiltered light and resulted in the formation of some 1-bromo-1,2,2,3-tetrafluorocyclopropane via the highly reactive bromofluorocarbene intermediate. A series of experiments using Barr and Stroud interference filters of band width 10 nm and having transmission bands centred at 254, 265, 313, 366 and 420 nm were conducted with trifluoroethylene and tribromofluoromethane to determine the effect of wavelength on substituted cyclopropane formation. Table 1.1 gives the average relative product concentrations.

Table 1.1 Variation of Wavelength - Average Concentration Ratios

$[CFBr_3] = 2.22 \times 10^{-3}$ mol l^{-1}; $[CHF{=}CF_2] = 1.11 \times 10^{-3}$ mol l^{-1}

$e_1 = [CFBr_2CHFCF_2Br]$; $e_2 = [CFBr_2CF_2CHFBr]$

λ (nm)	temp °C	time h	$\frac{[C_3HF_4Br]}{e_1}$	$\frac{[C_3HF_4Br]}{[CHFBrCF_2Br]}$	$\frac{[CHFBrCF_2Br]}{e_1}$	$\frac{e_2}{e_1}$
254	150	1.43	0.13	0.37	0.36	0.36
265	150	1.33	0.17	0.56	0.31	0.39
313	150	0.66	0.08	0.33	0.24	0.34
366	182	4.00	0.02	0.21	0.12	0.34
366	144	1.00	0.03	0.21	0.16	0.46
366	91	15.90	0.06	0.27	0.21	0.33
420	156	2.50	0.00	0.00	0.03	0.38

The significant features are:

i) the relatively reduced amount of substituted cyclopropane and dibromide formation as the energy of the incident light diminishes,

ii) the relative constancy of the reverse to normal adduct ratio.

2) Variation of Temperature

Two series of experiments were conducted using different wavelengths of incident light (265 and 366 nm).

i) Wavelength 265 nm

$[CFBr_3] = 1.01 \times 10^{-3}$ mol l^{-1}, $[CHF{=}CF_2] = .51 \times 10^{-3}$ mol l^{-1}

a_1 = area of $CFBr_2CHFCF_2Br$ peak, a_2 = area of $CFBr_2CF_2CHFBr$ peak

e_1 = $[CFBr_2CHFCF_2Br]$, e_2 = $[CFBr_2CF_2CHFBr]$

The peak areas were measured relative to $CFBr_3$ peak set equal to 100.

a) 88.5°C, 10.90 h

a_1	a_2	e_1/e_2	
10.44	3.00	3.48	
11.72	3.45	3.40	
10.32	3.12	3.31	
12.56	3.64	3.45	
11.26	3.30	3.41	Mean

b) 112°C, 11.55 h

a_1	a_2	e_1/e_2	
12.44	4.00	3.11	
13.78	4.34	3.18	
12.80	4.06	3.15	
13.60	4.24	3.21	
13.16	4.16	3.16	Mean

c) 134°C, 10.88 h

20.72	7.29	2.84	
24.00	8.20	2.93	
21.20	8.00	2.65	
21.00	7.60	2.76	
21.73	7.77	2.80	Mean

d) 153°C, 8.98 h

36.90	13.60	2.71	
39.00	14.26	2.75	
32.40	12.78	2.54	
36.10	13.53	2.67	Mean

e) 173.5°C, 8.12 h

30.40	11.36	2.68	
32.40	13.40	2.42	
32.80	13.00	2.52	
32.80	12.59	2.54	Mean

The plot of log e_1/e_2 versus $10^3/T$, by the least squares method, gave: gradient = 0.25 ± 0.05; intercept = -0.17 ± 0.02

ii) Wavelength 366 nm

$[CFBr_3] = 2.22 \times 10^{-3}$ mol l^{-1}, $[CHF{=}CF_2] = 1.11 \times 10^{-3}$ mol l^{-1}

a_1 = area of $CFBr_2CHFCF_2Br$ peak, e_1 = $[CFBr_2CHFCF_2Br]$

a_2 = area of $CFBr_2CF_2CHFBr$ peak, e_2 = $[CFBr_2CF_2CHFBr]$

The peak areas were measured relative to $CFBr_3$ peak set equal to 100.

a) 54°C, 18.0 h

1.95	0.46	4.28	
1.96	0.45	4.34	
1.94	0.45	4.27	
1.96	0.45	4.39	
1.95	0.45	4.32	Mean

b) 76°C, 43.0 h

9.20	2.35	3.91	
9.44	2.42	3.90	
9.48	2.40	3.95	
9.60	2.69	3.57	
9.43	2.47	3.83	Mean

c) 101°C, 20.95 h

a_1	a_2	e_1/e_2	
8.46	2.53	3.34	
8.64	2.58	3.35	
8.48	2.53	3.35	
8.48	2.59	3.26	
8.51	2.56	3.33	Mean

d) 123.5°C, 18.69 h

a_1	a_2	e_1/e_2	
14.00	4.60	3.04	
14.16	4.60	3.08	
13.80	4.60	3.00	
13.80	4.60	3.00	
13.94	4.60	3.03	Mean

The plot of log e_1/e_2 versus $10^3/T$, by the least squares method, gave: gradient 0.29 $\pm$ 0.02; intercept = -0.25 $\pm$ 0.01

Combining the results from the 265 and 366 nm temperature variation series gives: gradient = 0.29 $\pm$ 0.03; intercept = -0.25 $\pm$ 0.01

Table 1.2 Trifluoroethylene adduct ratios as a function of temperature

λ (nm)	Temp°C	$10^3/T$	$\frac{[CFBr_2CHFCF_2Br]}{[CFBr_2CF_2CHFBr]}$	$\log \frac{[CFBr_2CHFCF_2Br]}{[CFBr_2CF_2CHFBr]}$
366	54	3.058	4.32	0.635
366	76	2.865	3.83	0.583
265	88.5	2.766	3.41	0.533
366	101	2.674	3.33	0.522
265	112	2.597	3.16	0.500
366	123.5	2.522	3.03	0.481
265	134	2.457	2.80	0.447
265	153	2.347	2.67	0.425
265	173.5	2.240	2.54	0.405

The reactions of tribromofluoromethane with trifluoroethylene and ethylene

A series of competitive addition reactions between ethylene and trifluoroethylene to determine the relative rates of formation of the ethylene and normal trifluoroethylene adducts were conducted over the temperature range 100-174°C. The relative rates of formation of ethylene to reverse trifluorethylene adducts were calculated through the intermediacy of the normal to reverse adduct ratios from the experiments in the absence of ethylene: this method gives more accurate results.

$[CFBr_3] = 2.22 \times 10^{-3}$ mol l^{-1}, $[CHF{=}CF_2] = 0.74 \times 10^{-3}$ mol l^{-1}, $[C_2H_4] = 0.37 \times 10^{-3}$ mol l^{-1}, a_1 = area of $CFBr_2CHFCF_2Br$ peak $e_1 = [CFBr_2CHFCF_2Br]$, a_2 = area of $CFBr_2CF_2CHFBr$ peak, $e_2 = [CFBr_2CF_2CHFBr]$, a_3 = area of $CFBr_2CH_2CH_2Br$ peak, $e_3 = [CFBr_2CH_2CH_2Br]$ $e_t = e_1 + e_2$

Peak areas were measured relative to $CFBr_3$ set equal to 100.

a) 100°C, 14.75 h

a_1	a_2	a_3	
2.68	0.82	14.4	
2.64	0.84	14.4	
2.98	1.01	15.1	
2.88	1.00	14.8	
2.80	0.92	14.7	Mean
4.64	1.52	29.20	Conc mol l^{-1} x 10^5

78.93 % C_2H_4 reaction
8.32 %$CHF{=}CF_2$ "
1.33 e_t/e_1

b) 123°C, 16.60 h

a_1	a_2	a_3	
4.00	1.28	15.40	
3.74	1.28	14.20	
3.87	1.28	14.80	Mean
6.42	2.12	29.45	Conc mol l^{-1} x 10^5

79.60 %C_2H_4 reaction
11.55 %$CHF{=}CF_2$ "
1.33 e_t/e_1

c) 148°C, 7.38 h

0.90	0.30	4.12	
0.80	0.29	3.60	
0.80	0.28	3.40	
0.95	0.33	4.22	
0.86	0.30	3.84	Mean
1.43	0.50	7.63	Conc mol l^{-1} x 10^5

20.63 %C_2H_4 reaction
2.61 %$CHF{=}CF_2$ "
1.35 e_t/e_1

d) 174°C, 2.72 h

0.60	0.22	2.08	
0.58	0.20	2.20	
0.57	0.21	1.94	
0.59	0.26	2.26	
0.58	0.22	2.12	Mean
0.97	0.37	4.22	Conc mol l^{-1} x 10^5

11.40 %C_2H_4 reaction
1.81 %$CHF{=}CF_2$ "
1.38 e_t/e_1

The plot of $\log[e_t/e_1 \log g/\log h]$ versus $10^3/T$, by the least squares method, gave: gradient = 0.94 ± 0.10, intercept = -1.15 ± 0.04

Table 1.3 Ethylene to normal trifluoroethylene adduct ratios as a function of temperature

Equation 29 is relevant:

$$\log[e_t/e_1 \log g/\log h] = \log A_3 - \log A_1 + (E_1-E_3)/2.303\ RT$$

where $e_t = e_1 + e_2 = [CFBr_2CHFCF_2Br] + [CFBr_2CF_2CHFBr]$

h = the fraction of reacted trifluoroethylene

g = the fraction of reacted ethylene

Temp °C	$10^3/T$	$(e_t/e_1)\log g/\log h$	$\log[(e_t/e_1) \log g/\log h]$
100	2.681	23.80	1.377
123	2.525	17.17	1.235
148	2.375	11.79	1.071
174	2.237	9.24	0.966

The reactions of tribromofluoromethane with 1,1-difluoroethylene

i) A series of experiments with variation in temperature using light of 366 nm gave the normal and reverse adducts as the only significant products. The rate of addition was very slow, particularly to the $=CF_2$ group, and this necessitated long photolytic times to give measurable adduct peaks.

$[CFBr_3] = 1.00 \times 10^{-3}$ mol l^{-1}, $[CH_2=CF_2] = 0.75 \times 10^{-3}$ mol l^{-1}

Photolysis by a Hanovia 500 watt mercury UV lamp placed 5 cm from the oven mouth.

a_1 = area of $CFBr_2CH_2CF_2Br$ peak, $e_1 = [CFBr_2CH_2CF_2Br]$

a_2 = area of $CFBr_2CF_2CH_2Br$ peak, $e_2 = [CFBr_2CF_2CH_2Br]$

a) 125°C, 47.70 h

a_1	a_2	e_1/e_2	
2.05	0.019	107.9	
2.65	0.025	104.8	
3.05	0.029	105.2	
2.57	0.024	106.0	Mean

b) 136°C, 72.00 h

a_1	a_2	e_1/e_2	
3.00	0.041	73.2	
2.91	0.041	71.0	
2.93	0.041	71.5	
3.00	0.041	7.32	
2.95	0.041	72.0	
2.96	0.041	72.2	Mean

c) 144°C, 22.60 h

a_1	a_2	e_1/e_2	
2.78	0.042	66.19	
3.15	0.048	65.63	
3.25	0.049	66.33	
2.62	0.037	70.81	
2.95	0.044	67.24	Mean

d) 154°C, 25.75 h

a_1	a_2	e_1/e_2	
1.58	0.030	52.7	
1.76	0.030	58.7	
1.91	0.032	59.8	
1.57	0.028	56.1	
1.60	0.030	53.3	
1.68	0.030	56.1	Mean

e) 167.5°C, 68.20 h

11.24	0.294	38.23	
11.22	0.286	39.23	
11.20	0.264	42.40	
12.76	0.300	42.50	
12.56	0.282	44.50	
11.80	0.285	41.40	Mean

The plot of log e_1/e_2 versus $10^3/T$ by the least squares method, gave: gradient 1.59 ± 0.35; intercept: -1.99 ± 0.15

Table 1.4 1,1-difluoroethylene adduct ratios as a function of temperature (λ = 366 nm)

Temp °C	$10^3/T$	$[CFBr_2CH_2CF_2Br]/[CFBr_2CF_2CH_2Br]$	$\log \frac{[CFBr_2CH_2CF_2Br]}{[CFBr_2CF_2CH_2Br]}$
125	2.513	106.0	2.025
136	2.445	72.2	1.859
144	2.398	67.2	1.828
154	2.342	56.1	1.749
167.5	2.270	41.40	1.617

ii) A series of experiments with 1,1-difluoroethylene using unfiltered light over the temperature range 125-170°C greatly increased the rate of adduct formation and changed the observed adduct ratios. The loss in selectivity may be attributed to addition occurring predominantly by excited radicals.

$[CFBr_3] = 1.00 \times 10^{-3}$ mol l^{-1}; $[CH_2{=}CF_2] = 0.50 \times 10^{-3}$ mol l^{-1} except for reaction f where:
$[CFBr_3] = 2.00 \times 10^{-3}$ mol l^{-1}; $[CH_2{=}CF_2] = 1.75 \times 10^{-3}$ mol l^{-1}
a_1 = area of $CFBr_2CH_2CF_2Br$ peak $e_1 = [CFBr_2CH_2CF_2Br]$
a_2 = area of $CFBr_2CF_2CH_2Br$ peak $e_2 = [CFBr_2CF_2CH_2Br]$
The peak areas were measured relative to $CFBr_3$ set equal to 100.

a) 110°C, 1.00 h

a_1	a_2	e_1/e_2	
2.08	0.142	14.65	
2.00	0.126	15.87	
2.00	0.136	14.71	
2.12	0.140	15.14	
		15.09	Mean

b) 113°C, 2.25 h

a_1	a_2	e_1/e_2	
4.40	0.298	14.77	
4.70	0.338	13.91	
4.20	0.292	14.38	
4.35	0.290	15.00	
		14.52	Mean

c) 144°C, 1.87 h

5.33	0.38	14.03	
5.90	0.42	14.05	
5.90	0.42	14.05	
		14.04	Mean

d) 167°C, 1.25 h

8.80	0.511	17.22	
9.38	0.528	17.77	
9.32	0.580	16.07	
9.58	0.578	16.57	
		16.91	Mean

e) 190°C, 1.00 h

8.60	0.480	17.92	
9.36	0.500	18.72	
9.80	0.552	17.75	
10.44	0.556	18.78	
		18.29	Mean

f) 211°C, 1.83 h

47.36	3.01	15.73	
46.64	3.04	15.34	
46.48	3.04	15.29	
		15.46	Mean

The plot of log e_1/e_2 versus $10^3/T$, by the least squares method, gave: gradient = -0.112 ± 0.185, intercept = 1.46 ± 0.08

Table 1.5 Effect of unfiltered light on 1,1-difluoroethylene adduct ratios

Temp °C	$10^3/T$	$[CFBr_2CH_2CF_2Br]/[CFBr_2CF_2CH_2Br]$	$\log \frac{[CFBr_2CH_2CF_2Br]}{[CFBr_2CF_2CH_2Br]}$
110	2.611	15.09	1.179
113	2.591	14.52	1.162
144	2.398	14.04	1.147
167	2.273	16.91	1.228
190	2.160	18.29	1.262
211	2.067	15.46	1.189

The reactions of tribromofluoromethane with 1,1-difluoroethylene and ethylene

A series of photolyses was carried out at 366 nm in which tribromofluoromethane was reacted competitively with 1,1-difluoroethylene and ethylene. Accurate measurement of the very small

reverse adduct peak was not possible. The mathematical analyses allowing for consumption of 1,1-difluoroethylene requires the normal to reverse adduct ratios corresponding to the experimental temperatures. These ratio values were taken from the graph (log e_1/e_2 versus $10^3/T$) of the preceding experimental series with tribromofluoromethane and 1,1-difluoroethylene.

$[CFBr_3] = 1.00 \times 10^{-3}$ mol l^{-1}, $[CH_2{=}CF_2] = 0.33 \times 10^{-3}$ mol l^{-1}
$[C_2H_4] = 0.17 \times 10^{-3}$ mol l^{-1}

Photolysis by a Hanovia 500 watt mercury UV lamp placed 5 cm from the oven mouth.

a_1 = area of $CFBr_2CH_2CF_2Br$ peak
a_3 = area of $CFBr_2CH_2CH_2Br$ peak

$e_1 = [CFBr_2CH_2CF_2Br]$
$e_2 = [CFBr_2CF_2CH_2Br]$
$e_3 = [CFBr_2CH_2CH_2Br]$
$e_t = e_1 + e_2$

Peak areas were measured relative to $CFBr_3$ set equal to 100.

a) 115°C, 17.63 h

a_1	a_3	
0.171	0.610	
0.176	0.600	
0.172	0.612	
0.168	0.601	
0.172	0.606	Mean
0.136	0.543	Conc mol $l^{-1} \times 10^5$
	3.259	$\%C_2H_4$ reaction
	0.4113	$\%CH_2{=}CF_2$ reaction
	1.007	e_t/e_1

b) 120°C, 21.40 h

a_1	a_3	
0.296	1.06	
0.304	1.04	
0.316	1.08	
0.305	1.06	Mean
0.241	0.950	Conc mol $l^{-1} \times 10^5$
	5.701	$\%C_2H_4$ reaction
	0.7301	$\%CH_2{=}CF_2$ reaction
	1.008	e_t/e_1

c) 134°C, 67.6 h

1.12	3.63	
1.14	3.60	
1.22	3.85	
1.11	3.48	
1.15	3.64	Mean
0.908	3.26	Conc mol $l^{-1} \times 10^5$
	19.58	$\%C_2H_4$ reaction
	2.755	$\%CH_2{=}CF_2$ reaction
	1.012	e_t/e_1

d) 156°C, 6.45 h

0.34	1.07	
0.32	1.02	
0.34	1.06	
0.33	1.05	
0.33	1.05	Mean
0.261	0.943	Conc mol $l^{-1} \times 10^5$
	5.658	$\%C_2H_4$ reaction
	0.7985	$\%CH_2{=}CF_2$ reaction
	1.019	e_t/e_1

e) 175°C, 3.20 h

a_1	a_3
0.37	1.22
0.42	1.24
0.42	1.24
0.42	1.30
0.41	1.25 Mean
0.324	1.120 Conc mol l^{-1} x 10^5

6.718 % C_2H_4 reaction

1.001 % $CH_2{=}CF_2$ reaction

1.029 e_t/e_1

The plot of $\log[e_t/e_1$ log g/log h] versus $10^3/T$, by the least squares method, gave:
gradient = 0.17 ± 0.05,
intercept = 0.46 ± 0.02

Table 1.6 Ethylene to normal 1,1-difluoroethylene adduct ratios as a function of temperature

Equation 29 is relevant: $\log [(e_t/e_1)\log g/\log h] = \log A_3 - \log A_1 + (E_1-E_3)/2.303\ RT$

where $e_t = e_1 + e_2 = [CFBr_2CH_2CF_2Br] + [CFBr_2CF_2CH_2Br]$

h = the fraction of reacted 1,1-difluoroethylene

g = the fraction of reacted ethylene

Temp °C	$10^3/T$	$(e_t/e_1)\log g/\log h$	$\log[(e_t/e_1)\log g/\log h]$
115	2.577	8.059	0.9063
120	2.545	8.036	0.9050
134	2.457	7.906	0.8979
156	2.331	7.369	0.8674
175	2.232	7.059	0.8488

The reactions of tribromofluoromethane with vinyl fluoride

A series of photolyses at 366 nm was carried out with tribromofluoromethane and vinyl fluoride. The temperature was varied in the range 100-205°C and reaction times were of the order of 20 h. The only measurable products were the two adducts, but traces of $CHFBr_2$ and $C_3H_3F_2Br$ were also observed.

$[CFBr_3] = 2.22 \times 10^{-3}$ mol l^{-1}, $[CH_2{=}CHF] = 1.11 \times 10^{-3}$ mol l^{-1}

Photolysis by a Hanovia 500 watt mercury UV lamp placed 5 cm from the oven mouth.

a_1 = area of $CFBr_2CH_2CHFBr$ peak $e_1 = [CFBr_2CH_2CHFBr]$

a_2 = area of $CFBr_2CHFCH_2Br$ peak $e_2 = [CFBr_2CHFCH_2Br]$

The peak areas were measured relative to $CFBr_3$ set equal to 100.

a) 106°C, 22.68 h

a_1	a_2	e_1/e_2	
1.18	0.078	15.1	
1.14	0.076	15.0	
1.44	0.086	16.7	
1.24	0.078	15.9	
1.20	0.078	15.4	
1.24	0.079	15.65	Mean

b) 128.5°C, 21.80 h

a_1	a_2	e_1/e_2	
1.86	0.14	13.3	
1.84	0.14	13.2	
1.85	0.14	13.3	
1.88	0.14	13.4	
1.86	0.14	13.30	Mean

c) 150°C, 23.10 h

2.20	0.18	12.2	
2.16	0.18	12.3	
2.28	0.20	11.4	
2.24	0.19	11.7	
2.22	0.19	11.88	Mean

d) 162°C, 6.03 h

1.64	0.160	10.25	
1.96	0.170	11.53	
1.74	0.166	10.48	
1.96	0.166	11.81	
1.83	0.166	11.02	Mean

e) 201°C, 27.25 h

20.7	2.20	9.42	
22.0	2.36	9.32	
21.6	2.40	9.00	
20.0	2.20	9.09	
21.2	2.40	8.83	
21.10	2.31	9.13	Mean

The plot of log e_1/e_2 versus $10^3/T$, by the least squares method, gave:

gradient = 0.44 ± 0.02

intercept = 0.033 ± 0.008

Table 1.7 Vinyl fluoride adduct ratios as a function of temperature

Temp °C	$10^3/T$	$[CFBr_2CH_2CHFBr]/[CFBr_2CHFCH_2Br]$	$\log \frac{[CFBr_2CH_2CHFBr]}{[CFBr_2CHFCH_2Br]}$
106	2.639	15.65	1.195
128.5	2.491	13.30	1.124
150	2.364	11.88	1.075
162	2.299	11.02	1.042
201	2.110	9.13	0.961

The reactions of tribromofluoromethane with vinyl fluoride and ethylene

A series of photolyses was carried out at 366 nm in which tribromofluoromethane was reacted competitively with vinyl fluoride and ethylene. The small reverse adduct peak was superimposed upon the tail of the ethylene adduct peak and could not be measured. The

experimental normal to reverse adduct ratios used in the mathematical analyses were taken from the graph (log e_1/e_2 versus $10^3/T$) of the preceding experimental series with tribromofluoromethane and vinyl fluoride.

$[CFBr_3] = 1.00 \times 10^{-3}$ mol l^{-1}; $[CHF{=}CF_2] = 0.33 \times 10^{-3}$ mol l^{-1}; $[C_2H_4] = 0.17 \times 10^{-3}$ mol l^{-1}.

Photolysis by a Hanovia 500 watt mercury UV lamp placed 5 cm in front of the oven mouth.

a_1 = area of $CFBr_2CH_2CHFBr$ peak $e_1 = [CFBr_2CH_2CHFBr]$

a_3 = area of $CFBr_2CH_2CH_2Br$ peak $e_2 = [CFBr_2CHFCH_2Br]$

$e_t = e_1 + e_2$ $e_3 = [CFBr_2CH_2CH_2Br]$

Peak areas were measured relative to $CFBr_3$ set equal to 100.

a) 113°C, 19.05 h

a_1	a_3	
2.08	3.25	
2.09	3.25	
2.01	3.25	
2.04	3.24	
2.07	3.20	
2.06	3.24	Mean
1.730	2.903	Conc mol $l^{-1} \times 10^5$
17.42		$\%C_2H_4$ reaction
5.54		$\%CH_2{=}CHF$ reaction
1.067		e_t/e_1

b) 129°C, 25.65 h

a_1	a_3	
3.48	5.23	
3.54	5.29	
3.61	5.41	
3.54	5.23	
3.54	5.29	Mean
2.98	4.74	Conc mol $l^{-1} \times 10^5$
28.43		$\%C_2H_4$ reaction
9.60		$\%CH_2{=}CHF$ reaction
1.075		e_t/e_1

c) 147°C, 17.35 h

2.66	4.12	
2.65	3.95	
2.65	4.00	
2.71	4.02	
2.67	4.03	Mean
2.24	3.61	Conc mol $l^{-1} \times 10^5$
21.65		$\%C_2H_4$ reaction
7.29		$\%CH_2{=}CHF$ reaction
1.083		e_t/e_1

d) 162°C, 5.55 h

1.72	2.58	
1.60	2.45	
1.65	2.57	
1.64	2.49	
1.65	2.52	Mean
1.39	2.26	Conc mol $l^{-1} \times 10^5$
13.55		$\%C_2H_4$ reaction
4.54		$\%CH_2{=}CHF$ reaction
1.090		e_t/e_1

e) 177.5°C, 5.85 h

a_1	a_3	
1.92	2.88	
1.92	2.95	
1.92	2.88	
1.95	2.91	
1.93	2.91	Mean
1.62	2.60	Conc mol $l^{-1} \times 10^5$
15.62		$\%C_2H_4$ reaction
5.34		$\%CH_2$=CHF reaction
1.098		e_t/e_1

The plot of $\log[e_t/e_1 \log g/\log h]$ versus $10^3/T$, by the least squares method, gave:

gradient = 0.069 ± 0.024

intercept = 0.38 ± 0.01

Table 1.8 Ethylene to normal vinyl fluoride adduct ratios as a function of temperature

Equation 29 is relevant: $\log[e_t/e_1 \log g/\log h] = \log A_3 - \log A_1 + (E_1 - E_3)/2.303\ RT$

where $e_t = e_1 + e_2 = [CFBr_2CH_2CHFBr] + [CFBr_2CHFCH_2Br]$

h = the fraction of reacted vinyl fluoride

g = the fraction of reacted ethylene

Temp °C	$10^3/T$	$e_t/e_1 \log g/\log h$	$\log[(e_t/e_1)\log g/\log h]$
113	2.591	3.586	0.5546
129	2.488	3.566	0.5521
147	2.381	3.486	0.5424
162	2.299	3.409	0.5326
177.5	2.220	3.405	0.5321

The reactions of tribromofluoromethane with ethylene and tetrafluoroethylene

A series of photolyses was carried out at 366 nm in which a three fold excess of tribromofluoromethane was reacted competitively with equal quantities of ethylene and tetrafluoroethylene. Three significant products were formed, namely, the two adducts ($CFBr_2CH_2CH_2Br$ and $CFBr_2CF_2CF_2Br$) and the mixed telomer ($CFBr_2CF_2CF_2CH_2CH_2Br$).

$[CFBr_3] = 1.00 \times 10^{-3}$ mol l^{-1}; $[C_2F_4] = 0.67 \times 10^{-3}$ mol l^{-1}; $[C_2H_4] = 0.67 \times 10^{-3}$ mol l^{-1}.

Photolysis by a Hanovia 500 watt mercury UV lamp placed 5 cm in front of the oven mouth.

e^1 = area of $CFBr_2CH_2CH_2Br$ peak e = $[CFBr_2CH_2CH_2Br]$

f^1 = area of $CFBr_2CF_2CF_2Br$ peak f = $[CFBr_2CF_2CF_2Br]$

g^1 = area of $CFBr_2CF_2CF_2CH_2CH_2Br$ peak g = $[CFBr_2CF_2CF_2CH_2CH_2Br]$

Peak areas were measured relative to $CFBr_3$ set equal to 100.

a) 79.5°C, 2.50 h

e^1	f^1	g^1	
2.64	0.18	0.58	
2.57	0.20	0.60	
2.65	0.20	0.62	
2.56	0.18	0.62	
2.60	0.18	0.60	
2.61	0.19	0.60	Mean
2.34	0.13	0.40	Conc mol l^{-1} x 10^5
	16.38		$\%C_2H_4$ reaction
	3.17		$\%C_2F_4$ reaction
	0.855		e/(e+g)

b) 99°C, 1.50 h

e^1	f^1	g^1	
3.92	0.18	1.04	
4.70	0.20	1.25	
4.55	0.17	1.24	
4.25	0.17	1.16	
3.90	0.16	1.16	
4.26	0.176	1.17	Mean
3.82	0.124	0.766	Conc mol l^{-1} x 10^5
	27.52		$\%C_2H_4$ reaction
	5.34		$\%C_2F_4$ reaction
	0.833		e/(e+g)

c) 109°C, 1.00 h

3.08	0.19	0.94	
3.04	0.20	0.99	
3.12	0.20	0.98	
3.16	0.21	1.02	
3.05	0.20	0.94	
3.09	0.20	0.98	Mean
2.77	0.14	0.64	Conc mol l^{-1} x 10^5
	20.44		$\%C_2H_4$ reaction
	4.67		$\%C_2F_4$ reaction
	0.813		e/(e+g)

d) 130°C, 1.00 h

5.40	0.27	1.77	
5.34	0.31	1.77	
5.34	0.33	1.67	
5.34	0.33	1.70	
5.36	0.31	1.73	Mean
4.80	0.22	1.13	Conc mol l^{-1} x 10^5
	35.58		$\%C_2H_4$ reaction
	8.09		$\%C_2F_4$ reaction
	0.809		e/(e+g)

e) 147°C, 1.00 h

5.91	0.56	1.64	
6.83	0.59	1.83	
7.22	0.56	1.89	
6.85	0.60	1.80	
6.70	0.58	1.79	Mean
6.01	0.41	1.17	Conc mol l^{-1}x10^5
	43.08		$\%C_2H_4$ reaction
	9.49		$\%C_2F_4$ reaction
	0.837		e/(e+g)

f) 168°C, 1.00 h

7.39	0.84	2.31	
7.38	0.84	2.28	
7.40	0.77	2.38	
7.30	0.80	2.20	
7.42	0.84	2.22	
7.38	0.82	2.28	Mean
6.61	0.58	1.49	Conc mol l^{-1}x10^5
	48.64		$\%C_2H_4$ reaction
	12.43		$\%C_2F_4$ reaction
	0.816		e/(e+g)

g) 180°C, 1.00 h

e^{-1}	t^{-1}	g^{-1}	
8.9	1.24	2.50	
8.3	1.16	2.11	
8.7	1.09	2.22	
8.8	1.17	2.43	
8.7	1.16	2.29	
8.68	1.17	2.31	Mean
7.78	0.825	1.51	Conc mol l^{-1} x 10^5
	55.77		$\%C_2H_4$ reaction
	14.02		$\%C_2F_4$ reaction
	0.837		e/(e+g)

The plot of log $\left[\frac{e}{e+g}\log p/\log t\right]$ versus $10^3/T$, by the least squares method, gave: gradient = 0.046 ± 0.176; intercept = 0.53 ± 0.07

Table 1.9 Temperature dependent data on relative rate of $CFBr_2\cdot$ addition to ethylene and tetrafluoroethylene

Equation 60 is relevant

$$\log\left[\frac{e}{e+g}\ \frac{\log p}{\log t}\right] = \log A_2 - \log A_4 + [E_4 - E_2]/2.303\ RT$$

where e = $[CFBr_2CH_2CH_2Br]$

g = $[CFBr_2CF_2CF_2CH_2CH_2Br]$

p = the fraction of reacted ethylene

t = the fraction of reacted tetrafluoroethylene

Temp °C	$10^3/T$	$\frac{e}{e+g}\ \frac{\log p}{\log t}$	$\log \frac{e}{e+g}\ \frac{\log p}{\log t}$	$\frac{e}{e+g}$
79.5	2.837	4.77	0.679	0.855
99	2.688	4.88	0.688	0.833
109	2.619	3.89	0.590	0.813
130	2.481	4.21	0.624	0.809
147	2.381	4.72	0.674	0.837
168	2.268	4.09	0.612	0.816
180	2.208	4.52	0.655	0.837

DISCUSSION

The bond dissociation energy of a carbon-bromine bond in tribromofluoromethane is approximately 49 kcal mol^{-1}, and the energy supplied by a medium pressure mercury arc at 254 nm is equivalent to 113 kcal mol^{-1}, so there is sufficient energy for the fission of a carbon-bromine bond to give a dibromofluoromethyl radical and a bromine atom, and for the fission of two carbon-bromine bonds to give a bromofluorocarbene and a bromine molecule.

$$CFBr_3 + h\nu \xrightarrow{\emptyset I_a} \cdot CFBr_2 + Br\cdot \qquad 1$$

$$CFBr_3 + h\nu \xrightarrow{\emptyset' I_a} :CFBr + Br_2 \qquad 1'$$

Carbenes add readily to olefins to give cyclopropanes. For all the olefins except tetrafluoroethylene products having the molecular formulae of the substituted cyclopropanes were observed. The decomposition ions of the mass spectra were in good agreement with the observations of Deen and Roboz[45]. Cohen and Heicklen[46] observed that difluoromethylene ($:CF_2$) reacted with tetrafluoroethylene to give perfluorocyclopropane as the only product . The The effect of wavelength on the initiation process was examined for the reaction with trifluoroethylene (see table 1-1). The ratio of substituted cyclopropane to adduct decreased as wavelength increased. The total amount of incident radiation varied from one wavelength to another, but the dibromide probably gives an approximate measure of the rate of initiation. With increasing wavelength the relative amount of substituted cyclopropane to dibromide decreased and the relative amount of adduct to dibromide increased. At the shortest wavelengths the two initiation processes are of comparable importance, but at longer wavelengths $\emptyset' << \emptyset$ and very little carbene is formed. Photolyses of $CFBr_3$ and $CHF=CF_2$ mixtures at 265 nm at lower temperatures gave a significant proportion of carbene products (Table 1-10). In the series of photolyses at 366 nm carbene products were negligible. The ratio of the two adducts from the 366 nm experiments is plotted against

Table 1-10 Variation of Temperature in the Photolysis of $CFBr_3$ with $CHF{=}CF_2$ at 265 nm.

Temp °C	C_3HF_4Br	$CFBr{=}CFBr$	$CHFBrCF_2Br$	$CFBr_2CHFCF_2Br$	$CFBr_2CF_2CHFBr$
88.5	12.9	1.2	46.9	21.7	6.3
112	13.3	1.4	40.6	23.9	7.6
134	11.0	2.3	45.5	41.9	15.0
153	11.5	5.1	58.6	84.3	31.6
173.5	27.6	5.8	49.2	82.3	32.5

Rates of formation of products in mol $l^{-1}s^{-1} \times 10^{10}$
initial $[CFBr_3] = 1.01 \times 10^{-3}$ mol l^{-1}
initial $[CHF{=}CF_2] = 0.51 \times 10^{-3}$ mol l^{-1}
Traces of telomers were also detected

$10^3/T$ in fig 1-3 together with the adduct ratios from the experiments at 265 nm. The two sets of data form a single straight line which shows that the two initiations (1) and (1') are independent of each other, and that the carbene intermediate does not interfere with the radical chain process. Kinetic experiments with the other olefins were carried out at 366 nm, where substituted cyclopropane formation was negligible.

The mechanism for formation of the main products in the preparative experiments may be written as follows:

$$\cdot CFBr_2 + E \longrightarrow CFBr_2E\cdot \qquad 2$$

$$:CFBr + E \longrightarrow CFBrE \qquad 2'$$

$$CFBr_2E\cdot + CFBr_3 \longrightarrow CFBr_2EBr + \cdot CFBr_2 \qquad 3$$

$$Br_2 + E \longrightarrow EBr_2 \qquad 4$$

$$\cdot CFBr_2 + \cdot CFBr_2 \longrightarrow CFBr_2CFBr_2 \qquad 5$$

The main termination step for the radical chain is the combination of two dibromofluoromethyl radicals (5) as the dimer was detected, but none of the other radical combination or disproportionation products. The dimer may decompose by loss of bromine to form 1,2-dibromodifluoroethylene which was detected in the photolyses with ethylene, 1,1-difluoroethylene and trifluoroethylene.

$$CFBr_2CFBr_2 \longrightarrow CFBr{=}CFBr + Br_2 \qquad 6$$

Alternatively CFBr=CFBr could be formed by dimerisation of bromofluorocarbene; addition of bromine to this olefin would also produce the dimer.

The dibromides may be formed by the addition of bromine atoms followed by bromine abstraction from $CFBr_3$, or by ionic addition of molecular bromine in the solution phase upon distillation of reaction mixtures into sample tubes after completion of photolyses.

$$Br^{\cdot} + E \rightleftharpoons {\cdot}EBr \qquad 7$$

$${\cdot}EBr + CFBr_3 \longrightarrow BrEBr + {\cdot}CFBr_2 \qquad 8$$

The activation energy for the addition of bromine[47,48] atoms to ethylene is approximately 2.9 kcal mol^{-1}, but the reverse reaction[49] may be important (-7). Sources of bromine atoms are the fission of a carbon-bromine bond in the primary photolysis step (1), or the photolysis of the bromine formed in the carbene formation step (1'). Bromine abstraction from $CFBr_3$ by a bromine atom will be unimportant owing to a high activation energy. The activation energy for the analogous abstraction of bromine from CCl_3Br by a bromine atom[50] is 10.3 kcal mol^{-1}.

$$Br^{\cdot} + CFBr_3 \not\longrightarrow Br_2 + {\cdot}CFBr_2 \qquad 9$$

Therefore bromine atoms do not participate in a chain reaction and to the first approximation the rate of dibromide formation is equal to the rate of initiation and termination. In the kinetic experiments the rate of adduct formation was far in excess of the rate of dimer and dibromide formation indicating that the chain length was long.

In the preparative reactions with the olefins containing two or more hydrogen atoms the products of hydrogen abstraction reactions were identified.

$$\cdot CFBr_2 + RH \longrightarrow CHFBr_2 + R\cdot \qquad 10$$

$$CFBr_2E\cdot + RH \longrightarrow CFBr_2EH + R\cdot \qquad 11$$

$$BrE\cdot + RH \longrightarrow BrEH + R\cdot \qquad 12$$

The products $CHFBr_2$, $CFBr_2CH_2CH_3$ and C_2H_5Br, formed in the ethylene reaction, can be accounted for in this way. The ethyl bromide could also be formed by the addition of HBr, produced in a similar hydrogen abstraction process with bromine atoms, to the starting ethylene. The major sources of hydrogen are probably the reaction products, since hydrogen abstraction from the fluoroethylenes is considerably slower than the addition step[51]. In the ethylene reaction, traces of CH_2=CHBr were identifed which suggests that abstraction from this olefin may occur to a minor extent.

$$\cdot CFBr_2 + CH_2{=}CH_2 \longrightarrow CHFBr_2 + CH_2{=}\dot{C}H \qquad 13$$

$$CH_2{=}\dot{C}H + CFBr_3 \longrightarrow CH_2{=}CHBr + CFBr_2\cdot \qquad 14$$

In the preparative reactions with the olefins containing two or more fluorine atoms, telomers were found amongst the reaction products.

$$CFBr_2E\cdot + E \longrightarrow CFBr_2E_2\cdot \qquad 15$$

$$CFBr_2E_2\cdot + CFBr_3 \longrightarrow CFBr_2E_2Br + \cdot CFBr_2 \qquad 16$$

The rate of telomerisation increases as the fluorine content of the olefin increases. In the preparative reaction with ethylene and tetrafluoroethylene both the bromine atom and dibromofluoromethyl radical cross telomers were obtained.

$$\cdot CFBr_2 + F' \longrightarrow CFBr_2F'\cdot \qquad 17$$

$$CFBr_2F'\cdot + E \longrightarrow CFBr_2F'E\cdot \qquad 18$$

$$CFBr_2F'E\cdot + CFBr_3 \longrightarrow CFBr_2F'EBr \qquad 19$$

where $F' = C_2F_4$ and $E = C_2H_4$

Similarly for cross telomer formation with bromine atoms. More cross telomer by route 19 was formed than tetrafluoroethylene adduct by 3: this highlights the increasing competitive nature of

bromine abstraction and addition as the number of fluorine atoms increase on the intermediate halopropyl radical. With the intermediate n-heptafluoropropyl radical addition to ethylene occurs approximately three times faster than bromine abstraction from $CFBr_3$. The propyl radical is a substituted trifluoromethyl radical and $\cdot CF_3$ adds readily to ethylene with an activation energy[8] of 2.0 kcal mol^{-1}. Therefore this competitive nature of perfluoroalkyl radicals, for addition and bromine abstraction, indicates the necessity for using perfluoroalkyliodides in competitive addition to olefins as the rate of iodine abstraction is approximately two orders of magnitude greater than bromine abstraction[6]. Formation of the cross telomer in preference to the 2:1 tetrafluoroethylene telomer is due to the lower activation energy for the addition of highly fluorinated alkyl radicals to ethylene.

Mathematical Treatment of Rate Data

The dibromofluoromethyl radical adds to the fluoroethylenes with a high degree of selectivity. Experimentally this occasionally requires a relatively high percentage consumption of the fluoroolefin to facilitate measurement of the reverse adduct peak. To retain accuracy the variable olefin concentration during reaction must be taken into account in the mathematical treatment of the reaction mechanism. The salient features of the reaction mechanism are:-

(i) Photolytic initiation, whereby the homolytic fission of a C-Br bond gives a dibromofluoromethyl radical and a bromine atom.

$$CFBr_3 \xrightarrow{h\nu} CFBr_2\cdot + Br\cdot \quad \emptyset I_a \qquad (1)$$

(ii) Addition of a dibromofluoromethyl radical to an olefin giving an intermediate adduct radical. With unsymmetrical olefins addition to the least substituted end gives the normal adduct radical and addition to the most substituted end gives the reverse adduct radical.

$$\text{eg. } CFBr_2\cdot + CHF{=}CF_2 \xrightarrow{k_x} \underset{\text{normal adduct radical}}{CFBr_2CHFCF_2\cdot} \qquad (2)$$

$$CFBr_2\cdot + CHF{=}CF_2 \xrightarrow{k'_x} \underset{\text{reverse adduct radical}}{CFBr_2CF_2CHF\cdot} \qquad (2')$$

The addition step (k_x) is the rate determining step.

(iii) Each adduct radical upon abstraction of a bromine atom from the tribromofluoromethane, which is in excess, gives an adduct molecule and a dibromofluoromethyl radical. The normal and reverse adduct radicals give the normal and reverse adducts respectively.

$$\text{eg. } CFBr_2CHFCF_2\cdot + CFBr_3 \xrightarrow{k_3} \underset{\text{normal adduct}}{CFBr_2CHFCF_2Br} + CFBr_2\cdot \qquad (3)$$

$$CFBr_2CF_2CHF\cdot + CFBr_3 \xrightarrow{k'_3} \underset{\text{reverse adduct}}{CFBr_2CF_2CHFBr} + CFBr_2\cdot \qquad (3')$$

(iv) The termination step is represented by the combination of two dibromofluoromethyl radicals. Although the collision of any two radicals can give a termination product, the dimer ($CFBr_2CFBr_2$) was the only one observed.

$$2CFBr_2\cdot \xrightarrow{k_t} CFBr_2CFBr_2 \qquad (4)$$

In the following derivation it is assumed that the olefins were only consumed in the formation of the adducts. This neglects the olefin incorporated in the dibromides (a non chain product) and other trace products.

Formation of a single adduct from a symmetrical olefin

$$\text{eg. } CFBr_3 + CH_2{=}CH_2 \longrightarrow CFBr_2CH_2CH_2Br$$

let $X\cdot = CFBr_2\cdot$

E = the concentration of olefin at any time t

E_o = initial concentration of olefin

e_3 = final concentration of adduct

e = variable concentration of adduct

$\therefore E_o - e_3$ = final concentration of olefin

$\therefore E_o - e$ = variable concentration of olefin

Rate of adduct formation

$$de/dt = k_3[XE\cdot][XBr] \tag{5}$$

The Stationary State Approximation gives:

$$d[XE\cdot]/dt = 0 = -k_3[XBr][XE\cdot] + k_x[X\cdot][E] \tag{6}$$

$$\therefore \quad de/dt = k_x[X\cdot][E] \tag{7}$$

Let $x = E_o - e$

$\therefore dx = -de$

From equation 7: $de/(E_o - e) = k_x[X\cdot]dt$ (8)

$$\therefore \quad -dx/x = k_x[X\cdot]dt \tag{9}$$

Integration of equation (9) between the initial and final olefin concentration gives:

$$-\ln (1-e_3/E_o) = k_x[X\cdot]t \tag{10}$$

Invoking the relationship

$$k_x = A_x \exp(-E_x/RT) \tag{11}$$

where A_x = Arrhenius parameter in $1\ mol^{-1}s^{-1}$
E_x = activation energy in $cal\ mol^{-1}$
T = temperature in degrees Kelvin
R = Gas Constant = $1.987\ deg^{-1}mol^{-1}cal$

Then:

$$-\ln(1-e_3/E_o) = [X\cdot]tA_x\exp(-E_x/RT) \tag{12}$$

<u>Formation of two adducts from an unsymmetrical olefin</u>

eg. $CFBr_3 + CHF{=}CF_2 \longrightarrow CFBr_2CHFCF_2Br + CFBr_2CF_2CHFBr$

Let $X\cdot = CFBr_2\cdot$
E = [olefin] at any time t
E_o = initial concentration of olefin
e_1 = final concentration of the normal adduct
e_2 = final concentration of the reverse adduct
$e_t = e_1 + e_2$
e_1' = variable concentration of the normal adduct
e_2' = variable concentration of the reverse adduct
$\therefore E_o - e_1 - e_2$ = final concentration of olefin
$\therefore E_o - e_1' - e_2'$ = variable concentration of olefin

(i) Formation of the normal and reverse adducts

Equation (7) applies in the form:

$$de_1'/dt = k_1[X\cdot][E_o - e_1' - e_2'] \quad (13)$$

$$de_2'/dt = k_2[X\cdot][E_o - e_1' - e_2'] \quad (14)$$

where k_1 and k_2 are the rate constants for the addition steps in the formation of the normal and reverse adducts.

$$\therefore de_1'/k_1 = de_2'/k_2 \quad (15)$$

Integration of equation (15) gives:

$$e_1/e_2 = k_1/k_2 \quad (16)$$

(ii) Formation of the normal adduct

$$\text{Let } x = E_o - e_1' - e_2' \qquad \therefore de_1'/dt = k_1[X\cdot]x \quad (17)$$

$$\therefore dx = -de_1' - de_2' \quad (18)$$

Substitution of equation (15) into (18) gives:

$$dx = -(1+k_2/k_1)de_1' \quad (19)$$

Substituting equation (17) into (19) gives:

$$dx/x = -(1+k_2/k_1)k_1[X\cdot]dt \quad (20)$$

Integration of equation (20) between initial and final olefin concentrations gives:

$$-\ln(1-e_t/E_o)/(1+e_2/e_1) = k_1[X\cdot]t \quad (21)$$

$$= [X\cdot]t\ A_1\exp(-E_1/RT) \quad (22)$$

(iii) Formation of the reverse adduct

By analogy with the formation of the normal adduct, the expression for formation of the reverse adduct is:

$$-\ln(1-e_t/E_o)/(1+e_1/e_2) = [X\cdot]t\ A_2\exp(-E_2/RT) \quad (23)$$

The series of reactions with varying temperature were conducted competitively, allowing measurement of the relative rates of adduct formation and calculation of Arrhenius parameters and activation energy differences with respect to addition to ethylene.

Competitive addition to an unsymmetrical fluoroethylene

The ratio of normal to reverse adduct formation for the addition of dibromofluoromethyl radicals to each of the unsymmetrical fluoroethylenes (vinyl fluoride, 1,1-difluoroethylene and trifluoroethylene) is independent of olefin concentration and is represented by equation (16).

$$e_1/e_2 = k_1/k_2$$

$$\therefore \quad e_1/e_2 = A_1\exp(-E_1/RT)/A_2\exp(-E_2/RT) \qquad (23)'$$

Taking logs of both sides gives:

$$\log e_1/e_2 = \log A_1 - \log A_2 + (E_2-E_1)/2.303\ RT \qquad (24)$$

Plotting the log of the adduct ratio against $10^3/T$ gives:

(i) from the intercept, the difference in the Arrhenius parameter (A-factor) for addition to the opposite ends of the unsymmetrical olefin,

$$\text{intercept} = \log A_1 - \log A_2 \ (1\ \text{mol}^{-1}\text{s}^{-1}) \qquad (25)$$

(ii) from the slope, the difference in activation energy.

$$E_2-E_1 = 2.303.R.\text{slope} \ (\text{kcal mol}^{-1}) \qquad (26)$$

Competitive addition to ethylene and an unsymmetrical olefin

The ratio of formation of ethylene adduct to normal fluoroethylene adduct is given by equation 12 divided by equation 22.

$$\frac{\ln(1-e_3/E_o)}{\ln(1-e_t/E'_o)/(1+e_2/e_1)} = \frac{A_3\exp(-E_3/RT)}{A_1\exp(-E_1/RT)} \qquad (27)$$

where: E_o = initial concentration of ethylene, E'_o = initial concentration of fluoroethylene.

Converting the natural logarithms to logarithms to base ten and taking logarithms of both sides gives:

$$\log[(1+e_2/e_1)\log(1-e_3/E_o)/\log(1-e_t/E'_o)] = \log A_3 - \log A_1 + (E_1-E_3)/2.303\ RT \qquad (28)$$

Now $(1-e_3/E_o)$ = the fraction of reacted ethylene

$(1-e_t/E'_o)$ = the fraction of reacted fluoroethylene

let $1-e_3/E_o = g$, and $1-e_t/E'_o = h$

Therefore equation (28) simplifies to:

$$\log[(e_t/e_1)\log g/\log h] = \log A_3 - \log A_1 + (E_1-E_3)/2.303\ RT \qquad (29)$$

Plotting the LHS against $10^3/T$ gives:

(i) from the intercept, the A-factor difference for the competitive addition between ethylene and the least substituted end of the fluoroethylene,

$$\text{intercept} = \log A_3 - \log A_1\ (1\ \text{mol}^{-1}\text{s}^{-1}) \qquad (30)$$

(ii) from the slope, the difference in activation energy.

$$E_1-E_3 = 2.303\ R.\text{slope}\ (\text{kcal mol}^{-1}) \qquad (31)$$

The ratio of formation of ethylene adduct to reverse fluoroethylene adduct is, by analogy with equation 29, given by:

$$\log[(e_t/e_2)\log g/\log h] = \log A_3 - \log A_2 + (E_2-E_3)/2.303\ RT \qquad (32)$$

From which:

(i) the intercept gives the A-factor difference,

$$\text{intercept} = \log A_3 - \log A_2\ (1\ \text{mol}^{-1}\ \text{s}^{-1}) \qquad (33)$$

(ii) the slope gives the activation energy difference.

$$E_2-E_3 = 2.303\ R.\text{slope}\ (\text{kcal mol}^{-1}) \qquad (34)$$

The more accurate experimental method of obtaining the ratio of ethylene adduct to each reverse fluoroethylene adduct requires consideration of two reaction series; the competitive series between ethylene and each fluoroethylene which gives the ethylene to normal fluoroethylene adduct ratio, and the series in the absence of ethylene which gives the normal to reverse fluoroethylene adduct ratio. That is, the sum of equations (24) and (28) give an experimentally more accurate ethylene adduct to reverse fluoroethylene adduct ratio than equation (32).

Competitive addition to ethylene and tetrafluoroethylene

The competitive addition of tribromofluoromethane to ethylene and tetrafluoroethylene, with a three fold excess of

tribromofluoromethane and equal quantities of olefins, gave three significant products, namely, the two adducts ($CFBr_2CH_2CH_2Br$ and $CFBr_2CF_2CF_2Br$) and a cross telomer ($CFBr_2CF_2CF_2CH_2CH_2Br$).

The reaction mechanism representing the formation of these products is:

$$XBr + h\nu \xrightarrow{k_1} X\cdot + Br\cdot \quad (35)$$

$$X\cdot + E \xrightarrow{k_2} XE\cdot \quad (36)$$

$$XE\cdot + XBr \xrightarrow{k_3} XEBr + X\cdot \quad (37)$$

$$X\cdot + F \xrightarrow{k_4} XF\cdot \quad (38)$$

$$XF\cdot + XBr \xrightarrow{k_5} XFBr + X\cdot \quad (39)$$

$$XF\cdot + E \xrightarrow{k_6} XFE\cdot \quad (40)$$

$$XFE\cdot + XBr \xrightarrow{k_7} XFEBr + X\cdot \quad (41)$$

$$2X\cdot \xrightarrow{k_8} X_2 \quad (42)$$

where $X\cdot = CFBr_2\cdot$, E = ethylene, F = tetrafluoroethylene

Application of the Steady State Approximation gives:

$$d[XE\cdot]/dt = k_2[X\cdot][E] - k_3[XE\cdot][XBr] = 0 \quad (43)$$

$$d[XF\cdot]/dt = k_4[X\cdot][F] - k_5[XF\cdot][XBr] - k_6[XF\cdot][E] = 0 \quad (44)$$

$$d[XFE\cdot]/dt = k_6[XF\cdot][E] - k_7[XFE\cdot][XBr] = 0 \quad (45)$$

Let $e = CFBr_2CH_2CH_2Br$

$f = CFBr_2CF_2CF_2Br$

$g = CFBr_2CF_2CF_2CH_2CH_2Br$

$$\therefore \quad de/dt = k_2[X\cdot][E] \quad (46)$$

$$\therefore \quad df/dt = k_4[X\cdot][F]/[1 + k_6[E]/k_5[XBr]] \quad (47)$$

$$\therefore \quad dg/dt = k_4[X\cdot][F]/[1 + k_5[XBr]/k_6[E]] \quad (48)$$

$$\therefore \quad [df + dg]/dt = k_4[X\cdot][F] \quad (49)$$

The variable ethylene concentration (E) is:

$$E = E_o - e - g \quad (50)$$

Let $e + g = ce$ where c is a constant. (51)

The experimental variation of the constant (c) over the temperature range of 80-180°C is less than 6%. (See table 1-9)

$$\therefore \quad dE = -cde \quad (52)$$

from equations (46) and (52):

$$-dE/cE = k_2[X^{\cdot}]dt \qquad (53)$$

integration between the limits of ethylene concentration and over the duration of the reaction gives:

$$-(1/c)\ln[1 - ce/E_o] = k_2[X^{\cdot}]t \qquad (54)$$

The variable tetrafluoroethylene concentration (F) is:

$$F = F_o - f - g \qquad (55)$$

$$\therefore \quad dF = -(df + dg) \qquad (56)$$

from equations (49) and (56)

$$-dF/F = k_4[X^{\cdot}]dt \qquad (57)$$

integration between the limits of tetrafluoroethylene concentration and over the duration of the reaction gives:

$$-\ln[1 - (f+g)/F_o] = k_4[X^{\cdot}]t \qquad (58)$$

substituting equation (51) into equation (54) and dividing by equation (58) gives:

$$\frac{e}{e+g} \cdot \frac{\ln[1 - (e+g)/E_o]}{\ln[1 - (f+g)/F_o]} = \frac{k_2}{k_4} = \frac{A_2\exp(-E_2/RT)}{A_4\exp(-E_4/RT)} \qquad (59)$$

$$\therefore \log \frac{e}{e+g} \cdot \frac{\log[1 - (e+g)/E_o]}{\log[1 - (f+g)/F_o]} = \log A_2 - \log A_4 + [E_4 - E_2]/2.303RT \qquad (60)$$

A plot of the L.H.S. against $10^3/T$ gives:

i) from the intercept, the A-factor difference,

$$\text{intercept} = \log A_{C_2H_4} - \log A_{C_2F_4} \ (1\ \text{mol}^{-1}\ \text{s}^{-1}) \qquad (61)$$

ii) from the slope, the difference in activation energy for the addition steps of dibromofluoromethyl radical to ethylene and tetrafluoroethylene,

$$E_{C_2H_4} - E_{C_2F_4} = -2.303\ R.\ \text{slope}\ (\text{kcal mol}^{-1}) \qquad (62)$$

The rate determining step in the addition of tribromofluoromethane to ethylene and the fluoroethylenes is the radical addition step.

$$CFBr_2^{\cdot} + E \xrightarrow{k_2} CFBr_2E^{\cdot}$$

The presence of only trace amounts of the dimer indicates that the

chain length is long and that the bromine abstraction step yielding the adducts is fast. Therefore the adduct ratios are equal to the relative rates of the addition steps.

Ethylene was reacted competitively with vinyl fluoride, 1,1-difluoroethylene, trifluoroethylene and tetrafluoroethylene. The competitive series with the unsymmetrical olefins gave the ethylene adduct to the normal fluoroethylene adduct ratios. The competitive series with tetrafluoroethylene gave the ethylene adduct to the tetrafluoroethylene adduct plus cross telomer ($CFBr_2CF_2CF_2CH_2CH_2Br$) ratio. The unsymmetrical olefins were reacted singly and gave the normal to reverse adduct ratios. The kinetic reaction series were conducted over a range of temperature. The Arrhenius plots are shown in figs 1-2 and 3. From the least squares treatment of the log of adduct ratio versus $10^3/T$ the relative activation energies, Arrhenius parameters and the addition rates were calculated (Table 1-11). The main features of table 1-11 are:

i) With attack at the $CH_2=$ group fluorine atoms on the carbon atom β to the site of attack reduce the rate of addition and conversely with attack at the $CF_2=$ group fluorine atoms on the carbon atom β to the site of attack increase the rate of addition.

ii) With addition to the $CH_2=$ group increasing the fluorine substituents on the carbon atom β to the site of attack slightly increases the activation energy.

iii) With addition to the $CF_2=$ group increasing the fluorine substituents on the carbon atom β to the site of attack greatly reduces the activation energy.

iv) For a constant terminal group in the adduct radical containing the lone electron, increasing the fluorine substituents on the carbon atom under attack greatly increases the activation energy with the exception of addition to tetrafluoroethylene.

v) The A factors favour addition to the most substituted ends of the unsymmetrical fluoroethylenes.

Fig 1-2 Arrhenius plots for competitive addition of $CFBr_2\cdot$ radicals to vinyl fluoride (⊗), 1,1-difluoroethylene (O) and trifluoroethylene (◑) in the presence of ethylene.

e_1 = normal fluoroethylene adduct; e_3 = ethylene adduct.

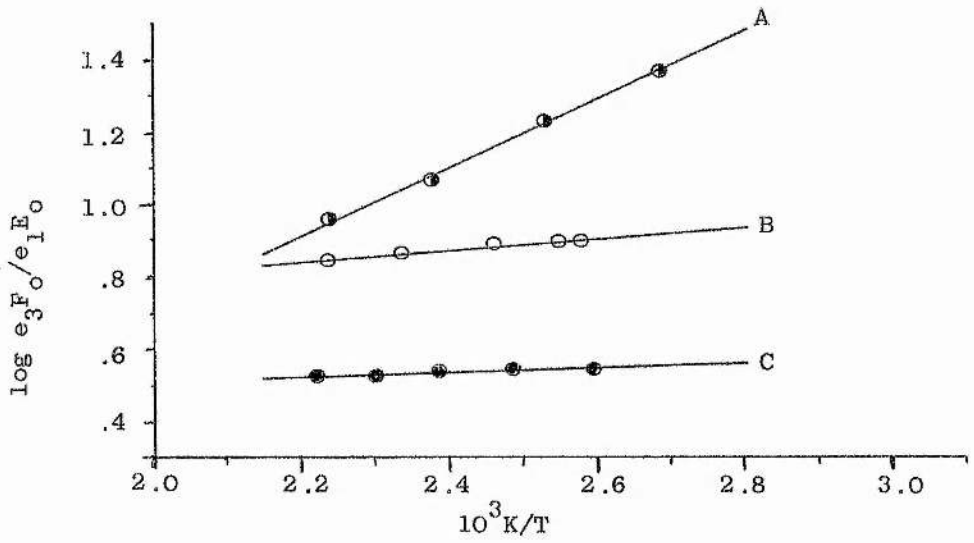

Fig 1-3 Arrhenius plots for addition of $CFBr_2\cdot$ radicals to vinyl fluoride (◑), 1,1-difluoroethylene (O) and trifluoroethylene (◑ for 366 nm and + for 265 nm). e_1 = normal adduct;

e_2 = reverse adduct.

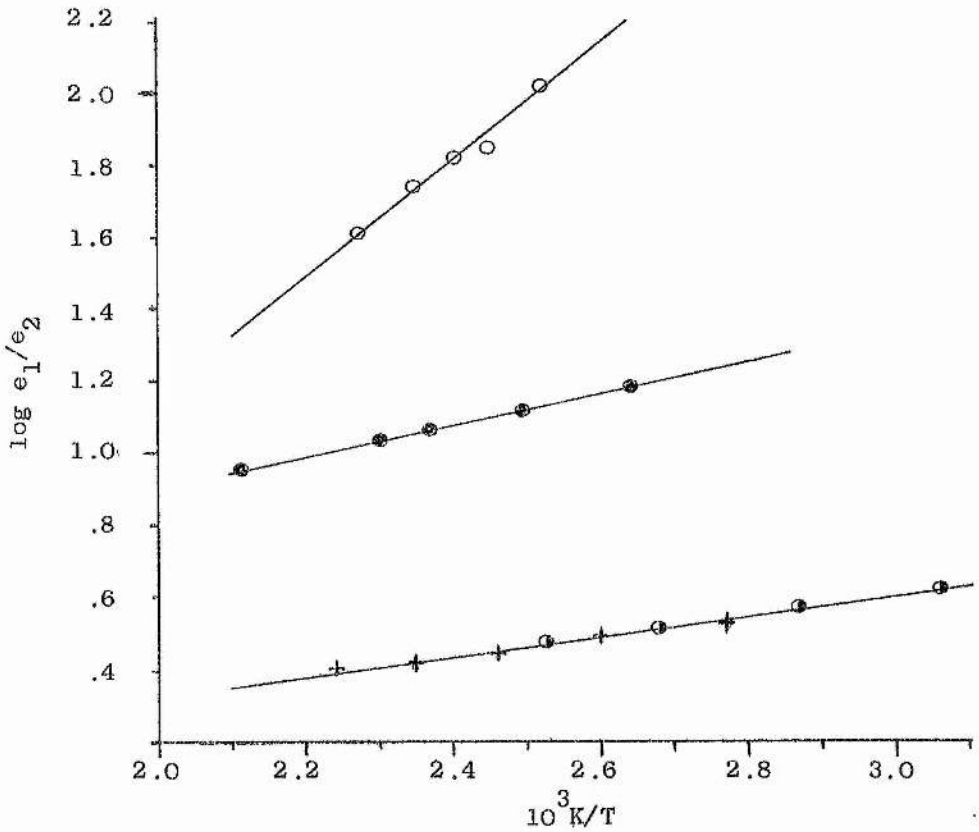

Table 1-11 The addition of $CFBr_2\cdot$ radicals to fluoroethylenes relative to ethylene.

Olefin	k_2/k_2' at 150°C	$\log A_2 - \log A_2'$	$E_2 - E_2'$
$^*CH_2{=}CH_2$	1.00	0.00	0.00
$^*CH_2{=}CHF$	0.28	-0.38 ± 0.01	0.32 ± 0.11
$^*CH_2{=}CF_2$	0.14	-0.46 ± 0.02	0.78 ± 0.23
$^*CHF{=}CH_2$	0.024	-0.41 ± 0.02	2.33 ± 0.20
$^*CHF{=}CF_2$	0.09	1.15 ± 0.04	4.30 ± 0.46
$^*CF_2{=}CH_2$	0.0024	1.53 ± 0.17	8.06 ± 1.83
$^*CF_2{=}CHF$	0.033	1.40 ± 0.05	5.63 ± 0.60
$^*CF_2{=}CF_2$	0.23	-0.53 ± 0.07	0.23 ± 0.82

* denotes the site of addition

k_2, A_2 and E_2 refer to addition to the fluoroethylene

k_2', A_2' and E_2' refer to addition to ethylene

A_2 and A_2' in 1 mol^{-1} s^{-1}

E_2 and E_2' in k cal mol^{-1}

The results highlight the inadequacy of Mayo and Walling's[10] initial theory that orientation of addition is determined by the resonance stabilization of the unpaired electron in the intermediate radical. Haszeldine[15] postulated that radical stability decreases as the number of hydrogen atoms directly attached to the carbon atom carrying the lone electron increases. This gives the order of reducing radical stability.

$$-CF_2\cdot > -CHF\cdot > -CH_2\cdot$$

The affinity of the electronegative fluorine atoms for the unpaired electron contribute towards increasing the stability of the intermediate radical. The experimental results are not in accord with the simple theory for addition to a $CH_2=$ group, however, there is agreement for addition to a $CF_2=$ group and for competitive addition to both ends of the unsymmetrical fluoroethylenes. The orientation ratios for addition of $CFBr_2\cdot$ to the unsymmetrical olefins at 150°C are $CH_2=CHF$ 1:0.085, $CH_2=CF_2$ 1:0.017, $CHF=CF_2$ 1:0.37. The suggestion of Waters[3] that electrophilic radicals preferentially attack the point of highest electron density is also not in accord for addition to the $CH_2=$ group in vinyl fluoride and 1,1-difluoroethylene relative to ethylene. These observations are general for the haloalkyl radical series $CFBr_2\cdot$, $CCl_3\cdot$, $C_3F_7\cdot$, $CF_2Br\cdot$, and $CF_3\cdot$. The rates of addition to the fluoroethylenes relative to ethylene for this series of radicals are shown in table 1-12.

The rate of haloalkyl radical addition to the fluoroethylenes varies with the number of fluorine atoms attached to the olefins. Upon increasing the fluorine atoms from zero to three, the rate of addition decreases to a minimum with trifluoroethylene and then increases to tetrafluoroethylene, with the exception of $C_3F_7\cdot$ which shows a continuous decrease. The overall rates of addition obtained from adding together the adducts from addition to both ends of the olefins are shown in table 1-13.

The selectivities in addition reactions to vinyl fluoride, 1,1-difluoroethylene and trifluoroethylene are compared in table 1-14.

Table 1-12 The Relative Rates of Addition of $CF_3^{\cdot}$, $C_3F_7^{\cdot}$, $CF_2Br^{\cdot}$, $CCl_3^{\cdot}$ and $CFBr_2^{\cdot}$ Radicals to Specific Sites in Fluoroethylenes at 150°C, Taking Ethylene as Standard.

OLEFIN	RADICALS				
	$CF_3^{\cdot}$	$C_3F_7^{\cdot}$	$CF_2Br^{\cdot}$	$CCl_3^{\cdot}$	$CFBr_2^{\cdot}$
$^{*}CH_2{=}CH_2$	1.0	1.0	1.0	1.0	1.0
$^{*}CH_2{=}CHF$	0.48	0.63	0.76	1.40	0.56
$^{*}CH_2{=}CF_2$	0.15	0.38	0.25	0.48	0.28
$^{*}CHF{=}CH_2$	0.052	0.067	0.070	0.10	0.048
$^{*}CHF{=}CF_2$	0.029	0.088	0.16	0.32	0.17
$^{*}CF_2{=}CH_2$	0.0049	0.0044	0.0074	0.0037	0.0048
$^{*}CF_2{=}CHF$	0.015	0.021	0.085	0.12	0.066
$^{*}CF_2{=}CF_2$	0.11	0.0056	0.11	1.00	0.23

* denote site of addition

The relative rates of addition are expressed per active site.

Table 1-13 Overall Rates of Addition to the Fluoroethylenes Relative to Ethylene at 150°C.

OLEFIN	No. of F ATOMS	RADICALS				
		$CF_3\cdot$	$C_3F_7\cdot$	$CF_2Br\cdot$	$CCl_3\cdot$	$CFBr_2\cdot$
$CH_2=CH_2$	0	1.0	1.0	1.0	1.0	1.0
$CH_2=CHF$	1	0.27	0.35	0.42	0.75	0.30
$CH_2=CF_2$	2	0.08	0.19	0.13	0.24	0.14
$CHF=CF_2$	3	0.022	0.055	0.12	0.22	0.12
$CF_2=CF_2$	4	0.11	0.0056	0.11	1.00	0.23

Table 1-14 Orientation of Radical Addition to Fluoroethylenes in the Gas Phase at 150°C.

RADICAL RADIUS[52] A°	RADICAL	$CH_2=CHF$	$CH_2=CF_2$	$CHF=CF_2$	REF.
3.92	$CF_3\cdot$	1:0.094	1:0.032	1:0.50	20
4.46	$CF_2Br\cdot$	1:0.089	1:0.030	1:0.46	22
5.16	$C_2F_5\cdot$	1:0.054	1:0.011	1:0.29	41
5.26	$CCl_3\cdot$	1:0.070	1:0.012	1:0.29	39
5.41	$CFBr_2\cdot$	1:0.085	1:0.017	1:0.37	This work
5.42	$C_3F_7\cdot$	1:0.050	1:0.009	1:0.25	21
6.62	$(CF_3)_2CF\cdot$	1:0.020	1:0.001	1:0.062	41

The main features of table 1-14 are:

i) Within the radical series under consideration, changes in the orientation ratios are consistent for the three unsymmetrical fluoroethylenes.

ii) The orientation ratio is a function of radical size and electronegativity, but radical size is of primary importance.

iii) The selectivity increases with increasing radical size with the exceptions of $C_2F_5\cdot$, $CCl_3\cdot$, and $CFBr_2\cdot$: these give an inverted order.

iv) The inverted selectivity order of $C_2F_5\cdot$, $CCl_3\cdot$, and $CFBr_2\cdot$ can be rationalised by accepting that in these cases the controlling factor is the electronegativity which decreases in the order

$$C_2F_5\cdot > CCl_3\cdot > CFBr_2\cdot$$

The correlation of radical radii with the logarithm of the orientation ratios for addition to vinyl fluoride, 1,1-difluoroethylene and trifluoroethylene are shown in figs 1-4a,b and c respectively. Although a considerable scatter of points is obtained, a reasonable trend is observed.

Coulson's[54] Free Valency Index (F_μ) and the π electron charge (Q_μ) are two parameters associated with the olefins for which correlations have been observed. Coulson's free valency index as calculated by simple Huckel theory is given by:

$$F_\mu = N_{max} - N_\mu$$

where N_μ is the sum of the π electron bond orders emitting from atom μ and N_{max} is the maximum possible value, usually taken as $\sqrt{3}$.

Kooyman and Farenhorst[55] showed that the logarithms of the rate constants for the addition of $CCl_3\cdot$ to aromatics was proportional to the free valence indices of the reactive sites. Walton[39] observed a similar trend for the addition of $CCl_3\cdot$, and Winton[21] for the addition of $C_3F_7\cdot$, to the fluoroethylenes.

The π electron charge density (Q_μ) at atom μ is the sum over all the occupied molecular orbitals of the electron densities at atom μ.

Fig 1-4 Plot of radical radii for the radical series $(CF_3)_2CF\cdot$, $C_3F_7\cdot$, $CFBr_2\cdot$, $CCl_3\cdot$, $C_2F_5\cdot$, $CF_2Br\cdot$, and $CF_3\cdot$ against the logarithm of the orientation ratio for addition to: a) - vinyl fluoride (●), b) - 1,1-difluoroethylene (○) and c) - trifluoroethylene (◐). e_1 = normal adduct, e_2 = reverse adduct.

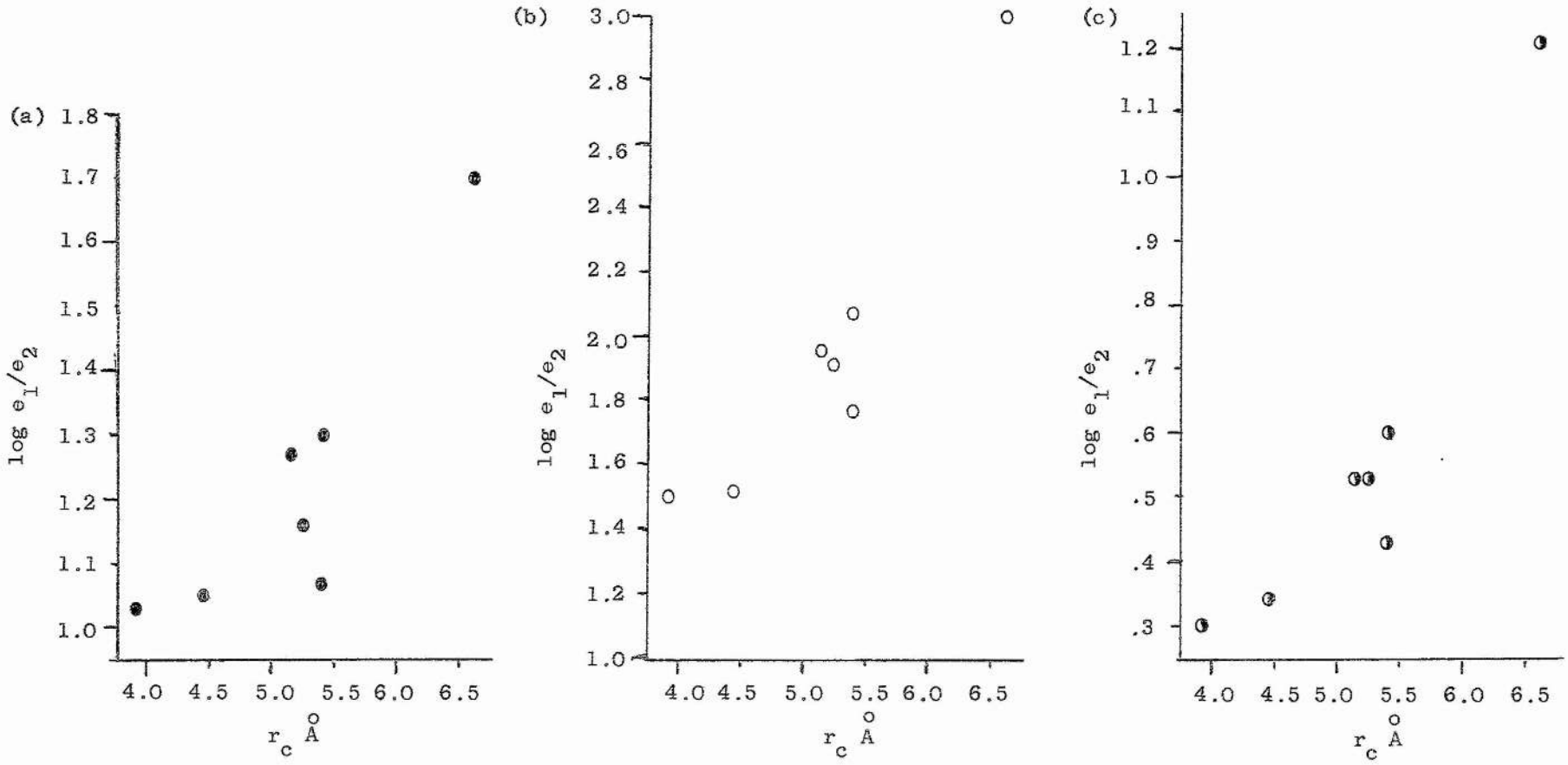

The free valence indices and the charge densities are shown in table 1-15. Accepting $CFBr_2\cdot$ as an electrophilic radical then both the F_μ and the charge densities correctly predict the preferred orientation of addition to each unsymmetrical olefin, but not the rate of addition to the $CH_2=$ ends of vinyl fluoride and 1,1-difluoroethylene relative to ethylene. The F_μ values of Landau[56] et al are plotted against the logarithms of the relative rate constants, taking addition to ethylene as standard, in fig 1-5. The correlation is rather poor.

Taking the addition of trifluoromethyl radicals to the fluoroethylenes as a standard series of reactions, and plotting the activation energy differences relative to ethylene (ΔE_a) for these standard reactions against the corresponding ΔE_a values for the addition of $CFBr_2\cdot$, $CCl_3\cdot$, C_3F_7 and $CF_3\cdot$ illustrates the similarities among this closely related family (fig 1-6). The correlations are approximately linear with the exception of $CFBr_2\cdot$ which may project a curve. The general trend is towards greater activation energies as the size of the radical increases.

The A-factors for addition of a particular radical show variation from one site of addition to another (Table 1-16). Increasing the fluorine content on the site of addition increases the A-factor for addition of the large radicals, $CFBr_2\cdot$, $CCl_3\cdot$ and $C_3F_7\cdot$, with the exception of tetrafluoroethylene where a decrease is observed for $CFBr_2\cdot$ and $C_3F_7\cdot$; the inverse situation applies with addition of the smaller $CF_3\cdot$ and $CF_2Br\cdot$ radicals. Increasing the fluorine content on the carbon atom β to the site of addition increases the A-factors for addition of $CFBr_2\cdot$, $CCl_3\cdot$, $CF_2Br\cdot$, $C_3F_7\cdot$, and $CF_3\cdot$ radicals, with the exceptions of $CFBr_2\cdot$ addition to tetrafluoroethylene (this result may be viewed with suspicion) and $C_3F_7\cdot$ addition to the $CF_2=$ group of the fluoroethylenes where the opposite trend was observed. Thus the experimental observations indicate that fluorine substitution in the fluoroethylenes is accompanied by greater A-factors as the radical size increases. The opposite trend

Table 1-15 Free Valence Indices and Charge Densities in Ethylene and the Fluoroethylenes, and log k_2/k_2' for Addition of $CFBr_2$·

OLEFIN	FREE VALENCE INDEX		Charge Densities (Q_μ)		
	ref. 16	ref. 56	ref. 16	ref. 56	log k_2/k_2'
*CH_2=CH_2	0.732	0.732	1.00	1.00	0
*CH_2=CHF	0.768	0.750	1.13	1.075	-0.25
*CH_2=CF_2	0.811	0.770	1.25	1.145	-0.65
*CHF=CH_2	0.513	0.571	0.93	0.956	-1.32
*CHF=CF_2	0.622	0.622	1.17	1.097	-0.77
*CF_2=CH_2	0.291	0.401	0.87	0.917	-2.32
*CF_2=CHF	0.350	0.434	0.98	0.985	-1.18
*CF_2=CF_2	0.419	0.470	1.05	1.052	-0.64

* denotes the carbon atom under consideration

k_2' refers to the rate of addition to ethylene per active site

k_2 " " " " " " to the fluoroethylenes per active site.

Fig 1-5 Correlation of relative rate constants with free valence indices (F_μ),

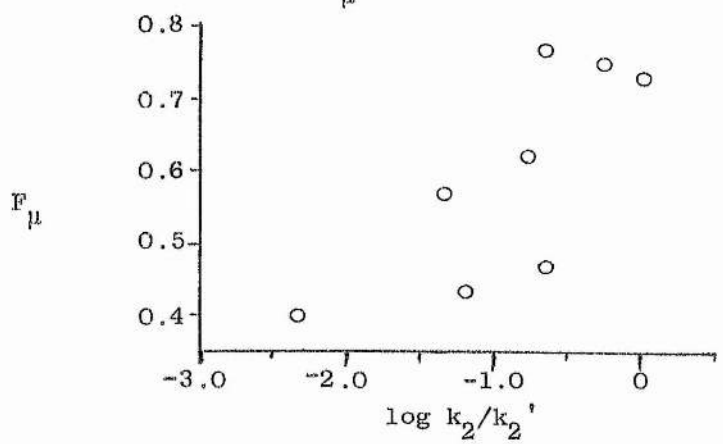

Fig 1-6 Plot of activation energy differences ($\triangle E_a$) for addition of $CFBr_2\cdot$ (+), $CCl_3\cdot$ (⊕), $C_3F_7\cdot$ (○) and $CF_3\cdot$ radicals against $\triangle E_a$ for addition of $CF_3\cdot$ radicals to the fluoroethylenes relative to ethylene.

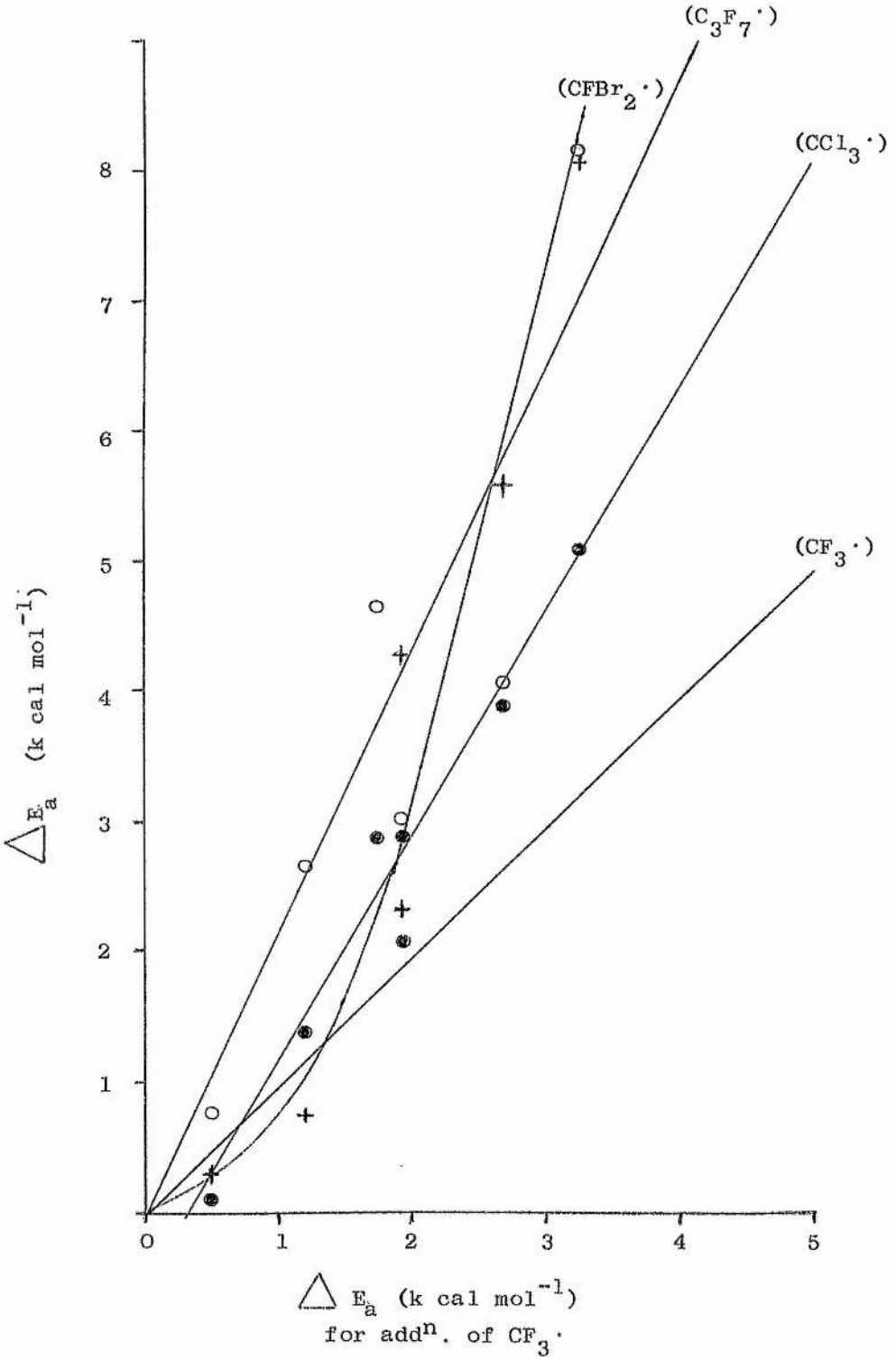

is expected owing to the slightly smaller size of a hydrogen atom. Other contributing factors are the geometric positions of the hydrogen and fluorine atoms in the olefins and the direction of approach by the radicals. The increase in A-factors accompanied by increasing the fluorine content in the fluoroethylenes is shown in fig 1-7 by the increment in the slopes as the size of the radical increases in going from vinyl fluoride to trifluoroethylene. The fig 1-7 shows a plot of the sum of the A-factor differences for addition to both ends of the unsymmetrical olefins relative to ethylene against the radii of the free radical series $CFBr_2^{\cdot}$, $CCl_3^{\cdot}$, $CF_2Br^{\cdot}$, $C_3F_7^{\cdot}$, and $CF_3^{\cdot}$. Each line also gives a correlation although rather poor. The A-factor differences for the normal trifluoroethylene and reverse trifluoroethylene adducts relative to ethylene are plotted against radical size in figs 1-8. Once again correlations are obtained although they are rather poor.

Tedder and Walton[11] proposed that the primary consideration should be given to the site of attack and not the site of the odd electron in the addend radical. This is substantiated in Table 1-16 where the activation energy differences in going down the columns for attack at constant sites are quite small. On the other hand, on going along the rows where the site of attack varies from a $CH_2=$ group to a $CF_2=$ group the activation energy changes are quite large. This confirms the general nature of Tedder and Walton's observations that the rate of $CCl_3^{\cdot}$ addition to olefins is determined principally by the substituents on the attacked carbon atom and only to a lesser extent on the carbon atom surrounded by the unpaired electron. They also proposed that the orientation of radical addition is determined principally by the relative strengths of the two bonds formed, but this leads to the same orientation predictions as Mayo and Walling's initial theory, when the stronger bond is assumed to be the one which gives the greater resonance stabilization of the unpaired electron in the intermediate radical.

Many attempts have been made to correlate rates of addition and

Fig 1-7 Plots of the sum of the A-factor differences for add^{n}. to both ends of vinyl fluoride (⊖,A), 1,1-difluoroethylene (O,B) and trifluoroethylene (◑,C) relative to ethylene against the radii of $CFBr_2\cdot$, $CF_2Br\cdot$, $CCl_3\cdot$, $C_3F_7\cdot$ and $CF_3\cdot$ radicals.

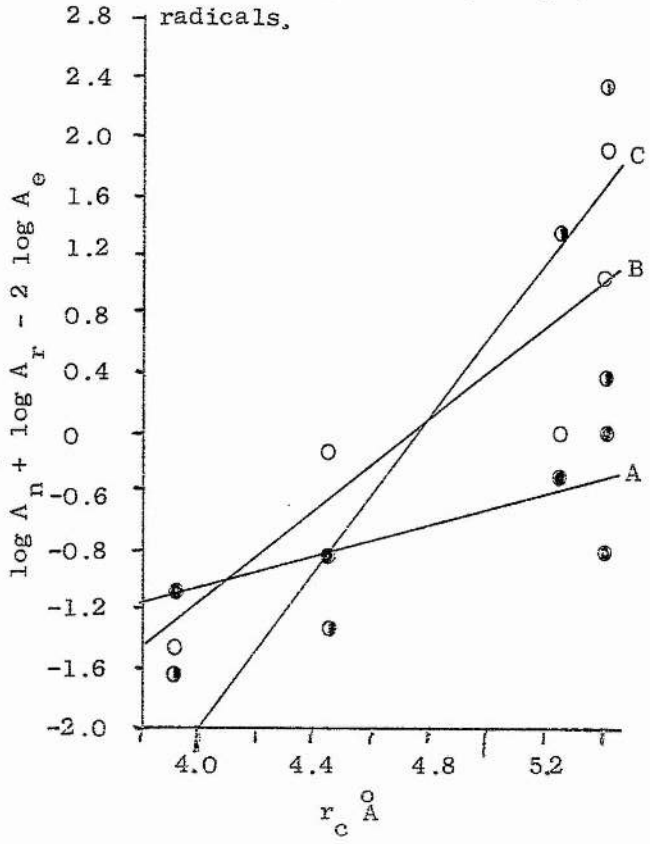

Fig 1-8 Plot of radii of $CFBr_2\cdot$, $CF_2Br\cdot$, $CCl_3\cdot$ and $CF_3\cdot$ radicals against the A-factor differences relative to ethylene for a) normal and b) reverse trifluoroethylene adducts.

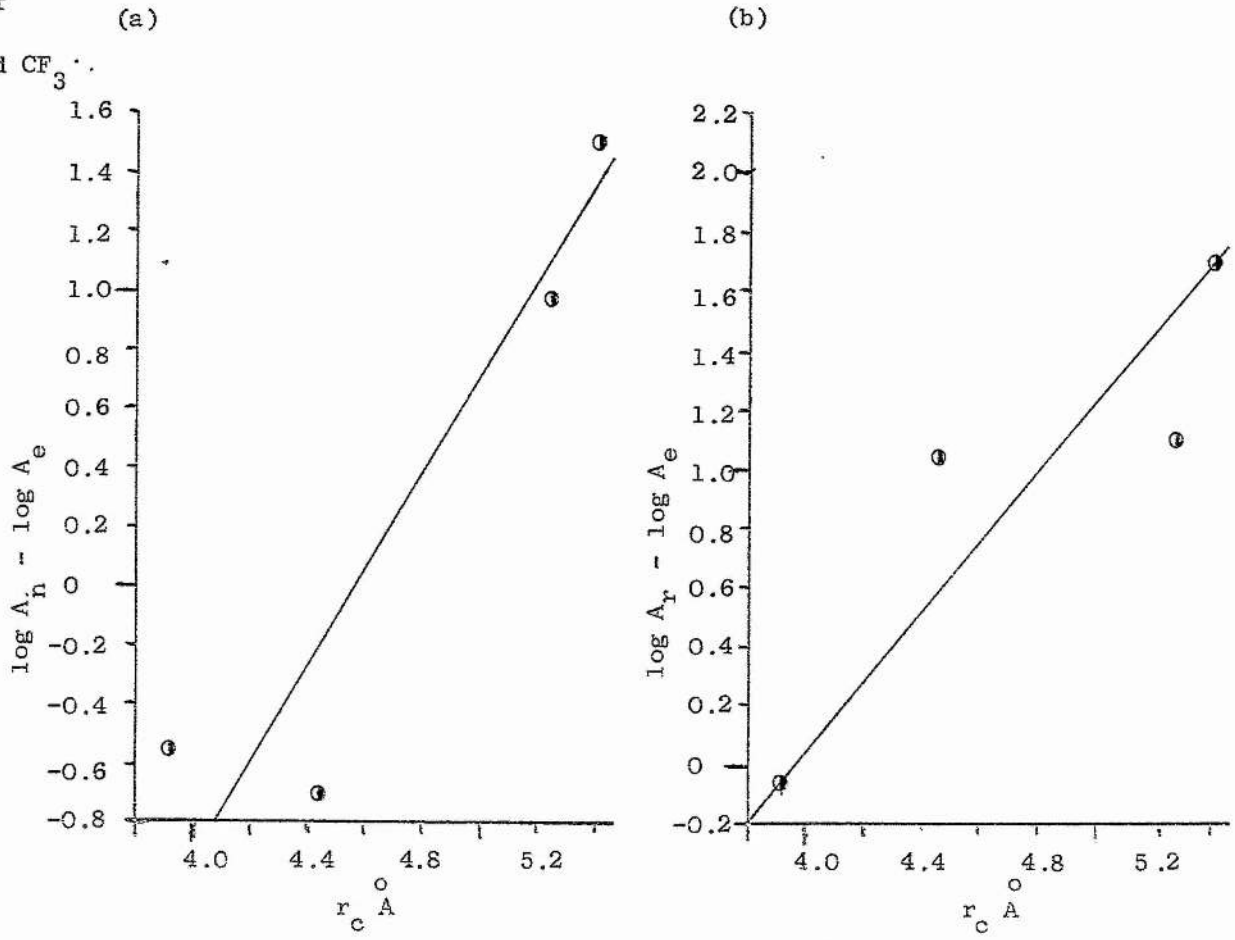

Table 1-16 Addition of Halomethyl Radicals to Fluoroethylenes in the Gas Phase

RADICAL	Addn. to CH_2=	$\log A_2 - \log A_2'$	$E_2 - E_2'$	Addn. to CHF=	$\log A_2 - \log A_2'$	$E_2 - E_2'$	Addn. to CF_2=	$\log A_2 - \log A_2'$	$E_2 - E_2'$	REF.
	$CH_2=CH_2$	0.0	0.0	$CHF=CH_2$	-0.11 ± 0.02	2.33 ± 0.20	$CF_2=CH_2$	1.83 ± 0.17	8.06 ± 1.83	
$CFBr_2\cdot$	$CH_2=CHF$	-0.08 ± 0.01	0.32 ± 0.11	-			$CF_2=CHF$	1.70 ± 0.05	5.63 ± 0.60	This Work
	$CH_2=CF_2$	-0.16 ± 0.02	0.78 ± 0.23	$CHF=CF_2$	1.45 ± 0.04	4.30 ± 0.46	$CF_2=CF_2$	-0.53 ± 0.07	0.23 ± 0.82	
	$CH_2=CH_2$	0.0	0.0	$CHF=CH_2$	0.1 ± 0.5	2.1 ± 0.5	$CF_2=CH_2$	0.2 ± 0.6	5.1 ± 0.8	
$CCl_3\cdot$	$CH_2=CHF$	0.2 ± 0.5	0.1 ± 0.5	-			CF_2CHF	1.1 ± 0.7	3.9 ± 1.0	39
	$CH_2=CF_2$	0.4 ± 0.6	1.4 ± 0.6	$CHF=CF_2$	1.0 ± 0.7	2.9 ± 1.1	$CF_2=CF_2$	1.5 ± 0.8	2.9 ± 0.7	
	$CH_2=CH_2$	0.0	0.0	$CHF=CH_2$	-0.31 ± 0.12	1.64 ± 0.45	$CF_2=CH_2$	0.16 ± 0.04	4.43 ± 0.57	
$CF_2Br\cdot$	$CH_2=CHF$	0.09 ± 0.04	0.40 ± 0.15	-			$CF_2=CHF$	-0.04 ± 0.08	2.00 ± 0.70	22
	$CH_2=CF_2$	0.33 ± 0.03	1.80 ± 0.40	$CHF=CF_2$	-0.69 ± 0.20	0.22 ± 0.50	$CF_2=CF_2$	1.05 ± 0.10	3.90 ± 0.80	
	$CH_2=CH_2$	0.0	0.0	$CHF=CH_2$	0.39 ± 0.10	3.03 ± 1.05	$CF_2=CH_2$	1.87 ± 0.13	8.19 ± 1.28	
$C_3F_7\cdot$	$CH_2=CHF$	0.21 ± 0.04	0.79 ± 0.41	-			$CF_2=CHF$	0.44 ± 0.07	4.09 ± 0.82	21
	$CH_2=CF_2$	0.96 ± 0.02	2.67 ± 0.23	$CHF=CF_2$	0.52 ± 0.04	3.05 ± 0.46	$CF_2=CF_2$	0.16 ± 0.12	4.67 ± 1.51	
	$CH_2=CH_2$	0.0	0.0	$CHF=CH_2$	-0.29 ± 0.08	1.92 ± 0.46	$CF_2=CH_2$	-0.64 ± 0.13	3.24 ± 0.96	
$CF_3\cdot$	$CH_2=CHF$	-0.07 ± 0.03	0.49 ± 0.13	-			$CF_2=CHF$	-0.46 ± 0.07	2.65 ± 0.72	20
	$CH_2=CF_2$	-0.22 ± 0.04	1.20 ± 0.34	$CHF=CF_2$	-0.55 ± 0.02	1.91 ± 0.50	$CF_2=CF_2$	-0.06 ± 0.04	1.74 ± 0.22	

A_2 and E_2 refer to addition to the fluoroethylenes

A_2' and E_2' refer to addition to the ethylene

The 'A' factor differences are expressed per active site

activation energies using Huckel Molecular Orbital theory. Two transition states have been proposed[19], a π and a σ~ transition state (figs 1-9a and b). The formation of a π complex is described by means of a π bond localisation process[57] and suggests that the activation energy will correlate with the bond localisation energies. Cvetanović[58] proposed a π-transition state for the addition of oxygen atoms to olefins, and Stefani[19] concluded that the highly nucleophilic cyclopropyl radical also adds to olefins through a π transition state. In the σ~ complex a well-defined primary valence bond between the radical and the substrate is developed and the structure of the complex is essentially like that of the product radical. In the Molecular Orbital theory the activation process resulting in a σ~ transition state is related to the localisation of an electron on the carbon atom of the substrate which undergoes rehybridisation during the reaction. Activation energies for radical addition to olefins involving a σ~ transition state are expected to correlate with atom localisation energies.

Winton[59] executed potential energy surface calculations on an IBM 360/44 computer using the program CNINDO[60] (intermediate neglect of differential overlap) for the addition of methyl radicals to the CH_2= end of vinyl fluoride. The main conclusions were:

i) The carbon-carbon bond between the radical and the olefin was relatively long in the transition state, showing that the transition state resembles the reactants rather than the products.

ii) That the most energetically favourable direction of attack was directly on to the carbon atom at right angles to the plane of the molecule.

iii) Attack on the double bond was not favoured.

Winton's results combined with the experimental observations that the addition of haloalkyl radicals correlate better with atom rather than bond localisation energies indicate that reactions proceed by σ~ transition states. Furthermore, the observation that different

Fig 1-9 Schematic representations of reaction pathways via a) a π transition state and b) a σ transition state for addition of halomethyl radicals to an unsymmetrical fluoroethylene.

E_a = activation energy

(n) refers to normal fluoroethylene adduct

(r) refers to reverse fluoroethylene adduct

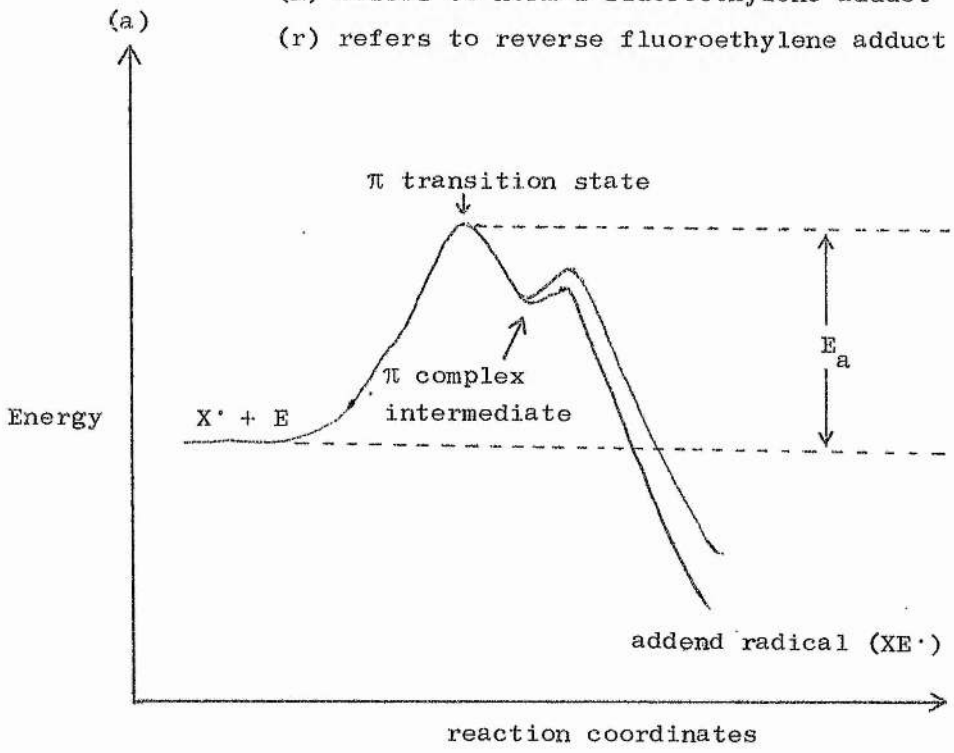

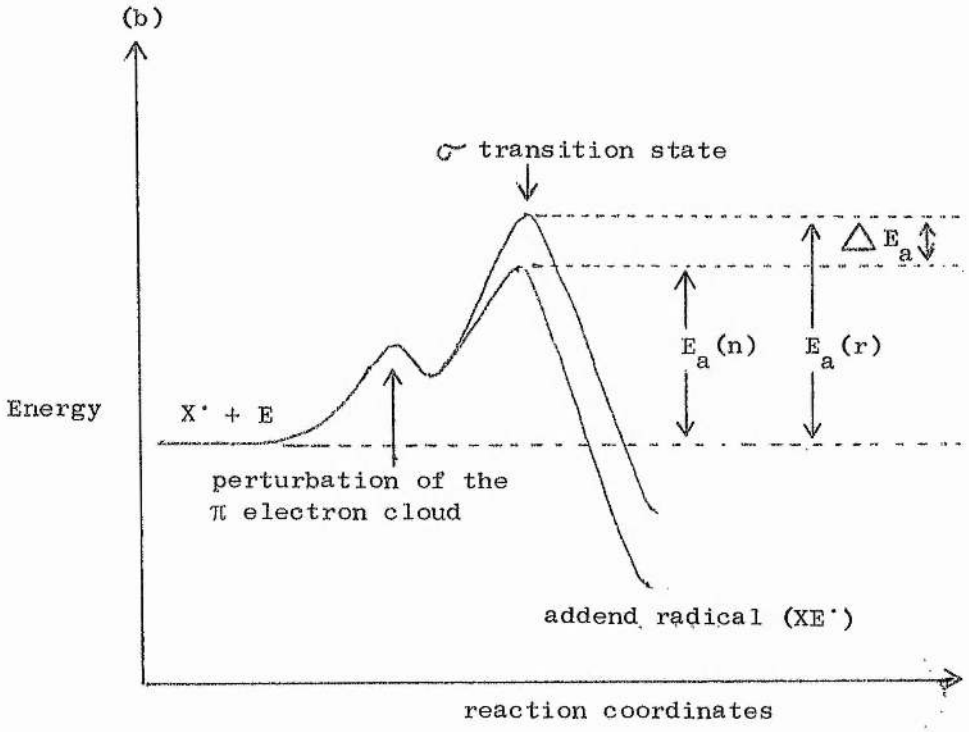

activation energies were obtained for addition to the two ends of each unsymmetrical fluoroethylene is excellent experimental proof that the top of the potential energy barrier corresponds to a σ- transition state (c.f. fig 1-9b).

The atom localisation energy (L_μ) is the energy required to localise one of the π electrons at a particular atom and can be calculated using Huckel Molecular Orbital theory.

$$L_\mu = E_\pi - E_\pi'$$

Where E_π is the π energy of the fully delocalised molecule and E_π' is the π energy of the molecule having one electron localised at atom μ. The π electron energies for the fluoroethylenes have been calculated using values for the fluorine coulomb (α_F) and resonance (β_{FC}) integrals

$$\alpha_F = \alpha_C + h\beta_{CC}; \quad \beta_{FC} = k\beta_{CC}$$

Streitweiser[61] suggested values for these integrals from the properties of aromatic compounds. Walton[39] using the range of values recommended by Streitweiser observed similar correlations between localisation energy and activation energy for the addition of $CCl_3^\cdot$ to the fluoroethylenes. The localisation energies are shown in table 1-17 using the integral values:

$$\alpha_C = 10\beta_o, \; \alpha_F = 12.73\beta_o, \; \beta_{FC} = 0.908\beta_o$$

The correlation of atom localisation energy with activation energy for addition of $CFBr_2^\cdot$ to the fluoroethylenes relative to ethylene is shown in fig 1-10. A reasonable correlation is obtained. The experimental points fall naturally into three groups. From left to right the first three points are for addition to $CH_2=$ groups, the next two points are for addition to $CHF=$ groups and the final three points are for addition to $CF_2=$ groups. Each of these three sets define three additional straight lines (a, b and c) for which the activation energy differences correlate with the atom localisation energy.

A polar term was introduced by Tedder and Walton[62] to improve the correlation in the addition of $CCl_3^\cdot$ radicals by consideration of the

Fig 1-10 Correlation of activation energy relative to ethylene with Lμ.

subsiduary correlations are:

line a = add^{n}. to $=CH_2$ sites (⊗)

line b = add^{n}. to =CHF sites (◑)

line c = add^{n}. to $=CF_2$ sites (○)

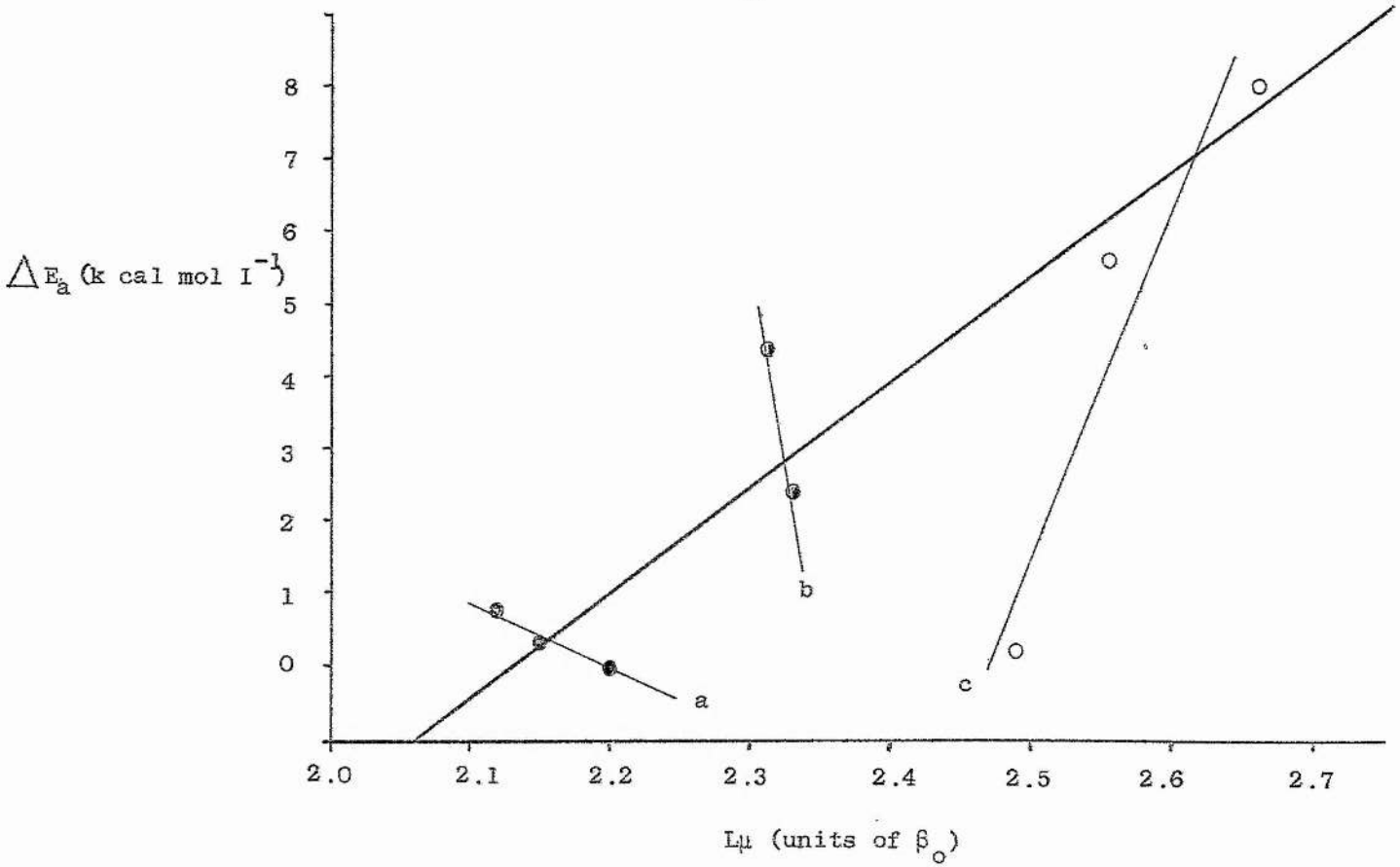

coulombic repulsion between the radical and the attacked site in the olefin. The repulsion was considered proportional to the charge on the radical and on the attacked site, but the charge on the radical is constant for the series of additions so the new term is set proportional to the net charge on the attacked carbon atom. The correlation between the activation energy differences and the refined localisation energy parameter is represented by;

$$E_2 - E_2' \propto L_\mu - B\delta Q_\mu$$

where: E_2 = activation energy for addition to the fluoroethylenes

E_2' = " " " " " " ethylene

B = a constant

The correlations of the activation energy differences for the addition of $CFBr_2^\cdot$, $CCl_3^\cdot$, $C_3F_7^\cdot$ and $CF_3^\cdot$ to the fluoroethylenes with the new parameter ($L_\mu - B\delta Q_\mu$) are shown in fig 1-11. The correlations are quite good, and they correctly predict the orientation ratios for addition to both the $CH_2=$ and $CF_2=$ groups of the fluoroethylenes relative to ethylene, but once again three additional lines are evident, one for attack at each of the different sites in the fluoroethylenes. This point is illustrated in fig 1-12 which shows a plot of $L_\mu - B\delta Q_\mu$ against the activation energy differences for the addition of the series of haloalkyl radicals to the three different types of sites ($CH_2=$, $CHF=$, $CF_2=$) in the fluoroethylenes relative to ethylene. The activation energy differences for addition to $CH_2=$ groups (●) and for addition to $CF_2=$ groups (○) correlate well with $L_\mu - B\delta Q_\mu$: much scatter is shown for addition to $CHF=$ groups (◑).

An improved overall correlation is obtained by optimising the contribution from the coulombic repulsion term for addition to each type of site. The improved correlation is shown in fig 1-13. Zero coulombic repulsion for addition to the $CF_2=$ group gives the best fit. The optimum values of B for addition to the $CH_2=$ group were: $CFBr_2^\cdot$, 0.5; $CCl_3^\cdot$, 0.8; $C_3F_7^\cdot$, 0.9; $CF_3^\cdot$, 0.9. Intermediate values

Fig 1-11 Correlation of the refined localisation energy parameter with ΔE_a for addition of:

a) $CFBr_2\cdot$ (B = 0.5) and $CCl_3\cdot$ (B = 0.7)

b) $C_3F_7\cdot$ (B = 0.9) and $CF_3\cdot$ (B = 0.9)

Fig 1-12 Correlation diagram of ΔE_a with $L\mu - B\delta Q\mu$ for addition of $CFBr_2\cdot$, $CCl_3\cdot$, $C_3F_7\cdot$ and $CF_3\cdot$ radicals to $=CH_2$ (⊕), $=CHF$ (◑) and $=CF_2$ (O) sites in fluoroethylenes.

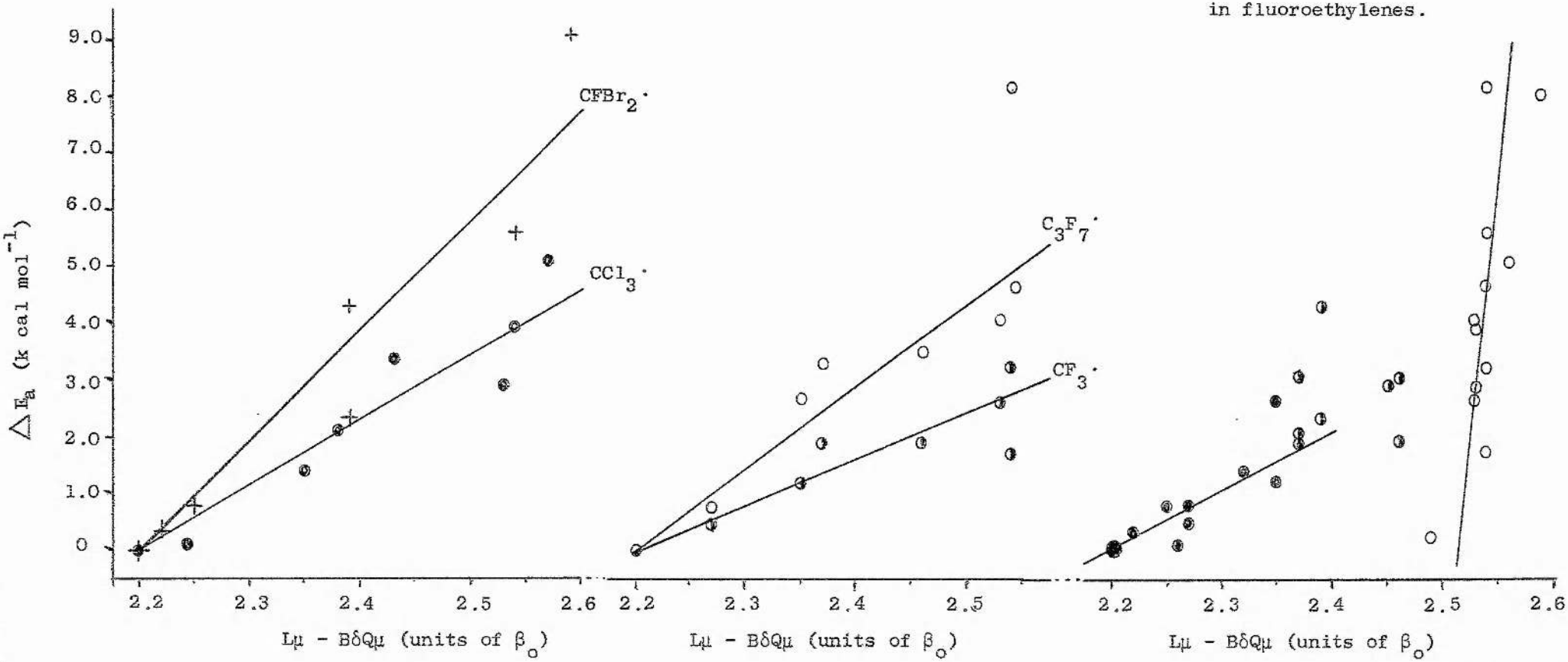

were used for addition to the CHF= group although higher values give better fits.

The outstanding observations from fig 1-13 are:

i) That the atom localisation energy is proportional to the activation energy for the addition of haloalkyl radicals to CF_2= sites in the fluoroethylenes.

ii) That for addition to CH_2= sites in the fluoroethylenes the atom localisation energy requires modifying to take into account the coulombic repulsion between the radical and the CH_2= sites for correlation with activation energies.

Table 1-17

OLEFIN	L_μ	δQ_μ	$L_\mu - 0.5\delta Q_\mu$	$L_\mu - 0.7\delta Q_\mu$	$L_\mu - 0.9\delta Q_\mu$	Δ Ea (k cal mol^{-1}) $CFBr_2\cdot$	$CCl_3\cdot$	$C_3F_7\cdot$	$CF_3\cdot$
$CH_2=CH_2$	2.20	0.00	2.20	2.20	2.20	0.00	0.00	0.00	0.00
$CH_2=CHF$	2.15	-0.13	2.22	2.24	2.27	0.32	0.10	0.79	0.49
$CH_2=CF_2$	2.12	-0.25	2.25	2.30	2.35	0.78	1.40	2.67	1.20
$CHF=CH_2$	2.43	+0.07	2.39	2.38	2.37	2.33	2.10	3.03	1.92
$CHF=CF_2$	2.31	-0.17	2.39	2.43	2.46	4.30	2.90	3.05	1.91
$CF_2=CH_2$	2.66	+0.13	2.59	2.57	2.54	8.06	5.10	8.19	3.24
$CF_2=CHF$	2.55	+0.02	2.54	2.54	2.53	5.63	3.90	4.09	2.65
$CF_2=CF_2$	2.49	-0.05	2.51	2.53	2.54	0.23	2.90	4.67	1.74

Fig 1-13 Correlation of $L_\mu - B\delta Q\mu$ with $\triangle E_a$ for add^n. of $CFBr_3\cdot$, $CCl_3\cdot$, $C_3F_7\cdot$ and $CF_3\cdot$ radicals to the fluoroethylenes. For add^n. to CH_2= sites values of B were: $CFBr_2\cdot$, 0.5; $CCl_3\cdot$, 0.8; $C_3F_7\cdot$ and $CF_3\cdot$, 0.9. For add^n. to CF_2= sites B = 0. For add^n. to CHF= sites intermediate values of B were used.

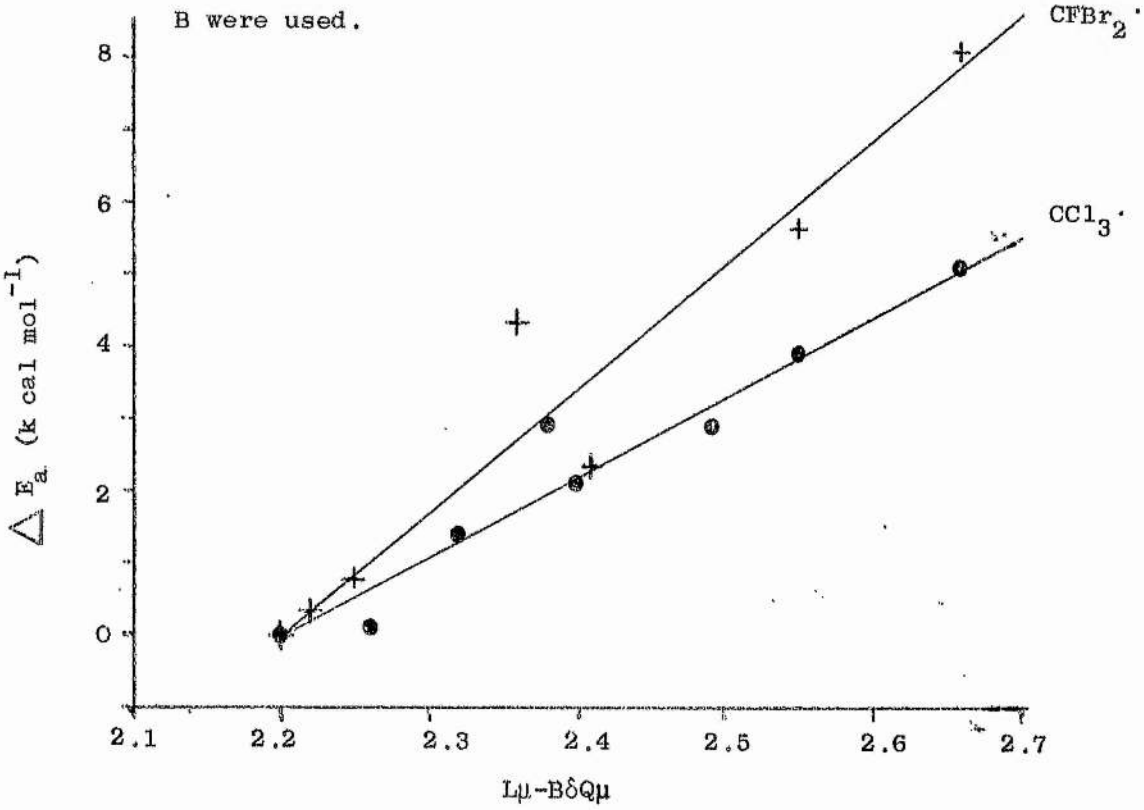

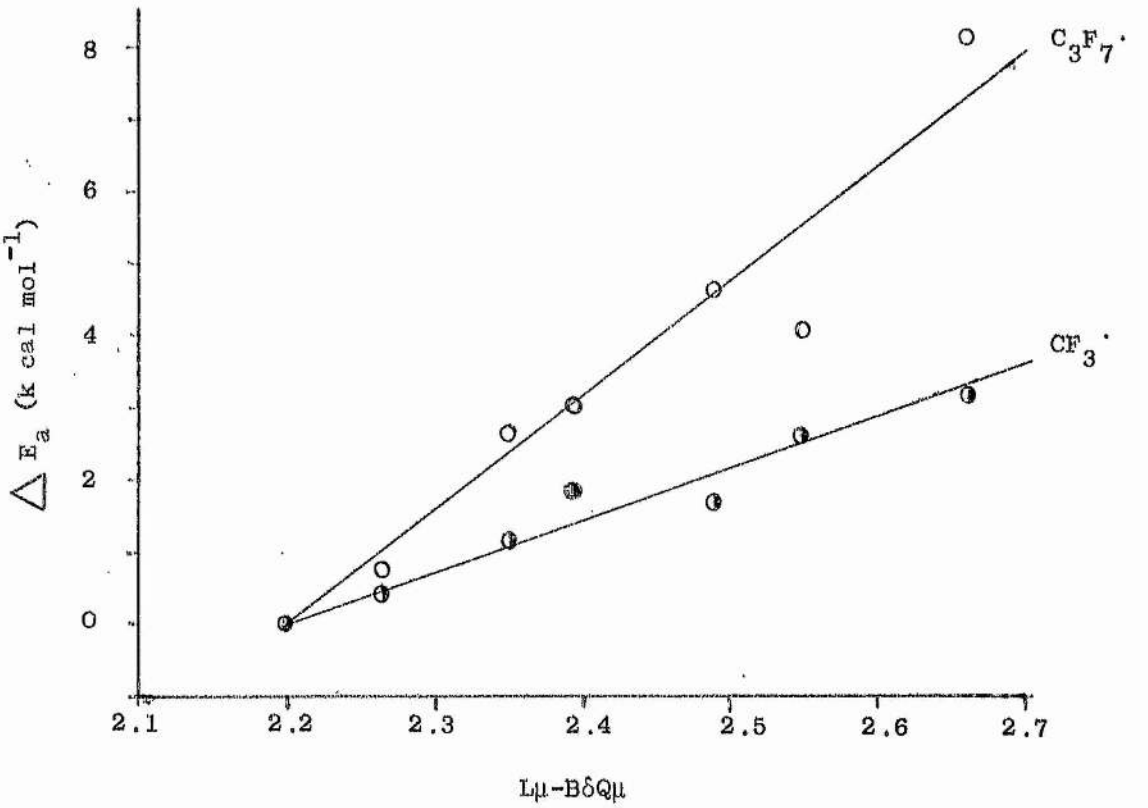

PART 2

The Addition of Difluoromethyl and Difluoroiodomethyl Radicals to Fluoroethylenes

Introduction

A survey of the chemical literature reveals, a few methods for preparing difluoroiodomethane (CHF_2I) together with values of several physical constants, and data on the geometry and reactions of difluoromethyl radicals. Difluoroiodomethyl radicals are not mentioned in the literature.

Ruff[74] et al. prepared CHF_2I by taking various proportions of iodoform, mercurous fluoride and calcium fluoride and gradually heating the mixtures to about 150°C. The reaction products were condensed in liquid air and separated by fractional distillation. The boiling point (bp 21.6°C) and freezing point (fp 122.0°C) were determined. Simons[75] et al. reacted iodine pentafluoride with iodoform in a copper reaction vessel and obtained two products, trifluoromethane and difluoroiodomethane in the ratio of fifteen to one. Haszeldine[76] prepared many fluorohalomethanes, including difluoroiodomethane, by the reactions of silver salts of fluorohalogeno-acids with chlorine, bromine and iodine. Haszeldine postulated a free radical mechanism for this general class of reactions:

$$CYZFCO_2Ag + X_2 \longrightarrow CYZFCO_2X + AgX$$

$$CYZFCO_2X \xrightarrow{\text{heat}} CYZF\cdot + CO_2 + X\cdot$$

$$CYZF\cdot + X_2 \longrightarrow CXYZF + X\cdot$$

where Y,Z = H,F,Cl,Br ; $X_2 = Cl_2, Br_2, I_2$

Haszeldine also gives the order of radical reactivity,

$CFBr_2\cdot < CFCl_2\cdot < CF_2Cl\cdot < CHFCl\cdot < CHF_2\cdot < CF_3\cdot < C_2F_5\cdot$,

and observes that difluoromethyl radicals undergo some dimerisation and react with glass to give silicon tetrafluoride and carbon dioxide. In a similar reaction Yarovenko[77] et al. prepared CHF_2I by slowly heating a mixture of Mercury II difluoroacetate and iodine. Rowland and Smail[78] studied the insertion reactions of monofluoro-carbene ($:CH^{18}F$) and difluorocarbene ($:CF^{18}F$) with hydrogen halides.

The fluorocarbenes were produced by secondary decomposition reactions of excited ^{18}F-labelled molecules formed by hot ^{18}F atom reactions with various precursor molecules, including CF_4, CHF_3, $C_2H_2F_4$ and C_2F_4. The insertion reaction of difluorocarbene with hydrogen iodide occurs readily to give excited difluoroiodomethane, with 19k cal mol^{-1} vibrational energy in excess of the C-I bond dissociation energy, which upon collisional deactivation gives the stable molecule: the exothermicity of the analogous reaction forming fluoroiodomethane is sufficiently great to cause complete decomposition to fluoromethyl radicals and iodine atoms. Blume[79] et al. prepared CHF_2I by reacting iodoform with silver fluoride giving $CHFI_2$ (35%) and CHF_2I (15 %)

Maslov and Maslov[36], from the elements in the gaseous state at 25°C, determined the heats of formation for numerous halomethanes including CHF_2I (92k cal mol^{-1}). Papulov[80] et al. have calculated the energies of carbon-hydrogen and carbon-halogen bond cleavages for 70 halomethanes (CXYZQ : X,Y,Z,Q = H,F,Cl,Br,I) as a linear function of the atomic dissociation parameters of X,Y,Z and Q. Lossing[81] has calculated the ionisation potentials and bond dissociation energies of chloromethyl and fluoromethyl radicals.

Hine and Ketley[82] studied the reaction of CHF_2I with ethanolic potassium hydroxide and observed the formation of CHF_3 and $CH_3CH_2OCHF_2$. From their study of the reaction kinetics they concluded that the reaction is initiated by a concerted α - dehydroiodination to yield difluoromethylene directly in one step. From further work by Hine and Langford[83], hydrolysis rate data indicated that fluorine atoms stabilise dihalomethylenes much better that other halogen atoms, and that two fluorine atoms add so greatly to the tendency of the carbanion to decompose to the dihalomethylene that decomposition is instantaneous. That is, as the removal of the haloform hydrogen begins, the negative charge thus placed on carbon atom causes the synchronised cleavage of the carbon-iodine bond.

$$HO^- + CHF_2I \longrightarrow \overset{\delta-}{HO}\cdots H\cdots \overset{\delta-}{CF_2}\cdots \overset{\delta-}{I} \longrightarrow HOH + :CF_2 + I^-$$

Several hydrogen abstraction reactions of difluoromethyl radicals have been studied. Perona and Pritchard[84] examined the hydrogen abstraction reactions of difluoromethyl radicals with $(CHF_2)_2CO$, H_2, D_2, CH_4, C_2H_6, $n\text{-}C_4H_{10}$ and $iso\text{-}C_4H_{10}$: the activation energy varied in the range of 9.3 k cal mol^{-1} for $iso\text{-}C_4H_{10}$ to 16.8 k cal mol^{-1} for CH_4. Kerr and Timlin studied the hydrogen abstraction reactions of difluoromethyl radicals with tetramethylsilane[85] and trichlorosilane[86] and compared the results for the fluoromethyl radical series. For the hydrogen abstraction reactions with tetramethylsilane, the activation energies were interpreted in terms of the enthalpy changes for the reactions and a polar effect operative between the attacking fluoromethyl radicals and the substrate which tends to reduce the activation energies progressively as the fluorine content of the radical increases. This polar effect, which decreases the activation energy for hydrogen abstraction from tetramethylsilane in the series $CH_3\cdot$ to $CF_3\cdot$, is in marked contrast to the polar repulsion between the fluorinated radicals and trichlorosilane which was tentatively proposed to explain the increase in the activation energy for hydrogen abstraction from $SiHCl_3$.

Numerous studies have been conducted on the disproportionation and combination of fluoromethyl radicals. Gunning[87] et al. studied the mercury photosensitised photolysis of chlorodifluoromethane and under the operative experimental conditions observed both the radical-radical disproportionation reaction giving difluorocarbene, and the dimersation reaction giving 1,1,2,2-tetrafluoroethane: the experimental recombination to disproportionation ratio was approximately five to one.

$$2CHF_2\cdot \longrightarrow CH_2F_2 + :CF_2$$

$$2CHF_2\cdot \longrightarrow CHF_2CHF_2$$

Bryant and Pritchard[88] generated difluoromethyl radicals by the photolysis of $(CHF_2)_2CO$ and by contrast observed the combination-

elimination reaction producing trifluoroethylene and hydrogen flouride.

$$2CHF_2\cdot \longrightarrow CHF{=}CF_2 + HF$$

Low pressures favour the elimination of HF and high pressures favour the formation of difluoromethylene. Pritchard and coworkers also studied the combination-disproportionation reaction of $CH_3\cdot$ plus $CHF_2\cdot$ radicals[89] generated from the photolysis of CH_3COCHF_2, and of $CF_3\cdot$ plus $CHF_2\cdot$ radicals[90] generated from the photolysis of CF_3COCHF_2, and observed that increasing the fluorine content of excited fluoroethanes reduces the rate of HF elimination. Follmer and Pritchard[91] observed a deuterium isotope effect in the disproportionation of $CHF_2\cdot$ and $CDF_2\cdot$ radicals generated from CHF_2COCHF_2 and CDF_2COCDF_2.

Fessenden and Schuler[92] obtained and identified the esr spectrum of $CHF_2\cdot$ after irradiation of methylene fluoride in solid xenon at -188°C. The carbon-13 hyperfine interactions provided an estimate of the s-character of the free radical electron from which a deviation from planarity of 12.7° was deduced. Ayscough[93] et al. observed the esr spectra of the three fluoromethyl radicals, $CF_3\cdot$, $CHF_2\cdot$ and $CH_2F\cdot$, generated by the photolyses of lead IV fluoroalkanoates, $(RCOO)_4Pb$, at 77°K. The fluoromethyl radicals reacted further by abstracting α-hydrogen atoms from the fluoroalkanoates. Andrews and Carver[94] obtained the infra red spectrum of difluoromethyl radical when CHF_2Br and CDF_2Br, at high dilution in argon, were codeposited with an atomic beam of lithium on a cesium iodide window, and calculated the force constants. Berces and Forgeteg[95] calculated the entropies of 44 simple organic free radicals, including $CHF_2\cdot$, by thermodynamic methods involving assumptions concerning the structural differences between the radicals and their parent molecules. Pople[96] et al. have demonstrated that INDO (intermediate neglect of differential overlap) approximation predicts molecular geometries fairly reliably. They observed that unpaired

spin populations in valence s orbitals show a good linear correlation with experimentally observed isotropic hyperfine coupling constants over a large number of free radicals. The predicted geometry for the difluoromethyl radical is 109° for the F-C-F bond and 116° for the H-C-F bonds. Biddles and Hudson[97], using the INDO method, have established the equilibrium geometries and hyperfine coupling constants for the series of radicals CH_nF_{3-n}, CH_nCl_{3-n} and CCl_nF_{3-n}.

Part 2 reports the photolytic reactions of CHF_2I, at various temperatures, with vinyl fluoride, and the competitive photolyses with vinyl fluoride, 1,1 difluoroethylene, trifluoroethylene and tetrafluoroethylene in the presence of ethylene. Two additional competitive series of reactions were conducted, over a range of concentration, between 1,1 difluoroethylene and ethylene at 100°C and 150°C. Part of the discussion section is sub divided: the addition reactions of $CF_2I\cdot$ radicals are discussed prior to the addition of $CHF_2\cdot$ radicals. The experimental work of part 2 was conducted after much of that of part 3 in an attempt to find an explanation for the observed anamolous behaviour of $CH_2F\cdot$ radicals which showed increasing selectivity with increasing temperature in addition reactions to the fluoroethylenes. The cause was eventually traced to the participation of excited CHF_2* and CH_2F*, (CF_2I cannot be excited since they are secondary radicals) and substantiated by a final series of reactions conducted with non-excited $CH_2F\cdot$ radicals generated thermally by the action of methyl radicals produced from the decomposition of di-t-butyl peroxide. The resultant product ratios showed normal behaviour. It is appropriate to discuss the final interpretation of the results at the end of part 3 after reporting the results of the thermally initiated experimental series.

EXPERIMENTAL

REACTANTS

1) Difluoroiodomethane (bp 21.6°C) was prepared by the action of mercurous fluoride on iodoform. Under an atmosphere of nitrogen, dry iodoform (0.3 moles) was heated with stirring until it began to melt, then, with reduced heat, anhydrous mercurous fluoride (0.1 mole) was slowly added through a Fieser apparatus. The products, consisting mainly of difluoroiodomethane and fluorodiiodomethane distilled directly into the receiver flask. The fluorodiiodomethane was separated from the product mixture and reacted in a similar manner to increase the total yield of difluoroiodomethane (2ml). Final purification was achieved by preparative glc which gave a product of approximately 99.1% purity. Several highly volatile impurity peaks were present, all of which defied analysis by glc - ms. These peaks gave a consistent reproducible pattern on the chromatograms from the kinetic series of reactions.

2) The fluoroethylenes were obtained commercially and purified by trap to trap distillation.

APPARATUS

The apparatus was as described in part 1 except for two minor changes: the reactor was a cylindrical "pyrex" glass vessel (202ml) which allowed transmission within the 290 to 420 nm range and alleviated the need to use an interference filter; and the light source was exclusively a 'Hanovia' UVS 220 medium pressure mercury arc.

EXPERIMENTAL PROCEDURE

The experimental procedure was basically the same as described in part 1. The difluoroiodomethane (bp 21.6°C) was stored in a two litre glass storage bulb fitted with a glass side arm which was surrounded by liquid nitrogen. The fluoroethylenes were

generally measured into bulb E (70ml) and ethylene into a small bulb F (17ml) to maintain accuracy in measuring the small concentrations used in the series of kinetic runs.

ANALYSIS

The analyses were conducted on the Griffin and George D6 gas density balance chromatograph and the Du Pont curve resolver as described in Part 1. The modifications involved a different technique for injecting samples and the use of several chromatographic columns and operating conditions in an attempt to optimise the resolution of peaks.

The sample injection technique involved cooling the 4μl capillary needle in liquid nitrogen immediately prior to immersing into the cold product mixture and transference of the sample onto the column. Failure to observe this technique resulted in very small injections accompanied by the appearance of broad water peaks.

Several chromatographic columns consisting of 3ft sections of stainless steel with an internal diameter of 3/16in were used. Most of the analyses were conducted on a 12ft column consisting of 6ft of 15% silanised silicone oil plus 6ft of 20% silicone oil packed on 60-100 mesh embacel. The column temperature was maintained at approximately 85^{o}C. The carrier gas was nitrogen which was maintained at a flow rate of approximately 40ml min^{-1}. The chart speed was 24 in h^{-1} for elution of the initial peaks and 12 in h^{-1} for elution of the diiodide peaks. A few additional analyses for each of 1,1-difluoroethylene and trifluoroethylene in competitive reactions with ethylene were conducted on an 18ft column consisting of 3ft of 15% tritolylphosphate plus 15ft of 20% silicone oil packed on 60-100 mesh embacel. The column temperature was maintained at 130^{o}C and the nitrogen carrier gas flow rate was maintained at 40ml min^{-1}. The products from the

photolyses of vinyl fluoride in the presence and absence of ethylene were analysed exclusively on a 6ft column of 15% silanised silicone oil on 60-100 mesh embacel. This column was maintained at 50°C and the nitrogen carrier gas flow rate was set at 40ml min^{-1}.

IDENTIFICATION of PRODUCTS

The products were identified exclusively by glc - ms as described in part 1 with the exceptions of $CF_2ICF_2CH_2I$ and CF_2ICF_2CHFI : the identities of these diiodides were assumed. The circumstantial evidence is that no further additional peaks appeared on the chromatograms and the relative retention times of the assumed peaks were as expected.

The ultraviolet spectrum, mass spectrum and ^1H and ^{19}F nuclear magnetic resonance spectra of CHF_2I were recorded.

U. V. Spectrum of CHF_2I

The ultraviolet spectrum of difluoroiodomethane was recorded in the gas phase over the concentration range of 10^{-3} to 10^{-2} mol l^{-1} using a quartz gas cell and a Unicam SP 800 ultraviolet spectrophotometer. One peak was observed with an absorbance maximum at 257.5nm. The molar extinction coefficient (ε) was calculated,

$$\varepsilon_{257.5} = 23.8 \pm 0.6 \ cm^{-1} \ mol^{-1} \ l.$$

MASS SPECTRUM of CHF_2I

m/e	Relative Intensity	Assignment
31	27	CF^+
32	17	CHF^+
50	6	CF_2^+
51	55	CHF_2^+
127	100	I^+
128	8	HI^+

m/e	Relative Intensity	Assignment
139	3	CI^+
140	4	CHI^+
159	23	$CHFI^+$
178	16	CHF_2I^+

^{1}H nmr spectrum of CHF_2I

The ^{1}H nmr spectrum of difluoroiodomethane was recorded on a 60MHz spectrometer using carbon tetrachloride as solvent and tetramethylsilane as internal reference. The proton resonance is split into a triplet by the two equivalent fluorine atoms.

chemical shift τ = 2.338 ppm

coupling constant J_{HF} = 55.8 Hz

^{19}F nmr spectrum of CHF_2I

The ^{19}F nmr spectrum of difluoroiodomethane was recorded on a 100 MHz spectrometer using carbon tetrachloride as solvent and trichlorofluoromethane as internal reference. The two equivalent fluorine atoms gave a doublet by interaction with the hydrogen atom.

chemical shift $\phi_{F_1} = \phi_{F_2}$ = 66.29 ppm

coupling constant J_{HF} = 56 Hz

G-ethylene

A preparative run was carried out with CHF_2I (1.00×10^{-3} mol l^{-1}) and $CH_2{=}CH_2$ (0.50×10^{-3} mol l^{-1}) in a pyrex reaction vessel. Four product peaks were observed and identified by glc - ms.

Peak G - 1

m/e	Relative Intensity	Assignment
31	15	CF^+
50	6	CF_2^+
127	80	I^+

m/e	Relative Intensity	Assignment
128	26	HI^+
177	100	CF_2I^+
254	23	I_2^+
266	1	CI_2^+
285	5	CFI_2^+
304	21	$CF_2I_2^+$

Identified as difluorodiiodomethane (CF_2I_2)

Peak G - 2

127	44	I^+
128	16	HI^+
155	100	$C_2H_4I^+$
254	16	I_2^+
282	3	$C_2H_4I_2^+$

Identified as 1,2 - diiodoethane (CH_2ICH_2I)

Peak G - 3

32	17	CHF^+
51	77	CHF_2^+
55	4	C_3F^+
57	4	$C_3H_2F^+$
59	44	$C_3H_4F^+$
60	3	$C_3H_5F^+$
77	12	$C_3H_3F_2^+$
79	44	$C_3H_5F_2^+$
127	29	I^+
128	14	HI^+
141	11	CH_2I^+
155	5	$C_2H_4I^+$
206	100	$C_3H_5F_2I^+$
207	3	$^{13}CC_2H_5F_2I^+$

Identified as the ethylene adduct, 1,1-difluoro-3-iodopropane ($CHF_2CH_2CH_2I$)

Peak G - 4

m/e	Relative Intensity	Assignment
50	3	CF_2^+
51	31	CHF_2^+
55	12	C_3F^+
57	8	$C_3H_2F^+$
59	12	$C_3H_4F^+$
75	6	$C_3HF_2^+$
77	77	$C_3H_3F_2^+$
78	15	$C_3H_4F_2^+$
127	45	I^+
128	24	HI^+
141	63	CH_2I^+
155	14	$C_2H_4I^+$
159	5	$CHFI^+$
177	6	CF_2I^+
185	2	$C_3H_3FI^+$
205	100	$C_3H_4F_2I^+$
254	6	I_2^+
332	7	$C_3H_4F_2I_2^+$

Identified as the diiodide, 1,1-difluoro-1,3-diiodopropane ($CF_2ICH_2CH_2I$)

H-vinyl fluoride

A preparative run was carried out with CHF_2I (1.00×10^{-3} mol l^{-1}) and $CH_2{=}CHF$ (1.00×10^{-3} mol l^{-1}) in a pyrex reaction vessel. Four product peaks were observed and identified by glc - ms.

Peak H - I

31	7	CF^+
32	36	CHF^+
44	6	C_2HF^+
45	7	$C_2H_2F^+$

m/e	Relative Intensity	Assignment
46	9	$C_2H_3F^+$
50	2	CF_2^+
51	73	CHF_2^+
57	2	$C_3H_2F^+$
77	10	$C_3H_3F_2^+$
97	100	$C_3H_4F_3^+$
127	22	I^+
128	9	HI^+
141	2	CH_2I^+
153	10	$C_2H_2I^+$
154	1	$C_2H_3I^+$
159	10	$CHFI^+$
224	22	$C_3H_4F_3I^+$

On the basis of previous work[16,44] it was expected that the normal adduct from addition to the CH_2= end would be eluted first. The relative ratio of the significant ions at m/e 141 (CH_2I^+) and m/e 159 ($CHFI^+$) facilitate assigning peak 1 to the normal adduct and peak 2 to the reverse adduct.

Identified as the normal adduct, 1,1,3-trifluoro-3-iodopropane (CHF_2CH_2CHFI)

Peak H - 2

31	10	CF^+
32	184	CHF^+
51	84	CHF_2^+
57	3	$C_2H_2F^+$
77	27	$C_3H_3F_2^+$
95	5	$C_3H_2F_3^+$
97	48	$C_3H_4F_3^+$
127	47	I^+
128	44	HI^+

m/e	Relative Intensity	Assignment
141	16	CH_2I^+
153	19	$C_2H_2I^+$
159	5	$CHFI^+$
173	19	$C_2H_3FI^+$
224	100	$C_3H_4F_3I^+$

Identified as the reverse adduct, 1,1,2-trifluoro-3-iodopropane (CHF_2 $CHFCH_2I$)

Peak H - 3

31	15	CF^+
32	33	CHF^+
44	9	C_2HF^+
45	11	$C_2H_2F^+$
46	15	$C_2H_3F^+$
50	3	CF_2^+
51	19	CHF_2^+
64	3	$C_2H_2F_2^+$
75	8	$C_3HF_2^+$
77	22	$C_3H_3F_2^+$
95	17	$C_3H_2F_3^+$
96	4	$C_3H_3F_3^+$
127	38	I^+
128	17	HI^+
153	5	$C_2H_2I^+$
159	64	$CHFI^+$
177	25	CF_2I^+
203	12	$C_3H_2F_2I^+$
223	100	$C_3H_3F_3I^+$
254	3	I_2^+
350	0.8	$C_3H_3F_3I_2^+$

Identified as the normal diiodide adduct, 1,1,3-trifluoro-1,3-diiodopropane (CF_2I CH_2CHFI)., from the addition of difluoroiodomethyl

radicals to the CH_2= end of vinyl fluoride.

Peak H - 4

m/e	Relative Intensity	Assignment
31	8	CF^+
32	205	CHF^+
44	25	C_2HF^+
45	10	$C_2H_2F^+$
46	13	$C_2H_3F^+$
50	4	CF_2^+
51	17	CHF_2^+
64	5	$C_2H_2F_2^+$
75	9	$C_3HF_2^+$
77	36	$C_3H_3F_2^+$
95	17	$C_3H_2F_3^+$
96	5	$C_3H_3F_3^+$
127	46	I^+
128	43	HI^+
141	19	CH_2I^+
153	8	$C_2H_2I^+$
159	17	$CHFI^+$
173	4	$C_2H_3FI^+$
177	11	CF_2I^+
203	12	$C_3H_2F_2I^+$
223	100	$C_3H_3F_3I^+$
254	7	I_2^+
350	8	$C_3H_3F_3I_2^+$

Identified as the reverse diiodide adduct, 1,1,2-trifluoro-1,3-diiodopropane (CF_2I $CHFCH_2I$)

I- 1,1-difluoroethylene

A preparative run was carried out with CHF_2I (2.00×10^{-3} mol l^{-1}) and $CH_2{=}CF_2$ (2.00×10^{-3} mol l^{-1}) in a pyrex reaction vessel. Four product peaks were observed and identified by glc - ms.

Peak I - 1

m/e	Relative Intensity	Assignment
31	34	CF^+
32	391	CHF^+
45	21	$C_2H_2F^+$
50	11	CF_2^+
51	52	CHF_2^+
63	13	$C_2HF_2^+$
64	115	$C_2H_2F_2^+$
74	6	$C_3F_2^+$
75	24	$C_3HF_2^+$
76	9	$C_3H_2F_2^+$
93	13	$C_3F_3^+$
94	9	$C_3HF_3^+$
95	98	$C_3H_2F_3^+$
113	87	$C_3HF_4^+$
114	100	$C_3H_2F_4^+$

Identified as 1,1,3,3-tetrafluoroprop-1-ene ($CF_2{=}CHCHF_2$).

Peak I - 2

31	7	CF^+
32	105	CHF^+
45	12	$C_2H_2F^+$
46	4	$C_2H_3F^+$
50	2	CF_2^+
51	95	CHF_2^+
64	14	$C_2H_2F_2^+$

m/e	Relative Intensity	Assignment
65	5	$C_2H_3F_2^+$
75	3	$C_3HF_2^+$
77	5	$C_3H_3F_2^+$
95	7	$C_3H_2F_3^+$
113	3	$C_3HF_4^+$
115	100	$C_3H_3F_4^+$
116	4	$^{13}CC_2H_3F_4^+$
127	32	I^+
128	10	HI^+
153	2	$C_2H_2I^+$
159	8	$CHFI^+$
177	10	CF_2I^+
203	1.5	$C_3H_2F_2I^+$
223	1.2	$C_3H_3F_3I^+$
242	2	$C_3H_3F_4I^+$

Identified as the normal adduct, 1,1,3,3-tetrafluoro-1-iodopropane ($CHF_2CH_2CF_2I$)

Peak I - 3

31	20	CF^+
32	897	CHF^+
50	6	CF_2^+
51	111	CHF_2^+
63	6	$C_2HF_2^+$
64	56	$C_2H_2F_2^+$
65	8	$C_2H_3F_2^+$
77	17	$C_3H_3F_2^+$
95	12	$C_3H_2F_3^+$

m/e	Relative Intensity	Assignment
128	82	HI^+
141	18	CH_2I^+
191	55	$C_2H_2F_2I^+$
242	100	$C_3H_3F_4I^+$

Identified as the reverse adduct, 1,1,2,2-tetrafluoro-3-iodopropane ($CHF_2CF_2CH_2I$).

Peak I - 4

31	7	CF^+
32	127	CHF^+
44	12	C_2HF^+
45	6	$C_2H_2F^+$
50	2	CF_2^+
51	4	CHF_2^+
64	18	$C_2H_2F_2^+$
75	4	$C_3HF_2^+$
95	2	$C_3H_2F_3^+$
113	7	$C_3HF_4^+$
127	32	I^+
128	21	HI^+
177	79	CF_2I^+
191	1	$C_2H_2F_2I^+$
241	100	$C_3H_2F_4I^+$
254	3	I_2^+
386	0.7	$C_3H_2F_4I_2^+$

Identified as the normal diiodide adduct, 1,1,3,3-tetrafluoro-1,3-diiodopropane ($CF_2ICH_2CF_2I$).

A small peak was present at the expected position of the reverse diiodide adduct but a mass spectrum was not obtained. In the results section the identity of the reverse diiodide adduct, 1,1,2,2-tetrafluoro-1,3-diiodopropane ($CF_2ICF_2CH_2I$), is assumed.

J-trifluoroethylene

A preparative run was carried out with CHF_2I (2.00×10^{-3} mol l^{-1}) and $CHF{=}CF_2$ (2.00×10^{-3} mol l^{-1}) in a pyrex reaction vessel. Five product peaks were observed and identified by glc and ms.

Peak J - 1

m/e	Relative Intensity	Assignment
31	16	CF^+
32	59	CHF^+
50	2	CF_2^+
51	118	CHF_2^+
63	5	$C_2HF_2^+$
64	9	$C_2H_2F_2^+$
82	16	$C_2HF_3^+$
95	7	$C_3H_2F_3^+$
113	4	$C_3HF_4^+$
127	32	I^+
128	7	HI^+
133	100	$C_3H_2F_5^+$
159	5	$CHFI^+$
171	3	C_2HFI^+
177	17	CF_2I^+
190	16	$C_2HF_2I^+$
209	1	$C_2HF_3I^+$
260	10	$C_3H_2F_5I^+$

Identified as the normal trifluoroethylene adduct, 1,1,2,3,3-pentafluoro-1-iodopropane (CHF_2CHFCF_2I).

Peak J - 2

m/e	Relative Intensity	Assignment
31	28	CF^+
32	113	CHF^+
51	225	CHF_2^+
63	8	$C_2HF_2^+$
64	14	$C_2H_2F_2^+$
82	33	$C_2HF_3^+$
95	16	$C_3H_2F_3^+$
113	6	$C_3HF_4^+$
127	62	I^+
128	12	HI^+
133	14	$C_3H_2F_5^+$
159	35	$CHFI^+$
171	5	C_2HFI^+
177	8	CF_2I^+
190	10	$C_2HF_2I^+$
209	8	$C_2HF_3I^+$
221	1.3	$C_3HF_3I^+$
260	100	$C_3H_2F_5I^+$

Identified as the reverse trifluoroethylene adduct, 1,1,2,2,3-pentafluoro-3-iodopropane (CHF_2CF_2CHFI).

Peak J - 3

31	26	CF^+
32	23	CHF^+
50	4	CF_2^+
51	32	CHF_2^+
63	10	$C_2HF_2^+$

m/e	Relative Intensity	Assignment
82	41	$C_2HF_3^+$
113	49	$C_3HF_4^+$
127	67	I^+
128	19	HI^+
131	3	$C_3F_5^+$
132	2	$C_3HF_5^+$
133	3	$C_3H_2F_5^+$
158	4	CFI^+
159	11	$CHFI^+$
177	100	CF_2I^+
190	6	$C_2HF_2I^+$
209	1.5	$C_2HF_3I^+$
240	2	$C_3HF_4I^+$
254	7	I_2^+
259	100	$C_3HF_5I^+$
386	8	$C_3HF_5I_2^+$

Identified as the normal diiodide adduct, 1,1,2,3,3-pentafluoro-1,3-diiodopropane ($CF_2ICHFCF_2I$). A small peak was present at the expected position of the reverse diiodide adduct but a mass spectrum was not obtained. In the results section the identity of the reverse diiodide adduct, 1,1,2,2,3-pentafluoro-1,3-diiodopropane (CF_2ICF_2CHFI), is assumed.

Peak J - 4

31	32	CF^+
32	600	CHF^+
51	375	CHF_2^+
127	118	I^+
128	104	HI^+
133	29	$C_3H_2F_5^+$
145	100	$C_4H_2F_5^+$

m/e	Relative Intensity	Assignment
159	61	$CHFI^+$
177	25	CF_2I^+
190	18	$C_2HF_2I^+$
209	14	$C_2HF_3I^+$
215	18	$C_4H_2F_2I^+$
259	11	$C_3HF_5I^+$
342	54	$C_5H_3F_8I^+$

Identified as the two to one telomer, 1,1,2,3,3,4,4,5-octafluoro-5-iodopentane ($CHF_2CHFCF_2CF_2CHFI$).

Peak J - 5

31	21	CF^+
32	247	CHF^+
51	46	CHF_2^+
127	71	I^+
128	39	HI^+
131	17	$C_3F_5^+$
177	100	CF_2I^+
195	36	$C_5H_2F_7^+$
254	10	I_2^+
259	7	$C_3HF_5I^+$
342	35	$C_5H_3F_8I^+$

Identified as the two to one telomer, 1,1,2,3,3,4,5,5-octafluoro-1-iodopentane ($CHF_2CHFCF_2CHFCF_2I$).

K-tetrafluoroethylene

A preparative run was carried out with CHF_2I (1.20×10^{-3} mol l^{-1}) and $CF_2=CF_2$ (1.20×10^{-3} mol l^{-1}) in a pyrex reaction vessel. Seven product peaks were observed and identified by glc -ms.

Peak K - 1

m/e	Relative Intensity	Assignment
31	34	CF^+
32	109	CHF^+
50	8	CF_2^+
51	159	CHF_2^+
82	30	$C_2HF_3^+$
93	2	$C_2F_3^+$
100	21	$C_2F_4^+$
101	11	$C_2HF_4^+$
113	25	$C_3HF_4^+$
127	98	I^+
128	12	HI^+
131	3	$C_3F_5^+$
132	3	$C_3HF_5^+$
151	100	$C_3HF_6^+$
158	6	CFI^+
159	4	$CHFI^+$
177	51	CF_2I^+
189	1.3	$C_2F_2I^+$
208	6	$C_2F_3I^+$
227	3	$C_2F_4I^+$
278	28	$C_3HF_6I^+$

Identified as the tetrafluoroethylene adduct, 1,1,2,2,3,3-hexafluoro-1-iodopropane ($CHF_2CF_2CF_2I$)

Peak K - 2

31	40	CF^+
32	77	CHF^+
50	11	CF_2^+
51	316	CHF_2^+
93	11	$C_3F_3^+$

m/e	Relative Intensity	Assignment
100	48	$C_2F_4^+$
101	47	$C_2HF_4^+$
112	6	$C_3F_4^+$
113	17	$C_3HF_4^+$
119	32	$C_2F_5^+$
127	100	I^+
128	9	HI^+
131	43	$C_3F_5^+$
151	7	$C_3HF_6^+$
158	5	CFI^+
163	11	$C_4HF_6^+$
169	4	$C_3F_7^+$
177	68	CF_2I^+
181	28	$C_4F_7^+$
208	9	$C_2F_3I^+$
213	6	$C_5HF_8^+$
227	9	$C_2F_4I^+$
239	5	$C_3F_4I^+$
251	36	$C_5HF_{10}^+$
289	3	$C_4F_6I^+$
378	10	$C_5HF_{10}I^+$

Identified as the two to one tetrafluoroethylene telomer ($CHF_2(CF_2CF_2)_2I$).

Peak K ~ 3

31	43	CF^+
32	152	CHF^+
50	18	CF_2^+
51	20	CHF_2^+
81	13	$C_2F_3^+$

m/e	Relative Intensity	Assignment
100	57	$C_2F_4^+$
127	65	I^+
128	33	HI^+
158	12	CFI^+
177	30	CF_2I^+
208	20	$C_2F_3I^+$
227	100	$C_2F_4I^+$
254	100	I_2^+
354	27	$C_2F_4I_2^+$

Identified as the diiodide, 1,1,2,2-tetrafluoro-1,2-diiodoethane (CF_2ICF_2I).

Peak K - 4

31	25	CF^+
32	153	CHF^+
50	11	CF_2^+
51	311	CHF_2^+
93	15	$C_3F_3^+$
100	42	$C_2F_4^+$
101	58	$C_2HF_4^+$
113	17	$C_3HF_4^+$
119	41	$C_2F_5^+$
127	100	I^+
128	13	HI^+
131	61	$C_3F_5^+$
151	16	$C_3HF_6^+$
158	6	CFI^+
163	5	$C_4HF_6^+$
169	13	$C_3F_7^+$
177	67	CF_2I^+
181	11	$C_4F_7^+$

m/e	Relative Intensity	Assignment
208	8	$C_2F_3I^+$
213	3	$C_5HF_8^+$
219	8	$C_4F_9^+$
227	12	$C_2F_4I^+$
231	4	$C_5F_9^+$
239	3	$C_3F_4I^+$
263	2	$C_6HF_{10}^+$
281	23	$C_6F_{11}^+$
313	2	$C_7HF_{12}^+$
351	8	$C_7HF_{14}^+$

Identified as the three to one tetrafluoroethylene telomer ($CHF_2(CF_2CF_2)_3I$).

Peak K - 5

31	42	CF^+
32	80	CHF^+
50	10	CF_2^+
51	5	CHF_2^+
93	5	$C_3F_3^+$
100	42	$C_2F_4^+$
127	87	I^+
128	10	HI^+
131	18	$C_3F_5^+$
139	4	CI^+
150	8	$C_3F_6^+$
158	9	CFI^+
177	100	CF_2I^+
208	8	$C_2F_3I^+$
254	4	I_2^+
258	4	$C_3F_5I^+$

m/e	Relative Intensity	Assignment
277	98	$C_3F_6I^+$
404	11	$C_3F_6I_2^+$

Identified as the diiodide adduct 1,3-diiodoperfluoropropane ($CF_2ICF_2CF_2I$).

Peak K - 6

32	600	CHF^+
50	32	CF_2^+
51	80	CHF_2^+
93	24	$C_3F_3^+$
100	96	$C_2F_4^+$
101	20	$C_2HF_4^+$
119	20	$C_2F_5^+$
127	192	I^+
128	40	HI^+
131	64	$C_3F_5^+$
177	64	CF_2I^+
181	40	$C_4F_7^+$
208	28	$C_2F_3I^+$
227	28	$C_2F_4I^+$
239	16	$C_3F_4I^+$
254	8	I_2^+
327	100	$C_4F_8I^+$

Identified as the two to one telomer 1,4-diiodoperfluorobutane ($CF_2ICF_2CF_2CF_2I$), from the addition of iodine atoms to tetrafluoroethylene.

Peak K - 7

31	24	CF^+
32	91	CHF^+
50	9	CF_2^+
51	10	CHF_2^+
93	8	$C_3F_3^+$

m/e	Relative Intensity	Assignment
100	32	$C_2F_4^+$
112	8	$C_3F_4^+$
119	11	$C_2F_5^+$
127	100	I^+
128	10	HI^+
131	46	$C_3F_5^+$
177	51	CF_2I^+
181	8	$C_4F_7^+$
208	6	$C_2F_3I^+$
227	9	$C_2F_4I^+$
231	13	$C_5F_9^+$
239	6	$C_3F_4I^+$
254	9	I_2^+
377	19	$C_5F_{10}I^+$

Identified as the two to one telomer, 1,5-diiodoperfluoropentane ($CF_2I(CF_2CF_2)_2I$), from the addition of difluoroiodomethyl radicals to tetrafluoroethylene.

L-tetrafluoroethylene plus ethylene

A preparative run was carried out with CHF_2I (2.00×10^{-3} mol l^{-1}), $CF_2=CF_2$ (0.67×10^{-3} mol l^{-1}) and $CH_2=CH_2$ (0.33×10^{-3} mol l^{-1}) in a pyrex reaction vessel. Three product peaks were observed and identified by glc - ms in addition to the tetrafluoroethylene and ethylene adducts.

Peak L - 1

31	11	CF^+
32	38	CHF^+
39	15	$C_3H_3^+$
47	14	$C_2H_4F^+$
50	4	CF_2^+
51	141	CHF_2^+

m/e	Relative Intensity	Assignment
57	10	$C_3H_2F^+$
59	15	$C_3H_4F^+$
64	4	$C_2H_2F_2^+$
65	36	$C_2H_3F_2^+$
75	10	$C_3HF_2^+$
77	66	$C_3H_3F_2^+$
89	18	$C_4H_3F_2^+$
95	26	$C_3H_2F_3^+$
100	5	$C_2F_4^+$
101	26	$C_2HF_4^+$
109	45	$C_4H_4F_3^+$
113	8	$C_3HF_4^+$
115	8	$C_3H_3F_4^+$
119	3	$C_2F_5^+$
127	45	$I^+/C_4H_3F_4^+$
128	36	$HI^+/C_4H_4F_4^+$
139	11	$CI^+/C_5H_3F_4^+$
141	44	$CH_2I^+/C_5H_5F_4^+$
155	19	$C_2H_4I^+$
159	34	$CHFI^+/C_5H_4F_5^+$
177	4	$C_5H_3F_6^+$
179	5	$C_5H_5F_6^+$
203	14	$C_3H_2F_2I^+$
205	4	$C_3H_4F_2I^+$
306	100	$C_5H_5F_6I^+$

Identified as the cross telomer 1,1,2,2,3,3-hexafluoro-5-iodopentane ($CHF_2CF_2CF_2CH_2CH_2I$) from the addition of difluoromethyl radicals to tetrafluoroethylene, followed by addition of the intermediate radicals to ethylene.

Peak L - 2

m/e	Relative Intensity	Assignment
32	396	CHF^+
51	38	CHF_2^+
77	93	$C_3H_3F_2^+$
108	27	$C_4H_3F_3^+$
109	17	$C_4H_4F_3^+$
127	83	$I^+/C_4H_3F_4^+$
128	24	$HI^+/C_4H_4F_4^+$
141	38	CH_2I^+
155	24	$C_2H_4I^+$
177	38	CF_2I^+
208	3	$C_2F_3I^+$
227	3	$C_2F_4I^+$
254	100	$I_2^+/C_4H_3F_4I^+$
382	9	$C_4H_4F_4I_2^+$

Identified as the cross telomer 1,1,2,2-tetrafluoro-1,4-diiodobutane ($CF_2ICF_2CH_2CH_2I$) from the addition of iodine atoms to tetrafluoroethylene, followed by addition of the intermediate radicals to ethylene.

Peak L - 3

31	19	CF^+
32	340	CHF^+
39	70	$C_3H_3^+$
50	29	CF_2^+
51	55	CHF_2^+
55	19	C_3F^+
57	16	$C_3H_2F^+$
59	34	$C_3H_4F^+$
63	17	$C_2HF_2^+$
64	30	$C_2H_2F_2^+$
65	55	$C_2H_3F_2^+$

m/e	Relative Intensity	Assignment
75	26	$C_3HF_2^+$
77	150	$C_3H_3F_2^+$
78	50	$C_3H_4F_2^+$
91	71	$C_4H_5F_2^+$
95	33	$C_3H_2F_3^+$
107	29	$C_4H_2F_3^+$
108	37	$C_4H_3F_3^+$
109	16	$C_4H_4F_3^+$
127	78	$I^+/C_4H_3F_4^+$
128	111	$HI^+/C_4H_4F_4^+$
137	25	$C_5HF_4^+$
141	61	CH_2I^+
165	25	$C_4H_3F_6^+$
177	38	CF_2I^+
254	7	$I_2^+/C_4H_3F_4I^+$
305	100	$C_5H_4F_6I^+$
432	1.7	$C_5H_4F_6I_2^+$

Identified as the cross telomer 1,1,2,2,3,3-hexafluoro-1-5-diiodopentane ($CF_2ICF_2CF_2CH_2CH_2I$) from the addition of difluoroiodomethyl radicals to tetrafluoroethylene, followed by addition of the intermediate radicals to ethylene.

Relative Chromatograph Retention Times

The chromatographic retention times of the products were determined using sereral columns in an effort to optimise peak resolution. All the columns consisted of 3ft sections of stainless steel of 3/16in internal diameter and were packed with the liquid phase on 60-100 mesh embacel.

Details of the experimental columns, including the average operating conditions, were:

i) Column 12ft consisting of 6ft of 15% silanised silicone oil plus 6ft of 20% silicone oil

OVEN TEMP. 72-97°C

CARRIER GAS NITROGEN - flow rate 20-50 ml min^{-1}

ii) Column 18ft consisting of 3ft of 15% tritolylphospate plus 15ft of 20% silicone oil

OVEN TEMP. 130°C

CARRIER GAS NITROGEN - flow rate 40-47 ml min^{-1}

iii) Column 6ft of 15% silanised silicone oil

OVEN TEMP. 34-69°C

CARRIER GAS NITROGEN - flow rate 25-60 ml min^{-1}

The retention times (R_t^1) relative to the retention times for the ethylene adduct ($CHF_2CH_2CH_2I$) are quoted for columns i,ii and iii.

ADDUCTS

	R_t^1 (i)	(ii)	(iii)
$CHF_2CF_2CF_2I$	0.38	0.50	
CHF_2CHFCF_2I	0.52	0.62	
CHF_2CF_2CHFI	0.57	0.68	
$CHF_2CH_2CF_2I$	0.55	0.62	0.51
$CHF_2CF_2CH_2I$	0.69	0.76	0.65
CHF_2CH_2CHFI	0.89		0.78

	R_t^1 (i)	(ii)	(iii)
ADDUCTS			
CHF_2CHFCH_2I	1.14		1.18
$CHF_2CH_2CH_2I$	1.00	1.00	1.00
$CF_2ICF_2CF_2I$	1.60	1.59	
$CF_2ICHFCF_2I$	2.64	2.51	
CF_2ICF_2CHFI	2.89	2.71	
$CF_2ICH_2CF_2I$	2.91	2.62	2.76
$CF_2ICF_2CH_2I$	3.50	3.10	
CF_2ICH_2CHFI	4.58		3.70
$CF_2ICHFCH_2I$	5.52		4.50
$CF_2ICH_2CH_2I$	4.23	3.52	3.40
CROSSTELOMERS			
$CHF_2CF_2CF_2CH_2CH_2I$	1.94	1.44	
$CF_2ICF_2CF_2CH_2CH_2I$	6.68	4.77	
OLEFINS			
$CF_2=CF_2$	0.12		
$CHF=CF_2$	0.15		
$CH_2=CF_2$	0.17	0.26	0.09
$CH_2=CHF$	0.15	0.27	0.10
MISC.			
CHF_2I	0.23	0.38	0.14
CF_2I_2	0.80	1.03	0.39
CF_2ICF_2I			0.50

RESULTS

The reactions of difluoroiodomethane with vinyl fluoride

A series of photolyses was carried out with CHF_2I (0.75×10^{-3} mol l^{-1}) and CH_2=CHF (0.38×10^{-3} mol l^{-1}). The temperature was varied in the range 47-170°C and the reaction time in the range 6-40 h. The only measurable products were the two adducts from the addition of difluoromethyl radicals, and the two adducts from the addition of difluoroiodomethyl radicals to both ends of vinyl fluoride, and difluorodiiodomethane. Although CF_2I_2 was produced in all of the kinetic runs the relative amounts were not measured, mainly due to poor resolution of the chromatographic peak.

let e_1 = the relative concentration of CHF_2CH_2CHFI

e_2 = the relative concentration of CHF_2CHFCH_2I

h_1 = the relative concentration of CF_2ICH_2CHFI

h_2 = the relative concentration of $CF_2ICHFCH_2I$

a) temp. 47°C, time 39.90 h

i) e_1	e_2	ii) h_1	h_2
100	34.0	100	19.2
100	34.3	100	17.4
100	34.0	100	15.5
100	35.1	100	16.0
100	34.0		
100	34.3 mean value	100	17.0 mean value
	2.92 e_1/e_2		5.88 h_1/h_2

b) temp. 75°C, time 30.60 h

i)			ii)		
100	27.0		100	18.9	
100	28.0		100	17.8	
100	29.0		100	17.0	
100	28.8				
100	29.0				
100	28.4 mean value		100	17.9 mean value	
	3.53 e_1/e_2			5.59 h_1/h_2	

c) temp.94°C, 21.28 h

i) e_1	e_2	ii) h_1	h_2
100	24.9	100	18.0
100	24.0	100	19.0
100	27.0	100	18.8
100	26.2	100	18.5
100	25.5 mean value	100	18.6 mean value
	3.92 e_1/e_2		5.38 h_1/h_2

d) temp. 120°C, 16.77 h

i)		ii)	
100	21.0	100	17.7
100	21.3	100	18.0
100	21.0	100	17.1
100	21.2	100	17.3
100	20.0	100	18.3
100	20.9 mean value	100	17.7 mean value
	4.79 e_1/e_2		5.66 h_1/h_2

e) temp. 147°C, time 16.25 h

i)		ii)	
100	21.0	100	24.0
100	20.0	100	23.0
100	21.0	100	23.0
100	20.0		
100	20.5 mean value	100	23.3 mean value
	4.88 e_1/e_2		4.27 h_1/h_2

f) temp. 170°C, time 5.53 h

i)		ii)	
100	22.0	100	21.2
100	21.0	100	21.0
100	18.0	100	22.8
100	19.0	100	21.0
100	19.8		
100	19.9 mean value	100	21.5 mean value
	5.01 e_1/e_2		4.65 h_1/h_2

Plots of i) log e_1/e_2 and ii) log h_1/h_2 against $10^3/T$, by the least squares method, gave:

i) (add^n. of CHF_2.) gradient = -0.29 ± 0.09; intercept = 1.37 ± 0.03

ii) (add^n. of CF_2I·) gradient = 0.14 ± 0.13; intercept = 0.35 ± 0.05

Table 2-1

Temp ^{o}C	e_1/e_2	log e_1/e_2	h_1/h_2	log h_1/h_2
47	2.92	0.465	5.88	0.770
75	3.53	0.547	5.59	0.747
94	3.92	0.593	5.38	0.731
120	4.79	0.680	5.66	0.753
147	4.88	0.688	4.27	0.630
170	5.01	0.700	4.65	0.668

The reactions of difluoroiodomethane with vinyl fluoride and ethylene

A series of photolyses was carried out with CHF_2I (0.75×10^{-3} mol l^{-1}), CH_2=CHF (0.25×10^{-3} mol l^{-1}) and CH_2=CH_2 (0.06×10^{-3} mol l^{-1}). The temperature was varied in the range 38-180^{o}C and the reaction time in the range 3-25h. The measurable products included the normal vinyl fluoride and ethylene adducts from the addition of both difluoromethyl and difluoroiodomethyl radicals. Both of the reverse vinyl fluoride adduct peaks were present in rather small quantities for accurate measurement: the small reverse adduct peak from addition of difluoromethyl radicals was superimposed upon the tail of the corresponding ethylene adduct peak. No other significant peaks were present.

let a_1 = the relative area of CHF_2CH_2CHFI peak

a_3 = the relative area of $CHF_2CH_2CH_2I$ peak

g_1 = the relative area of CF_2ICH_2CHFI peak

g_3 = the relative area of $CF_2ICH_2CH_2I$ peak

e_1, e_3, h_1 and h_3 = the corresponding relative concentrations

a) temp. 38^{o}C, time 24.18h

i)

a_1	a_3	
100	70.3	
100	68.5	
100	69.0	
100	72.4	
100	70.1	mean value
76.5	59.0	rel. conc.
	3.09	$4e_3/e_1$

ii)

g_1	g_3	
100	78.6	
100	76.0	
100	76.0	
100	79.0	
100	77.4	mean value
46.6	38.2	rel. conc.
	3.28	$4h_3/h_1$

b) temp. 39.5°C, time 16.35h

i) a_1	a_3	ii) g_1	g_3
100	77	100	80.0
100	85	100	77.6
		100	82.0
100	81 mean value		
76.5	68.2 rel. conc.	100	79.9 mean value
	3.57 $4e_3/e_1$	46.6	39.4 rel. conc.
			3.38 $4h_3/h_1$

c) temp. 63.5°C, time 16.92h

i) a_1	a_3	ii) g_1	g_3
100	78	100	74
100	78	100	74
100	80	100	76
100	82	100	80
		100	70
100	79.5 mean value		
76.5	67.0 rel. conc.	100	75 mean value
	3.50 $4e_3/e_1$	46.6	36.9 rel. conc.
			3.17 $4h_3/h_1$

d) temp. 84°C, 23.93h

i) a_1	a_3	ii) g_1	g_3
100	73.2	100	76
100	67.8	100	57
100	72.4	100	73
100	71.1 mean value	100	68.7 mean value
76.5	59.9 rel. conc.	46.6	33.9 rel. conc.
	3.13 $4e_3/e_1$		2.91 $4h_3/h_1$

e) temp. 107°C, 16.67h

i) a_1	a_3	ii) g_1	g_3
100	70.0	100	66
100	70.0	100	63
100	68.5	100	65
100	68.8	100	67
100	70.0	100	68
100	69.5 mean value	100	65.8 mean value
76.5	58.5 rel. conc.	46.6	32.5 rel. conc.
	3.06 $4e_3/e_1$		2.79 $4h_3/h_1$

f) temp. 133°C, time 17.43h

i) a_1	a_3	ii) g_1	g_3
100	67.2	100	68.0
100	66.0	100	66.0
100	70.2	100	63.5
		100	63.4
100	67.8 mean value		
76.5	57.1 rel. conc.	100	65.2 mean value
	2.99 $4e_3/e_1$	46.6	32.2 rel. conc.
			2.76 $4h_3/h_1$

g) temp. 150°C, time 5.23h

i) a_1	a_3	ii) g_1	g_3
100	69	100	63
100	71	100	61
100	70	100	63
100	71	100	64
100	70.5	100	61
100	70.3 mean value	100	62.4 mean value
76.5	59.2 rel. conc.	46.6	30.8 rel. conc.
	3.10 $4e_3/e_1$		2.64 $4h_3/h_1$

h) temp. 180°C, time 3.17 h

i) a_1	a_3	ii) g_1	g_3
100	68	100	61
100	67	100	54
100	64	100	64
100	65	100	61
100	72	100	59
100	67.3 mean value	100	60 mean value
76.5	56.7 rel. conc.	46.6	29.5 rel. conc.
	2.96 $4e_3/e_1$		2.53 $4h_3/h_1$

Plots of i) log $4e_3/e_1$ and ii) log $4h_3/h_1$ against $10^3/T$, by the least squares method, gave:

i) (add^n. of $CHF_2\cdot$) gradient = 0.056 $\pm$ 0.066 intercept = 0.35 $\pm$ 0.02

ii) (add^n. of $CF_2I\cdot$) gradient = 0.12 $\pm$ 0.02 intercept = 0.14 $\pm$ 0.01

Table 2-2

Temp °C	$4e_3/e_1$	log $4e_3/e_1$	$4h_3/h_1$	log $4h_3/h_1$
38	3.09	0.489	3.28	0.516
39.5	3.57	0.552	3.38	0.529
63.5	3.50	0.545	3.17	0.501
84	3.13	0.496	2.91	0.464
107	3.06	0.486	2.79	0.445
133	2.99	0.475	2.76	0.441
150	3.10	0.491	2.64	0.422
180	2.96	0.472	2.53	0.403

The reactions of difluoroiodomethane with 1,1-difluoroethylene and ethylene

Three series of photolyses were carried out with difluoroiodomethane, 1,1-difluoroethylene and ethylene. The six measurable product peaks were the normal and reverse 1,1-difluoroethylene and ethylene adducts from addition of difluoromethyl and difluoroiodomethyl radicals to the olefins.

The first series of photolyses was carried out with CHF_2I (0.75×10^{-3} mol l^{-1}), $CH_2=CF_2$ (0.25×10^{-3} mol l^{-1}) and $CH_2=CH_2$ (0.06×10^{-3} mol l^{-1}) over the temperature range of 45-180°C, and reaction time range of 2.5-47h, except for the two reactions at 144°C and 179.5°C in which the ethylene concentration was increased by a factor of two.

The concentration of the reactants was progressively increased during the second and third photolytic series conducted at 100°C and 150°C respectively. The reactant ratios were kept constant at:

CHF_2I	:	$CH_2=CF_2$	:	$CH_2=CH_2$
12	:	4	:	1

let a_1 = the relative area of $CHF_2CH_2CF_2I$
a_2 = the relative area of $CHF_2CF_2CH_2I$
a_3 = the relative area of $CHF_2CH_2CH_2I$
g_1 = the relative area of $CF_2ICH_2CF_2I$
g_2 = the relative area of $CF_2ICF_2CH_2I$
g_3 = the relative area of $CF_2ICH_2CH_2I$

e_1, e_2, e_3, h_1, h_2, h_3 = the corresponding concentrations.

A - Variation of temperature

a) temp. 45.5°C, time 46.6h

i) e_1	e_2	ii) a_1	a_3
100	34	107.8	100
100	35	109.0	100
100	36	110.8	100
100	33	105.0	100
100	34	111.6	100
100	34.4 mean value	108.8	100 mean value
	2.91 e_1/e_2	76.9	84.2 rel. conc.
			4.38 $4e_3/e_1$

b) temp. 66°C, time ~40h

i) e_1	e_2	ii) a_1	a_3
100	30	77	100
100	31	77	100
100	30	78	100
100	30.3 mean value	77.3	100 mean value
	3.30 e_1/e_2	54.7	84.2 rel. conc.
			6.16 $4e_3/e_1$

iii) g_1	g_3
16.2	100
16.0	100
16.0	100
16.6	100
16.2	100 mean value
7.15	49.3 rel. conc.
	27.61 $4h_3/h_1$

c) temp. 93°C, time 18.17h

i) e_1	e_2	ii) a_1	a_3
100	21.5	65.4	100
100	22.6	61.0	100
100	22.2	62.0	100
100	22.1 mean value	62.8	100 mean value
	4.53 e_1/e_2	44.4	84.2 rel. conc.
			7.59 $4e_3/e_1$

iii)

g_1	g_3
22.8	100
23.2	100
23.0	100
23.0	100 mean value
10.2	49.3 rel. conc.
	19.5 $4h_3/h_1$

d) temp. 130°C, time 22.28h

i)

e_1	e_2
100	20.8
100	22.0
100	21.0
100	21.1
100	21.2 mean value
	4.71 e_1/e_2

ii)

a_1	a_3
55.0	100
53.7	100
54.2	100
58.2	100
55.3	100 mean value
39.1	84.2 rel. conc.
	8.62 $4h_3/h_1$

iii)

g_1	g_3
25.0	100
25.8	100
25.0	100
27.2	100
25.8	100 mean value
11.4	49.3 rel. conc.
	17.4 $4h_3/h_1$

e) temp. 132°C, time 16.60h

i)

e_1	e_2
100	23
100	21
100	23
100	23
100	23
100	22.6 mean value
	4.42 e_1/e_2

ii)

a_1	a_3
64	100
56	100
59	100
57	100
59	100 mean value
41.7	84.2 rel. conc.
	8.08 $4e_3/e_1$

iii)

g_1	g_3
24	100
23	100
24	100
24	100
24	100
23.8	100 mean value
10.5	49.3 rel. conc.
	18.8 $4h_3/h_1$

f) temp. 160°C, time 6.00h

i)

e_1	e_2
100	16
100	14
100	15.5
100	14
100	14.9 mean value
	6.70 e_1/e_2

ii)

a_1	a_3
53	100
50	100
53	100
54	100
52.5	100 mean value
37.1	84.2 rel. conc.
	9.08 $4e_3/e_1$

iii)

g_1	g_3
29.6	100
29	100
28	100
29	100
28.9	100 mean value
12.8	49.3 rel. conc.
	15.5 $4h_3/h_1$

g) temp. 160°C, time 6.08h

ii)

a_1	a_3
48.0	100
47.4	100
46.8	100
47.4	100 mean value
33.5	84.2 rel. conc.
	10.1 $4e_3/e_1$

iii)

g_1	g_3
30	100
30	100
29	100
30	100
29.7	100 mean value
13.1	49.3 rel. conc.
	15.1 $4h_3/h_1$

h) temp. 189°C, time 4.43h

i) e_1	e_2	ii) a_1	a_3
100	16.7	51	100
100	16.1	51.3	100
100	16.0	49	100
100	15.0	51.3	100
100	14.8	54	100
100	15.7 mean value	51.3	100 mean value
	6.36 e_1/e_2	36.3	84.2 rel. conc.
			9.29 $4e_3/e_1$

iii) g_1	g_3	iv) h_1	h_2
27.0	100	100	32.5
28.2	100	100	32.1
27.0	100	100	32.0
25.5	100	100	33.3
30.0	100		
27.5	100 mean value	100	32.5 mean value
12.2	49.3 rel. conc.		3.08 h_1/h_2
	16.2 $4h_3/h_1$		

i) temp. 33.5°C, time 14.45h

i) e_1	e_2	iii) g_1	g_3
100	34.3	12.4	100
100	36.0	12.2	100
100	36.2	12.1	100
100	35.8	14.0	100
100	35.6 mean value	12.7	100 mean value
	2.81 e_1/e_2	5.59	49.3 rel. conc.
			35.3 $4h_3/h_1$

j) temp. 64°C, time 14.75h

i) e_1	e_2	iii) g_1	g_3
100	32	14.2	100
100	31	14.0	100
100	31	15.2	100
100	30	15.0	100
100	31 mean value	14.6	100 mean value
	3.23 e_1/e_2	6.44	49.3 rel. conc.
			30.6 $4h_3/h_1$

k) temp. 116°C, time 6.00h

i) e_1	e_2	ii) g_1	g_3
100	17	27.6	100
100	19	23.0	100
100	17	27.8	100
100	18	27.0	100
100	17.8 mean value	26.4	100 mean value
	5.62 e_1/e_2	11.6	49.3 rel. conc.
			17.0 $4h_3/h_1$

l) temp. 144°C, time 4.43h (ethylene conc. doubled)

i) e_1	e_2	ii) g_1	g_3
100	15.9	15.1	100
100	15.9	14.2	100
100	14.3	15.0	100
100	14.8	14.3	100
100	14.8	15.0	100
100	15.1 mean value	14.7	100 mean value
	6.61 e_1/e_2	6.49	49.3 rel. conc.
			15.2 $2h_3/h_1$

m) temp. 179.5°C, time 2.60h (ethylene conc. doubled)

i) e_1	e_2	ii) g_1	g_3
100	14.7	16.4	100
100	15.1	16.0	100
100	16.1	16.0	100
100	15.6	15.6	100
100	17.0	15.5	100
		16.2	100
100	15.7 mean value		
	6.37 e_1/e_2	16.0	100 mean value
		7.04	49.3 rel. conc.
			14.0 $2h_3/h_1$

Plots of i) log e_1/e_2, ii) log $4e_3/e_1$, iii) log h_1/h_2 and iv) log $4h_3/h_1$, against $10^3/T$, by the least squares method, gave:

i) (add^n. of $CHF_2^{\cdot}$) gradient = -0.37 ± 0.11; intercept = 1.64 ± 0.04

ii) (add^n. of $CHF_2\cdot$) gradient = -0.33 ± 0.12; intercept = 1.72 ± 0.05

iii) (add^n. of $CF_2I\cdot$) gradient = 0.30 ± 0.06; intercept = -0.16 ± 0.02

iv) (add^n. of $CF_2I^{\cdot}$) gradient = 0.36 ± 0.09; intercept = 0.35 ± 0.04

Table 2-3

Temp °C	e_1/e_2	log e_1/e_2	$4e_3/e_1$	log $4e_3/e_1$	h_1/h_2	log h_1/h_2	$4h_3/h_1$	log $4h_3/h_1$
45.5	2.91	0.463	4.38	0.642	-		-	
66	3.30	0.519	6.16	0.790	-		27.61	1.44
93	4.53	0.657	7.59	0.880	-		19.5	1.29
130	4.71	0.673	8.62	0.936	-		17.4	1.24
132	4.42	0.646	8.08	0.907	-		18.8	1.27
160	6.70	0.826	9.08	0.958	-		15.5	1.19
160	-	-	10.1	1.003	-		15.1	1.18
189	6.36	0.804	9.29	0.968	3.08	0.488	16.2	1.21
33.5	2.81	0.449	-		-		35.3	1.55
64	3.23	0.510	-		-		30.6	1.49
116	5.62	0.750	-		-		17.0	1.23
							$2h_3/h_1$	log $2h_3/h_1$
144	6.61	0.820	-		-		15.2	1.18
179.5	6.37	0.804	-		-		14.0	1.15
							$4h_3/h_1$	log $4h_3/h_1$
* 100	-				4.36	0.640	21.3	1.33
* 150	-				3.43	0.536	18.3	1.26

* Data from the conc^{n} - variation series

B - Variation of concentration at 100°C

a) $[CHF_2I]$ 0.22×10^{-3} mol l^{-1},
temp. 98°C, time 64.92h

i) e_1	e_2	ii) a_1	a_3
100	56.8	60.5	100
100	56.5	56.0	100
100	56.8	58.0	100
100	57.0	64.0	100
100	56.8 mean value	59.6	100 mean value
	1.76 e_1/e_2	42.2	84.2 rel. conc.
	0.568 e_2/e_1		7.99 $4e_3/e_1$
	0.0711 $e_2/4e_3$		

b) $[CHF_2I]$ 0.38×10^{-3} mol l^{-1}, temp. 100°C, time 46.08h

i) e_1	e_2	ii) a_1	a_3
100	47.8	63	100
100	46.3	61	100
100	46.7	64	100
100	46.9 mean value	62.7	100 mean value
	2.13 e_1/e_2	44.3	84.2 rel. conc.
	0.469 e_2/e_1		7.61 $4e_3/e_1$
	0.0616 $e_2/4e_3$		

c) $[CHF_2I]$ 1.5×10^{-3} mol l^{-1}, temp. 100°C, time 45.50h

i) e_1	e_2	ii) a_1	a_3
100	34.2	65	100
100	33.7	66	100
100	32.9	67	100
100	34.8	66	100
100	33.9 mean value	66	100 mean value
	2.95 e_1/e_2	46.7	84.2 rel. conc.
	0.339 e_2/e_1		7.21 $4e_3/e_1$
	0.0470 $e_2/4e_3$		

iii) g_1	g_3	iv) h_1	h_2
20	100	100	25.0
21	100	100	21.0
22	100	100	21.0
21	100	100	21.8
21	100	100	25.8
21.0	100 mean value	100	22.9 mean value
9.27	49.3 rel. conc.		4.36 h_1/h_2
	21.3 $4h_3/h_1$		

A plot of the reciprocal concentration of CHF_2I against

i) e_2/e_1 and ii) $e_2/4e_3$, by the least squares method, gave the following intercepts and slopes:

i) intercept = 0.304 $\pm$ 0.004; slope = 0.059 $\pm$ 0.013

ii) intercept = 0.044 $\pm$ 0.001; slope = 0.0062 $\pm$ 0.0022

Table 2-4

$[CHF_2I] \times 10^3$ mol l^{-1}	e_2/e_1	e_2E_o/e_3F_o
0.22	0.568	0.0711
0.38	0.469	0.0616
1.50	0.339	0.0470

C - Variation of concentration at 150°C.

a) $[CHF_2I]$ 0.22 x 10^{-3} mol l^{-1}, temp 150°C, time 20.28h

i) e_1	e_2	ii) a_1	a_3
100	34.5	39.0	100
100	33.0	42.8	100
100	36.3	41.4	100
100	34.6 mean value	41.1	100 mean value
	2.89 e_1/e_2	29.0	84.2 rel. conc.
	0.346 e_2/e_1		11.61 $4e_3/e_1$
	0.0298 $e_2/4e_3$		

b) $[CHF_2I]$ 0.38 x 10^{-3} mol l^{-1}, temp 150°C, time 20.00h

i) e_1	e_2	ii) a_1	a_3
100	33	46.2	100
100	33	44.0	100
100	30	46.2	100
100	31	44.0	100
100	31.8 mean value	45.1	100 mean value
	3.15 e_1/e_2	31.9	84.2 rel. conc.
	0.317 e_2/e_1		10.57 $4e_3/e_1$
	0.0300 $e_2/4e_3$		

e) $[CHF_2I]$ 1.50 x 10^{-3} mol l^{-1}, temp. 150°C, time 18.67h

i) e_1	e_2	ii) a_1	a_3
100	23.2	50	100
100	22.6	50	100
100	23.2	53	100
100	22.2	53	100
100	22.8 mean value	51.5	100 mean value
	4.39 e_1/e_2	36.4	84.2 rel. conc.
	0.228 e_2/e_1		9.26 $4e_3/e_1$
	0.0246 $e_2/4e_3$		

iii) g_1	g_3	iv) h_1	h_2
25	100	100	28
25	100	100	30
24	100	100	32.5
24	100	100	26
24.5	100 mean value	100	29.1 mean value
10.8	49.3 rel. conc.		3.43 h_1/h_2
	18.3 $4h_3/h_1$		

A plot of the reciprocal concentration of CHF_2I against i) e_2/e_1 and ii) $e_2/4e_3$, by the least squares method, gave the following intercepts and slopes:

i) intercept = 0.217 ± 0.009; slope = 0.030 ± 0.027

ii) intercept = 0.025 ± 0.001; slope = 0.0013 ± 0.0025

Table 2-5

$[CHF_2I] \times 10^3$ mol l^{-1}	e_2/e_1	e_2E_o/e_3F_o
0.22	0.346	0.0298
0.38	0.317	0.0300
1.50	0.228	0.0246

Table 2-6

$[CHF_2I] \times 10^3$ mol l^{-1}	Temp °C	$4e_3/e_1$	$e_2/4e_3$	e_2/e_1
0.22	98	7.99	0.0711	0.568
0.38	100	7.61	0.0616	0.469
1.50	100	7.21	0.0470	0.339
0.22	150	11.61	0.0298	0.346
0.38	150	10.57	0.0300	0.317
1.50	150	9.26	0.0246	0.228

The reactions of difluoroiodomethane with trifluoroethylene and ethylene

A series of photolyses was carried out with CHF_2I (0.75×10^{-3} mol l^{-1}), $CHF{=}CH_2$ (0.25×10^{-3} mol l^{-1}) and $CH_2{=}CH_2$ (0.13×10^{-3} mol l^{-1}). The temperature was varied in the range 50-217°C and the reaction time in the range 2-48h. The six measurable product peaks were the normal and reverse trifluoroethylene and the ethylene adducts from addition of difluoromethyl and difluoroiodomethyl radicals.

let a_1 = the relative area of CHF_2CHFCF_2I
a_2 = the relative area of CHF_2CF_2CHFI
a_3 = the relative area of $CHF_2CH_2CH_2I$
g_1 = the relative area of $CF_2ICHFCF_2I$
g_2 = the relative area of CF_2ICF_2CHFI
g_3 = the relative area of $CF_2ICH_2CH_2I$

e_1, e_2, e_3, h_1, h_2, h_3 = the corresponding relative concentrations.

a) temp. 50°C, time 47.20h

i) e_1	e_2	ii) a_1	a_3
100	86.3	91.2	100
100	88.0	88.0	100
100	85.0	88.8	100
100	85.0	83.8	100
100	84.3	88.8	100
100	85.7 mean value	88.1	100 mean value
	1.17 e_1/e_2	57.0	84.2 rel. conc.
			2.96 $2e_3/e_1$

b) temp. 66°C, time 21.50h

i) e_1	e_2	ii) a_1	a_3
100	84	64	100
100	79	66	100
100	77	62	100
100	80 mean value	64	100 mean value
	1.25 e_1/e_2	41.4	84.2 rel. conc.
			4.10 $2e_3/e_1$

iii) h_1	h_2	iv) g_1	g_3
100	42	21.0	100
100	46	15.8	100
100	44 mean value	18.4	100 mean value
	2.27 h_1/h_2	7.7	49.3 rel. conc.
			12.8 $2h_3/h_1$

c) temp. 92°C, time 20.23h

i) e_1	e_2	ii) a_1	a_3
100	90.7	55.2	100
100	89.8	53.7	100
100	87.8	56.2	100
100	87.8	58.0	100
100	85.0	54.0	100
100	88.2 mean value	55.4	100 mean value
	1.13 e_1/e_2	35.8	84.2 rel. conc.
			4.70 $2e_3/e_1$

iii)

h_1	h_2	g_1	g_3
100	44.4	31.8	100
100	49.0	28.8	100
100	53.0	29.6	100
100	52.8	26.8	100
100	47.1	27.2	100
100	49.3 mean value	28.8	100 mean value
	2.03 h_1/h_2	12.1	49.3 rel. conc.
			8.17 $2h_3/h_1$

d) temp. 106°C, time 12.80h

i)

e_1	e_2
100	92
100	87
100	86
100	84
100	87.2 mean value
	1.15 e_1/e_2

ii)

a_1	a_3
47.0	100
52.5	100
52.0	100
43.6	100
48.8	100 mean value
27.3	84.2 rel. conc.
	5.35 $2e_3/e_1$

iii)

h_1	h_2
100	48.0
100	50.4
100	47.8
100	52.0
100	49.6 mean value
	2.02 h_1/h_2

iv)

g_1	g_3
24.9	100
20.1	100
23.0	100
22.9	100
22.7	100 mean value
9.52	49.3 rel. conc.
	10.36 $2h_3/h_1$

e) temp. 135°C, time 5.10h

i)

e_1	e_2
100	89.7
100	90.8
100	92.8
100	91.1 mean value
	1.10 e_1/e_2

ii)

a_1	a_3
41.8	100
42.1	100
38.0	100
40.6	100 mean value
26.3	84.2 rel. conc.
	6.42 $2e_3/e_1$

iii)

h_1	h_2
100	52
100	55
100	54
100	53
100	56
100	54 mean value
	1.85 h_1/h_2

iv)

g_1	g_3
19.3	100
19.3	100
18.8	100
18.3	100
22.2	100
19.6	100 mean value
8.20	49.3 rel. conc.
	12.30 $2h_3/h_1$

f) temp. 136°C, time 15.52h

i)

e_1	e_2
100	82
100	83
100	85
100	83
100	83
100	83 mean value
	1.20 e_1/e_2

ii)

a_1	a_3
48.9	100
51.0	100
46.2	100
48.9	100
54.4	100
49.9	100 mean value
32.2	84.2 rel. conc.
	5.23 $2e_3/e_1$

iii)

h_1	h_2
100	64
100	64
100	65
100	61
100	62
100	63.2 mean value
	1.58 e_1/e_2

iv)

g_1	g_3
29.0	100
29.8	100
30.0	100
29.6	100 mean value
12.4	49.3 rel. conc.
	7.96 $2h_3/h_1$

g) temp. 162°C, time 6.00h

i)

e_1	e_2
100	95.8
100	92.5
100	93.0
100	92.4
100	93.4 mean value
	1.07 e_1/e_2

ii)

a_1	a_3
40.8	100
40.0	100
40.1	100
39.2	100
40.0	100 mean value
25.9	84.2 rel. conc.
	6.51 $2e_3/e_1$

iii)

h_1	h_2	g_1	g_3
100	69.6	25.0	100
100	70.0	27.1	100
100	65.4	25.2	100
100	64.0	21.0	100
100	66.2	23.2	100
100	67.0 mean value	24.3	100 mean value
	1.49 h_1/h_2	10.2	49.3 rel. conc.
			9.69 $2h_3/h_1$

h) temp. 217°C, time 2.33h

i)

e_1	e_2
100	104.2
100	105.0
100	101.3
100	100.0
100	102.6 mean value
	0.975 e_1/e_2

ii)

a_1	a_3
34.9	100
35.0	100
33.6	100
37.0	100
35.1	100 mean value
22.7	84.2 rel. conc.
	7.42 $2e_3/e_1$

i) temp. 54.5°C, time 9.80h

i)

e_1	e_2
100	82
100	83
100	79
100	80
100	80
100	80.8 mean value
	1.24 e_1/e_2

j) temp, 81°C, time 5.70h

i)

e_1	e_2
100	81
100	84
100	83
100	84
100	80
100	82.4 mean value
	1.21 e_1/e_2

k) temp, 127°C, time 2.00h

i)

e_1	e_2
100	92
100	93
100	89
100	93
100	91.8 mean value
	1.09 e_1/e_2

l) temp. 148°C, time 2.00h

i)

e_1	e_2
100	92
100	94
100	95
100	93.8 mean value
	1.07 e_1/e_2

m) temp. 170°C, time 2.08h

i) e_1	e_2	
100	96	
100	98	
100	96	
100	95	
100	96	
100	96.2	mean value
	1.04	e_1/e_2

Plots of i) log e_1/e_2, ii) log $2e_3/e_1$, iii) log h_1/h_2 and iv) log $2h_3/h_1$ against $10^3/T$, by the least squares method, gave:

i) (add^n. of $CHF_2\cdot$) gradient = 0.085 $\pm$ 0.040; intercept = -0.17 $\pm$ 0.02

ii) (add^n. of $CHF_2\cdot$) gradient = -0.35 $\pm$ 0.12; intercept = 1.62 $\pm$ 0.05

iii) (add^n. of $CF_2I\cdot$) gradient = 0.28 $\pm$ 0.14; intercept = -0.44 $\pm$ 0.05

iv) (add^n. of $CF_2I\cdot$) gradient = 0.12 $\pm$ 0.44; intercept = 0.69 $\pm$ 0.17

Table 2-7

Temp °C	e_1/e_2	log e_1/e_2	$2e_3/e_1$	log $2e_3/e_1$	h_1/h_2	log h_1/h_2	$2h_3/h_1$	log $2h_3/h_1$
50	1.17	0.0671	2.96	0.471	-	-	-	-
66	1.25	0.0976	4.10	0.613	2.27	0.357	12.8	1.11
92	1.13	0.0546	4.70	0.673	2.03	0.308	8.17	0.912
106	1.15	0.0588	5.35	0.728	2.02	0.305	10.36	1.015
135	1.10	0.0407	6.42	0.807	1.85	0.268	12.03	1.080
136	1.20	0.0802	4.23	0.718	1.58	0.200	7.96	0.901
162	1.07	0.0294	6.51	0.814	1.49	0.175	9.69	0.986
217	0.975	-0.0111	7.42	0.871	-	-	-	-
54.5	1.24	0.0923						
81	1.21	0.0842						
127	1.09	0.0374						
148	1.07	0.0280						
170	1.04	0.0167						

The reactions of difluoroiodomethane with tetrafluoroethylene and ethylene

A series of photolyses was carried out with CHF_2I (0.75×10^{-3} mol l^{-1}), $CF_2{=}CF_2$ (0.19×10^{-3} mol l^{-1}) and $CH_2{=}CH_2$ (0.19×10^{-3} mol l^{-1}). The temperature and time were varied in the ranges of 40-230°C and 1.5-22h. The six measurable products were the tetrafluoroethylene and ethylene adducts and the cross telomers from the addition of difluoromethyl and difluoroiodomethyl radicals: the cross telomers were from addition of the halomethyl radicals to tetrafluoroethylene followed by the intermediate substituted propyl radicals adding to ethylene ($CHF_2CF_2CF_2CH_2CH_2I$ and $CF_2ICF_2CF_2CH_2CH_2I$).

let a_1 = the relative area of $CHF_2CF_2CF_2I$

a_2 = the relative area of $CHF_2CF_2CF_2CH_2CH_2I$

a_3 = the relative area of $CHF_2CH_2CH_2I$

g_1 = the relative area of $CF_2ICF_2CF_2I$

g_2 = the relative area of $CF_2ICF_2CF_2CH_2CH_2I$

g_3 = the relative area of $CF_2ICH_2CH_2I$

e_1, e_2, e_3, h_1, h_2, h_3 = the corresponding relative concentrations.

a) temp. 40°C, time 21.68h

i) a_1	a_2	a_3	ii) g_1	g_2	g_3
162	18.0	100	100	132	288
150	21.3	100	100	184	320
155	21.1	100	100	196	442
			100	129	296
156	20.1	100 mean value			
93.4	10.9	84.2 rel. conc.	100	160	337 mean value
		1.24 $(e_1 + e_2)/e_3$	39.9	59.5	166 rel. conc.
					2.00 $h_3/(h_1 + h_2)$

b) temp. 63°C, time 18.63h

i) a_1	a_2	a_3	ii) g_1	g_2	g_3
126	36.2	100	100	204	389
132	37.6	100	100	208	464
129	36.9	100 mean value	100	206	426 mean value
77.4	19.9	84.2 rel. conc.	39.9	76.5	210 rel. conc.
		1.16 $(e_1 + e_2)/e_3$			1.81 $h_3/(h_1 + h_2)$

c) temp. 93°C, time 18.60h

i) a_1	a_2	a_3	ii) g_1	g_2	g_3
152	33	100	100	236	448
139	39	100	100	245	462
112	41	100	100	224	456
115	40	100	100	200	448
117	38	100			
127	38	100 mean value	100	226	454 mean value
76.1	20.6	84.2 rel. conc.	39.9	84.0	224 rel. conc.
		1.15 $(e_1 + e_2)/e_3$			1.81 $h_3/(h_1 + h_2)$

d) temp. 108°C, time 16.43h

ii) g_1	g_2	g_3
100	102	234
100	108	256
100	105	245 mean value
39.9	39.0	120.9 rel. conc.
		1.53 $h_3/(h_1 + h_2)$

e) temp. 132°C, time 19.77h

i) a_1	a_2	a_3	ii) g_1	g_2	g_3
110.0	48.9	100	100	241	327
122.5	48.0	100	100	296	430
100.0	56.8	100	100	312	418
104.5	54.3	100			
109.3	52.0	100 mean value	100	283	392 mean value
65.5	28.0	84.2 rel. conc.	39.9	105	193 rel. conc.
		1.11 $(e_1 + e_2)/e_3$			1.33 $h_3/(h_1 + h_2)$

f) temp. 160°C, time 5.77h

i) a_1	a_2	a_3
107.0	52.3	100
117.5	54.4	100
109.3	52.0	100
105.0	55.8	100
112.5	45.9	100
110.3	52.1	100 mean value
66.1	28.1	84.2 rel. conc.
		1.12 $(e_1 + e_2)/e_3$

g) temp. 181°C, time 3.00h

i)

a_1	a_2	a_3	
100.4	45.6	100	
110.8	43.7	100	
106.4	44.0	100	
105.0	47.5	100	
105.7	45.2	100	mean value
63.4	24.4	84.2	rel. conc.
		1.04	$(e_1 + e_2)/e_3$

h) temp. 230°C, time 1.50h

i)

a_1	a_2	a_3	
116.0	52.0	100	
97.0	57.3	100	
95.8	54.6	100	
99.5	55.5	100	
86.3	65.0	100	
98.9	56.9	100	mean value
59.3	30.7	84.2	rel. conc.
		1.07	$(e_1 + e_2)/e_3$

Plots of i) log $(e_1 + e_2)/e_3$ and ii) log $h_3/(h_1 + h_2)$ against $10^3/T$, by the least squares method, gave:

i) (add^n. of $CHF_2\cdot$) gradient = 0.052 $\pm$ 0.026; intercept = -0.081 $\pm$ 0.010

ii) (add^n. of $CF_2I\cdot$) gradient = 0.22 $\pm$ 0.16; intercept = -0.40 $\pm$ 0.06

Table 2-8

Temp°C	$\frac{e_1+e_2}{e_3}$	log $\frac{e_1+e_2}{e_3}$	$\frac{h_3}{h_1+h_2}$	log $\frac{h_3}{h_1+h_2}$
40	1.24	0.0923	2.00	0.302
63	1.16	0.0626	1.81	0.257
93	1.15	0.0595	1.81	0.257
108	-	-	1.53	0.185
132	1.11	0.0457	1.33	0.125
160	1.12	0.0487	-	-
181	1.04	0.0178	-	-
230	1.07	0.0286	-	-

DISCUSSION

The primary photolytic process in the photolyses of halomethanes is the homolytic fission of the weakest carbon-halogen bond giving halomethyl radicals and halogen atoms. Goodeve and Porret[118] represented the primary process in the photolysis of CH_3I at 254 nm by the formation of excited CH_3^* radicals and $I^*(^2P_{\frac{1}{2}})$ atoms. The excitation energy of iodine atoms from the ground ($^2P_{3/2}$) to the excited ($^2P_{\frac{1}{2}}$) state is 21.6 k cal mol^{-1}. With the use of a pyrex reaction vessel the main incident wavelengths during the photolysis of CHF_2I were 313 and 366 nm corresponding to 92 and 78 k cal mol^{-1} respectively. The dissociation energy of the carbon-iodine bond in CHF_2I is approximately 50 k cal mol^{-1} which leaves sufficient energy for the primary photolytic process to give excited CHF_2^* radicals to the extent of approx. 20 k cal mol^{-1} and excited I^* atoms.

$$CHF_2I + h\nu \xrightarrow{\text{ØIa}} CHF_2^* + I^* \ (^2P_{\frac{1}{2}}) \qquad 1$$

Pryor[99] notes that hydrogen abstractions from alkanes by iodine atoms is appreciably endothermic whereas on the other hand iodine atoms abstract I from alkyl iodides: although participation of excited I^* will affect the situation the preference for I abstraction should remain. In the competitive H and I abstraction reactions of iodine atoms the strengths of the I-I (36.1 k cal mol^{-1}) and H-I (71.4 k cal mol^{-1}) bonds formed favour hydrogen abstraction but this is more than counter-balanced by the strengths of the C-H (approx. 95 k cal mol^{-1}) and C-I (approx. 50 k cal mol^{-1}) bonds broken during the abstraction processes.

Abstraction of H from CHF_2I by the excited I^* atoms formed in the primary photolytic process produces a system in which both $CHF_2\cdot$ and $CF_2I\cdot$ radicals are generated: the contribution to the formation of $CF_2I\cdot$ from the abstraction of H by $CHF_2\cdot$ may be of minor importance.

$$I^* (^2P_{\frac{1}{2}}) + CHF_2I \longrightarrow CF_2I\cdot + HI \qquad 1'$$

The abstraction of I by excited I^* atoms contributes to the formation of nonexcited $CHF_2\cdot$ radicals.

$$I^* (^2P_{\frac{1}{2}}) + CHF_2I \longrightarrow CHF_2\cdot + I_2 \qquad 1''$$

The formation of $CF_2I\cdot$ radicals occurs by a secondary process and the resultant radicals remain in ground states.

Gunning[87] et al. observed the analogous abstraction of H by Cl· atoms from difluorochloromethane giving $CF_2Cl\cdot$ radicals: $CHF_2\cdot$ radicals also abstracted H from CHF_2Cl giving $CF_2Cl\cdot$ radicals. Similar competitive abstraction reactions were observed by Tedder[98] et al. during the photolysis of bromodichloromethane: the dichloromethyl radicals competitively abstracted hydrogen and bromine from $CHCl_2Br$ giving a system in which $CHCl_2\cdot$ and $CCl_2Br\cdot$ radicals were generated. Szwarc[7] and co-workers observed that hydrogen abstraction is competitive with bromine and iodine abstraction from alkyl bromides and iodides by methyl radicals. Whittle[100] and co-workers showed that hydrogen abstraction from chloromethane by trifluoromethyl radicals was faster than chlorine abstraction.

In the kinetic series of photolyses with the fluoroethylenes and ethylene the adducts from the addition of $CHF_2\cdot$ and $CF_2I\cdot$ radicals were observed; the identities of the reverse 1,1-difluoroethylene and trifluoroethylene adducts from the

addition of $CF_2I\cdot$ radicals were assumed.

$$X\cdot + E \longrightarrow XE\cdot \qquad 2$$

$$XE\cdot + CHF_2I \longrightarrow XEI + CHF_2\cdot \qquad 3$$

where: $X\cdot = CHF_2\cdot$, $CH_2I\cdot$; E = olefin

Additionally, in the presence of tetrafluoroethylene and ethylene, the cross telomers were formed from the addition of the halomethyl radicals to tetrafluoroethylene followed by addition of the intermediate radicals to ethylene ($X\,CF_2CF_2CH_2CH_2I$).

$$X\cdot + E' \longrightarrow XE'\cdot \qquad 4$$

$$XE\cdot' + E \longrightarrow XE'E\cdot \qquad 5$$

$$XE'E\cdot + CHF_2I \longrightarrow XE'EI + CHF_2\cdot \qquad 6$$

where: $X = CHF_2\cdot$, $CF_2I\cdot$; $E' = CF_2{=}CF_2$, $E = CH_2{=}CH_2$

Also difluorodiiodomethane was formed in all of the kinetic reactions.

$$CF_2I\cdot + CHF_2I \longrightarrow CF_2I_2 + CHF_2\cdot \qquad 7$$

In the preparative runs a few additional products were observed. Only one dehydroiodination product was identified.

$$CHF_2CH_2CF_2I \xrightarrow{-HI} CHF_2CH{=}CF_2 + HI \qquad 8$$

Two of the two to one telomers from the addition of $CHF_2\cdot$ radicals to trifluoroethylene were observed ($CHF_2CHFCF_2CHFCF_2I$ and $CHF_2CHFCF_2CF_2CHF\ I$). The two to one telomers from the addition of $CHF_2\cdot$ and $CF_2I\cdot$ radicals and the three to one telomer from the addition of $CHF_2\cdot$ radicals to tetrafluoroethylene were identified.

$$X\,CF_2CF_2\cdot + CF_2{=}CF_2 \longrightarrow X(CF_2CF_2)_2\cdot \qquad 9$$

$$X(CF_2CF_2)_2\cdot + CHF_2I \longrightarrow X(CF_2CF_2)_2I + CHF_2\cdot \qquad 10$$

$$CHF_2(CF_2CF_2)_2\cdot + CF_2{=}CF_2 \longrightarrow CHF_2(CF_2CF_2)_3\cdot \qquad 11$$

$$CHF_2\,(CF_2CF_2)_3\cdot + CHF_2I \longrightarrow CHF_2(CF_2CF_2)_3I + CHF_2\cdot \qquad 12$$

where $X\cdot = CHF_2\cdot$, $CF_2I\cdot$

Several diiodides were obtained from the addition of excited iodine atoms; these included the ethylene and tetrafluoroethylene diiodides (CH_2ICH_2I and CF_2ICF_2I), the tetrafluoroethylene two to one cross telomer ($I(CF_2CF_2)_2I$ and the cross telomer from addition to tetrafluoroethylene followed by addition to ethylene ($ICF_2CF_2CH_2CH_2I$). Formation of the ethylene diiodide is not favoured owing to the endothermic addition step, but addition of excited I^* is slightly exothermic.

$$I\cdot + CH_2{=}CH_2 \longrightarrow CH_2ICH_2\cdot \qquad \triangle H = 7 \text{ k cal mol}^{-1} \qquad 13$$

The extent of formation of the other diiodides indicates that iodine atom addition to an unsaturated carbon atom having two fluorine substituents is more favourable. Rather than adding to olefins, iodine atoms prefer to react with alkyl iodides by abstracting iodine.

$$I\cdot + RI \longrightarrow R\cdot + I_2 \qquad 14$$

MATHEMATICAL TREATMENT OF RATE DATA

The $CHF_2\cdot$ and $CF_2I\cdot$ radicals are less selective than $CFBr_2\cdot$ radicals in addition reactions to the fluoroethylenes, and this facilitates the measurement of product peaks from reactions of low percentage conversion (<10%). Consequently simplified expressions of the rate equations derived in part 1 are adequate. Expansion of the series ln (1+x) where $-1 < x < 1$ gives:

$$\ln(1+x) = x - x^2/2 + x^3/3 - x^4/4 + \ldots\ldots + (-1)^m x^{m-1}/(m-1) + R_m \qquad 15$$

and introducing the approximation that ln(1+x) equals x into equations 28 and 60 of part 1 gives simplified expressions. Equation 28 of part 1 for the competitive addition to ethylene and an unsymmetrical fluoroethylene reduces to:

$$\log e_3F_o/e_1E_o = \log A_3 - \log A_1 + (E_1 - E_3)/2.303RT \quad 16$$

where F_o = initial concentration of the assymmetrical fluoroethylene

E_o = " " " ethylene

e_3 = ethylene adduct concentration

e_1 = an unsymmetrical fluoroethylene adduct concentration

From plots of $\log e_3F_o/e_1E_o$ versus $10^3/T$,

i) the intercepts give the A-factor differences,

$$\text{intercept} = \log A_3 - \log A_1 \quad (1 \text{ mol}^{-1} \text{ s}^{-1}) \quad 17$$

ii) the slopes give the activation energy differences.

$$E_1 - E_3 = 2.303R \text{ . slope} \quad (\text{k cal mol}^{-1}) \quad 18$$

Equation 60 of part 1 for the competitive addition to ethylene and tetrafluoroethylene resulting in the formation of the adducts and the cross telomers ($XCF_2CF_2CH_2CH_2I$; $X = CHF_2\cdot, CF_2I\cdot$) reduces to:

$$\log eF_o/(f+g)E_o = k_2/k_4 = \log A_2 - \log A_4 + (E_4 - E_2)/2.303RT \quad 19$$

where F_o = initial concentration of tetrafluoroethylene

E_o = " " " ethylene

e_3 = ethylene adduct concentration

f = tetrafluoroethylene adduct concentration

g = cross telomer concentration

From a plot of $\log eF_o/(f+g)\ E_o$ versus $10^3/T$,

i) the intercept gives the A-factor difference,

$$\text{intercept} = \log A_2 - \log A_4 \quad (1 \text{ mol}^{-1} \text{ s}^{-1}) \quad 20$$

ii) the slope gives the activation energy difference.

$$E_4 - E_2 = 2.303R \text{ . slope} \quad 21$$

Equation 24 of part 1 for the competitive addition to an unsymmetrical olefin remains unaltered.

Addition of difluoroiodomethyl radicals ($CF_2I\cdot$) to the fluoroethylenes.

This is the first report of reactions of difluoroiodomethyl radicals. The addition reactions of $CF_2I\cdot$ to the fluoroethylenes are analogous to the closely related halomethyl radical addition reactions discussed in part 1. In the kinetic runs the dimer (CF_2ICF_2I) was not observed and, by analogy with the $CFBr_2\cdot$ addition system, the chain reactions were considered to be long and the addition steps to be rate determining. Although both $CHF_2\cdot$ and $CF_2I\cdot$ radicals were generated in the same system a direct comparison between the relative rates of addition of $CHF_2\cdot$ and $CF_2I\cdot$ radicals to a particular olefin was not possible. The products derived from $CHF_2\cdot$ radicals exceeded those from $CF_2I\cdot$ radicals by a factor of approximately 2. Formation of each molecule of the $CF_2I\cdot$ addition products was accompanied by generation of another $CHF_2\cdot$ radical due to the overwhelming preference of the intermediate radical to abstract iodine from CHF_2I.

$$CF_2IE\cdot + CHF_2I \longrightarrow CF_2IEI + CHF_2\cdot \qquad 22$$

where E = olefin

Abstraction of hydrogen by the intermediate radicals was not observed.

$$CF_2IE\cdot + CHF_2I \not\longrightarrow CF_2IEH + CF_2I\cdot \qquad 23$$

This circumstantially confirms the expectation that difluoromethyl radicals abstract iodine more readily than hydrogen from CHF_2I.

$$CHF_2\cdot + CHF_2I \xrightarrow{kx} CHF_2I + CHF_2\cdot \qquad 24$$

$$CHF_2\cdot + CHF_2I \xrightarrow{ky} CH_2F_2 + CF_2I\cdot \qquad 25$$

i.e. $kx > ky$

Formation of both hydrogen and bromine abstraction products in almost equal quantities from the analogous addition reactions of $CHCl_2^{\bullet}$ and $CBrCl_2^{\bullet}$ to the fluoroethylenes from the photolysis of $CHCl_2Br$ implies that hydrogen and bromine abstraction by the halomethyl radicals are of comparable importance.[98]

$$CHCl_2^{\bullet} + CHCl_2Br \xrightarrow{k_x} CHCl_2Br + CHCl_2^{\bullet} \qquad 26$$

$$CHCl_2^{\bullet} + CHCl_2Br \xrightarrow{k_y} CH_2Cl_2 + CCl_2Br^{\bullet} \qquad 27$$

i.e. $k_x \sim k_y$

Methyl radicals[99] abstract I relative to H from $CHCl_2I$ 500 times faster than the corresponding abstractions from $CHCl_2Br$. This may explain the differences in the related $CHF_2^{\bullet}$ and $CHCl_2^{\bullet}$ systems provided the halomethyl radicals follow the same trend as methyl radicals.

The kinetic series of reactions were conducted over the temperature range of 33 - 217°C. The Arrhenius plots are shown in figs. 2 - 1a and 1b. The rates of addition, A-factors and activation energies for the addition of $CF_2I^{\bullet}$ radicals to the fluoroethylenes relative to ethylene were calculated from plots of the adduct ratios versus $10^3/T$ by the least squares method (Table 2-9). Large error factors are associated with the competitive addition of $CF_2I^{\bullet}$ to ethylene and trifluoroethylene owing to the scatter of experimental points (fig. 2-1a). Nevertheless, several deductions can be drawn from the experimental series. The main features of table 2-9 are the same as those outlined on page 62 for the addition of $CFBr_2^{\bullet}$ radicals with the exception that when the constant terminal group is CF_2= increasing the fluorine substituents on the carbon atom under attack reduces the activation energy. The rates of addition of $CF_2I^{\bullet}$ to specific sites and the overall rates of addition to the fluoroethylenes follow the

Fig 2-1a Arrhenius plots for competitive addition of $CF_2I\cdot$ radicals to vinyl fluoride (◉), 1,1-difluoroethylene (○), trifluoroethylene (◑) and tetrafluoroethylene (+) in the presence of ethylene.

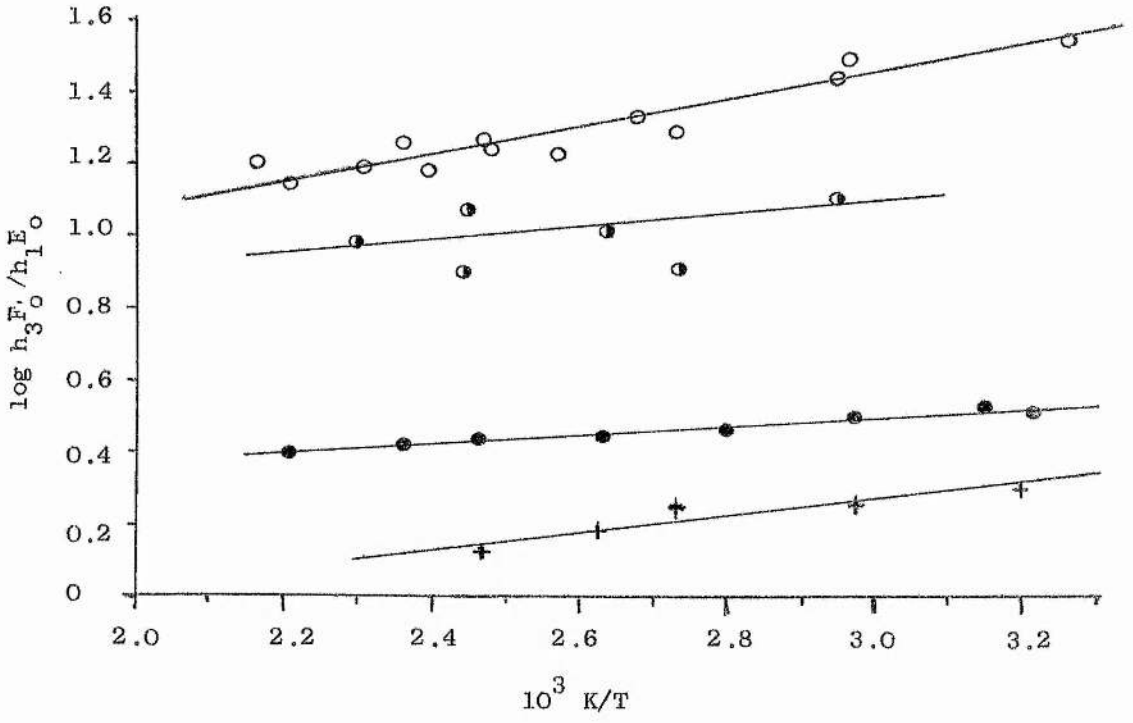

Fig 2-1b Arrhenius plots for addition of $CF_2I\cdot$ radicals to vinyl fluoride (◉), 1,1-difluoroethylene (○) and trifluoroethylene (◑).

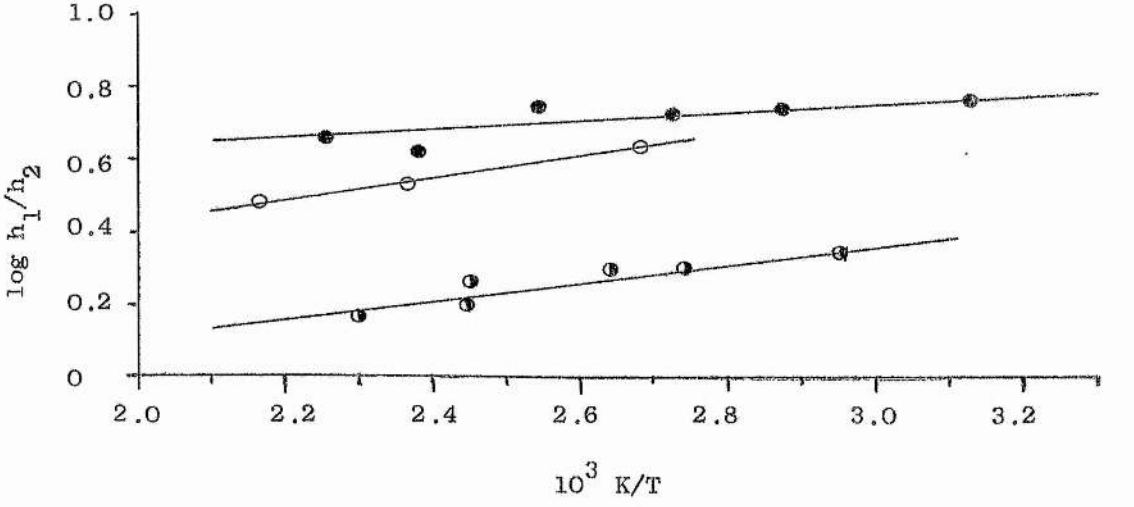

same pattern as the other halomethyl radicals (Table 2-10; c.f. Tables 1-12 and 13).

Table 2 - 9 The addition of difluoroiodomethyl ($CF_2I\cdot$) radicals to fluoroethylenes relative to ethylene

Olefin	k_2/k_2' at 150°C	$\log A_2 - \log A_2'$	$E_2 - E_2'$
$\overset{*}{C}H_2=CH_2$	1.0	0.0	0.0
$\overset{*}{C}H_2=CHF$	0.38	-0.14 ± 0.01	0.55 ± 0.09
$\overset{*}{C}H_2=CF_2$	0.13	-0.05 ± 0.04	1.65 ± 0.41
$\overset{*}{C}HF=CH_2$	0.079	-0.49 ± 0.06	1.19 ± 0.68
$\overset{*}{C}HF=CF_2$	0.10	-0.69 ± 0.17	0.55 ± 2.01
$\overset{*}{C}F_2=CH_2$	0.018	-0.19 ± 0.06	3.02 ± 0.69
$\overset{*}{C}F_2=CHF$	0.064	-0.25 ± 0.22	1.83 ± 2.65
$\overset{*}{C}F_2=CF_2$	0.76	0.40 ± 0.06	1.01 ± 0.73

* denotes the site of addition

k_2, A_2 and E_2 refer to addition to the fluoroethylenes

k_2', A_2' and E_2' " " " " ethylene

A_2 and A_2' in 1 mol^{-1} s^{-1}

E_2 and E_2' in k cal mol^{-1}

Table 2 - 10 A The rates of $CF_2I^\bullet$ add^n. to specific sites in the fluoroethylenes relative to ethylene at 150°C.

B The overall rates of $CF_2I^\bullet$ add^n. to the fluoroethylenes relative to ethylene at 150°C.

A		B		
Olefin	$CF_2I^\bullet$	Olefin	No. of F atoms	$CF_2I^\bullet$
$\overset{*}{C}H_2=CH_2$	1.0	$CH_2=CH_2$	0	1.0
$\overset{*}{C}H_2=CHF$	0.38	$CH_2=CHF$	1	0.92
$\overset{*}{C}H_2=CF_2$	0.13	$CH_2=CF_2$	2	0.30
$\overset{*}{C}HF=CH_2$	0.079	$CHF=CF_2$	3	0.32
$\overset{*}{C}HF=CF_2$	0.1	$CF_2=CF_2$	4	0.76
$\overset{*}{C}F_2=CH_2$	0.018			
$\overset{*}{C}F_2=CHF$	0.064			
$\overset{*}{C}F_2=CF_2$	0.76			

* denotes the site of addition: the values are expressed per active site.

The orientation ratios for addition of $CF_2I^\bullet$ to the unsymmetrical olefins at 150°C are $CH_2=CHF$ 1 : 0.21, $CH_2=CF_2$ 1: 0.14, $CHF=CF_2$ 1 : 0.64. The relatively low selectivity of the $CF_2I^\bullet$ radical is not consistent with its size (r = 4.98Å) in relation to the results for the other halomethyl radicals (c.f. Table 1-14). The low selectivity combined with the large radius of $CF_2I^\bullet$ excludes it from fitting the correlation pattern obtained from plotting the log of the adduct ratios against the radii of halomethyl radicals as illustrated in fig. 1-4. The relative A-factors are within the normal range and show only slight variations. The free valence indices and the charge densities of the reactive sites in the

olefins correctly predict the preferred orientation of addition to each unsymmetrical olefin. However, the rate of addition to the CH_2= ends of vinyl fluoride and 1,1-difluoroethylene relative to ethylene are not in accord with f.v.i. and change density predictions. The results are in agreement with those for addition of the other halomethyl radicals. The activation energy differences for CF_3·, C_3F_7·, CCl_3· and $CFBr_2$· radicals gave a good correlation with the modified atom localisation energy parameter $L_\mu - B\delta Q_\mu$ (fig. 1-13) where the contribution from the coulombic repulsion term was optimised for each type of addition site by varying the value of the constant B. A similar correlation is observed with CF_2I· with B set equal to zero for addition to a CF_2= group, 1.1 for addition to a CH_2= group and an intermediate value for addition to a CHF group (fig. 2-2).

Addition of CF_2I· radicals to the fluoroethylenes follows the same pattern exhibited by the addition of CF_3·, C_3F_7· CCl_3·, CF_2Br· and $CFBr_2$· radicals. The main point of difference is the low selectivity of CF_2I·.

Addition of difluoromethyl radicals (CHF_2·) to the fluoroethylenes.

The apparent insignificance of termination, elimination and hydrogen abstraction products, and the presence of only the adducts and the cross tetrafluoroethylene-ethylene telomer from CHF_2· addition reactions to the olefins led to the initial deductions that the chain reactions were long and that the addition steps were rate determining. However, applying the least squares method to plots of the logarithms of the CHF_2· adduct ratios against $10^3/T$ gives mainly negative slopes, indicating divergence of adduct ratios with increasing temperature, and intercepts varying by up to three orders of magnitude implying that A-factors vary by factors of up to 1,000 (Table 2-11).

Fig 2-2 Correlation of $\triangle E_a$ with the modified atom localisation energy parameter for add^n. of $CF_2I\cdot$ radicals to the fluoroethylenes.

B = 1.1 for add^n. to $CH_2=$

B = 0.5 for add^n. to $CHF=$

B = 0 for add^n. to $CF_2=$

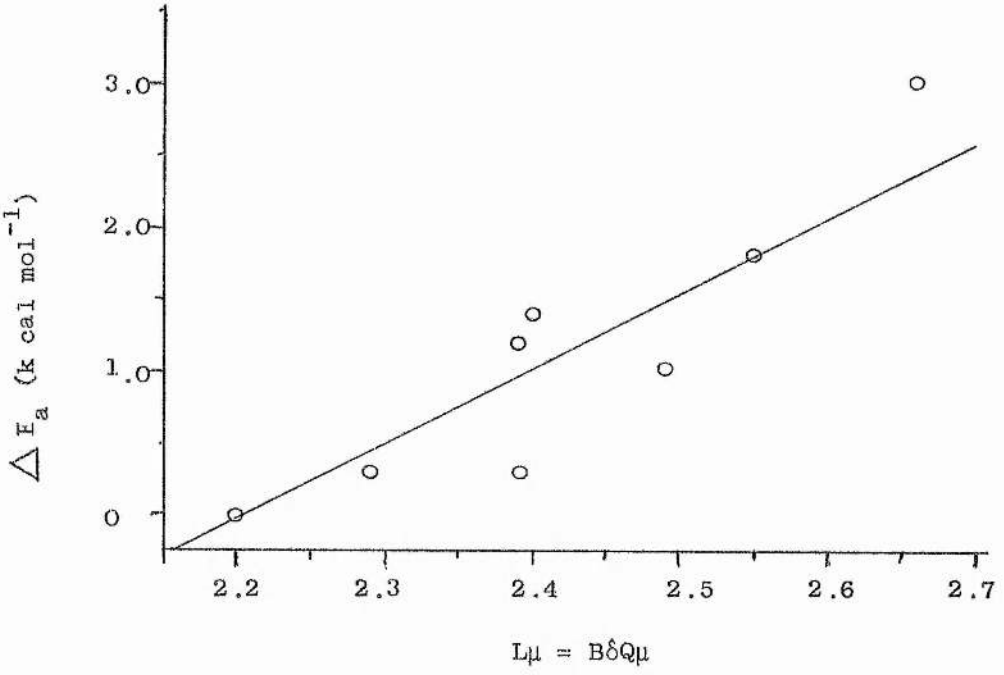

The improbability of these situations was recognised and much effort was directed towards finding satisfactory explanations.

The logarithms of the adduct ratios are plotted against $10^3/T$ for the competitive addition of difluoromethyl radicals to vinyl fluoride, 1,1-difluoroethylene, trifluoroethylene and tetrafluoroethylene relative to ethylene in fig. 2-3a, and for addition to both ends of each unsymmetrical olefin in fig. 2-3b. The only results showing normal behaviour, in competitive addition reactions with ethylene, are the two reaction series with vinyl fluoride and tetrafluoroethylene.

The rates of formation of these adducts and the cross telomer are of comparable magnitude and relatively fast. The Arrhenius plots for the competitive series with 1,1-difluoroethylene and trifluoroethylene appear to project curves.

Table 2-11 The addition of $CHF_2\cdot$ radicals to fluoroethylenes relative to ethylene.

Olefin	k_2/k_2' at 150°C	log A_2 - log A_2'	$E_2 - E_2'$
$\overset{*}{C}H_2=CH_2$	1.0	0.0	0.0
$\overset{*}{C}H_2=CHF$	0.68	-0.035 ± 0.020	0.26 ± 0.30
$\overset{*}{C}H_2=CF_2$	0.11	-1.72 ± 0.05	-1.51 ± 0.55
$\overset{*}{C}HF=CH_2$	0.14	-1.41 ± 0.05	-1.07 ± 0.71
$\overset{*}{C}HF=CF_2$	0.16	-1.62 ± 0.05	-1.60 ± 0.55
$\overset{*}{C}F_2=CH_2$	0.020	-3.36 ± 0.09	-3.20 ± 1.05
$\overset{*}{C}F_2=CHF$	0.15	-1.45 ± 0.07	-1.21 ± 0.73
$\overset{*}{C}F_2=CF_2$	0.90	0.08 ± 0.01	0.24 ± 0.12

* denotes the site of addition

k_2 , A_2 and E_2 refer to addition to the fluoroethylene

k_2', A_2' and E_2' " " " " ethylene

A_2 and A_2' in l mol^{-1} s^{-1}

E_2 " E_2' in k cal. mol^{-1}

Similarly, the Arrhenius plots for addition to both ends of vinyl fluoride and 1,1-difluoroethylene also appear to project curves. The common factor in the four Arrhenius plots showing curvature is that in each case one adduct predominates while the other adduct is formed to a minor extent. Although addition to both ends of trifluoroethylene gives a relatively straight line, the rates of formation of both the normal and reverse adducts

Fig 2-3a Arrhenius plots for competitive addition of $CHF_2\cdot$ radicals to vinyl fluoride (●), 1,1-difluoroethylene (○), trifluoroethylene (◐) and tetrafluoroethylene (+) relative to ethylene.

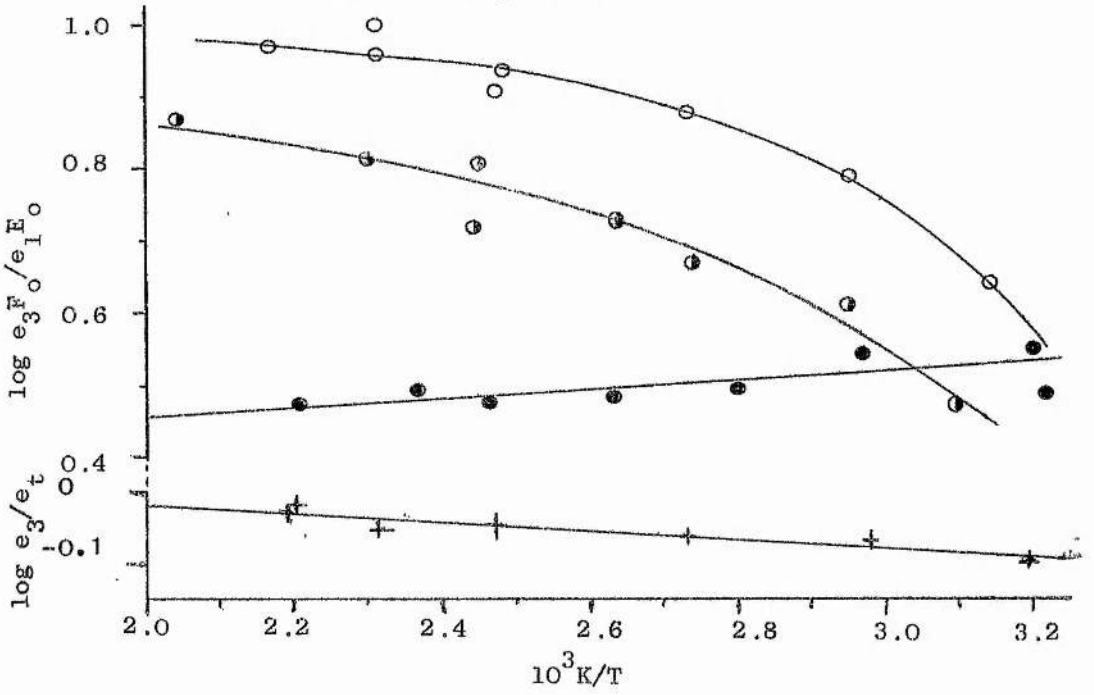

Fig 2-3b Arrhenius plots for addition of $CHF_2\cdot$ radicals to vinyl fluoride (●), 1,1-difluoroethylene (○) and trifluoroethylene (◐).

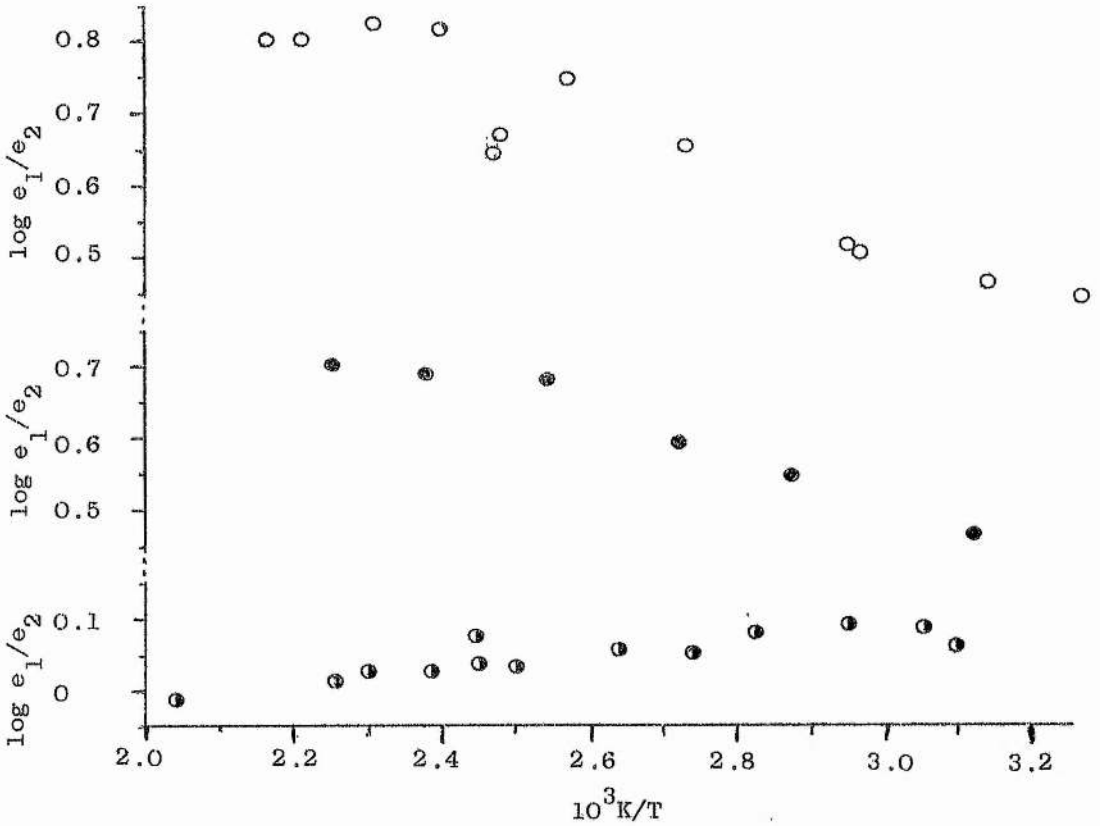

are about equal and of comparable magnitude to those of the minor adducts in the curved plots indicating that this straight line may fortuitously result from compensatory effects.

By tentatively assuming A-factors within the normal range and accepting the adduct ratios corresponding to the middle of the experimental temperature range as reasonably accurate, then explanations were sought in two combinations of alternative situations:

i) at high temperatures there is either an excess of major adduct or deficiency of minor adduct;

ii) at low temperatures there is either a deficiency of major adduct or an excess of minor adduct. Several possible causes of the observed anomalous effect require consideration:

a) elimination of hydrogen iodide from the adducts;

b) cross combination, dimerisation and disproportionation of radical species generated within the system;

c) the removal of adduct radicals from the system by hydrogen abstraction as well as by iodine abstraction;

d) the removal of adduct radicals by telomerisation;

e) reversibility of the addition step;

f) participation of excited radicals.

a - Elimination of hydrogen iodide from the adducts

Dehydrohalogenation reactions generally proceed by a molecular mechanism via a 4-centre transition state with activation energies falling in the range of 40-60 k cal mol^{-1}. The carbon-iodine bond in substituted propyl iodides is relatively weak and liable to thermal scission at moderate temperatures giving substituted propenes and hydrogen iodide. Propyl chloride decomposes[101] to propene and hydrogen chloride at about 300°C. Propyl iodide will decompose at lower temperatures. Nevertheless, Greig[20]

has studied the addition of trifluoromethyl radicals to the fluoroethylenes over the temperature range of 40^{o} - 170^{o}C and observed fast rates of addition, normal Arrhenius parameters and no tendency for the adducts to eliminate HI. The only difference between corresponding adducts derived from $CHF_2^{\cdot}$ and $CF_3^{\cdot}$ is the presence of a hydrogen substituent from $CHF_2^{\cdot}$ in place of the third fluorine substituent from $CF_3^{\cdot}$ on the γ- carbon atom of the substituted propyl iodides: the effects of this upon elimination of HI should be of minor importance. Furthermore, as elimination of HI is a high temperature effect, this will only explain the anomalous behaviour if elimination occurs preferentially from the minor adducts: this is contrary to expectations. The elimination of HI involves the loss of a hydrogen atom from the β-carbon atom with respect to the iodine atom, therefore reducing the number of hydrogen atoms on the β-carbon atom will statistically reduce the probability of elimination. With the reverse 1, 1-difluoroethylene adduct ($CHF_2CF_2CH_2I$) there are no hydrogen atoms on the β-carbon atom so elimination of HI is unlikely. Although the mass spectrum was obtained for one elimination product ($CHF_2CH{=}CF_2$) from the preparative runs, no elimination products were detected from the kinetic runs. The accumulated evidence conclusively supports the non participation of hydrogen iodide elimination under the experimental conditions employed here.

b- Cross combination, dimerisation and disproportionation reactions.

Radical-radical combination reactions are highly exothermic and readily occur. The initial combination products are generally

vibrationally excited and may either react further by disproportionation into two species or become collisionally deactivated by interaction with a third body. Most combination and disproportionation reactions are independent of temperature but show a pressure dependence; at low pressures (<10 torr) combinations tend to become third body dependent. No combination or disproportionation products were observed in kinetic runs. The rates of formation of the adducts in the kinetic runs is relatively slow at low temperatures, and the direction of looking for the anomalous behaviour, in terms of disproportionation and combination reactions, involves examining the reaction system for a proportionately greater loss of the most abundant adduct peaks at low temperatures.

i.e.

$$CHF_2CH_2CH_2\cdot + CHF_2\cdot \text{ (or X}\cdot\text{)} \xrightarrow{k_x} \begin{cases} CHF_2CH{=}CH_2 + CH_2F_2 \\ \quad (+ \text{ cross dispn.}) \\ CHF_2(CH_2)_2CHF_2 \; (+ CHF_2CH_2CH_2X) \end{cases} \quad 28$$

$$CHF_2CH_2CF_2\cdot + CHF_2\cdot \text{ (or X}\cdot\text{)} \xrightarrow{k_y} \begin{cases} CHF_2CH{=}CF_2 + CH_2F_2 \\ \quad (+ \text{ cross dispn.}) \\ CHF_2CH_2CF_2CHF_2 \; (+ CHF_2CH_2CF_2X) \end{cases} \quad 29$$

$$CHF_2CH_2CH_2\cdot + CHF_2I \xrightarrow{k_t} CHF_2CH_2CH_2I + CHF_2\cdot \quad 30$$

if at low temperature $k_t \sim k_x > k_y$

if at high " $k_t > k_x > k_y$

X· = any other radical within the system.

For a significant contribution from combination and disproportionation reactions a build up of adduct radicals within the system is necessary: short chains and a slow transfer step are conducive to meeting these requirements. However, the iodine transfer step is particularly fast and this will maintain the steady state concentration of adduct radicals at a low level and thus inhibit the contribution from combination and disproportionation reactions.

By analogy with similar systems the steady state concentrations of $CHF_2\cdot$ and $CF_2I\cdot$ radicals will exceed those of the corresponding adduct radicals and should facilitate the detection of the $CHF_2\cdot$ and $CF_2I\cdot$ combination and disproportionation products. Comparing the concentrations of the termination products with the corresponding concentrations of the addition products would give an estimate of the chain length. Unfortunately the termination products were not detected. This may be due to their formation in insignificant quantities, their chromatographic coincidence with the fluoroethylenes and CHF_2I peaks or partial loss of highly volatile termination products prior to injection onto the chromatographic column. Nevertheless, the nature of the termination products merits comment. The disproportionation/combination ratio[87] (kd/kc) of $CHF_2\cdot$ radicals is approximately 0.19, and the nature of the disproportionation reaction is pressure dependent. The main disproportionation reaction of the intermediate vibrationally excited tetrafluoroethane is the formation of difluoromethane and difluorocarbene, but at low pressures (<7 torr) elimination of hydrogen fluoride occurs.[88]

$$CHF_2CHF_2^* \longrightarrow CH_2F_2 + :CF_2 \qquad 31$$

$$CHF_2CHF_2^* \longrightarrow CHF{=}CF_2 + HF \qquad 32$$

In the mercury photosensitisation of chlorodifluoromethane Gunning[87] et al. observed ten per cent of C_3 products, and attributed these to the reactions of $:CF_2$ with $CHF_2\cdot$ and $CF_2Cl\cdot$ radicals followed by subsequent radical-radical combinations.

$$:CF_2 + CHF_2\cdot \longrightarrow CHF_2CF_2\cdot \qquad 33$$

$$:CF_2 + CF_2Cl\cdot \longrightarrow CClF_2CF_2\cdot \qquad 34$$

Perona and Pritchard[84] have expressed the view that reaction 33 does not occur during the photolysis of pentafluoroacetone. In the present kinetic system the fate of any haloethyl radicals produced, including $CF_2ICF_2\cdot$ radicals, would preferentially be

either addition to the olefins or abstraction of iodine from CHF_2I. These products were not observed. This is not surprising, even if much $:CF_2$ is generated, owing to the preferential addition of $:CF_2$ across double bonds of olefins giving substituted cyclopropanes[46]. This route for difluorocarbenes is greatly favoured by the large excess of olefin concentration over the concentrations of radical species. No substituted cyclopropanes were observed but detection of small quantities of these is almost outwith the scope of the analytical system.

Termination reactions of the adduct radicals in this work are of no significance and do not give an explanation for the anomalous behaviour of $CHF_2^{\bullet}$ radicals in addition reactions. Although short chain reactions could provide an explanation for the anomaly, failure to detect the termination products of the halomethyl radicals detracts from this, but the inadequacies of the analytical system must be borne in mind.

c- Hydrogen abstraction reactions.

Failure to observe hydrogen abstraction products of the intermediate adduct radicals, and the overwhelming preference for iodine rather than hydrogen abstraction rules out the possibility of finding an explanation for the anomaly in terms of hydrogen abstraction. In addition, Tedder[20-23] and co-workers have not observed hydrogen abstraction products from kinetic studies on the addition of other halomethyl radicals to the fluoroethylenes.

The hydrogen abstraction products from the addition of $CF_2I^{\bullet}$ radicals to the fluoroethylenes are isomers of the iodine abstraction products from addition of $CHF_2^{\bullet}$ radicals and should therefore easily have been observed, with the exceptions of addition to the $CH_2=$ end of 1,1-difluoroethylene, the CHF= end of trifluoroethylene, and tetrafluoroethylene where the corresponding products are identical.

e.g. $CF_2ICH_2CF_2\cdot + CHF_2I \longrightarrow CHF_2CH_2CF_2I + CF_2I\cdot$ 35

$CHF_2CH_2\ CF_2\cdot + CHF_2I \longrightarrow CHF_2CH_2CF_2I + CHF_2\cdot$ 36

Corresponding groups of isomers do not necessarily appear as coincident chromatographic peaks, as the normal and reverse adducts from the addition of a specific radical to a particular olefin are also isomers and the analytical conditions were chosen to give adequate separation. One of the observations from the addition of $CF_2I\cdot$ radicals to the fluoroethylenes was the apparently low selectivity of $CF_2I\cdot$ by comparison with the selectivities of other halomethyl radicals. A plausible explanation for this low selectivity of $CF_2I\cdot$ radicals and the negative slope (fig. 2-3b) for addition of CHF_2' radicals to 1,1-difluoroethylene is a significant competition between hydrogen and iodine abstraction by the normal adduct radicals derived from the addition of $CF_2I\cdot$.

i.e. k_H/k_I for $CF_2ICH_2CF_2\cdot > CF_2ICF_2CH_2\cdot$ 37

Hydrogen abstraction may occur from CHF_2I in the production of $CF_2I\cdot$ radicals, and $CF_3\cdot$ radicals abstract hydrogen from alkanes more readily than $CH_3\cdot$ radicals,[102] therefore it is reasonable to assume that the hydrogen abstraction order of the adduct radicals is $CF_2ICH_2CF_2\cdot > CF_2ICF_2CH_2\cdot$. A reduced rate of $CF_2ICH_2CF_2I$ adduct formation due to hydrogen abstraction is accompanied by a direct gain of $CHF_2CH_2CF_2I$. For a satisfactory explanation of the negative slope, $CHF_2\cdot$ radicals must preferentially add to the $CF_2=$ group of 1,1-difluoroethylene and $CHF_2CH_2CF_2I$ must be mainly formed from the addition of $CF_2I\cdot$ radicals followed by hydrogen abstraction. This situation is unlikely to arise, especially as none of the closely related halomethyl radicals previously studied add preferentially to the $CF_2=$ end of 1,1-difluoroethylene.

d- Telomerisation reactions

In the preparative runs several telomers were observed: the two to one telomers from the addition of $CHF_2^{\cdot}$ and $CF_2I^{\cdot}$ radicals, and the three to one telomer from the addition of $CHF_2^{\cdot}$ radicals to tetrafluoroethylene; two of the four possible two to one telomers from the addition of $CHF_2^{\cdot}$ radicals to trifluoroethylene; the cross telomers from the addition of $CHF_2^{\cdot}$ and $CF_2I^{\cdot}$ radicals to tetrafluoroethylene followed by the addition of the intermediate radicals to ethylene. The main point from the formation of telomers is that with the presence of two fluorine atoms on the carbon atom surrounded by the unpaired electron, addition of the intermediate adduct radical occurs preferentially to the least substituted centre. Nevertheless, telomerisation occurs readily with tetrafluoroethylene. When equal quantities of tetrafluoroethylene and ethylene are reacted competitively, the adduct radical of tetrafluoroethylene, with the unpaired electron centred on a $-CF_2$ group, adds preferentially to ethylene giving a C_5 radical with the odd electron centred on a $-CH_2$ group which inhibits further telomerisation.

The telomers are relatively involatile as they contain at least one iodine atom and are ideally suited for detection by chromatographic analysis. The telomers from the preparative runs gave well resolved chromatographic peaks, therefore their absence from the chromatograms of the kinetic runs excludes telomerisation as a solution of the anomalous negative slopes.

e- Reversibility of addition

In the addition of a halomethyl radical to mono-olefin a double bond is broken while a single carbon-carbon bond is formed resulting in an exothermic addition step: the reverse decomposition is endothermic. The activation energy for the addition of $CH_3^{\cdot}$ radicals to ethylene is 7 k cal mol^{-1} and the reverse decomposition reaction has an activation energy of 20 k cal mol^{-1}, giving an energy barrier

of 13 k cal mol^{-1} against reversibility of the addition step.

$$CH_3\cdot + CH_2{=}CH_2 \underset{k_{-2}}{\overset{k_2}{\rightleftharpoons}} CH_3CH_2CH_2\cdot$$

$$E_2 = 7 \text{ k cal mol}^{-1}, \quad E_{-2} = 20 \text{ k cal mol}^{-1}$$

The probability of reversibility is further reduced in a system allowing iodine atom transfer by a pathway involving a low energy of activation. Szwarc[103] and co-workers illustrated by two techniques that $CF_3\cdot$ radicals, generated by the photolysis of hexafluoroazomethane, add to olefins non reversibly. Tedder and Walton[102] showed that addition of $CCl_3\cdot$ to vinyl chloride is non reversible at temperatures up to 250°C. However, both $CF_3\cdot$ and $CCl_3\cdot$ radicals, which do not give reversible addition, show normal Arrhenius plots, whereas the addition of $CHF_2\cdot$ radicals show anomalous behaviour and this justifies consideration of the reversible addition process.

The reaction mechanism for the formation of the adducts, allowing for reversibility of the addition step, is:

$$CHF_2I + h\nu \xrightarrow{\emptyset I_a} CHF_2\cdot + I\cdot \qquad 38$$

$$CHF_2\cdot + E \underset{k_{-2}}{\overset{k_2}{\rightleftharpoons}} CHF_2E\cdot \qquad 39$$

$$CHF_2E\cdot + CHF_2I \xrightarrow{k_3} CHF_2EI + CHF_2\cdot \qquad 40$$

$$2CHF_2\cdot \xrightarrow{k_t} CHF_2CHF_2 \qquad 41$$

where E = olefin.

The Stationary State Approximation gives:

$$d[XE\cdot]/dt = k_2[X\cdot][E] - k_{-2}[XE\cdot] - k_3[XE\cdot][XI] = 0 \qquad 42$$

$$\therefore [XE\cdot] = k_2[X\cdot][E]/(k_{-2} + k_3[XI]) \qquad 43$$

where $X\cdot = CHF_2\cdot$

let $e = [XEI]$

$$\therefore de/dt = k_3[XI][XE\cdot] \qquad 44$$

substituting equation 43 into 44 gives :

$$de/dt = K_2k_3[E][X\cdot][XI]/\left(1 + \frac{k_3[XI]}{k_{-2}}\right) \qquad 45$$

where $K_2 = k_2/k_{-2}$

Assuming that the percentage reaction is small, i.e. [XI] and [E] are constant, then integration of equation 45 gives:

$$[XEI] = K_2 k_3 [E][X\cdot][XI]t \,/\left(1 + \frac{k_3[XI]}{k_{-2}}\right) \qquad 46$$

The corresponding equation for adduct formation by a non reversible pathway is:

$$[XEI] = k_2[E\cdot][X\cdot]\,t \qquad 47$$

For the formation of adducts which give normal Arrhenius plots, it is reasonable to assume that the addition step is non reversible. On the other hand, reversibility of the addition step may contribute to the anomalous behaviour of the other adducts. Assuming that the addition step in the formation of the ethylene adduct is non reversible and allowing for the possible reversibility of the addition step in the formation of the normal 1,1-difluoroethylene adduct, then the adduct ratio is given by equation 47 divided by equation 46.

$$e_3F_o/e_1E_o = k_2/k_2' + k_2k_{-2}'/k_2'\,k_3'[XI] \qquad 48$$

where $e_3 = [CHF_2CH_2CH_2I]$, $E_o = [CH_2{=}CH_2]$

$e_1 = [CHF_2CH_2CF_2I]$, $F_o = [CH_2{=}CF_2]$

k_2 refers to the ethylene reaction

k_2' , k_{-2}' and k_3' refers to the 1,1-difluoroethylene reaction.

If the addition step to the $CH_2{=}$ end of 1,1-difluoroethylene is non reversible then equation 48 reduces to the ratio of the relative rates of the addition step which is independent of the concentration of difluoroiodomethane.

$$e_3F_o/e_1E_o = k_2/k_2' \qquad 49$$

On the other hand, reversibility of the addition step gives an adduct ratio which is dependent on the concentration of CHF_2I. In this situation a plot of the adduct ratio (e_3F_o/e_1E_o) against $1/[CHF_2I]$ gives:

(i) from the intercept, the ratio of the rate constants for the addition processes,

$$\text{intercept} = k_2/k_2' \qquad 50$$

(ii) from the slope, the product of the rate constant ratio for the addition processes and the rate constant ratio for the reversible addition step (k_{-2}') and the iodine transfer step (k_3'),

$$\text{slope} = k_2/k_2' \times k_{-2}'/k_3' \qquad 51$$

(iii) from the slope divided by the intercept, the rate constant ratio for the reversible addition step (k_{-2}') and the iodine transfer step (k_3'),

$$\text{slope/intercept} = k_{-2}'/k_3' \qquad 52$$

(iv) from the slope divided by the product of the intercept and the concentration of CHF_2I, the ratio of the relative rates for the reversible decomposition and iodine transfer steps.

$$\text{slope/intercept} \times [CHF_2I] = R_{-2}/R_3 \qquad 53$$

One kinetic series was conducted at 100°C, and another at 150°C, in which the concentration of CHF_2I was progressively increased (0.22, 0.38 and 1.50 x 10^{-3} mol l^{-1}) in the presence of 1,1-difluoroethylene and ethylene while the ratio of the reactants was maintained constant at 12 : 4 : 1 respectively. The adduct ratios which gave positive slopes were determined for each experimental concentration of CHF_2I (table 2-6) and plotted against $10^3/[CHF_2I]$ (fig 2-4). A linear dependence on the inverse concentration of CHF_2I is evident. The intercepts and slopes were calculated by the least squares method and are presented in table 2-11 together with the relative rate constants and relative rates for the reversible decomposition and iodine transfer steps.

Fig 2-4 Plot of adduct ratios against $10^3/[CHF_2I]$ for the reaction series at 100°C and 150°C.

where $e_1 = [CHF_2CH_2CF_2I]$, $E_o = [CH_2{=}CH_2]$

$e_2 = [CHF_2CF_2CH_2I]$, $F_o = [CF_2{=}CF_2]$

$e_3 = [CHF_2CH_2CH_2I]$

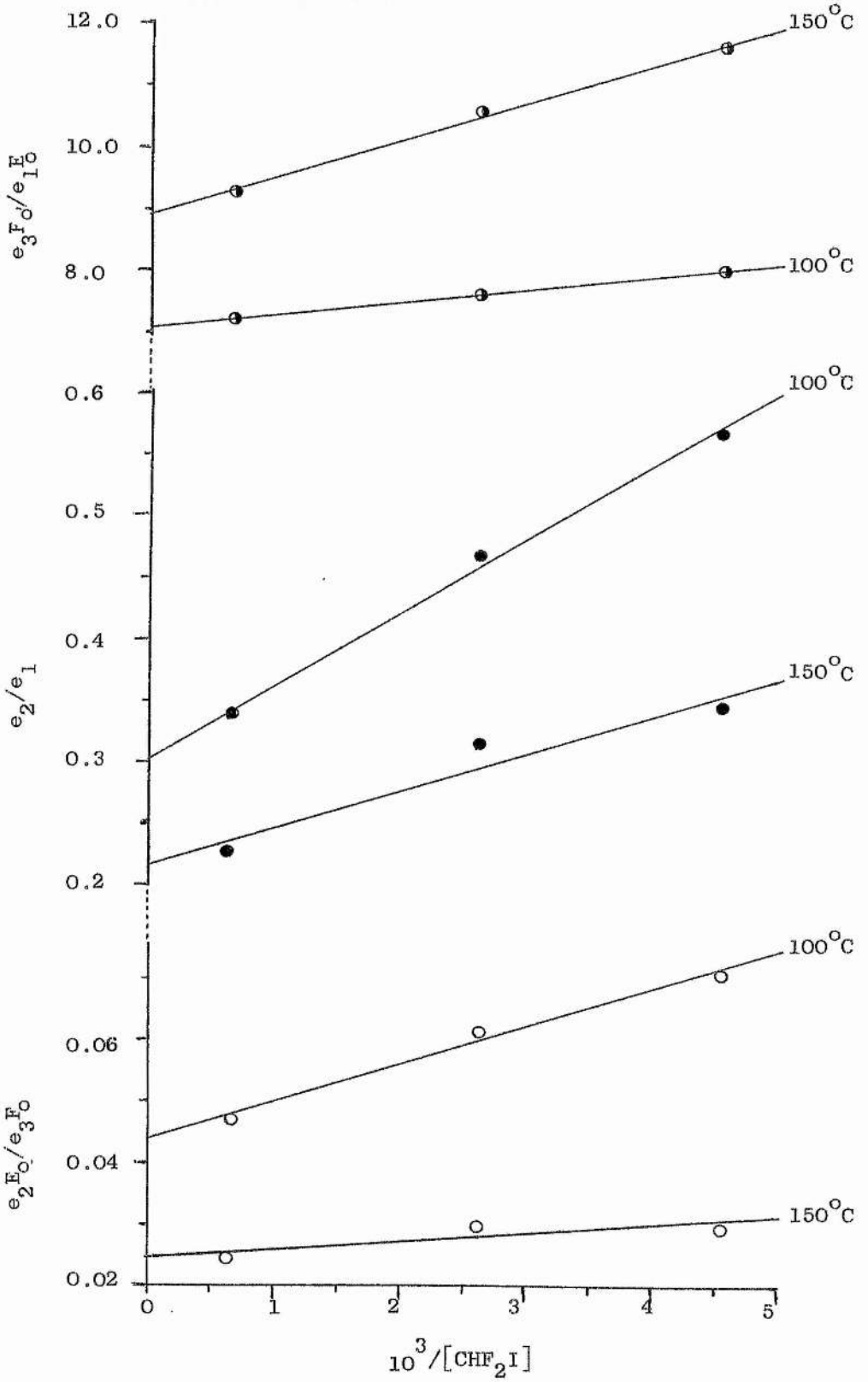

The positive slopes of fig. 2-4 and the relative rates for the decomposition and iodine transfer steps indicate that the significance of reversible decomposition in the adduct radicals decreases along the series

$$CHF_2CH_2CF_2\cdot > CHF_2CH_2CH_2\cdot > CHF_2CF_2CH_2\cdot$$

The results indicate that the initial assumption was wrong and that the addition of $CHF_2\cdot$ to ethylene is the most reversible addition step. Assuming that the addition of $CHF_2\cdot$ to the $=CF_2$ end of 1,1-difluoroethylene is non reversible then the relative rates of reversible decomposition (R_{-2}) and iodine transfer (R_3) steps at 100 and 150°C are:

	$^*CH_2=CF_2$	$CH_2=CH_2$	$^*CF_2=CH_2$
i) R_{-2}/R_3 at 100°C	0.26	0.19	0.00
ii) " " 150°C	0.18	0.07	0.00

* denotes the site of addition.

The inverted order is expected owing to:

i) the normal adduct radical of 1,1-difluoroethylene, with the unpaired electron centred on a $-CF_2$ group, has a lower activation energy for the iodine transfer step and this reduces the lifetime of the species and the probability of decomposition;

ii) the β carbon- γ carbon bond in $CHF_2-CF_2CH_2\cdot$ is probably slightly weaker than in $CHF_2-CH_2CH_2\cdot$ and therefore more liable to break in a reversible decomposition step;

iii) the shorter lifetime of a $CHF_2CH_2CF_2\cdot$ species is expected to make a greater contribution to relative decomposition rates than the strength of the β carbon - γ carbon bonds in the adduct radicals.

The intercepts of the adduct ratios from the concentration dependent series at 100°C and 150°C are the adduct ratios corresponding to the non reversible situation. The logarithms of these intercepts are plotted against $10^3/T$ in fig. 2-5. Negative slopes again result and are of similar magnitude to the corresponding negative slopes obtained from the temperature dependent kinetic series (fig. 2-3a and b). For a complete explanation of the anomalous behaviour in terms of reversibility of the addition steps, positive slopes are required from fig.2-5 and the magnitude of the negative slopes excludes reversibility from explaining the anomaly. Nevertheless, a dependence of the adduct ratios upon the concentration of CHF_2I has been established.

Table 2-11

a) 100°C

Adduct Ratio	Intercept	Gradient	$10^4\ k_{-2}/k_3$	R_{-2}/R_3
e_2E_o/e_3F_o	0.044 ± 0.001	0.0062 ± 0.0022	1.41 ± 0.50	0.188 ± 0.067
e_2/e_1	0.304 ± 0.004	0.059 ± 0.013	1.94 ± 0.43	0.259 ± 0.057
b) 150°C				
e_2E_o/e_3F_o	0.025 ± 0.001	0.0013 ± 0.0025	0.520 ± 1.00	0.069 ± 0.133
e_2/e_1	0.217 ± 0.009	0.030 ± 0.027	1.38 ± 1.24	0.184 ± 0.165

Notes:

i) the adduct in the numerator of the adduct ratios is assumed non reversible for the situation under consideration (e_2).

ii) the relative rate constants and relative rates for the reversible decomposition (k_{-2}, R_{-2}) and the iodine transfer (k_3, R_3) steps refer to the adducts appearing in the denominator of the adduct ratios (e_1, e_3).

Fig 2-5 Arrhenius plot of the adduct ratios at 100°C and 150°C from the intercepts of fig 2-4.

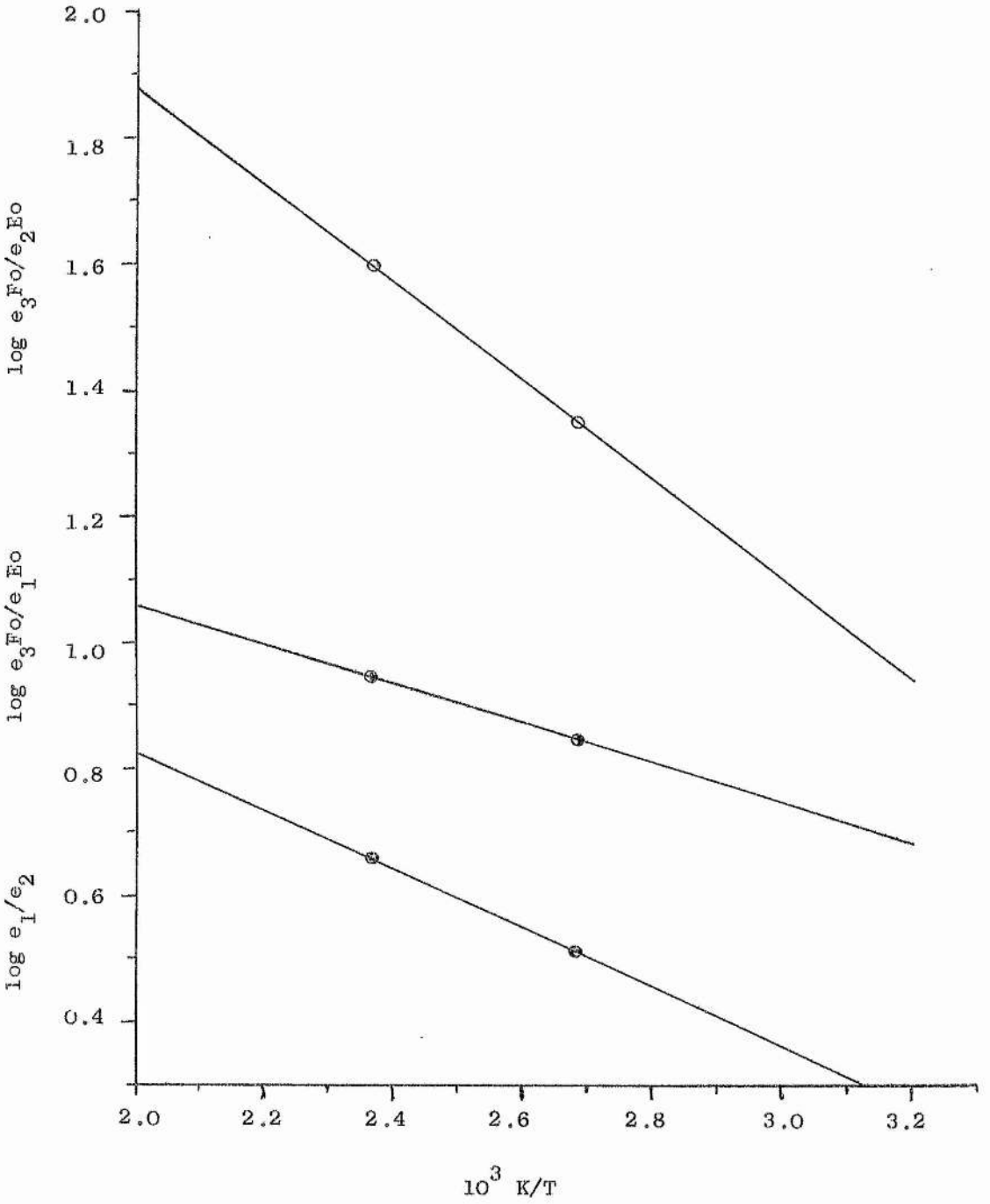

f- Participation of excited radicals

The carbon-iodine bond strength in CHF_2I is approximately 50 k cal mol^{-1} and the input energy from the medium pressure mercury arc, with use of a pyrex filter, is attributable mainly to the 313 and 366 nm wavelengths corresponding to 92 and 78 k cal mol^{-1}. This gives approximately 41 and 28 k cal mol^{-1} in excess of the carbon-iodine bond dissociation energy and will result in vibrationally excited radicals. In the event of chain lengths being short, vibrationally excited CHF_2^* radicals would contribute significantly to the formation of adducts, especially at low temperatures where the low selectivity of the excited radicals would result in a much reduced temperature dependence of the rates of adduct formation: the contribution to adduct formation from the much more selective and nonexcited $CHF_2\cdot$ radicals would be greatly diminished at low temperature. Although Rabinovitch[104] et al, recognised that at low pressures excited propyl radicals readily undergo decomposition into ethylene and methyl radicals, the conclusion from the previous section (e) excludes reversibility considerations from reaction schemes involving excited radicals in this work.

Simultaneous participation of excited and non excited radicals by the same reaction pathway is equivalent to the addition of two species, accompanied by different activation energies, to form identical products. Assuming that excited radicals have the same level of vibrational excitation and that the addition pathway for the excited and non excited radicals is:

$$X\cdot + E \longrightarrow XE\cdot \qquad 54$$

$$XE\cdot + XI \longrightarrow XEI + X\cdot \qquad 55$$

$$2X\cdot\ (+M) \longrightarrow X_2 \qquad 56$$

where $X\cdot = CHF_2\cdot, CHF_2^*$

then, the relative rate of normal to reverse adduct formation is:

$$e_1/e_2 = \frac{x_1 + y_1}{x_2 + y_2} \qquad 57$$

where x_1 = normal adduct formed by addition of non excited radicals

x_2 = reverse " " " " " " " "

y_1 = normal " " " " " excited radicals

y_2 = reverse " " " " " " "

With 1,1- difluoroethylene, at low temperatures excited radicals may predominate and at high temperatures non excited radicals may predominate, i.e. equation 57 simplifies to:

i) at low temp. $e_1/e_2 = y_1/y_2$ 58

provided $x_2 \ll y_2$ and $x_1 \ll y_1$

ii) at high temp. $e_1/e_2 = x_1/x_2$

provided $y_2 \ll x_2$ and $y_1 \ll x_1$ 59

At intermediate temperatures both excited and non excited radicals may make significant contributions to the adduct ratio.

Introducing the Arrhenius relationship:

$$k_m = A_m \exp^{-E_m/RT} \qquad 60$$

where $m = e_1, e_2, x_1, x_2, y_1$ and y_2

then, equation 57 becomes:

$$\frac{A_{e_1}}{A_{e_2}} \exp^{-(E_{e_1} - E_{e_2})/RT} = \frac{A_{x_1} \exp^{-E_{x_1}/RT} + A_{y_1} \exp^{-E_{y_1}/RT}}{A_{x_2} \exp^{-E_{x_2}/RT} + A_{y_2} \exp^{-E_{y_2}/RT}} \qquad 61$$

The Arrhenius exquation (61) corresponding to the low temperature situation of equation 58 is:

$$\log e_1/e_2 = \log A_{y_1} - \log A_{y_2} + (E_{y_2} - E_{y_1})/2.303\ RT \qquad 62$$

where, $\log A_{y_1} - \log A_{y_2}$ and $E_{y_2} - E_{y_1}$ are the A-factor and activation energy differences for the addition of excited CHF_2^* radicals to 1,1 - difluoroethylene. Similarly, the Arrhenius equation corresponding to the high temperature situation of equation 59 gives the A-factor and activation energy differences for the addition of non excited $CHF_2^{\cdot}$ radicals to 1,1 - difluoroethylene.

$$\log e_1/e_2 = \log A_{x_1} - \log A_{x_2} + (E_{x_2} - E_{x_1})/2.303\ RT \qquad 63$$

Individually the addition of non excited and excited ($CHF_2^{\cdot}$ and CHF_2^{*}) radicals would show normal Arrhenius behaviour with small A-factor differences and positive temperature coefficients. Plots of the logarithms of adduct ratios ($\log e_1/e_2$) against $10^3/T$ for the addition of excited radicals would give a relatively small positive slope and for addition of non excited radicals would give a relatively large positive slope. A system in which the major contribution to adduct ratio changes from excited to non excited radical addition as the temperature increases may show anomalous behaviour as illustrated in fig. 2-6.

Fig 2-6 Illustration of proposed Arrhenius behaviour for addition of non excited (a), excited (b) and a combination of non excited and excited (c) radicals to unsymmetrical fluoroethylenes.

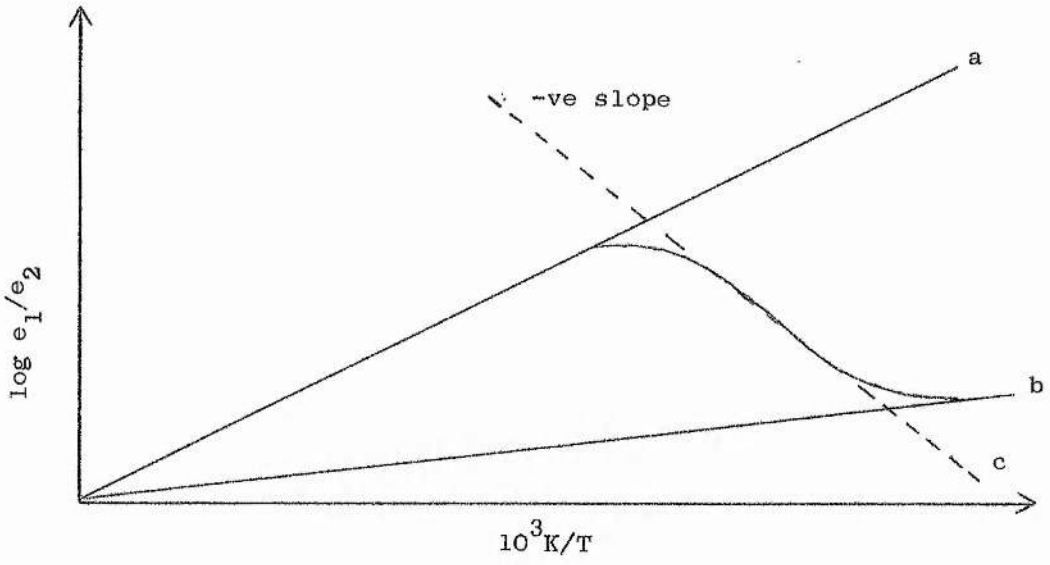

The predicted behaviour illustrated in fig.2-6 for contributions from excited and non excited radicals is in agreement with the observed Arrhenius plot for the addition of $CHF_2^{\cdot}$ to 1,1-difluoroethylene (fig. 2-3b) and may fully explain the observed anomalous behaviour. The topic is discussed further in the discussion section of part 3.

PART 3

The Addition of Fluoromethyl Radicals to Fluoroethylenes

Introduction

Fluoroiodomethane and difluoroiodomethane, being related compounds, share several common references in the chemical literature. A few synthetic methods for the preparation of CH_2FI are given and a few physical constants have been determined. Some data on the geometry, physical properties and reactions of fluoromethyl radicals has been recorded.

The methods previously used for synthesising CH_2FI include: the action of mercurous fluoride on diiodomethane[105] at 120°C; slowly heating an intimate mixture of silver monofluoroacetate and iodine[76] to 260°C; and the action of sodium iodide on CH_2FBr in methyl ethyl ketone[106] followed by fractionation.

Todd[107] detected CH_2FI as a product of hot F^{18} reaction with methane in the presence of iodine. The boiling point[105] of fluoroiodomethane is 53.4°C and the heat of formation[36] from the elements in the gas phase at 25°C is 44 k cal mol^{-1}.

Fluoromethyl radicals have been generated for kinetic studies by the reactions of sodium atoms with chlorofluoromethane[108] and bromine atoms with fluoromethane[109]. The ionisation potential and C-F bond dissociation energy of $CH_2F\cdot$ radicals have been determined[81]. The e.s.r. spectrum[110] of $CH_2F\cdot$ has been observed in krypton and xenon matrices near the temperature of liquid nitrogen following 2.8 Mev electron irradiation of fluoromethane. From the carbon-13 hyperfine splittings the pyramidal angle of the radical was determined to be 5° or less. The e.s.r. spectrum was also observed from the photolysis of $(CH_2FCOO)_4Pb$ at 77°K.[94] In support of a pyramidal structure, three molecular orbital calculations[96,111,112] have suggested that $CH_2F\cdot$ is slightly non planar. By using an ab initio LCAO-SCF-MO-CI method with Slater basis sets, the isotropic H, ^{19}F, and ^{13}C coupling constants of planar and non planar $CH_2F\cdot$ radicals have been calculated[113]. The infra red spectrum of $CH_2F\cdot$ was observed[114] during the ultra violet photolysis of fluoromethane in an argon matrix at 14°K.

Several hydrogen abstraction reactions of fluoromethyl radicals have been studied. Perona and Pritchard[84] studied the hydrogen abstraction reactions from $(CHF_2)_2CO$ and $n\text{-}C_4H_{10}$. Kerr and Timlin studied the hydrogen abstraction reactions from tetramethyl silane[85] and trichlorosilane[86] and compared the results for the series of fluoromethyl radicals.

Pritchard[115] et al. during a preliminary photolysis of $(CH_2F)_2CO$ observed vinyl fluoride as a main product. This was the first observed case of a disproportionation reaction between two substituted methyl or methyl radicals resulting in two molecules as opposed to a molecule and a methylene species. Pritchard and Thommarson[116] extended this work to the photolysis of CH_2FCOCH_3 and examined the rate of collisonal stabilisation versus HF elimination of the excited dimers, $C_2H_5F^*$ and $C_2H_4F_2^*$, as a function of temperature and pressure.

Sangster and Thynne[117] have studied the addition of fluoromethyl radicals to ethylene in the gas phase between 17°C and 182°C using the abstraction of hydrogen atoms from hydrogen sulphide as the competing reaction.

$$CH_2F\cdot + CH_2{=}CH_2 \xrightarrow{1} CH_2FCH_2CH_2\cdot$$

$$CH_2F\cdot + H_2S \xrightarrow{2} CH_3F + HS\cdot$$

$$CH_2FCH_2CH_2\cdot + H_2S \xrightarrow{3} CH_2FCH_2CH_3 + HS\cdot$$

$$E_1 - E_2 = 1.32 \pm 0.29 \text{ k cal mol}^{-1}$$

$$\log A_1 - \log A_2 = -0.91 \pm 0.18 \text{ l mol}^{-1} \text{ s}^{-1}$$

The fluoromethyl radicals added readily to ethylene with a reactivity intermediate between $CH_3\cdot$ and $CF_3\cdot$ radicals. The intermediate fluoropropyl radical was observed to be stable towards decomposition under the experimental conditions. The absolute values of the A-factor and activation energy for addition of fluoromethyl radicals to ethylene were calculated. ($\log A = 10.6$ l mol^{-1} s^{-1}, $E_A = 4.3$ k cal mol^{-1}).

Part 3 reports the photolytic reactions of CH_2FI over a range of temperature (40° - 200°C) with vinyl fluoride, 1,1-difluoroethylene, trifluoroethylene and tetrafluoroethylene in the presence of ethylene.

Two additional competitive series of photolytic reactions between trifluoroethylene and ethylene are recorded in which, i) the olefin concentration was varied while the temperature was held constant at 100°C, and ii) various amounts of carbon dioxide were added for a series at 150°C. Also, a thermally initiated competitive series between 1,1-difluoroethylene and ethylene over a range of temperature (103-182°C) is reported.

EXPERIMENTAL

REACTANTS

1) Fluoroiodomethane (bp 53.4°C) was prepared by the action of mercurous fluoride on diiodomethane. Diiodomethane (0.3 mole) was heated to about 120°C in an atmosphere of nitrogen and then mercurous fluoride (0.1 mole) was slowly added through a Fieser apparatus into the stirring reactant. Upon formation the fluoroiodomethane distilled directly into the receiver flask immersed in an ice bath. The yield was very small. Final purification was achieved by preparative g.l.c. which gave a product of approximately 99.4% purity. A few volatile impurity peaks were present on the chromatograms and all of them defied analysis by g.l.c.-m.s. These peaks gave a consistent reproducible pattern on the chromatograms from the kinetic series of reactions.

2) The fluoroethylenes were obtained commercially and purified by trap to trap distillation.

APPARATUS

The apparatus was described in part 1. The cylindrical quartz reaction vessel (140 ml) was used in conjunction with a pyrex filter for all reactions except the thermally initiated series, which was conducted in the cylindrical pyrex reaction vessel (202 ml). A Hanovia UVS 220 medium pressure mercury arc was used throughout.

EXPERIMENTAL PROCEDURE

The experimental procedure was basically the same as described in part 1. The fluoroiodomethane was stored in a small tube attached to the main line and surrounded with liquid nitrogen. For the kinetic series incorporating carbon dioxide, a small quantity of solid CO_2 was placed in a small sample tube attached to the line and thoroughly degassed prior to measurement of the required quantity into a calibrated bulb. One microlitre of CH_2Cl_2 was added to many of the product mixtures as a standard to facilitate more accurate measurement of the

product concentrations.

ANALYSIS

The analyses were conducted on the Griffin and George D6 gas density balance chromatograph and the Du Pont curve resolver as described in part 1. The modifications involved a different technique for injecting samples (described in part 2) and the use of two chromatographic columns in an effort to optimise the resolution of peaks.

Chromatographic columns consisting of 3ft sections of stainless steel with an internal diameter of 3/16in and interconnected with small bore u pieces were used. The majority of the analyses were conducted on an 18ft column consisting of 12ft of 15% tritolylphosphate plus 6ft of 24% dinonylphthalate packed on 60-100 mesh embacel. The column was maintained at approx. 150°C, the nitrogen carrier gas flow rate was set at 60 ml min^{-1} and the chart speed was 24in h^{-1}. The products from the temperature dependent photolytic series with difluoroethylene and trifluoroethylene were mainly analysed on a 12ft column of 15% tritolylphosphate packed with 60-100 mesh embacel. The column was maintained at 134°C, the nitrogen flow at 30 ml min^{-1} and the chart speed at 24in h^{-1}.

IDENTIFICATION OF PRODUCTS

The products were identified exclusively by g.l.c.-m.s. as described in part 1.

The ultraviolet spectrum, mass spectrum and ^{1}H and ^{19}F nuclear magnetic resonance spectra of CH_2FI were recorded.

U.V. spectrum of CH_2FI

The ultraviolet spectrum of fluoroiodomethane was recorded in the gas phase over the concentration range of 10^{-3} to 10^{-2} mol l^{-1} using a quartz gas cell and a UNICAM SP 800 ultraviolet spectrophotometer. One peak was observed with an absorbance maximum at 256.0 nm. The molar extinction coefficient (ε) was calculated.

$$\varepsilon_{256} = 23.3 \pm 0.8 \text{ cm}^{-1} \text{ mol}^{-1} \text{ l}$$

MASS SPECTRUM OF CH_2FI

m/e	Relative Intensity	Assignment
31	9	CF^+
32	6	CHF^+
33	84	CH_2F^+
127	69	I^+
128	6	HI^+
139	7	CI^+
140	3	CHI^+
141	31	CH_2I^+
158	1	CFI^+
159	4	$CHFI^+$
160	100	CH_2FI^+

^1H nmr spectrum of CH_2FI

The nmr spectrum of fluoroiodomethane was recorded on a 60 MHz spectrometer using carbon tetrachloride as solvent and tetramethylsilane as internal reference. The two protons are equivalent and gave a doublet by interaction with the fluorine atom.

chemical shift τ = 3.65 ppm

coupling constant J_{HF} = 49.4 Hz

^{19}F nmr spectrum of CH_2FI

The ^{19}F nmr spectrum of fluoroiodomethane was recorded on a 60 Mz spectrometer using carbon tetrachloride as solvent and trichlorofluoromethane as internal reference. The fluorine atom resonance is split into a triplet by the two equivalent hydrogen atoms.

chemical shift ϕ_F = 191.85 ppm

coupling constant J_{HF} = 49.4 Hz

M-vinyl fluoride

A preparative run was carried out with CH_2FI (2.00×10^{-3} mol l^{-1}) and CH_2=CHF (1.00×10^{-3} mol l^{-1}) at 183°C for 46 h with light filtered

through pyrex. Four product peaks were observed and identified by g.l.c.-m.s.

Peak M-1

m/e	Relative Intensity	Assignment
31	64	CF^+
32	10	CHF^+
33	14	CH_2F^+
77	29	$C_3H_3F_2^+$
78	14	$C_3H_4F_2^+$

Identified as 1,3-difluoroprop-1-ene ($CHF=CHCH_2F$).

Peak M-2

m/e	Relative Intensity	Assignment
31	5	CF^+
32	32	CHF^+
33	29	CH_2F^+
45	6	$C_2H_2F^+$
46	9	$C_2H_3F^+$
51	37	CHF_2^+
57	6	$C_3H_2F^+$
59	27	$C_3H_4F^+$
77	11	$C_3H_3F_2^+$
79	100	$C_3H_5F_2^+$
127	27	I^+
128	15	HI^+
141	2	CH_2I^+
159	4	$CHFI^+$
206	37	$C_3H_5F_2I^+$

Identified as the normal vinyl fluoride adduct,

1,3-difluoro-1-iodopropane (CH_2FCH_2CHFI).

Peak M-3

m/e	Relative Intensity	Assignment
32	178	CHF^+
33	48	CH_2F^+
45	17	$C_2H_2F^+$
46	20	$C_2H_3F^+$
51	67	CHF_2^+
59	59	$C_3H_4F^+$
77	19	$C_3H_3F_2^+$
79	9	$C_3H_5F_2^+$
127	44	I^+
128	26	HI^+
141	17	CH_2I^+
173	16	$C_2H_3FI^+$
206	100	$C_3H_5F_2I^+$

Identified as the reverse vinyl fluoride adduct, 1,2-difluoro-3-iodopropane ($CH_2FCHFCH_2I$).

Peak M-4

m/e	Relative Intensity	Assignment
127	59	I^+
128	4	HI^+
140	15	CHI^+
159	100	$CHFI^+$
254	19	I_2^+
266	4	CI_2^+
286	37	$CHFI_2^+$

Identified as fluorodiiodomethane ($CHFI_2$).

N-1,1-difluoroethylene

A preparative run was carried out with CH_2FI (2.00×10^{-3} mol l^{-1}) and $CH_2{=}CF_2$ (0.67×10^{-3} mol l^{-1}) at 204°C for 16h using unfiltered light. Three product peaks were observed and identified by g.l.c.-m.s.

Peak N-1

m/e	Relative Intensity	Assignment
31	46	CF^+
33	22	CH_2F^+
39	59	$C_3H_3^+$
46	48	$C_2H_3F^+$
51	100	CHF_2^+
75	37	$C_3HF_2^+$
76	18	$C_3H_2F_2^+$
77	100	$C_3H_3F_2^+$
95	68	$C_3H_2F_3^+$
96	51	$C_3H_3F_3^+$

Identified as 1,1,3-trifluoroprop-1-ene ($CH_2FCH{=}CF_2$).

Peak N-2

m/e	Relative Intensity	Assignment
33	39	CHF^+
45	13	$C_2H_2F^+$
46	7	$C_2H_3F^+$
47	6	$C_2H_4F^+$
64	8	$C_2H_2F_2^+$
77	30	$C_3H_3F_2^+$
78	4	$C_3H_4F_2^+$
95	6	$C_3H_2F_3^+$
97	100	$C_3H_4F_3^+$
127	26	I^+
128	6	HI^+
177	5	CF_2I^+
186	1	$C_3H_4FI^+$
203	1	$C_3H_2F_2I^+$
224	2	$C_3H_4F_3I^+$

Identified as the normal 1,1-difluoroethylene adduct, 1,1,3-trifluoro-1-iodopropane ($CH_2FCH_2CF_2I$).

Peak N-3

m/e	Relative Intensity	Assignment
33	34	CH_2F^+
45	4	$C_2H_2F^+$
46	4	$C_2H_3F^+$
47	3	$C_2H_4F^+$
57	8	$C_3H_2F^+$
64	35	$C_2H_2F_2^+$
75	4	$C_3HF_2^+$
77	38	$C_3H_3F_2^+$
78	8	$C_3H_4F_2^+$
83	5	$C_2H_2F_3^+$
95	5	$C_3H_2F_3^+$
97	6	$C_3H_4F_3^+$
127	32	I^+
128	4	HI^+
141	19	CH_2I^+
190	33	$C_2HF_2I^+$
224	100	$C_3H_4F_3I^+$

Identified as the reverse 1,1-difluoroethylene adduct, 1,2,2-trifluoro-3-iodopropane ($CH_2FCF_2CH_2I$).

O-trifluoroethylene plus ethylene

A preparative run was carried out with CH_2FI (2.00×10^{-3} mol l^{-1}), $CHF=CF_2$ (0.67×10^{-3} mol l^{-1}) and $CH_2=CH_2$ (0.33×10^{-3} mol l^{-1}) at 220°C for 6h using unfiltered light. Four products were observed and identified by g.l.c.-m.s.

Peak O-1

m/e	Relative Intensity	Assignment
27	32	$C_2H_3^+$
31	16	CF^+
32	137	CHF^+
33	21	CH_2F^+
36	5	C_3^+
37	16	C_3H^+
38	16	$C_3H_2^+$
39	100	$C_3H_3^+$
40	16	$C_3H_4^+$
41	26	$C_3H_5^+$
57	21	$C_3H_2F^+$
59	100	$C_3H_4F^+$
60	58	$C_3H_5F^+$

Identified as 1-fluoroprop-2-ene ($CH_2FCH=CH_2$).

Peak O-2

m/e	Relative Intensity	Assignment
31	30	CF^+
33	57	CH_2F^+
45	39	$C_2H_2F^+$
46	18	$C_2H_3F^+$
50	10	CF_2^+
64	16	$C_2H_2F_2^+$
65	34	$C_2H_3F_2^+$
77	26	$C_3H_3F_2^+$
82	35	$C_2HF_3^+$
95	39	$C_3H_2F_3^+$
96	12	$C_3H_3F_3^+$
109	17	$C_4H_4F_3^+$
115	100	$C_3H_3F_4^+$
127	70	I^+
128	16	HI^+
159	10	$CHFI^+$
177	14	CF_2I^+
242	12	$C_3H_3F_4I^+$

Identified as the normal trifluoroethylene adduct,

1,1,2,3-tetrafluoro-1-iodopropane ($CH_2FCHFCF_2I$).

Peak O-3

m/e	Relative Intensity	Assignment
31	57	CF^+
32	93	CHF^+
33	100	CH_2F^+
43	5	C_2F^+
44	19	C_2HF^+
45	21	$C_2H_2F^+$
46	14	$C_2H_3F^+$
50	11	CF_2^+
56	9	C_3HF^+
57	15	$C_3H_2F^+$
63	19	$C_2HF_2^+$
64	16	$C_2H_2F_2^+$
65	20	$C_2H_3F_2^+$
75	17	$C_3HF_2^+$
77	20	$C_3H_3F_2^+$
82	69	$C_2HF_3^+$
83	15	$C_2H_2F_3^+$
95	51	$C_3H_2F_3^+$
96	14	$C_3H_3F_3^+$
113	6	$C_3HF_4^+$
115	25	$C_3H_3F_4^+$
127	100	I^+
128	13	HI^+
159	54	$CHFI^+$
177	11	CF_2I^+
189	16	$C_2F_2I^+$
190	12	$C_2HF_2I^+$
209	11	$C_2HF_3I^+$
242	97	$C_3H_3F_4I^+$

Identified as the reverse trifluoroethylene adduct,

1,2,2,3-tetrafluoro-1-iodopropane (CH_2FCF_2CHFI).

Peak O-4

m/e	Relative Intensity	Assignment
27	33	$C_2H_3^+$
28	92	$C_2H_4^+$
31	3	CF^+
32	20	CHF^+
33	15	CH_2F^+
39	17	$C_3H_3^+$
41	45	$C_3H_5^+$
57	5	$C_3H_2F^+$
59	25	$C_3H_4F^+$
60	5	$C_3H_5F^+$
61	100	$C_3H_6F^+$
127	22	I^+
128	9	HI^+
141	5	CH_2I^+
155	4	$C_2H_4I^+$
188	60	$C_3H_6FI^+$

Identified as the ethylene adduct,

1-fluoro-3-iodopropane ($CH_2FCH_2CH_2I$).

P-tetrafluoroethylene

A preparative run was carried out with CH_2FI (2.00×10^{-3} mol l^{-1}) and $CF_2=CF_2$ (0.80×10^{-3} mol l^{-1}) at 152°C for 25h using light filtered through pyrex. Three product peaks were observed and identified by g.l.c.-m.s.

Peak P-1

m/e	Relative Intensity	Assignment
31	8	CF^+
32	4	CHF^+
33	18	CH_2F^+
44	2	C_2HF^+
45	3	$C_2H_2F^+$
50	2	CF_2^+
51	35	CHF_2^+
63	3	$C_2HF_2^+$
64	10	$C_2H_2F_2^+$
69	30	CF_3^+
75	2	$C_3HF_2^+$
82	4	$C_2HF_3^+$
83	24	$C_2H_2F_3^+$
95	8	$C_3H_2F_3^+$
100	6	$C_2F_4^+$
113	5	$C_3HF_4^+$
114	3	$C_3H_2F_4^+$
127	22	I^+
128	6	HI^+
133	100	$C_3H_2F_5^+$
177	20	CF_2I^+
208	2	$C_2F_3I^+$
221	1	$C_3HF_3I^+$
227	2	$C_2F_4I^+$
260	31	$C_3H_2F_5I^+$

Identified as the tetrafluoroethylene adduct,

1,1,2,2,3-pentafluoro-1-iodopropane ($CH_2FCF_2CF_2I$).

Peak P-2

m/e	Relative Intensity	Assignment
31	16	CF^+
32	39	CHF^+
33	39	CH_2F^+
51	148	CHF_2^+
64	6	$C_2H_2F_2^+$
69	84	CF_3^+
83	61	$C_2H_2F_3^+$
93	6	$C_3F_3^+$
95	10	$C_3H_2F_3^+$
100	26	$C_2F_4^+$
113	23	$C_3HF_4^+$
119	19	$C_2F_5^+$
127	45	I^+
128	32	HI^+
131	29	$C_3F_5^+$
133	6	$C_3H_2F_5^+$
163	100	$C_4HF_6^+$
169	6	$C_3F_7^+$
177	45	CF_2I^+
181	5	$C_4F_7^+$
195	5	$C_5H_2F_7^+$
208	6	$C_2F_3I^+$
213	13	$C_5HF_8^+$
227	6	$C_2F_4I^+$
233	29	$C_5H_2F_9^+$
277	3	$C_3F_6I^+$
360	10	$C_5H_2F_9I^+$

Identified as the two to one telomer of tetrafluoroethylene, 1,1-dihydro-5-iodoperfluoropentane ($CH_2F(CF_2CF_2)_2I$).

Peak P-3

m/e	Relative Intensity	Assignment
31	23	CF^+
32	37	CHF^+
33	23	CH_2F^+
51	300	CHF_2^+
63	13	$C_2HF_2^+$
69	173	CF_3^+
75	13	$C_3HF_2^+$
82	60	$C_2HF_3^+$
83	80	$C_2H_2F_3^+$
93	7	$C_3F_3^+$
95	17	$C_3H_2F_3^+$
100	27	$C_2F_4^+$
101	53	$C_2HF_4^+$
113	73	$C_3HF_4^+$
119	30	$C_2F_5^+$
127	93	I^+
128	27	HI^+
131	47	$C_3F_5^+$
133	10	$C_3H_2F_5^+$
145	10	$C_4H_2F_5^+$
151	17	C_2I^+
159	50	$CHFI^+$
163	53	$C_4HF_6^+$
169	7	$C_3F_7^+$
177	43	CF_2I^+
181	7	$C_4F_7^+$
189	13	$C_2F_2I^+$
194	10	$C_5HF_7^+$
208	17	$C_2F_3I^+$
227	7	$C_2F_4I^+$
233	3	$C_5H_2F_9^+$
258	60	$C_3F_5I^+$
358	100	$C_5F_9I^+$
460	5	$C_7H_2F_{13}I^+$

Identified as the three to one telomer of tetrafluoroethylene, 1,1-dihydro-7-iodoperfluoroheptane ($CH_2F(CF_2CF_2)_3I$).

Q - tetrafluoroethylene plus ethylene

A preparative run was carried out with CH_2FI (2.00×10^{-3} mol l^{-1}), $CF_2=CF_2$ (0.17×10^{-3} mol l^{-1}) and $CH_2=CH_2$ (0.33×10^{-3} mol l^{-1}) at 151°C for 22h using light filtered through pyrex. One additional product peak was observed and identified by g.l.c.-m.s.

Peak Q-1

m/e	Relative Intensity	Assignment
32	161	CHF^+
33	13	CH_2F^+
77	74	$C_2H_3F_2^+$
83	55	$C_2H_2F_3^+$
127	23	I^+
128	15	HI^+
133	3	$C_3H_2F_5^+$
141	19	CH_2I^+
155	13	$C_2H_4I^+$
161	10	$C_5H_6F_5^+$
267	5	$C_5H_4F_4I^+$
288	100	$C_5H_6F_5I^+$

Identified as the cross telomer 1,2,2,3,3-pentafluoro-5-iodopentane ($CH_2FCF_2CF_2CH_2CH_2I$) from the addition of fluoromethyl radicals to tetrafluoroethylene, followed by addition of the intermediate radicals to ethylene.

RELATIVE CHROMATOGRAPHIC RETENTION TIMES

OPERATING CONDITIONS:

COLUMN	18' x 3/16" stainless steel consisting of 12' of 15% tritolylphosphate plus 6' of 24% dinonylphthalate packed on 60-100 mesh embacel. (Several additional analyses were conducted on a 12' column of 15% tritolyl-phosphate for which the R_t' values were similar).
OVEN TEMP.	approximately 150°C
CARRIER GAS	NITROGEN-flow rate 60 ml min^{-1}

The retention times (R_t') relative to the retention time for CH_2FI (approx. 6.5 minutes) are quoted.

ADDUCTS	R_t'
$CH_2FCF_2CF_2I$	1.42
$CH_2FCHFCF_2I$	2.20
CH_2FCF_2CHFI	2.56
$CH_2FCH_2CF_2I$	2.55
$CH_2FCF_2CH_2I$	3.32
CH_2FCH_2CHFI	3.47
$CH_2FCHFCH_2I$	5.03
$CH_2FCH_2CH_2I$	4.05
OLEFINS	
$CH_2FCH=CF_2$	0.38
$CH_2FCH=CH_2$	0.49

TELOMERS	R_t'
$CH_2F(CF_2CF_2)_2I$	2.46
$CH_2F(CF_2CF_2)_3I$	3.50
$CH_2F(CF_2CF_2)_4I$	4.54
CROSS TELOMER	
$CH_2FCF_2CF_2CH_2CH_2I$	6.60
HALOMETHANES	
CHF_2I	0.70
CF_2I_2	2.89
$CHFI_2$	6.63
CH_2I_2	8.38

RESULTS

The reactions of fluoroiodomethane with vinyl fluoride and ethylene

A series of photolyses was carried out with CH_2FI (2.00×10^{-3} mol l^{-1}), $CH_2{=}CHF$ (0.67×10^{-3} mol l^{-1}) and $CH_2{=}CH_2$ (0.33×10^{-3} mol l^{-1}). The temperature was varied in the range 43-193°C and the reaction time in the range 20-114h. The three measurable products were the normal and reverse vinyl fluoride adducts and the ethylene adduct. Three additional photolytic reactions were conducted in the absence of ethylene. One microlitre of CH_2Cl_2 was added to several product mixtures as a standard to facilitate more accurate measurement of the product concentrations.

let a_1 = the relative area of CH_2FCH_2CHFI

a_2 = the relative area of $CH_2FCHFCH_2I$

a_3 = the relative area of $CH_2FCH_2CH_2I$

e_1 = the relative concentration of CH_2FCH_2CHFI

e_2 = the relative concentration of $CH_2FCHFCH_2I$

e_3 = the relative concentration of $CH_2FCH_2CH_2I$

A = the relative area of CH_2FI

B = the relative area of CH_2Cl_2

a) temp. 43.5°C, time 113.47h

A	a_1	a_2	a_3	
28 000	66	24.0	100	
-	66	22.2	100	
31 500	65	23.0	100	
-	65	23.0	100	
-	66	19.4	100	
29 800	65.6	22.3	100	mean value
	3.27	1.11	5.54	conc. $\times 10^6$ mol l^{-1}
			2.94	e_1/e_2
			3.39	$2e_3/e_1$

b) temp. 60°C, time 94.00h

B	a_1	a_2	a_3
3 410	68.2	23	100
2 940	67.8	23	100
2 940	67.8	23	100
2 580	66.8	23	100
2 020	65.0	23	100
2 780	67.1	23	100 mean value
	1.74	0.59	2.88 conc. x 10^6 mol l^{-1}
			2.94 e_1/e_2
			3.32 $2e_3/e_1$

c) temp. 80°C, time 64.90h

B	a_1	a_2	a_3
-	65.2	22.0	100
-	64.8	22.3	100
1 910	62.6	22.2	100
1 830	63.8	22.8	100
2 640	62.5	22.6	100
2 130	63.8	22.4	100 mean value
	2.16	0.76	3.76 conc. x 10^6 mol l^{-1}
			2.85 e_1/e_2
			3.49 $2e_3/e_1$

d) temp. 97.5°C, time 64.75h

B	a_1	a_2	a_3
-	61.3	19.8	100
620	60.8	19.2	100
580	61.6	18.8	100
620	60.6	20.0	100
660	61.4	20.0	100
620	61.1	19.6	100 mean value
	7.09	2.27	12.90 conc. x 10^6 mol l^{-1}
		3.64 $2e_3/e_1$	3.13 e_1/e_2

e) temp. 117.5°C, time 65.50h

B	a_1	a_2	a_3
930	58.8	18.2	100
-	58.2	18.8	100
860	59.0	18.2	100
830	57.2	18.2	100
870	58.3	18.4	100 mean value
	4.80	1.51	9.17 conc. x 10^6 mol l^{-1}
			3.18 e_1/e_2
			3.82 $2e_3/e_1$

f) temp. 131.5°C, time 45.30h

B	a_1	a_2	a_3
960	61.0	18.0	100
980	60.6	18.1	100
1 070	63.0	20.0	100
-	63.4	18.8	100
840	60.5	18.0	100
963	61.7	18.6	100 mean value
	4.60	1.39	8.30 conc. x 10^6 mol l^{-1}
			3.32 e_1/e_2
			3.61 $2e_3/e_1$

g) temp. 139°C, time 47.00h

A	a_1	a_2	a_3
-	58.2	15.2	100
13 800	60.0	15.7	100
-	62.2	16.5	100
-	59.8	15.4	100
-	59.0	15.3	100
12 800	58.0	15.0	100
13 300	59.5	15.5	100 mean value
	6.64	1.73	12.40 conc. x 10^6 mol l^{-1}
			3.84 e_1/e_2
			3.74 $2e_3/e_1$

h) temp. 147°C, time 75.37h

a_1	a_2	a_3	
57.8	19.8	100	
59.0	19.2	100	
59.6	18.8	100	
60.0	19.4	100	
60.0	19.0	100	
59.3	19.2	100	mean value
21.3	6.91	39.9	rel. conc.
		3.08	e_1/e_2
		3.75	$2e_3/e_1$

i) temp. 164°C, time 22.65h

B	a_1	a_2	a_3	
1 060	65.0	17.2	100	
1 050	65.3	17.8	100	
1 020	65.0	17.8	100	
-	65.0	18.0	100	
950	65.0	18.8	100	
1 020	65.1	17.9	100	mean value
	4.58	1.26	7.83	conc. x 10^6 mol l^{-1}
			3.63	e_1/e_2
			3.42	$2e_3/e_1$

j) temp. 165.5°C, time 20.67h

A	a_1	a_2	a_3	
18 100	59.8	15.8	100	
-	61.0	16.3	100	
-	58.9	16.0	100	
18 700	63.2	17.0	100	
18 800	59.8	16.5	100	
18 500	60.5	16.3	100	mean value
	4.84	1.31	8.90	conc. x 10^6 mol l^{-1}
			3.71	e_1/e_2
			3.68	$2e_3/e_1$

k) temp, 192.5°C, time 20.30h

a_1	a_2	a_3
61	18	100
63	19	100
63	18	100
61	19	100
63	19	100
62.2	18.6	100 mean value
22.3	6.69	39.9 rel. conc.
		3.34 e_1/e_2
		3.58 $2e_3/e_1$

l) temp. 154°C, time 29.00h

e_1	e_2
100	28.8
100	29.6
100	30.0
100	29.0
100	29.4 mean value
	3.41 e_1/e_2

m) temp. 183°C, time 46.00h

e_1	e_2
100	30
100	35
100	32.5 mean value
	3.08 e_1/e_2

n) temp. 198°C, time 24.04h

e_1	e_2
100	29.5
100	30.5
100	32.0
100	30.8
100	31.0
100	30.8 mean value
	3.25 e_1/e_2

Plots of i) log e_1/e_2 and ii) log $2e_3/e_1$ against $10^3/T$, by the least squares method, gave:

i) gradient = -0.074 $\pm$ 0.071 intercept = 0.70 $\pm$ 0.03

ii) gradient = -0.034 $\pm$ 0.044 intercept = 0.64 $\pm$ 0.02

Table 3-1

Temp°C	e_1/e_2	log e_1/e_2	$2e_3/e_1$	log $2e_3/e_1$
43.5	2.94	0.468	3.39	0.531
60	2.94	0.468	3.32	0.520
80	2.85	0.455	3.49	0.543
97.5	3.13	0.495	3.64	0.561
117.5	3.18	0.502	3.82	0.582
131.5	3.32	0.523	3.61	0.557
139	3.84	0.584	3.74	0.573
147	3.08	0.489	3.75	0.574
164	3.63	0.561	3.42	0.534
165.5	3.71	0.569	3.68	0.565
192.5	3.34	0.523	3.58	0.554
154	3.41	0.532		
183	3.08	0.488		
198	3.25	0.512		

The reactions of fluoroiodomethane with 1,1-difluoroethylene and ethylene

A photolytic series and a thermally initiated series of temperature dependent addition reactions were conducted with 1,1-difluoroethylene and ethylene.

The series of photolyses was carried out with CH_2FI (2.00×10^{-3} mol l^{-1}), $CH_2{=}CF_2$ (0.67×10^{-3} mol l^{-1}) and $CH_2{=}CH_2$ (0.33×10^{-3} mol l^{-1}) over the

temperature range of 42-182°C. The reaction time was varied over the range of 20-116h. The three measurable products were the normal and reverse 1,1-difluoroethylene adducts and the ethylene adduct.

The thermal reactions were initiated by the decomposition of di-t-butylperoxide and were conducted with CH_2FI (1.00×10^{-3} mol l^{-1}), $CH_2{=}CF_2$ (0.38×10^{-3} mol l^{-1}), $CH_2{=}CH_2$ (0.13×10^{-3} mol l^{-1}) and $(t\text{-}BuO)_2$ (0.5×10^{-5} mol l^{-1}). The temperature was varied in the range 103-182°C and the reaction time in the range 3.5-91h. The three adducts from the addition of $CH_2F\cdot$ radicals to the olefins were observed and measured. Two additional poorly resolved peaks were observed and assumed to be the adducts from addition of $CHFI\cdot$ radicals to the $CH_2{=}$ groups of 1,1-difluoroethylene and ethylene. Some $CHFI_2$ was also formed. One microlitre of CH_2Cl_2 was added to several product mixtures as a standard to facilitate more accurate measurement of the product concentrations.

let a_1 = the relative area of $CH_2FCH_2CF_2I$

a_2 = the relative area of $CH_2FCF_2CH_2I$

a_3 = the relative area of $CH_2FCH_2CH_2I$

e_1 = the relative concentration of $CH_2FCH_2CF_2I$

e_2 = the relative concentration of $CH_2FCF_2CH_2I$

e_3 = the relative concentration $CH_2FCH_2CH_2I$

A = the relative area of CH_2FI

B = the relative area of CH_2Cl_2

PHOTOLYTIC SERIES

a) temp. 42°C, time 116.10h

A	a_1	a_2	a_3
48 300	58	30.9	100
47 500	59	31.8	100
51 500	62	32.5	100
-	66	33.0	100
48 600	61	33.5	100
49 000	61.2	32.3	100 mean value
	1.68	0.89	3.37 conc. x 10^6 mol l^{-1}
			1.89 e_1/e_2
			4.01 $2e_3/e_1$
			7.58 $2e_3/e_2$

b) temp. 60°C, time approx. 80h

B	a_1	a_2	a_3
2 570	57	32.0	100
2 550	55	31.8	100
2 560	58	31.8	100
2 500	54	32.0	100
2 550	57	31.0	100
2 550	56.2	31.7	100 mean value
	1.44	0.81	3.14 conc. x 10^6 mol l^{-1}
		7.72 e_3/e_2	1.77 e_1/e_2
			4.36 $2e_3/e_1$

c) temp. 76.5°C, time 77.70h

B	a_1	a_2	a_3
1 900	49	28.6	100
1 840	46	27.5	100
1 730	44	25.3	100
1 650	47	27.4	100
1 730	46	26.1	100
1 770	46.4	27.0	100 mean value
	1.71	0.99	4.51 conc. x 10^6 mol l^{-1}
			1.72 e_1/e_2
		9.08 $2e_3/e_2$	5.28 $2e_3/e_1$

d) temp. 82.5°C, time approx. 70h

A	a_1	a_2	a_3
20 900	34.0	17.8	100
-	35.4	19.0	100
21 400	35.6	19.2	100
19 200	36.0	19.2	100
20 000	35.0	18.2	100
20 400	35.2	18.7	100 mean value
	2.33	1.23	8.09 conc. x 10^6 mol l^{-1}
			1.88 e_1/e_2
			6.96 $2e_3/e_1$
			13.08 $2e_3/e_2$

e) temp. 98°C, time 41.38h

B	a_1	a_2	a_3
1 620	34.8	16	100
1 600	30.6	16	100
1 660	34.0	17	100
1 680	34.0	17	100
1 820	34.0	17	100
1 680	33.5	16.6	100 mean value
	1.30	0.65	4.77 conc. x 10^6 mol l^{-1}
		14.79 $2e_3/e_2$	2.02 e_1/e_2
			7.32 $2e_3/e_1$

f) temp. 100°C, time 39.40h

B	a_1	a_2	a_3
1 410	31.8	16	100
1 590	31.6	16	100
1 530	32.0	14.5	100
1 530	32.0	15	100
1 580	33.0	16	100
1 530	32.1	15.5	100 mean value
	1.37	0.66	5.23 conc. x 10^6 mol l^{-1}
	15.81 $2e_3/e_2$	7.64 $2e_3/e_1$	2.07 e_1/e_2

g) temp. 117°C, time 29.00h

B	a_1	a_2	a_3
1 700	28.0	13.5	100
1 550	28.8	13.0	100
1 550	27.5	12.5	100
1 330	27.0	13.0	100
1 390	28.4	13.0	100
1 500	27.9	13.0	100 mean value
	1.21	0.56	5.31 conc. x 10^6 mol l^{-1}
			2.15 e_1/e_2
			8.77 $2e_3/e_1$
			18.86 $2e_3/e_2$

h) temp. 129.5°C, time 23.25h

B	a_1	a_2	a_3
1 370	26.0	11.6	100
1 360	25.0	11.8	100
1 260	23.8	10.6	100
1 170	22.6	11.0	100
1 260	23.4	10.4	100
1 280	24.2	11.0	100 mean value
	1.23	0.56	6.22 conc. x 10^6 mol l^{-1}
			2.18 e_1/e_2
			10.13 $2e_3/e_1$
			22.08 $2e_3/e_2$

i) temp. 143.5°C, time 22.87h

A	a_1	a_2	a_3
28 000	22.8	9.3	100
27 200	21.0	8.8	100
-	22.8	9.3	100
-	22.0	8.8	100
-	22.0	8.5	100
-	21.6	-	100
27 600	22.0	8.94	100 mean value
	1.07	0.44	5.98 conc. x 10^6 mol l^{-1}
	27.36 $2e_3/e_2$	11.12 $2e_3/e_1$	2.46 e_1/e_2

j) temp. 151.5°C, time 21.55h

B	a_1	a_2	a_3	
1 240	24.0	11.0	100	
1 310	23.8	9.8	100	
1 270	24.6	10.3	100	
1 360	23.0	10.2	100	
1 260	24.2	10.8	100	
1 290	23.9	10.4	100	mean value
	1.21	0.53	6.20	conc. x 10^6 mol l^{-1}
			2.30	e_1/e_2
			10.24	$2e_3/e_1$
			23.55	$2e_3/e_2$

k) temp. 160°C, time 24.50h

A	a_1	a_2	a_3	
18 200	18.8	8.2	100	
-	19.8	7.3	100	
17 400	19.0	8.2	100	
-	20.0	9.2	100	
17 800	19.4	8.2	100	mean value
	1.47	0.62	9.27	conc. x 10^6 mol l^{-1}
			2.36	e_1/e_2
			12.63	$2e_3/e_1$
			29.81	$2e_3/e_2$

l) temp. 168.5°C, time 20.95h

B	a_1	a_2	a_3	
960	21.8	10.8	100	
1 010	22.0	10.0	100	
1 050	21.0	10.2	100	
950	20.4	9.9	100	
930	19.0	8.5	100	
980	20.8	9.9	100	mean value
	1.39	0.66	8.15	conc. x 10^6 mol l^{-1}
			2.11	e_1/e_2
			11.76	$2e_3/e_1$
			24.81	$2e_3/e_2$

m) temp. 182°C, time 21.05h

e_1	e_2
100	40
100	41
100	43
100	41.3 mean value
	2.42 e_1/e_2

Plots of i) log e_1/e_2, ii) log $2e_3/e_1$ and iii) log $2e_3/e_2$ against $10^3/T$, by the least squares method, gave:

i) gradient = -0.14 ± 0.07; intercept = 0.69 ± 0.03

ii) gradient = -0.57 ± 0.09; intercept = 2.39 ± 0.04

iii) gradient = -0.71 ± 0.16; intercept = 3.08 ± 0.07

Table 3-2

Temp°C	e_1/e_2	log e_1/e_2	$2e_3/e_1$	log $2e_3/e_1$	$2e_3/e_2$	log $2e_3/e_2$
42	1.89	0.277	4.01	0.603	7.58	0.880
60	1.77	0.248	4.36	0.641	7.72	0.889
76.5	1.72	0.235	5.28	0.723	9.08	0.958
82.5	1.88	0.275	6.96	0.843	13.08	1.118
98	2.02	0.305	7.32	0.864	14.79	1.169
100	2.07	0.316	7.64	0.883	15.81	1.199
117	2.15	0.332	8.77	0.943	18.86	1.275
129.5	2.18	0.339	10.13	1.006	22.08	1.345
143.5	2.46	0.392	11.12	1.046	27.36	1.438
151.5	2.30	0.361	10.24	1.010	23.55	1.371
160	2.36	0.373	12.63	1.101	29.81	1.474
168.5	2.11	0.324	11.76	1.070	24.81	1.394
182	2.42	0.384				

n) temp. 103°C, time 90.8h

a) e_1	e_2	b) a_1	a_2	a_3
104	100	6.8	6.6	100
107	100	7.6	7.2	100
107	100	6.4	6.1	100
98	100	6.8	7.0	100
100	100	7.0	7.0	100
103	100 mean value	6.9	6.8	100 mean value
	1.03 e_1/e_2	4.7	4.6	82.5 rel. conc.
				53.1 $3e_3/e_1$
				54.3 $3e_3/e_2$

o) temp. 123°C, time 39.5h

a) e_1	e_2	b) a_1	a_2	a_3
72.4	100	5.8	7.8	100
74.0	100	5.3	7.2	100
76.2	100	5.9	7.7	100
72.2	100	6.6	9.0	100
76.2	100	6.1	8.0	100
74.2	100 mean value	5.9	7.9	100 mean value
	0.742 e_1/e_2	4.0	5.4	82.5 rel. conc.
			46.2 $3e_3/e_2$	61.9 $3e_3/e_1$

p) temp. 139°C, time 20.0h

a) e_1	e_2	b) a_1	a_2	a_3
69.0	100	5.8	8.4	100
72.8	100	6.5	9.0	100
74.2	100	6.8	9.2	100
70.0	100	6.4	9.4	100
72.0	100	6.3	8.7	100
71.6	100			
71.6	100 mean value	6.4	8.9	100 mean value
	0.716 e_1/e_2	4.3	6.0	82.5 rel. conc.
				57.8 $3e_3/e_1$
				41.1 $3e_3/e_2$

q) temp. 163°C, time 6.3h

a) e_1	e_2	b) a_1	a_2	a_3
82.0	100	8.2	10.2	100
94.8	100	9.4	9.8	100
86.0	100	9.6	10.8	100
92.4	100	10.7	11.5	100
100.0	100	10.0	10.0	100
91.0	100 mean value	9.6	10.5	100 mean value
	0.910 e_1/e_2	6.5	7.0	82.5 rel. conc.
				38.4 $3e_3/e_1$
				35.1 $3e_3/e_2$

r) temp. 182°C, time 3.5h

a) e_1	e_2	b) a_1	a_2	a_3
152	100	15.2	10	100
136	100	13.6	10	100
146.5	100	14.4	10	100
137	100	14.0	10	100
140	100	14.0	10	100
142.3	100 mean value	14.2	10	100 mean value
	1.423 e_1/e_2	9.6	6.7	82.5 rel. conc.
				25.8 $3e_3/e_1$
				36.9 $3e_3/e_2$

Plots of i) log e_1/e_2, ii) log $3e_3/e_1$ and iii) log $3e_3/e_2$ against $10^3/T$, by the least squares method, gave:

i) gradient = -0.30 ± 0.83 intercept = 0.69 ± 0.34

ii) gradient = 0.71 ± 0.68 intercept = -0.06 ± 0.28

iii) gradient = 0.40 ± 0.17 intercept = 0.67 ± 0.07

Table 3-3

Temp°C	e_1/e_2	log e_1/e_2	$3e_3/e_1$	log $3e_3/e_1$	$3e_3/e_2$	log $3_e/e_2$
103	1.03	0.014	53.1	1.725	54.3	1.732
123	0.742	-0.130	61.9	1.791	46.2	1.667
139	0.716	-0.145	57.8	1.762	41.1	1.614
163	0.910	-0.041	38.4	1.584	35.1	1.546
182	1.423	0.153	25.8	1.412	36.9	1.567

The reactions of fluoroiodomethane with trifluoroethylene and ethylene

Three series of photolytic reactions were conducted with trifluoroethylene and ethylene. The variable parameters were i) temperature, ii) olefin concentration, and iii) addition of various amounts of carbon dioxide. Measurable quantities of the normal and reverse trifluoroethylene adducts and the ethylene adduct were obtained in all of the reactions. The initial concentration of fluoroiodomethane was kept constant at 2.00×10^{-3} mol l^{-1} and, with the exception of the variation of olefin concentration series, the initial concentrations of trifluoroethylene and ethylene were 0.67 and 0.33 $\times 10^{-3}$ mol l^{-1} respectively. One microlitre of CH_2Cl_2 was added to several product mixtures as a standard to facilitate more accurate measurement of the product concentrations.

let a_1 = the relative area of $CH_2FCHFCF_2I$

a_2 = the relative area of CH_2FCF_2CHFI

a_3 = the relative area of $CH_2FCH_2CH_2I$

e_1 = the relative concentration of $CH_2FCHFCF_2I$

e_2 = the relative concentration of CH_2FCF_2CHFI

e_3 = the relative concentration of $CH_2FCH_2CH_2I$

A = the relative area of CH_2FI

B = the relative area of CH_2Cl_2

i) variation of temperature

a) temp. 60°C, time 59.00h

B	a_1	a_2	a_3
2 590	52.8	110	100
2 560	54.9	114	100
2 520	58.6	115	100
2 680	61.0	115	100
2 880	57.8	118	100
2 650	57.0	114.4	100 mean value
	1.29	2.58	3.02 conc. $\times 10^6$ mol l^{-1}
			2.01 e_2/e_1
			2.34 $2e_3/e_2$

b) temp. 80.5°C, time 65.63h

B	a_1	a_2	a_3	
2 450	51.5	105.0	100	
2 240	53.0	104.0	100	
2 250	53.9	107.8	100	
2 370	50.6	103.2	100	
2 180	53.4	104.8	100	
2 300	52.5	105.0	100	mean value
	1.36	2.73	3.48	conc. x 10^6 mol l^{-1}
			2.02	e_2/e_1
			2.55	$2e_3/e_2$

c) temp. 100°C, time 27.25h

B	a_1	a_2	a_3	
2 290	47.6	98.0	100	
2 290	45.1	91.6	100	
2 250	49.5	97.0	100	
2 270	48.5	93.2	100	
2 240	49.4	95.0	100	
2 270	48.0	95.0	100	mean value
	1.26	2.50	3.52	conc. x 10^6 mol l^{-1}
			1.98	e_2/e_1
			2.82	$2e_3/e_2$

d) temp. 116°C, time 24.00h

B	a_1	a_2	a_3	
-	45.1	92.0	100	
3 380	44.1	89.0	100	
3 120	44.4	88.0	100	
3 100	45.3	92.0	100	
3 180	45.0	91.4	100	
3 200	44.8	90.5	100	mean value
	0.84	1.69	2.50	conc. x 10^6 mol l^{-1}
			2.02	e_2/e_1
			2.96	$2e_3/e_2$

e) temp. 131°C, time 23.05h

a_1	a_2	a_3	
41.8	82	100	
42.3	83	100	
42.8	84	100	
43.3	84	100	
42.3	83	100	
42.5	83.2	100	mean value
25.4	49.7	79.9	rel. conc.
		1.96	e_2/e_1
		3.22	$2e_3/e_2$

f) temp. 143°C, time 23.10h

B	a_1	a_2	a_3	
2 850	42.6	82	100	
2 380	41.3	81	100	
2 540	42.3	83	100	
2 580	43.4	85	100	
2 500	41.0	82	100	
2 570	42.1	82.6	100	mean value
	1.98	3.84	6.22	conc. x 10^6 mol l^{-1}
			1.97	e_2/e_1
			3.24	$2e_3/e_2$

g) temp. 160°C, time 21.57h

a_1	a_2	a_3	
36.7	78.0	100	
37.9	79.0	100	
41.1	77.5	100	
41.1	79.0	100	
39.2	78.4	100	mean value
23.4	46.8	79.9	rel. conc.
		2.00	e_2/e_1
		3.41	$2e_3/e_2$

h) temp. 168°C, time 21.65h

B	a_1	a_2	a_3
780	35.7	76.0	100
780	35.7	77.5	100
820	33.9	75.4	100
785	36.7	76.4	100
791	35.3	76.3	100 mean value
	2.68	5.76	10.10 conc. x 10^6 mol l^{-1}
			2.15 e_2/e_1
			3.50 $2e_3/e_2$

Plots of i) log e_2/e_1 and ii) log $2e_3/e_2$ against $10^3/T$, by the least squares method, gave:

i) gradient = -0.014 $\pm$ 0.049 intercept = 0.339 $\pm$ 0.019

ii) gradient = -0.24 $\pm$ 0.02 intercept = 1.09 $\pm$ 0.01

Table 3-4

Temp°C	e_2/e_1	log e_2/e_1	$2e_3/e_2$	log $2e_3/e_2$
60	2.01	0.303	2.34	0.369
80.5	2.02	0.304	2.55	0.406
100	1.98	0.297	2.82	0.450
116	2.02	0.305	2.96	0.471
131	1.96	0.292	3.22	0.507
143	1.97	0.295	3.24	0.510
160	2.00	0.301	3.41	0.533
168	2.15	0.332	3.50	0.545

ii) Variation of olefin concentration ($CHF=CF_2$: C_2H_4=2:1)

i) $[CHF=CF_2]$ = 0.17 x 10^{-3} mol l^{-1}; time 64.35h, temp 100°C

A	a_1	a_2	a_3	
-	40	79.8	100	
41 300	41	82.0	100	
36 800	39	78.8	100	
39 600	39	79.0	100	
-	40	79.8	100	
39 200	39.8	79.9	100	mean value
	1.25	2.51	4.20	conc. x 10^6 mol l^{-1}
	0.54	1.08	1.81	rate of formation x 10^{11} mol l^{-1} s^{-1}
	6.71 $2e_3/e_1$	3.35 $2e_3/e_2$	2.01 e_2/e_1	

j) $[CHF=CF_2]$ = 0.33 x 10^{-3} mol l^{-1}; time 20.00h, temp 97.5°C

A	a_1	a_2	a_3	
67 500	44	87.6	100	
67 000	44	84.0	100	
64 000	44	87.6	100	
66 500	42	80.2	100	
68 000	44	85.6	100	
66 600	43.6	85.0	100	mean value
	0.81	1.57	2.48	conc. x 10^6 mol l^{-1}
	1.13	2.18	3.44	rate of formation x 10^{11} mol l^{-1} s^{-1}
			1.95 e_2/e_1	
			3.15 $2e_3/e_2$	
			6.14 $2e_3/e_1$	

k) $[CHF=CF_2]$ = 0.67 x 10^{-3} mol l^{-1}; time 27.25h, temp. 100°C

B	a_1	a_2	a_3
22 900	47.6	98.0	100
22 900	45.1	91.6	100
22 500	49.5	97.0	100
22 700	48.5	93.2	100
22 400	49.4	95.0	100
22 700	48.0	95.0	100 mean value
	1.26	2.50	3.52 conc. x 10^6 mol l^{-1}
	1.28	2.55	3.59 rate of formation x 10^{11} mol l^{-1} s^{-1}
			1.98 e_2/e_1
			2.82 $2e_3/e_2$
			5.57 $2e_3/e_1$

l) $[CHF=CF_2]$ = 1.33 x 10^{-3} mol l^{-1}; time 16.77h, temp. 96°C

A	a_1	a_2	a_3
26 500	25.2	73.0	100
25 600	24.0	73.4	100
24 000	24.4	75.4	100
27 000	25.6	72.4	100
26 800	25.4	76.0	100
26 000	24.9	74.0	100 mean value
	1.18	3.51	6.35 conc. x 10^6 mol l^{-1}
	1.95	5.81	10.52 rate of formation x 10^{11} mol l^{-1} s^{-1}
			2.97 e_2/e_1
			3.61 $2e_3/e_2$
			10.73 $2e_3/e_1$

Table 3-5a

$[CHF=CF_2]$ x 10^3 mol l^{-1}	e_2/e_1	$2e_3/e_2$	$2e_3/e_1$
0.17	2.01	3.35	6.71
0.33	1.95	3.15	6.14
0.33*	2.03	2.82	5.62
0.67	1.98	2.82	5.57
1.33	2.97	3.61	10.73

* data corresponding to 100°C from the temperature variation series

Table 3.5b

$[CHF=CF_2]$ x 10^3 mol l^{-1}	R_{e_1}	(log R_{e_1} +12)	R_{e_2}	(log R_{e_2} +12)	R_{e_3}	(log R_{e_3} +12)
0.17	0.54	0.73	1.08	1.03	1.81	1.26
0.33	1.33	1.05	2.18	1.34	3.44	1.54
0.67	1.28	1.11	2.55	1.41	3.59	1.55
1.33	1.95	1.29	5.81	1.76	10.52	2.02

where R = rate of adduct formation x 10^{11} mol l^{-1} s^{-1}

A plot of (log R + 12) against log($[CHF=CF_2]$ x 10^4) for each of the adducts, by the least squares method, gave:

i) e_1 gradient = 0.58 $\pm$ 0.09

ii) e_2 gradient = 0.75 $\pm$ 0.10

iii) e_3 gradient = 0.77 $\pm$ 0.15

iii) addition of various amounts of carbon dioxide

m) $[CO_2]$ = 3.0 x 10^{-3} mol l^{-1}; time 18.53 h, temp. 146°C

A	a_1	a_2	a_3	
-	37	70	100	
27 800	36	73	100	
29 400	35	70	100	
-	35	71	100	
-	36	71	100	
29 400	36	70	100	
28 900	35.9	70.8	100	mean value
	1.53	3.03	5.71	conc. x 10^6 mol l^{-1}
	2.29	4.54	8.56	rate of formation x 10^{11} mol l^{-1} s^{-1}
			1.97	e_2/e_1
			3.78	$2e_3/e_2$
			7.45	$2e_3/e_1$

n) $[CO_2]$ = 6.0 x 10^{-3} mol l^{-1}; time 27.90h, temp. 148°C

A	a_1	a_2	a_3	
-	35.0	71.2	100	
21 800	34.8	70.0	100	
21 000	34.0	69.5	100	
19 600	33.6	70.0	100	
20 800	33.0	72.0	100	
-	37.0	73.8	100	
20 800	34.6	71.1	100	mean value
	2.05	4.21	7.93	conc. x 10^6 mol l^{-1}
	2.04	4.19	7.90	rate of formation x 10^{11} mol l^{-1} s^{-1}
			2.06	e_2/e_1
			3.76	$2e_3/e_2$
			7.74	$2e_3/e_1$

o) $[CO_2]$ = 18.0 x 10^{-3} mol l^{-1}; time approx. 60h, temp. 157.5°C

A	a_1	a_2	a_3	
12 900	29	66	100	
13 600	31	71	100	
-	29	66	100	
-	29	68	100	
-	30	72	100	
13 250	29.6	68.6	100	mean value
	2.75	6.38	12.45	conc. x 10^6 mol l^{-1}
	1.27	2.95	5.76	rate of formation x 10^{11} mol l^{-1} s^{-1}
			2.32	e_2/e_1
			3.90	$2e_3/e_2$
			9.05	$2e_3/e_1$

Table 3-6a

$[CO_2] \times 10^3$ mol l^{-1}	R_{e_1}	R_{e_2}	R_{e_3}
3.0	2.29	4.53	8.56
6.0	2.04	4.19	7.90
18.0	1.27	2.95	5.76

where R = rate of adduct formation x 10^{11} mol l^{-1} s^{-1}

Table 3-6b

$[CO_2] \times 10^3$ mol l^{-1}	e_2/e_1	$2e_3/e_2$	$2e_3/e_1$
0*	2.02	3.31	6.73
3.0	1.97	3.78	7.45
6.0	2.06	3.76	7.74
18.0	2.32	3.90	9.05

* data corresponding to 148°C from the temperature variation series

The reactions of fluoroiodomethane with tetrafluoroethylene and ethylene

A series of photolyses was carried out with CH_2FI (2.00 x 10^{-3} mol l^{-1}), $CF_2=CF_2$ (0.17 x 10^{-3} mol l^{-1}) and $CH_2=CH_2$ (0.33 x 10^{-3} mol l^{-1}). The temperature was varied in the range 43-168°C and the reaction time in the range 5-50h. The three measurable products were the tetrafluoroethylene and ethylene adducts and the cross telomer: the cross telomer was from the addition of fluoromethyl radicals to tetrafluoroethylene followed by the intermediate substituted propyl radicals adding to ethylene ($CH_2FCF_2CF_2CH_2CH_2I$).

let a_1 = the relative area of $CH_2FCF_2CF_2I$
a_2 = the relative area of $CH_2FCF_2CF_2CH_2CH_2I$
a_3 = the relative area of $CH_2FCH_2CH_2I$
e_1 = the relative concentration of $CH_2FCF_2CF_2I$
e_2 = the relative concentration of $CH_2FCF_2CF_2CH_2CH_2I$
e_3 = the relative concentration of $CH_2FCH_2CH_2I$
A = the relative area of CH_2FI

a) temp. 43.5°C, time 49.53h

A	a_1	a_2	a_3
32 000	41.7	50	208
-	46.2	50	206
-	42.1	50	216
33 400	45.0	50	212
31 000	41.4	50	212
32 100	43.3	50	210.7 mean value
	1.53	2.57	6.66 conc. x 10^6 mol l^{-1}
			6.38 $2(e_1 + e_2)/e_3$

b) temp. 68.0°C, time 43.10h

A	a_1	a_2	a_3
23 500	38.6	50	176.4
21 500	34.2	50	172.0
-	32.9	50	163.4
-	34.0	50	173.6
-	32.1	50	169.2
22 500	34.4	50	170.9 mean value
	1.74	3.67	7.71 conc. x 10^6 mol l^{-1}
			5.152e$(e_1 + e_2)/e_3$

c) temp. 88°C, time 28.33h

A	a_1	a_2	a_3
-	36	50	147
19 500	33	50	142
-	36	50	138
19 000	35	50	146
20 200	35	50	150
18 500	35	50	145
19 300	35	50	144.5 mean value
	2.06	4.28	7.60 conc. x 10^6 mol l^{-1}
			4.52 $2(e_1 + e_2)/e_3$

d) temp. 102°C, time 19.00h

a_1	a_2	a_3	
44	50	140	
40	50	144	
42	50	142	mean value
2.39	4.12	7.21	rel. conc.
		4.66	$2(e_1 + e_2)/e_3$

e) temp. 110°C, time 22.00h

A	a_1	a_2	a_3	
-	36.8	50	132	
18 600	38.2	50	136	
16 500	35.0	50	126	
16 000	35.4	50	129	
18 500	42.0	50	116	
17 400	37.5	50	127.8	mean value
	2.45	4.74	7.45	conc. x 10^6 mol l^{-1}
			4.18	$2(e_1 + e_2)/e_3$

f) temp. 132.5°C, time 24.50h

A	a_1	a_2	a_3	
10 700	38.2	50	114	
11 200	35.8	50	121	
11 500	35.5	50	118	
11 700	37.0	50	118	
11 400	38.0	50	119	
11 300	36.9	50	118	mean value
	3.71	7.30	10.61	conc. x 10^6 mol l^{-1}
			3.93	$2(e_1 + e_2)/e_3$

g) temp. 151°C, time 22.15h

A	a_1	a_2	a_3
16 600	45.0	50	102.8
-	46.0	50	103.5
15 200	43.5	50	105.5
15 900	44.8	50	103.9 mean value
	3.21	5.19	6.54 conc. x 10^6 mol l^{-1}
			3.76 $2(e_1 + e_2)/e_3$

h) temp. 167.5°C, time 18.10h

A	a_1	a_2	a_3
8 700	32	50	98.8
-	32	50	98.0
-	33	50	97.8
8 500	31	50	97.6
-	32	50	98.0
8 600	32	50	98.0 mean value
	4.23	9.59	11.57 conc. x 10^6 mol l^{-1}
			3.30 $2(e_1 + e_2)/e_3$

i) temp. 168°C, time 5.50h

A	a_1	a_2	a_3
16 800	55	50	80.0
16 800	56	50	77.8
16 800	55.5	50	78.9 mean value
	3.76	4.91	4.70 conc. x 10^6 mol l^{-1}
			3.44 $2(e_1 + e_2)/e_3$

A plot of log $2(e_1 + e_2)/e_3$ against $10^3/T$, by the least squares method, gave:

gradient = 0.29 ± 0.05

intercept = -0.12 ± 0.02

Table 3-8

Temp ^{o}C	$2(e_1 + e_2)/e_3$	$\log 2(e_1 + e_2)/e_3$
43.5	6.38	0.805
68	5.15	0.712
88	4.52	0.655
102	4.66	0.668
110	4.18	0.621
132.5	3.93	0.594
151	3.76	0.575
167.5	3.30	0.518
168	3.44	0.537

DISCUSSION

The photolyses of CH_2FI ($\lambda > 300$ nm) in the presence of the fluoroethylenes gave the adducts from the addition of fluoromethyl radicals followed by abstraction of iodine: in the presence of both tetrafluoroethylene and ethylene the cross telomer, $CH_2FCF_2CF_2CH_2CH_2I$, was also formed. Failure to observe other products in significant quantities led to the initial assumption that the reaction chains were long and that the addition step was rate determining.

$$CH_2FI + h\nu \longrightarrow CH_2F\cdot + I\cdot \qquad 1$$

$$CH_2F\cdot + E \longrightarrow CH_2FE\cdot \qquad 2$$

$$CH_2FE\cdot + CH_2FI \longrightarrow CH_2FEI + CH_2F\cdot \qquad 3$$

$$2CH_2F\cdot \longrightarrow CH_2FCH_2F \qquad 4$$

where E = olefin

This is the analogous reaction scheme initially adopted for the addition of $CHF_2\cdot$ radicals in part 2: the experimental work of part 3, with the exception of the thermally initiated series, was carried out before that of part 2. As only a small percentage of reactants is consumed in each reaction (<10%), equations 24 of part 1, and 16 and 19 of part 2 are applicable.

$$\log e_3F_o/e_1E_o = \log A_3 - \log A_1 + (E_1 - E_3)/2.303\ RT \qquad 5$$

$$\log e_1/e_2 = \log A_1 - \log A_2 + (E_2 - E_1)/2.303\ RT \qquad 6$$

$$\log e_4E_o/e_3F_o = \log A_4 - \log A_3 + (E_3 - E_4)/2.303\ RT \qquad 7$$

where:

e_1 = the concentration of a normal fluoroethylene adduct

e_2 = the concentration of the corresponding reverse fluoroethylene adduct

e_3 = the concentration of ethylene adduct

e_4 = the concentration of tetrafluoroethylene adduct plus cross telomer

E_o = the concentration of ethylene

F_o = the concentration of fluoroethylenes

The analogy between the $CHF_2\cdot$ and $CH_2F\cdot$ radical systems may extend to the participation of excited CH_2F^* radicals and iodine, $I^*(^2P_{\frac{1}{2}})$, atoms.

Fluorodiiodomethane was present as an impurity in CH_2FI, but was also formed as a minor product in the photolytic reactions.

$$CH_2FI + h\nu \longrightarrow CH_2F^* + I^*(^2P_{\frac{1}{2}}) \quad 8$$

$$I^*(^2P_{\frac{1}{2}}) + CH_2FI \longrightarrow CHFI\cdot + HI \quad 9$$

$$CHFI\cdot + CH_2FI \longrightarrow CHFI_2 + CH_2F\cdot \quad 10$$

This pathway also produces fluoroiodomethyl radicals. Although the addition products of $CHFI\cdot$ radicals were not identified, the chromatograms contained very small broad peaks of long retention time: these are analogous to the adducts from the addition of $CF_2I\cdot$ radicals to the fluoroethylenes (cf. part 2).

$$CHFI\cdot + E \longrightarrow CHFIE\cdot \quad 11$$

$$CHFIE\cdot + CH_2FI \longrightarrow CHFIEI + CH_2F\cdot \quad 12$$

where E = olefin

In the preparative runs with ethylene, vinyl fluoride and 1,1-difluoroethylene the propenes corresponding to the elimination of hydrogen iodide from the adducts were observed, but these were of no significance in the kinetic runs. The two and three to one telomers of tetrafluoroethylene, $CH_2F(CF_2CF_2)_3I$ and $CH_2F(CF_2CF_2)_3I$, were observed in the preparative run, but in the kinetic runs in the presence of ethylene the predominant product was the cross telomer, $CHF_2CF_2CF_2CH_2CH_2I$: no other telomers were observed and the tetrafluoroethylene adduct was the minor product.

The logarithms of the adduct ratios are plotted against $10^3/T$ for the addition of $CH_2F\cdot$ radicals to both ends of vinyl fluoride and 1,1-difluoroethylene (fig 3.1), the competitive addition to vinyl fluoride and 1,1-difluoroethylene relative to ethylene (fig 3.2), and the addition to both ends of trifluoroethylene and the competitive addition to trifluoroethylene and tetrafluoroethylene relative to ethylene (fig 3.3). The results follow the same trend as for the addition of $CHF_2\cdot$ radicals. In the competitive reactions between ethylene and the unsymmetrical fluoroethylenes the $CH_2F\cdot$ radicals add preferentially to ethylene. On the other hand, in the competitive reaction between

Fig. 3.1 Arrhenius plot for addition of $CH_2F^{\cdot}$ radicals to vinyl fluoride (●) and 1,1-difluoroethylene (○).

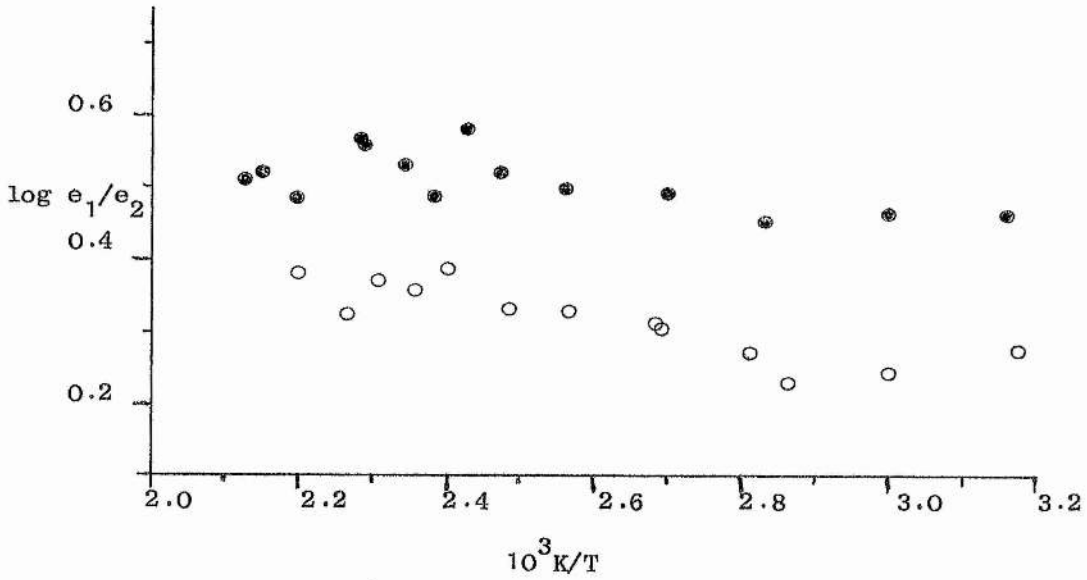

Fig. 3.2 Arrhenius plot for addition of $CH_2F^{\cdot}$ radicals to vinyl fluoride (●) and 1,1-difluoroethylene (○) in the presence of ethylene

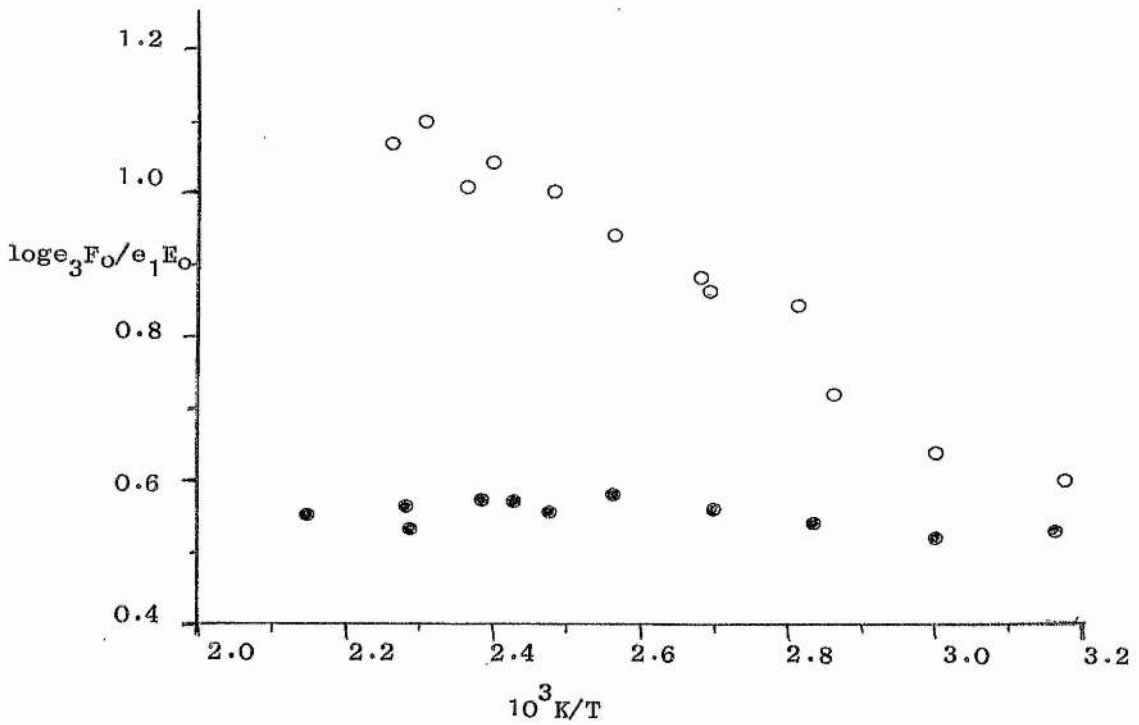

Fig. 3.3 Arrhenius plots for addition of $CH_2F^{\cdot}$ radicals to trifluoroethylene (O and ◑) and tetrafluoroethylene (◉) in the presence of ethylene.

$e_1 = [CH_2FCHFCF_2I]$; $e_2 = [CH_2FCF_2CHFI]$; $e_3 = [CH_2FCH_2CH_2I]$

$e_4 = [CH_2FCF_2CF_2I] + [CH_2FCF_2CF_2CH_2CH_2I]$

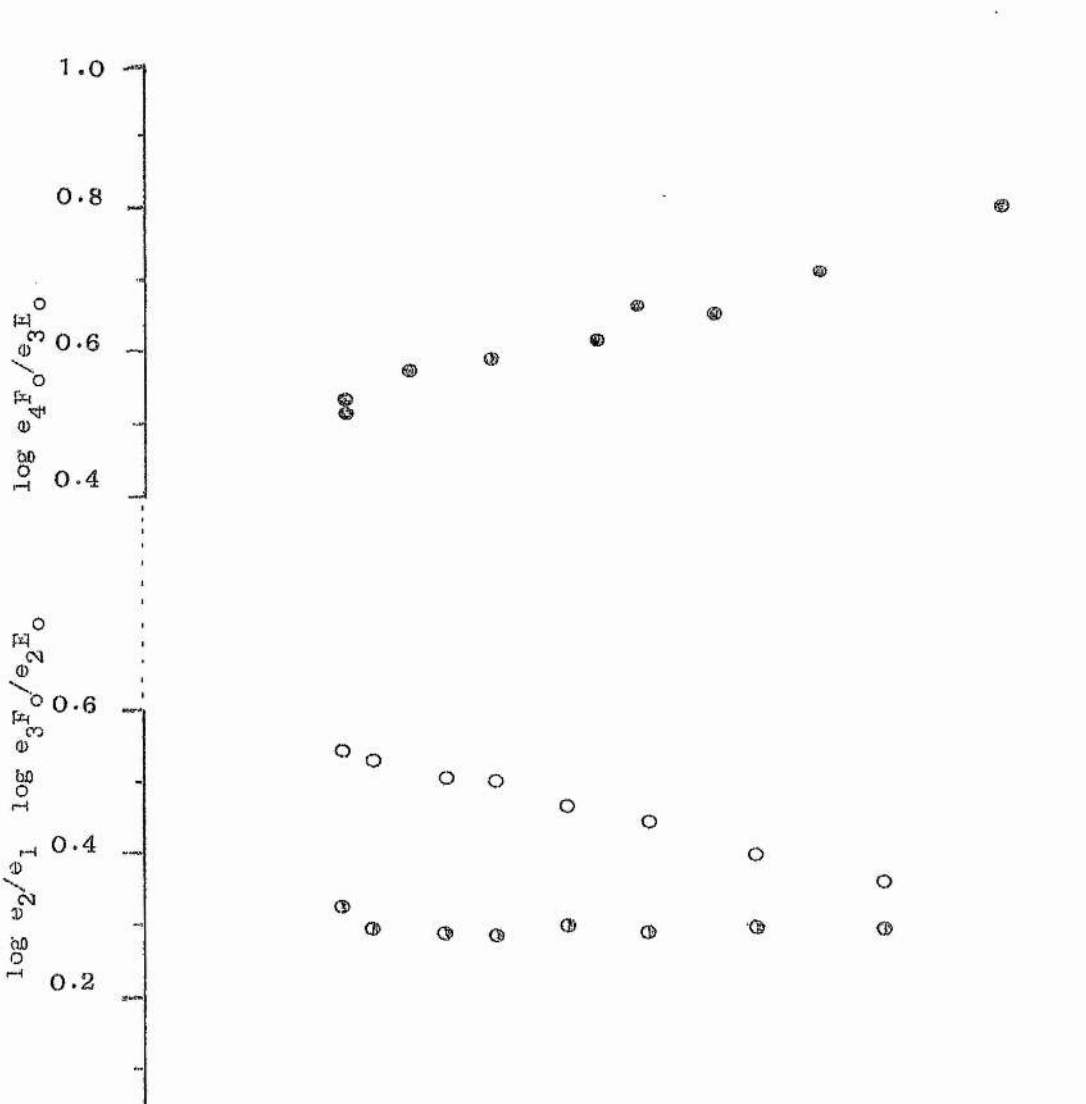

ethylene and tetrafluoroethylene the radicals add preferentially to tetrafluoroethylene. In the addition reactions to the unsymmetrical fluorcethylenes there is preferential addition to the least substituted ends of vinyl fluoride and 1,1-difluoroethylene and to the most substituted end in trifluoroethylene. The intercepts and slopes from the logarithms of the adduct ratios against $10^3/T$ were calculated by the least squares method and are shown in table 3.9. Once again an anomalous behaviour is observed. Negative slopes, corresponding to diverging adduct ratios with increasing temperature, and A-factors varying by up to three orders of magnitude from normal values were observed for the competitive addition to 1,1-difluoroethylene and trifluoroethylene in the presence of ethylene. The competitive addition between vinyl fluoride and ethylene gave a small negative slope, which is exceeded by the error factor, and a reasonably acceptable A-factor. The competitive addition between ethylene and tetrafluoroethylene shows normal behaviour. Once again, as was observed with the addition of $CHF_2\cdot$ radicals, normal behaviour is accompanied by relatively fast addition reactions and anomalous behaviour is associated with at least one relatively slow addition step. The results for the addition of $CHF_2\cdot$ and $CH_2F\cdot$ radicals complete the data for the competitive addition of the fluoromethyl radical series ($CF_3\cdot$, $CHF_2\cdot$, $CH_2F\cdot$ and $CH_3\cdot$) to ethylene and tetrafluoroethylene. The logarithms of the adduct ratios for the series of radicals are plotted against $10^3/T$ in fig 3.4.

The main points are:

i) the similarities of the A-factor differences,

ii) the stepwise change in slopes from $CF_3\cdot$ to $CH_3\cdot$,

iii) the change, from the preferential addition of the electrophilic $CF_3\cdot$ radical to ethylene, to the preferential addition of the less electrophilic or nucleophilic $CH_3\cdot$ radical to tetrafluoroethylene.

The orientation ratios at 150°C, and the A-factor and activation energy differences are shown in table 3.10.

The series of fluoromethyl radicals show graduated changes in structural

Table 3-9 The addition of $CH_2F^{\cdot}$ radicals to fluoroethylenes relative to ethylene.

OLEFIN	INTERCEPT	SLOPE
$^{*}CH_2=CH_2$	0.00	0.00
$^{*}CH_2=CHF$	0.64 ± 0.02	-0.034 ± 0.044
$^{*}CH_2=CF_2$	2.39 ± 0.04	-0.57 ± 0.09
$^{*}CHF=CH_2$	1.34 ± 0.05	-0.108 ± 0.115
$^{*}CHF=CF_2$	1.43 ± 0.029	-0.254 ± 0.069
$^{*}CF_2=CH_2$	3.08 ± 0.07	-0.71 ± 0.15
$^{*}CF_2=CHF$	1.09 ± 0.01	-0.24 ± 0.02
$^{*}CF_2=CF_2$	-0.12 ± 0.02	0.29 ± 0.05

* denotes the site of addition

Fig. 3.4 Arrhenius plot of log e_3/e_4 against $10^3/T$ for competitive addition of $CF_3^{\cdot}$ (O), $CHF_2^{\cdot}$ (◐), $CH_2F^{\cdot}$ (●), $CH_3^{\cdot}$ radicals between tetrafluoroethylene and ethylene.

e_3 = $[XCH_2CH_2I]$

e_4 = $[XCF_2CF_2I]$ + $[XCF_2CF_2CH_2CH_2I]$

X = $CF_3^{\cdot}$, $CHF_2^{\cdot}$, $CH_2F^{\cdot}$ and $CH_3^{\cdot}$

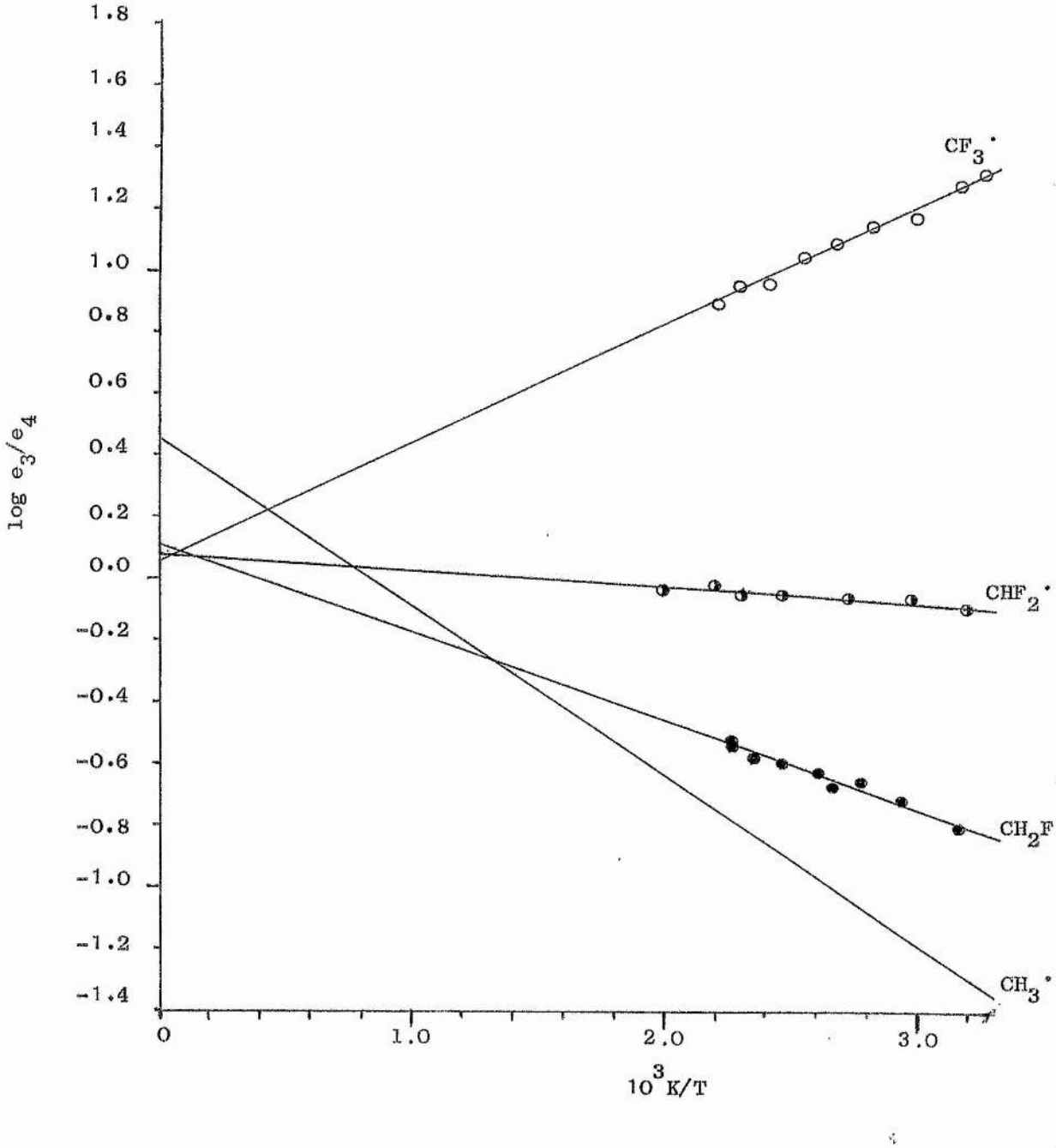

Table 3-10 Experimental data from the competitive addition of $CF_3^{\cdot}$, $CHF_2^{\cdot}$, $CH_2F^{\cdot}$ and $CH_3^{\cdot}$ radicals to tetrafluoroethylene and ethylene.

RADICAL	k_3/k_4 at 150°C	$\log A_3/A_4$ ($l\ mol^{-1}\ s^{-1}$)	$E_{C_2F_4} - E_{C_2H_4}$ (k cal mol^{-1})	ref.
$CF_3^{\cdot}$	9.10	0.06 ± 0.01	1.74 ± 0.22	20
$CHF_2^{\cdot}$	0.90	0.08 ± 0.01	-0.24 ± 0.12	this work
$CH_2F^{\cdot}$	0.27	0.12 ± 0.01	-1.33 ± 0.23	this work
$CH_3^{\cdot}$	0.15	0.47	-2.5	8

subscript 3 refers to addition to ethylene

subscript 4 refers to addition to tetrafluoroethylene

Table 3-11 The structural and polar nature of $CF_3^{\cdot}$, $CHF_2^{\cdot}$, $CH_2F^{\cdot}$ and $CH_3^{\cdot}$ radicals.

	Θ[1]	r_c[2]	$\sum_{\alpha} \sigma_I(\alpha)$
ref	92	32	32
$CF_3^{\cdot}$	17.8	3.92	1.56
$CHF_2^{\cdot}$	12.7	3.63	1.04
$CH_2F^{\cdot}$	<5	3.16	0.52
$CH_3^{\cdot}$	0	2.58	0.00

1 Θ = angle of deviation from planarity

2 r_c = radius of each fluoromethyl radical

and polar states. Methyl radicals are planar and the carbon atom is sp^2-hybridised with the unpaired electron in a p-orbital perpendicular to the plane of the sp^2-orbitals. On the other hand, trifluoromethyl radicals[92] are pyramidal with F-C-F angles of 111.1° and the unpaired electron in an orbital of 21% s character: the degree of non planarity, the angle between the bonds and a plane normal to the three fold axis of symmetry, is 17.8°. The $CH_2F\cdot$ and $CHF_2\cdot$ radicals have intermediate structures with deviations from planarity of <5° and 12.7° respectively. The sum of the Taft inductive substituent constants[119] (σ_I) for the substituent atoms (α) attached to the central carbon atom of each fluoromethyl radical is a measure of radical polarity. The structural and polar natures of the radicals are shown in Table 3.11. A combination of these structural and polar differences may contribute to the observed experimental behaviour. The A-factors show a slight preference for addition to ethylene, but the differences within the radical series are very small. The activation energy differences are plotted against the sum of the Taft inductive substituent constants and the radii of the fluoromethyl radicals in figs 3.5 and 6. The correlation of activation energies with Taft inductive substituent constants is approximately linear and illustrates the decreasing electrophilic nature of the radicals along the series from $CF_3\cdot$ to $CH_3\cdot$. The correlation with the radii of the radicals presents a curve showing that steric hindrance may also contribute to the observed activation energy differences.

All of the fully halogenated methyl radicals that have been studied in competitive addition reactions to tetrafluoroethylene and ethylene add preferentially to ethylene. With $CHF_2\cdot$ and $CH_2F\cdot$ radicals preferential addition occurs to tetrafluoroethylene. On the other hand, addition to 1,1-difluoroethylene, which also presents $=CH_2$ and $=CF_2$ reactive sites, results in preferential addition to $=CH_2$ groups. Consideration of these two situations may elucidate the factors influencing the direction of orientation. In both cases the competition is between addition to $=CH_2$ and $=CF_2$ sites with the difference arising in

Fig. 3.5 $E_{C_2F_4} - E_{C_2H_4}$ against the radical radii for $CF_3^{\cdot}$, $CHF_2^{\cdot}$, $CH_2F^{\cdot}$ and $CH_3^{\cdot}$ radicals.

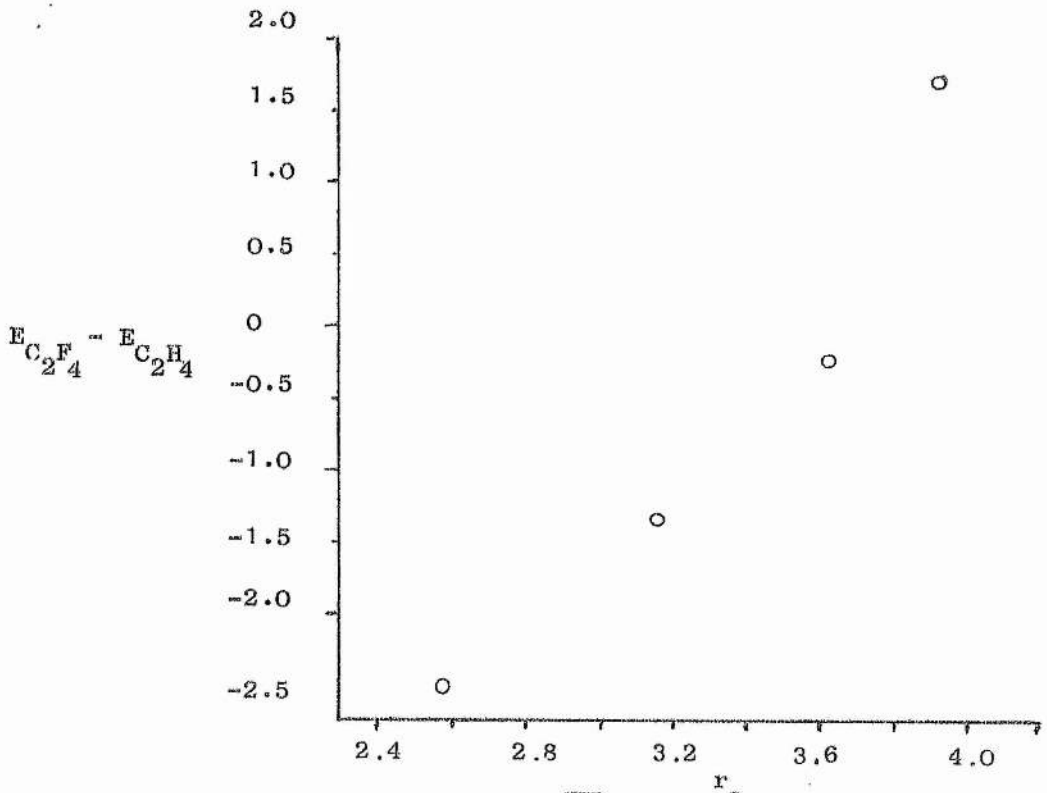

Fig. 3.6 $E_{C_2F_4} - E_{C_2H_4}$ against $\sum_{\alpha} \sigma_I$ (α) for $CF_3^{\cdot}$, $CH_2F^{\cdot}$ and $CH_3^{\cdot}$ radicals.

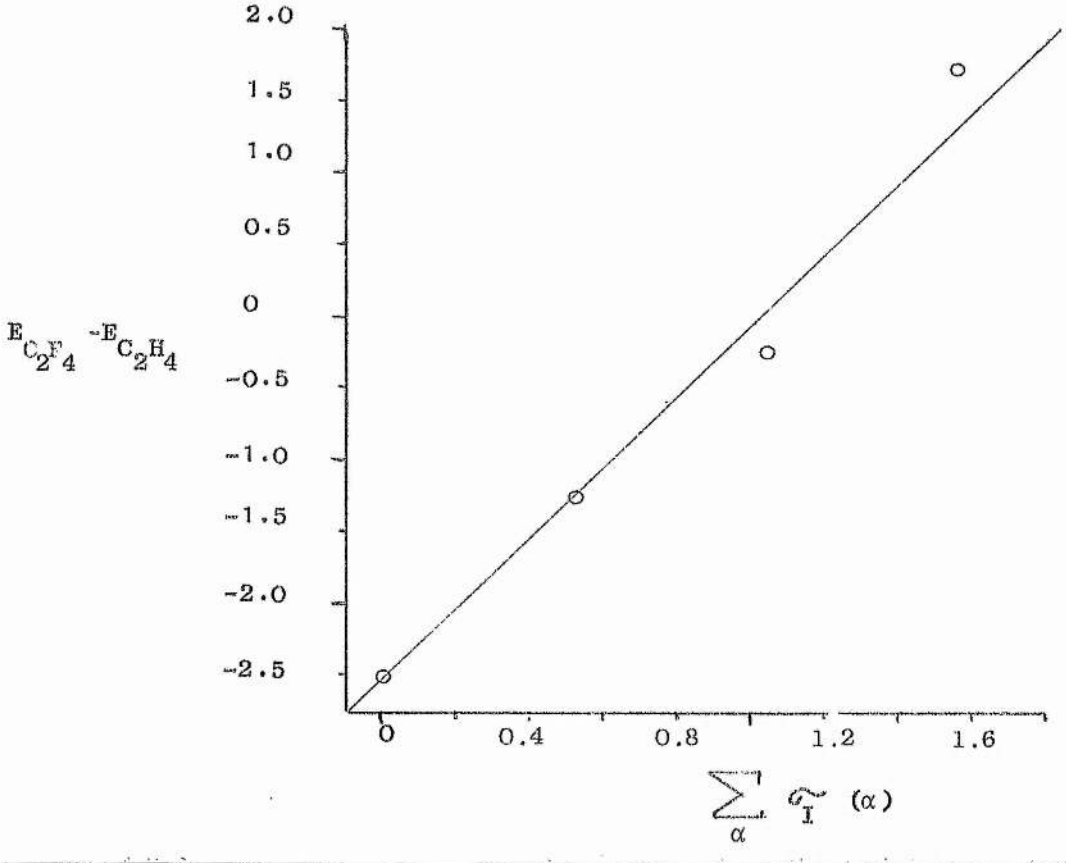

the substituents on the carbon atom β to the site of attack. Recent calculations by the INDO method[52,53] predict that the electron densities on the fluorinated carbon atoms of vinyl fluoride, 1,1-difluoroethylene and tetrafluoroethylene are less than unity. These are consistent with the observed preferential addition of electrophilic $CF_3\cdot$ radicals to ethylene and less electrophilic or nucleophilic $CHF_2\cdot$ and $CH_2F\cdot$ radicals to tetrafluoroethylene. Although $CH_2F\cdot$ radicals do not add preferentially to the $=CF_2$ end of 1,1-difluoroethylene, at least for the series of $CF_3\cdot$, $CHF_2\cdot$ and $CH_2F\cdot$ radicals the orientation ratios are moving in the right direction with decreasing preference for addition to the $=CH_2$ end. The observed results are consistent with addition to $=CH_2$ sites being assisted by the presence of $=CH_2$ groups β to the site of attack, and with addition to $=CF_2$ sites being assisted by the presence of $=CF_2$ groups β to the site of attack.

Two additional competitive series of reactions between trifluoroethylene and ethylene were conducted: in the first series various amounts of CO_2 were added to the system, and in the second series the olefin concentrations were varied, but the ratio of trifluoroethylene to ethylene was maintained constant.

The reaction series incorporating CO_2 was conducted at approx. 150°C: the corresponding rates of adduct formation and the adduct ratios are shown in tables 3.6a and b. Addition of CO_2 depresses the rate of adduct formation and increases the selectivity of the fluoromethyl radicals. These results are consistent with the joint participation of non excited $CH_2F\cdot$ and excited CH_2F^* radicals. Increasing collisional deactivation of excited species with increasing amounts of CO_2 may decrease the rate of adduct formation, and the proportionate decrease is greater for the trifluoroethylene adducts which is consistent with excited radicals making a greater contribution to their formation in the temperature dependent series. Similarly, increasing selectivity with increasing amounts of CO_2 is indicative of reduced participation of

excited species.

The reaction series dependent upon olefin concentration was conducted at 100°C: the corresponding adduct ratios and the rates of adduct formation are shown in tables 3.5a and b. Apart from the reaction at high olefin concentration, the normal to reverse trifluoroethylene adduct ratio is constant, and the slight variation in the ratios of the ethylene to trifluoroethylene adducts may be within the limits of experimental accuracy. The anomalous selectivities at high olefin concentration are due to the telomerisation of the trifluoroethylene addend radicals. The rate of formation of the ethylene adduct is, to the first approximation, 1st order with respect to ethylene. This evidence substantiates the proposed reaction mechanism. The partial order (0.58 ± 0.09) for formation of the normal trifluoroethylene adduct may deviate from unity as a result of some telomerisation at high olefin concentrations.

To test the hypothesis that excited radicals participate in the photochemical reactions, a series of reactions was initiated by the thermal decomposition of di-t-butylperoxide in the presence of ethylene and 1,1-difluoroethylene.

$$(CH_3)_3COOC(CH_3)_3 \xrightarrow{\text{heat}} 2(CH_3)_3CO\cdot \qquad 13$$

$$CH_3\text{-}\overset{\displaystyle CH_3}{\overset{|}{C}}\text{-}O\cdot \xrightarrow{\beta \text{ scission}} CH_3\cdot + CH_3\text{-}\overset{\displaystyle O}{\overset{\|}{C}}\text{-}CH_3 \qquad 14$$

$$CH_3\cdot + CH_2FI \longrightarrow CH_3I + CH_2F\cdot \qquad 15$$

The $CH_2F\cdot$ radicals are in their ground states as they are formed by secondary reactions. The logarithms of the adduct ratios are plotted against $10^3/T$ for both the thermally and photochemically initiated series in fig 3.7a and b. The intercepts and slopes as calculated by the least squares method are shown on pages 188 and 190. Although the ethylene to normal 1,1-difluoroethylene adduct ratios of the thermal series show approximately normal behaviour i.e. positive slope in the Arrhenius plot, an unknown factor contributing towards the loss of

normal adduct may be operative. The main points of interest from the ratios of the ethylene to reverse 1,1-difluoroethylene adducts are:

i) normal Arrhenius behaviour in the thermally initiated series,

ii) convergence of the adduct ratios for both the photolytic and thermal series with increasing temperature around 200°C,

iii) convergence, with decreasing temperature around 40°C, of the experimental curve to the proposed Arrhenius plot representing the addition of excited CH_2F^* radicals to the olefins. The proposed plot is based upon the conclusions of part 2 (page159), that the anomalous curved plots may arise from the joint participation of non excited and excited radicals in non reversible addition reactions to the fluoroethylenes, with non excited species predominating at high temperature and excited species predominating at low temperature.

The Arrhenius parameters for the thermal addition of $CH_2F^{\cdot}$ and the proposed plot for the addition of excited CHF_2^* are:

Radical	k_{e_3}/k_{e_2} at 150°C	$\log A_{e_2} - \log A_{e_3}$ ($l\ mol^{-1}\ s^{-1}$)	$E_{e_2} - E_{e_3}$ (k cal mol^{-1})
$CH_2F^{\cdot}$	41.3	-0.67 ± 0.07	1.83 ± 0.78
CH_2F^*	7.8	-0.67 ± 0.07	0.27

where e_2 = reverse 1,1-difluoroethylene adduct

e_3 = ethylene adduct

Assuming that the addition of both $CHF_2^{\cdot}$ and CHF_2^* to the fluoroethylenes involves the same transition states, then, the difference in the gradients for the thermal addition of $CH_2F^{\cdot}$ and the proposed Arrhenius plot for the addition of excited CH_2F^* radicals (Fig 3.7b) gives some indication of the vibrational energy of the excited species: this is approximately 1.6 k cal mol^{-1} for excited CH_2F^* radicals.

An analogous situation arose from the photolytic addition of $CFBr_2^{\cdot}$ radicals to 1,1-difluoroethylene (part 1) using unfiltered light and light of 366 nm. The logarithms of the adduct ratios are plotted against $10^3/T$ in fig 3.8. The corresponding Arrhenius parameters for formation of the normal (e_1) and reverse (e_2)

Fig. 3.7 Arrhenius plots for competitive addition of $CH_2F^{\cdot}$ to 1,1-difluoroethylene in the presence of ethylene by photolysis (O) and thermolysis (●)

$e_1 = [CH_2FCH_2CF_2I]$; $e_2 = [CH_2FCF_2CH_2I]$; $e_3 = [CH_2FCH_2CH_2I]$

a)

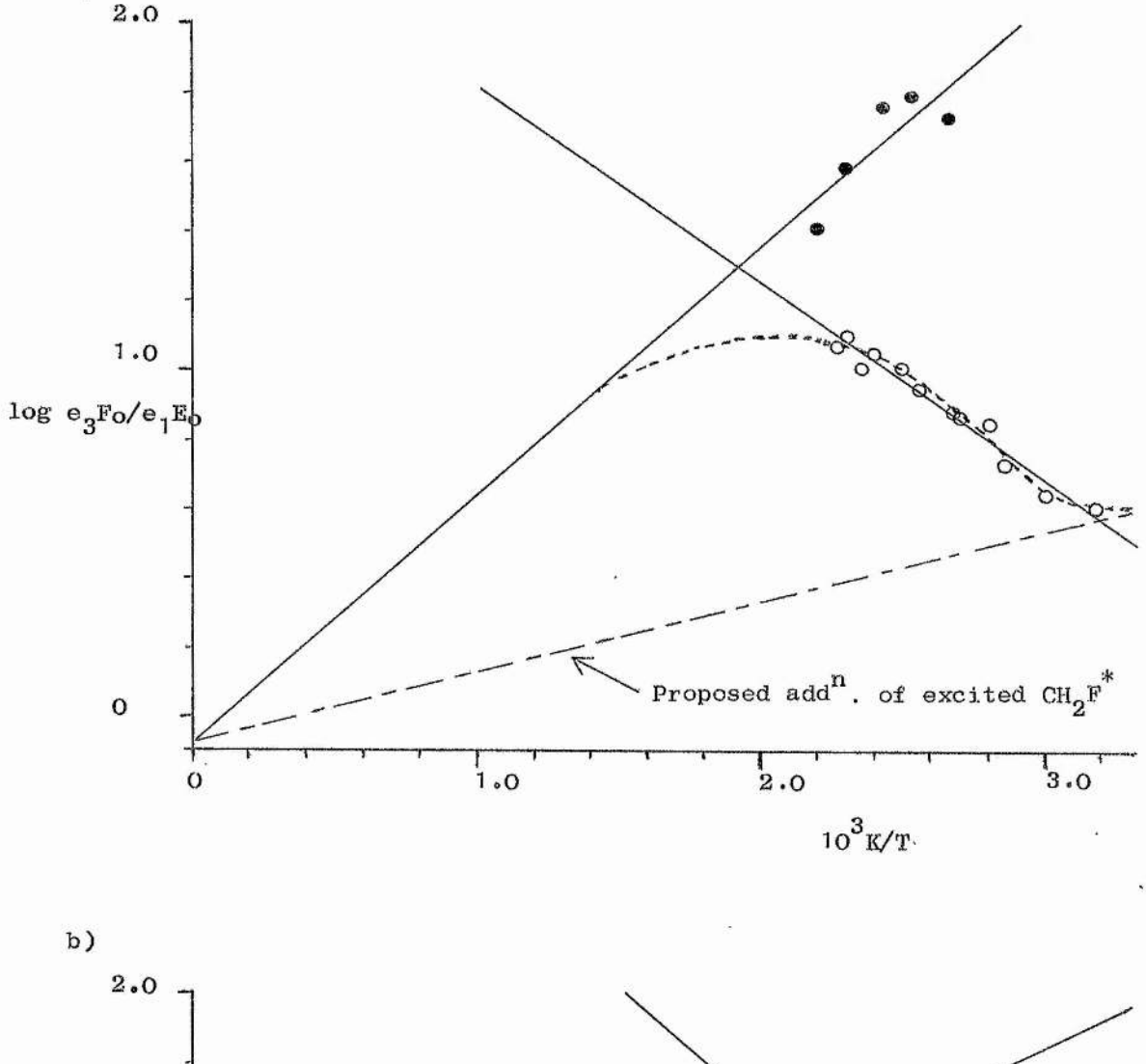

b)

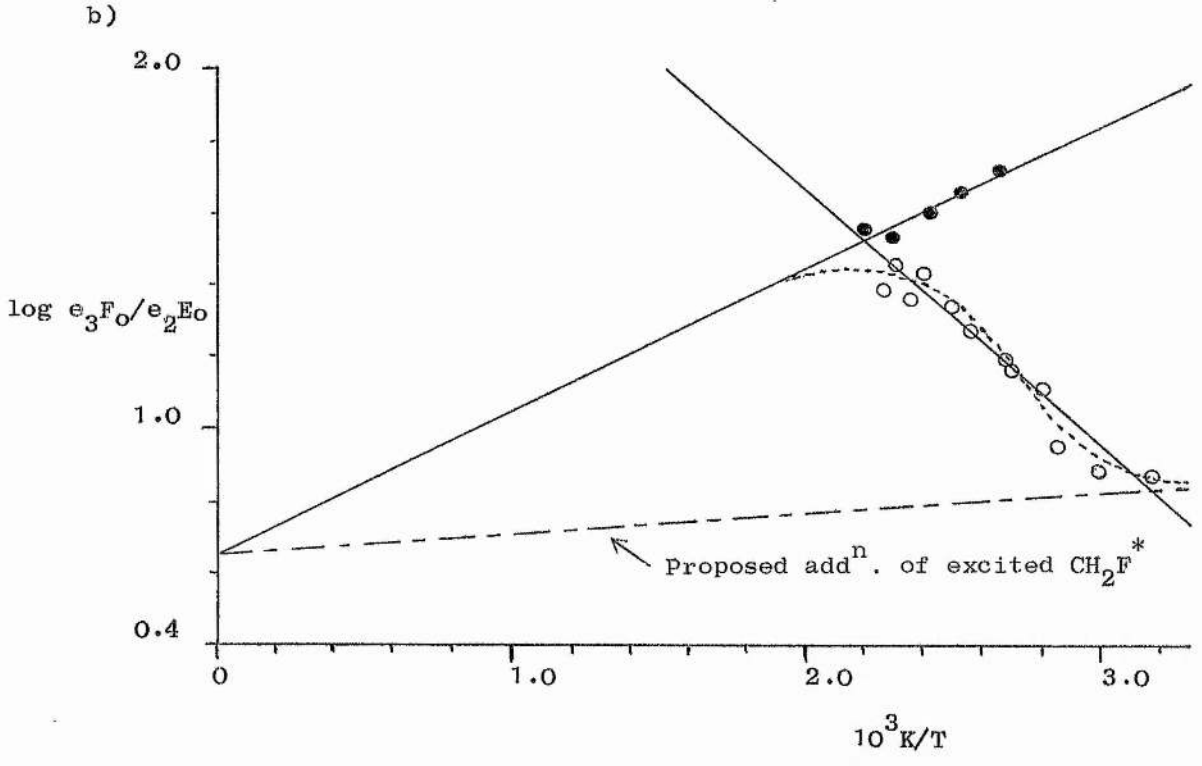

1,1-difluoroethylene adducts from addition of non excited $CFBr_2^{\cdot}$ and excited $CFBr_2^{*}$ radicals are:

Radical	k_{e_1}/k_{e_2} at 150°C	$\log A_{e_2} - \log A_{e_1}$ ($l\ mol^{-1}\ s^{-1}$)	$E_{e_2} - E_{e_1}$ (k cal mol^{-1})
$CFBr_2^{\cdot}$	55.0	1.99 ± 0.15	7.25 ± 1.60
$CFBr_2^{*}$	6.2	1.99 ± 0.15	5.42

Assuming that reaction of both the non excited and excited species proceed through the same transition state, then some indication of the level of vibrational excitation in $CFBr_2^{*}$ is given by the difference in the slopes of fig 3.8: this is equivalent to 1.8 k cal mol^{-1}.

The reaction pathway postulated in part 2 incorporated the non reversible addition of non excited and excited difluoromethyl radicals, with non excited radicals predominating at high temperatures, and excited radicals predominating at low temperatures. Fluoromethyl radicals have now been observed to show the same anomalous pattern of behaviour. The results from the kinetic series with variable CO_2 and olefin concentrations are in accord with the proposed mechanism which is finally verified by the results of the thermally initiated series.

The orientation ratios for the addition of $CF_3^{\cdot}$, $CHF_2^{\cdot}$, $CH_2F^{\cdot}$ and $CH_3^{\cdot}$ radicals to the unsymmetrical fluoroethylenes at 150°C are:

Radical	$CH_2{=}CHF$	$CH_2{=}CF_2$	$CHF{=}CF_2$
$CF_3^{\cdot}$	1:0.09	1:0.03	1:0.50
$CHF_2^{\cdot}$	1:0.19	1:0.18	1:0.95
$CH_2F^{\cdot}$	1:0.30	1:0.44	1:2.04
$CH_3^{\cdot}$	1:0.59	-	1:7.15

The obvious feature is the decreasing preference for addition to the least substituted ends of the fluoroethylenes as the attacking radicals become less electrophilic along the series from $CF_3^{\cdot}$ to $CH_3^{\cdot}$. These variations are influenced by steric and polar factors. The radical radii (r_c) and the sum of the Taft inductive substituent constants ($\sum_{\alpha} \sigma_I (\alpha)$) may be measures of steric and polar factors respectively. These values, individual and combined, along with adduct ratio data at 150°C are

Fig. 3.8 Arrhenius plots for photolytic addition of dibromofluoromethyl radicals to 1,1-difluoroethylene using unfiltered light (●) and light of 366 nm (○).

$e_1 = [CFBr_2CH_2CF_2Br]$; $e_2 = [CFBr_2CF_2CH_2Br]$

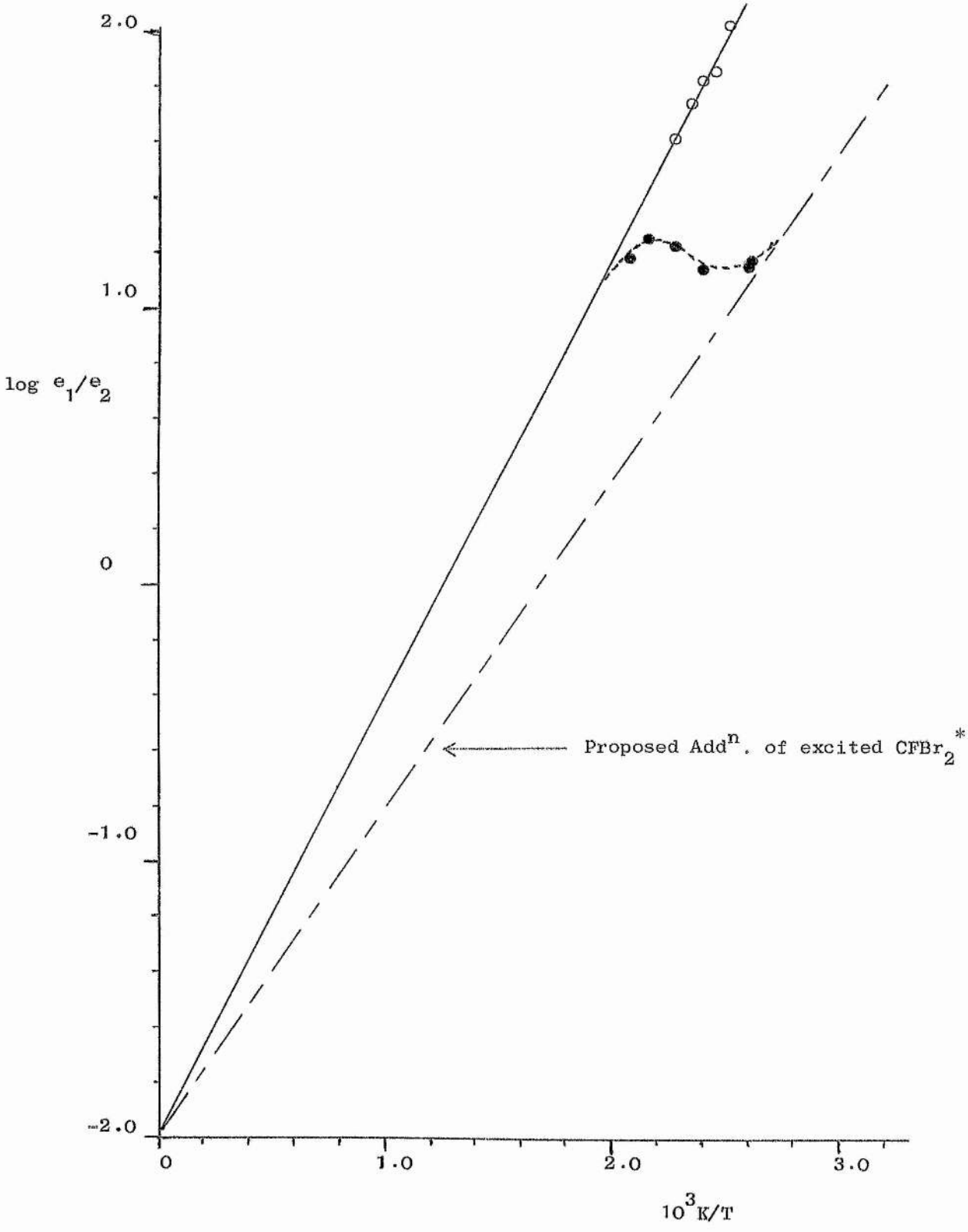

shown in table 3.12 for the addition of a series of haloalkyl radicals to the unsymmetrical fluoroethylenes. The correlation diagrams of the logarithms of the orientation ratios at 150°C with radical radii for addition to vinyl fluoride, 1,1-difluoroethylene and trifluoroethylene are shown in figs 3.9a, 10a and 11a respectively. Introducing the polar term to improve the correlation gives best results when the coefficient (B) is set equal to one.

Improved correlation term: $r_c + B \sum_{\alpha} \sigma_I (\alpha)$

where r_c = radical radii

B = 1 = the coefficient

$\sum_{\alpha} \sigma_I (\alpha)$ = sum of the Taft inductive constants for all substituents attached to the central carbon atom.

The improved correlations are shown in figs 3.9b, 10b and 11b. These highlight the contribution to determining the direction of orientation from the differing polarities of the carbon-halogen and carbon-hydrogen bonds in halomethyl radicals.

Table 3-12

RADICAL	RADIUS Å	$\sum_{\alpha}\sigma_I(\alpha)$	RADIUS Å+ $\sum_{\alpha}\sigma_I(\alpha)$	$CH_2=CHF$		$CH_2=CF_2$		$CHF=CF_2$		REF.
				e_1/e_2	log e_1/e_2	e_1/e_2	log e_1/e_2	e_1/e_2	log e_1/e_2	
$CH_3\cdot$	2.58	0.00	2.58	1.69	0.228	-	-	0.14	-.854	59
$CH_2F\cdot$	3.16	0.52	3.68	3.35	0.525	2.29	0.360	0.49	-0.31	this work
$CHF_2\cdot$	3.63	1.04	4.67	5.26	0.721	5.56	0.745	1.05	0.021	this work
$CF_3\cdot$	3.92	1.56	5.48	10.64	1.027	31.25	1.495	2.00	0.301	41
$CF_2Br\cdot$	4.45	1.49	5.93	11.24	1.051	34.48	1.538	2.13	0.328	22
$CF_3F_2\cdot$	5.16	1.46	6.62	18.52	1.268	90.91	1.959	3.45	0.538	41
$CCl_3\cdot$	5.26	1.41	6.67	14.29	1.155	83.33	1.921	3.45	0.538	39
$CFBr_2\cdot$	5.41	1.42	6.83	11.76	1.071	52.63	1.721	2.78	0.444	this work
$CHBr_2\cdot$	5.41	0.80	6.21	15.87	1.201	-	-	3.23	0.509	52
$CBr_3\cdot$	5.84	1.20	7.04	23.80	1.377	-	-	4.17	0.620	52
$(CF_3)_2CF\cdot$	6.62	1.34	7.96	50.00	1.699	1 000	3.000	16.13	1.205	41

Fig. 3.9 Correlation diagrams of logarithms of orientation ratios at 150°C with a) steric and b) steric plus polar factors for addition of haloalkyl radicals to vinyl fluoride.

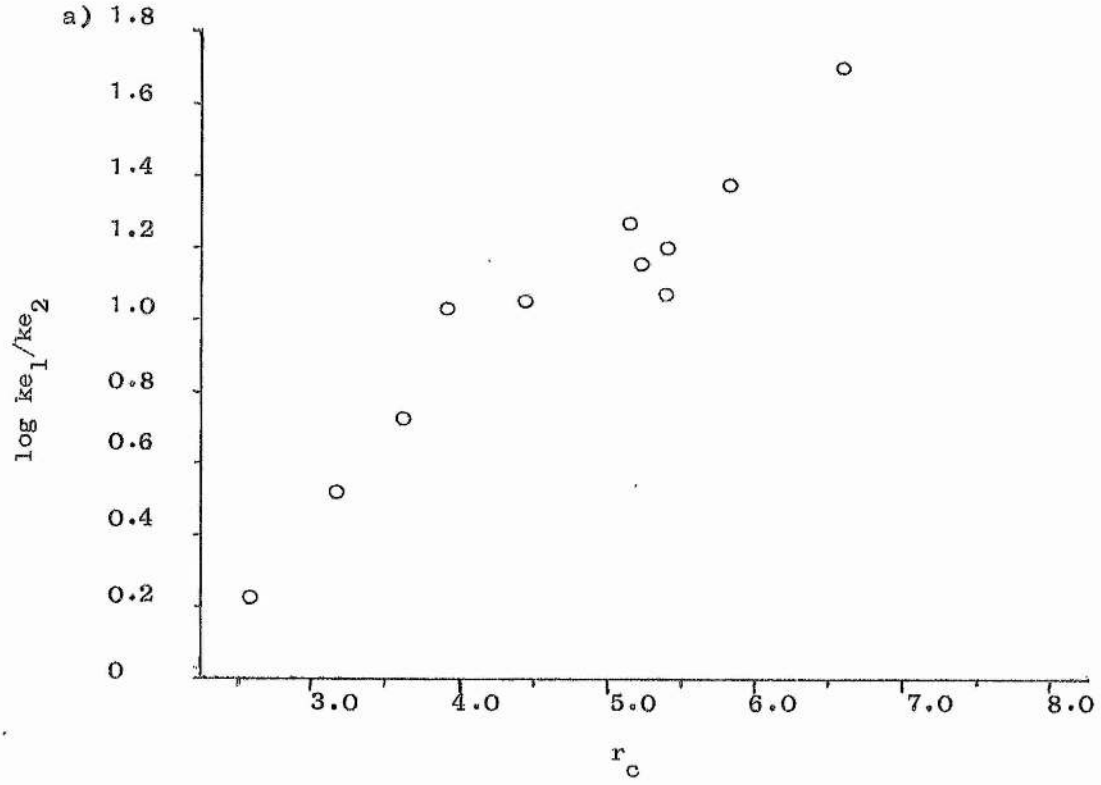

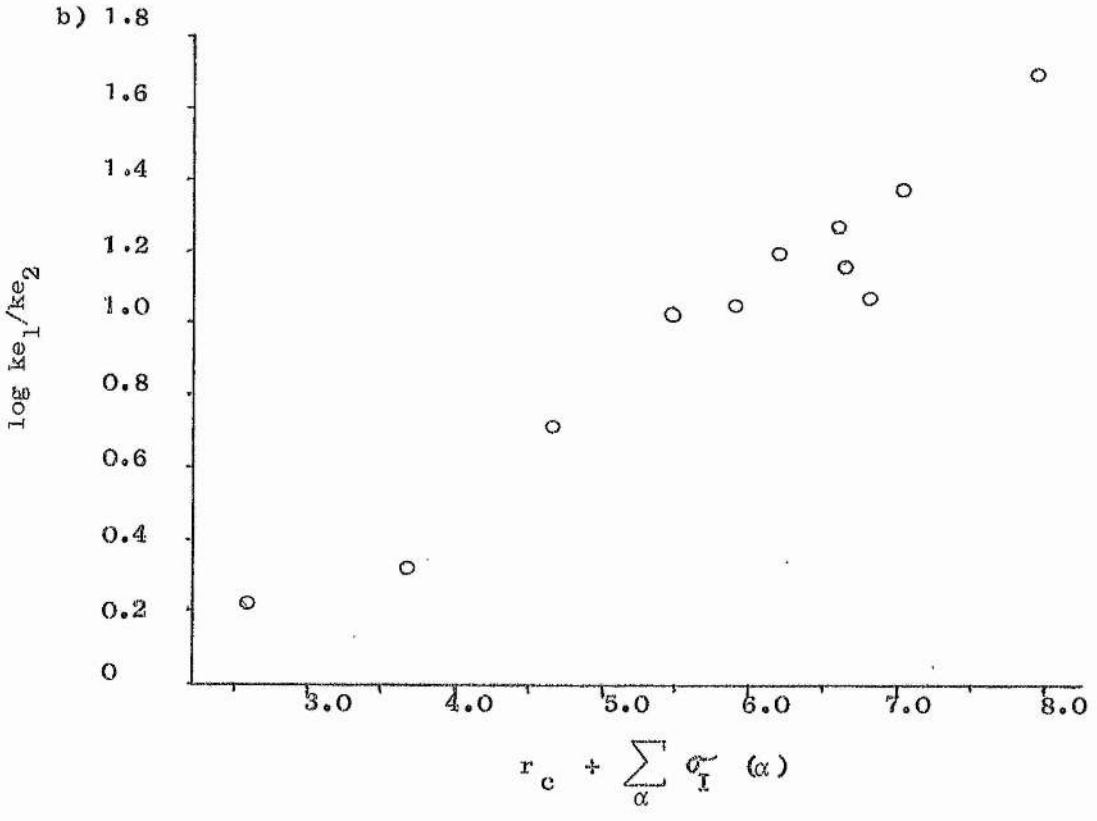

Fig. 3.10 Correlation diagrams of logarithms of orientation ratios at 150°C with a) steric and b) steric plus polar factors for addition of haloalkyl radicals to 1,1-difluoroethylene.

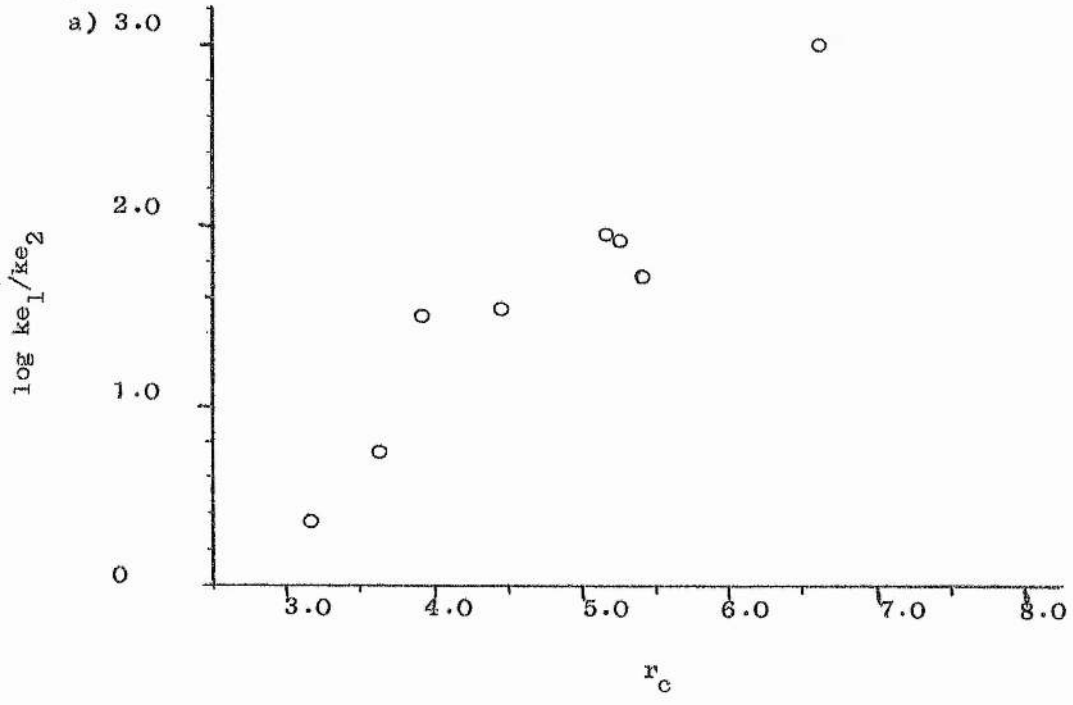

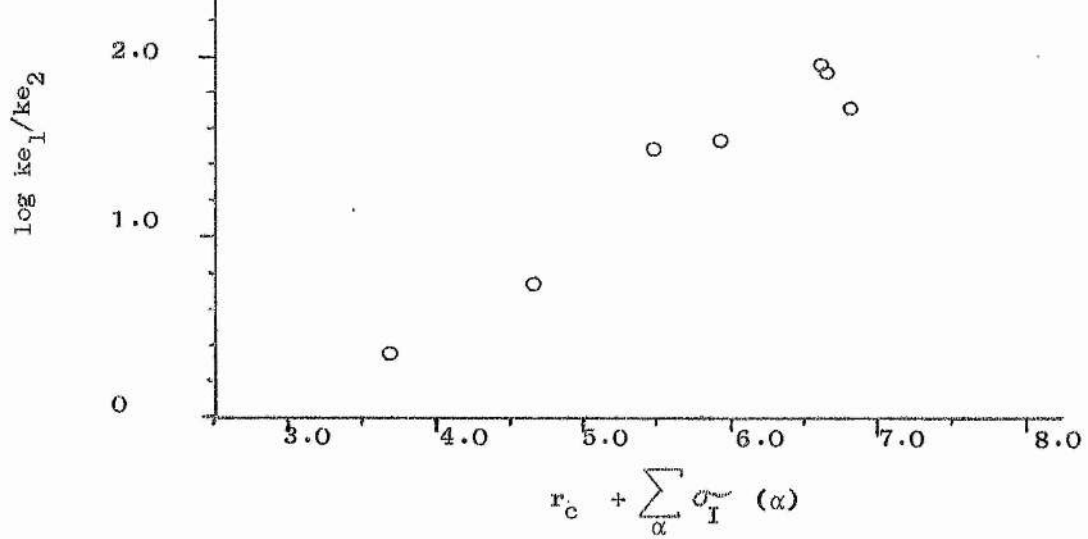

Fig. 3.11 Correlation diagrams of logarithms of orientation ratios at 150°C with a) steric and b) steric plus polar factors for addition of haloalkyl radicals to trifluoroethylene.

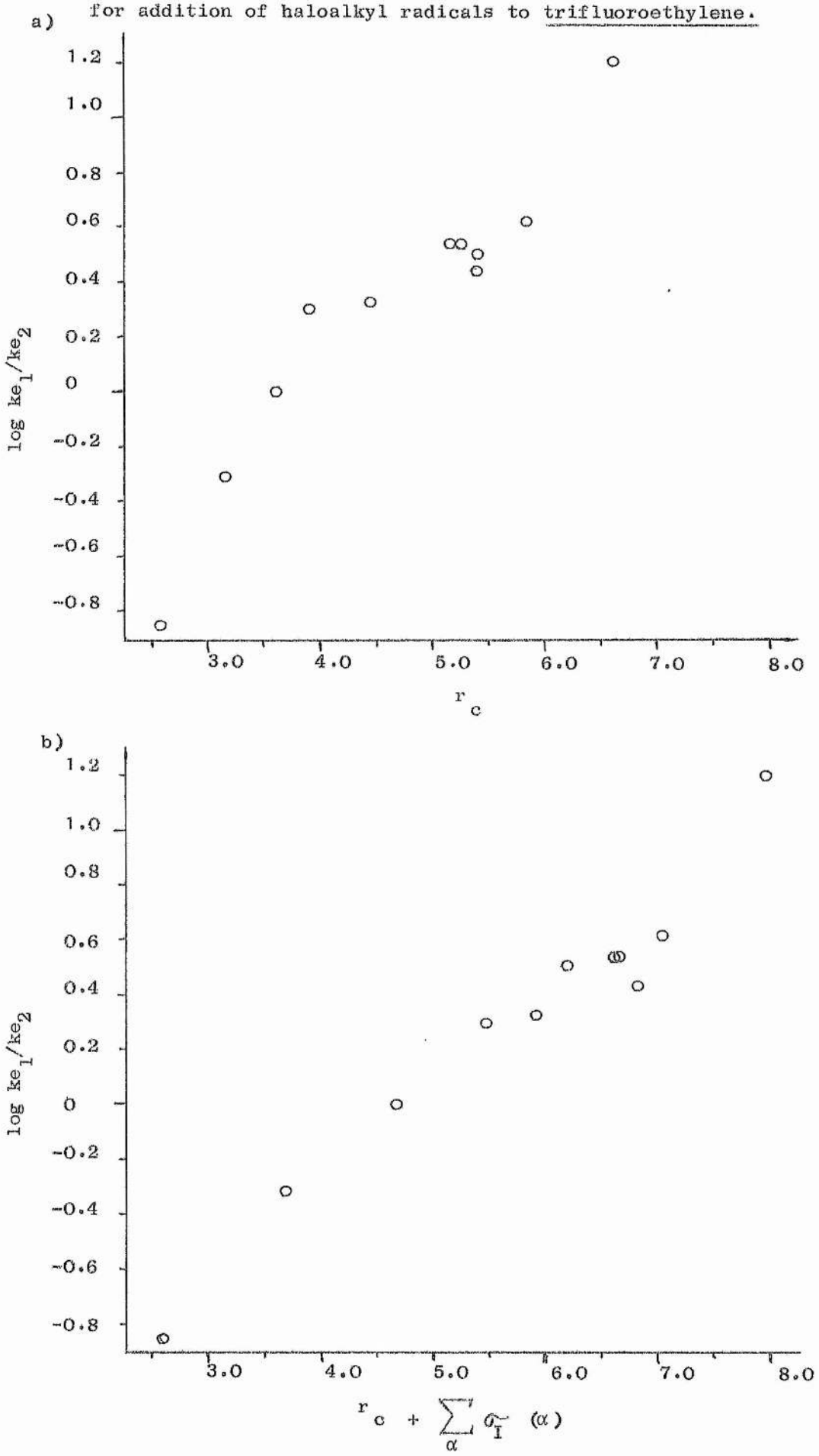

REFERENCES

1. M. Gomberg, J.Amer.Chem.Soc., 1900, 22, 757.
2. H.S. Taylor, Trans.Faraday Soc., 1925, 21, 560.
3. W. Hofeditz and F. Paneth, Chem.Ber., 1929, 62, 1335.
4. D.H. Hey and W.A. Waters, Chem.Revs., 1937, 21, 169.
5. J.A. Kerr and A.F. Trotman-Dickenson, Prog. in Reaction Kinetics, Vol. 1, 107.
6. F.W. Evans and M. Szwarc, Trans.Faraday Soc., 1961, 57, 1905.
7. F.W. Evans, R.I. Fox and M. Szwarc, Trans.Faraday Soc., 1961, 57, 1915.
8. J.A. Kerr and M.J. Parsonage, "Evaluated Kinetic Data On Gas Phase Addition Reactions", Butterworths, 1972.
9. J.I.G. Cadogan and D.H. Hey, Quart.Rev., 1954, 8, 308.
10. F.H. Mayo and C. Walling, Chem.Revs., 1940, 27, 351.
11. J.M. Tedder and J.C. Walton, Proc,Chem.Soc., 1964, 420.
12. M.G. Evans and M. Polanyi, Trans.Faraday Soc., 1938, 34, 11.
13. W.A. Waters, "Chemistry of Free Radicals", Oxford Univ.Press", 1946.
14. M.G. Evans, J. Gergely and E.C. Seaman, J. Polymer Sci., 1948, 3, 866.
15. i) R.N. Haszeldine, J.Chem.Soc., 1953, 3565.
    ii) R.N. Haszeldine, J.Chem.Soc., 1953, 3559.
    iii) R.N. Haszeldine and B.R. Steele, J.Chem.Soc., 1954, 923.
16. J.M. Tedder and J.C. Walton, Trans.Faraday Soc., 1966, 62, 1859.
17. J.M. Tedder and J.C. Walton, Trans.Faraday Soc., 1967, 63, 2678.
18. C.A. Coulson, Disc.Faraday Soc., 1947, 2, 351.
19. L.Y. Chuang, A.P. Stefani and H.E. Todd, J.Amer.Chem.Soc., 1970, 92, 4168.
20. A.C. Greig et al, in preparation.
21. J.M. Tedder, J.C. Walton and K.D.R. Winton, Trans.Faraday Soc., 1972, 68, 160.
22. J.M. Tedder and J.C. Walton, Trans.Faraday Soc., 1974, 70, 308.

23. J.M. Tedder and J.C. Walton, Trans.Faraday Soc., 1966, 62, 1859.

24. M. Hemptinne and J. Wouters, Nature, 1938, 141, 412.

25. A.I. Pisanskii and Y.P. Tsyashchenko, Ukr,Fiz.Zh (Russ.Ed.), 1970, 15, 1585.

26. F.F. Cleveland, A.G. Meister and S.E. Rosser, J.Chem.Phys., 1950, 18, 346.

27. B.J. Stepanov, Comptes Rendus, 1944, 45, 56.

28. M.L. Delwaulle and F. Francois,

i) Comptes Rendus, 1942, 214, 828,

ii) J.Phys.Radium, 1946, 7, 15,

iii) Contrib.e'tude structure mol. Vol. Commem. Victor Henri, 1947, 119.

29. I.P. Biryukov, V.T. Danilkin and M.G. Voronkov, Tear.Eksp.Khim., 1966, 2, 533.

30. G. Filipovich and G.V.D. Tiers, J.Phys.Chem., 1959, 63, 761.

31. I.K. Venkateswarlu and R. Thanalakshmi, J. Annamalai Univ., 1962, ptB24, 13 and 38.

32. H.J. Bernstein, J.Phys.Chem., 1965, 69, 1550.

33. J.C. Miller and C.P. Smyth, J.Chem.Phys., 1956, 24, 814.

34. J.C. Miller and C.P. Smyth, J.Amer.Chem.Soc., 1957, 79, 20.

35. E. Gelles and K.S. Pitzer, J.Amer.Chem.Soc., 1953, 75, 5259.

36. P.G. Maslov andY.P. Maslov, Khim. i Tekhnol.Topliv i Masel, 1958, 3, No. 10, 50.

37. M. Hellmann, E. Peters, W.J. Pummer and L.A. Wall, J.Amer.Chem. Soc., 1957, 79, 5654.

38. W.F. Edgell and L. Parts, J.Amer.Chem.Soc., 1955, 77, 5515.

39. J.C. Walton, Ph.D. Thesis, St. Andrews, 1966.

40. H.W. Sidebottom, J.M. Tedder and J.C. Walton, Trans.Faraday Soc., 1970, 66, 2038.

41. D.S. Ashton, A.F. Mackay, J.M. Tedder, D.C. Tipney and J.C. Walton, J.Chem.Soc.Chem.Comm., 1973, 496.

42. H. Rathsburg, Ber., 1918, 51, 669.

43. D.A. Brotchie, Private Communication.

44. J.M. Tedder and J.C. Walton, Trans.Faraday Soc., 1970, 66, 1135.

45. M.L. Deen and J. Roboz, Org.Mass Spec., 1970, 3, 155.

46. N. Cohen and J. Heicklen, J.Chem.Phys., 1965, 43, 871.

47. D.A. Armstrong and J.W.T. Spinks, Can.J.Chem., 1959, 37, 1210.

48. R.J. Cvetanović, Adv.Photochem., 1963, 1, 173.

49. P.I. Abell and R.J. Field, Trans.Faraday Soc., 1969, 65, 743.

50. N. Davidson and J.H. Sullivan, J.Chem.Phys., 1951, 19, 143.

51. R.J. Cvetanović and G.R. Wooley, J.Chem.Phys., 1969, 50, 4697.

52. J.C. Walton, Private Communication.

53. D.L. Beveridge and J.A. Pople, "Approximate Molecular Orbital Theory", McGraw-Hill, 1970.

54. C.A. Coulson, Trans.Faraday Soc., 1946, 42, 265.

55. E. Farenhorst and E.C. Kooyman, Trans.Faraday Soc., 1953, 49, 58.

56. S.S. Dubov, M. Landau and A.N. Medvedev, Russ.J.Phys.Chem., 1969, 43, 3.

57. M.J.S. Dewar, "The Molecular Orbital Theory of Organic Chemistry", McGraw-Hill, New York, 1969.

58. R.J. Cvetanović, Advan.Photochem., 1963, 1, 115.

59. K.D.R. Winton, Ph.D. Thesis, St. Andrews, 1973.

60. P.A. Dobosh, CNINDO, Q.C.P.E., Program No. 141.

61. A. Streitweiser Jr., "Molecular Orbital Theory for Organic Chemists", Wiley, New York, 1957.

62. J.M. Tedder and J.C. Walton, Progress in Reaction Kinetics, 1967, 4, 37.

63. J.P. Simons and A.J. Yarwood, Proc.Chem.Soc., 1962, 62.

64. N.J. Friswell and B.G. Gowenlock, Advances in Free Radical Chemistry, 1, 39.

65. R.F. Chambers, H.C. Clark and C.J. Willis, Chem. and Ind., 1960, 76.

66. C.J. Albisetti, D.D. Coffman, F.W. Hoover, E.L. Jenner and W.E. Mochel, J.Amer.Chem.Soc., 1959, 81, 1489.

67. J.F. Harris Jr. and F.W. Stacey, Organic Reactions, Wiley, 13, 150.

68. P. Gray and A. Williams, Chem.Rev., 1959, 59, 239.

69. E.W.R. Steacie, "Atomic and Free Radical Reactions", 2nd Edition, Reinhold, New York.

70. A.T. Coscia, J.Org.Chem., 1961, 26, 2995.

71. T.J. Dougherty, J.Amer.Chem.Soc., 1964, 86, 460.

72. G.H. Williams, "Homolytic Aromatic Substitution", Pergamon Press, 1960.

73. D.C. Nonhebel and J.C. Walton, "Free Radical Chemistry", Cambridge University Press, 1974.

74. O. Bretschneider, W. Luchsinger, G. Miltschitzky and O. Ruff, Ber., 1936, 69B, 299.

75. R.L. Bond, R.E. McArthur and J.H. Simons, J.Amer.Chem.Soc., 1940, 62, 3477.

76. R.N. Haszeldine, J.Chem.Soc., 1952, 4259.

77. M.A. Raksha, V.N. Shemanina, A.S. Vasil'eva and N.N. Yarovenko, Zhur.Obshcheĭ Khim., 1957, 27, 2246.

78. F.S. Rowland and T. Smail, J.Phys.Chem., 1970, 74, 1866.

79. G. Blume, R. Mathias and P. Weyerstahl, Tetrahedron Lett., 1973, 617 (Ger).

80. Yu.G. Papulov et al., Zh.Strukt.Khim., 1973, 13, 956 (Russ).

81. F.P. Lossing, Bull.Soc.Chim.Belg., 1972, 81, 125.

82. J. Hine and A.D. Ketley, J.Org.Chem., 1960, 25, 606.

83. J. Hine and P.B. Langford, J.Amer.Chem.Soc., 1957, 79, 5497.

84. M.J. Perona and G.O. Pritchard, Int.J.Chem.Kinet., 1969, 1, 509.

85. J.A. Kerr and D.M. Timlin, Int.J.Chem.Kinet., 1971, 3, 69.

86. J.A. Kerr and D.M. Timlin, Int.J.Chem.Kinet., 1971, 3, 1.

87. M.G. Bellas, H.E. Gunning and O.P. Strausz, Can.J.Chem., 1965, 43, 1022.

88. J.T. Bryant and G.O. Pritchard, J.Phys.Chem., 1965, 69, 1085.

89. J.T. Bryant and G.O. Pritchard, J.Phys.Chem., 1967, 71, 3439.

90. M.J. Perona, and G.O. Pritchard, Int.J.Chem.Kinet., 1969, 1, 413.

91. D.W. Follmer and G.O. Pritchard, Int.J.Chem.Kinet., 1973, 5, 169.

92. R.W. Fessenden and R.H. Schuler, J.Chem.Phys., 1965, 43, 2704.

93. P.B. Ayscough, K. Mach and J. Machova', J.Chem.Soc., Faraday Trans. II, 1973, 69, 750.

94. L. Andrews and T.G. Carver, J.Chem.Phys., 1969, 50, 5100.

95. T. Berces and S. Forgeteg, Acta Chim.Acad.Sci.Hung., 1967, 51, 205.

96. D.L. Beveridge, P.A. Dobosh and J.A. Pople, J.Chem.Phys., 1968, 48, 4802.

97. J. Biddles and A. Hudson, Mol.Physics, 1973, 25, 707.

98. i) J.C. Gibb, J.M. Tedder and J.C. Walton, J.Chem.Soc., Perkin II, 1974, 807,

ii) F.W. Evans and M. Szwarc, Trans.Faraday Soc., 1961, 57, 1905.

99. W.A. Pryor, "Free Radicals", McGraw-Hill, 1966.

100. W.G. Alcock and E. Whittle, Trans.Faraday Soc., 1965, 61, 244; W.G. Alcock and E. Whittle, Trans.Faraday Soc., 1966, 62, 134.

101. J.H. Knox, Trans.Faraday Soc., 1962, 58, 275.

102. J.M. Tedder and J.C. Walton, Prog.Reaction Kinetics, 1967, 4, 37.

103. H. Komazawa, A.P. Stefani and M. Szwarc, J.Amer.Chem.Soc., 1963, 85, 2043.

104. S.G. Davis, B.S. Rabinovitch and C.A. Winkler, Can.J.Research, 1943, B21, 251.

105. A.E. Arkel and E. Janetzky, Rec.trav.Chim., 1937, 56, 167.

106. W.H. Brader, S.J. Ehrenson and J. Hine, J.Amer.Chem.Soc., 1956, 78, 2282.

107. J.F.J. Todd, J.Phys.Chem., 1967, 71, 2875.

108. B.S. Rabinovitch and J.F. Reed, J.Phys.Chem., 1957, 61, 598.

109. J.W. Coomber, A.M. Tarr and E. Whittle, Trans.Faraday Soc., 1965, 61, 598.

110. R.W. Fessenden and R.H. Schuler, J.Chem.Phys., 1965, 43, 2704.

111. M. Karplus, K. Morokuma and L. Pedersen, J.Phys.Chem., 1968, 48, 4801.

112. A.D. Walsh, J.Chem.Soc., 1953, 2306.

113. H. Konishi and K. Morokuma, J.Amer.Chem.Soc., 1972, 94, 5603.

114. M.E. Jacox and D.E. Milligan, J.Chem.Phys., 1969, 50, 3252.

115. T.F. Graham, G.O. Pritchard and M. Venugopalan, J.Phys.Chem., 1964, 68, 1786.

116. G.O. Pritchard and R.L. Thomarson, J.Phys.Chem., 1967, 71, 1674.

117. J.M. Sangster and J.C.J. Thynne, Trans.Faraday Soc., 1969, 65, 2110.

118. D. Goodeve and C.F. Porret, Proc.Roy.Soc., 1938, A165, 31.

119. C.D. Ritchie and W.F. Sager, Progr.Phys.Org.Chem., 1964, 2, 323.